

INVESTIGATING THE ROLE OF THE GUT MICROBIOME AND THE GUT
METABOLOME IN THE DEVELOPMENT OF CHILDHOOD ECZEMA AND ASTHMA

By

Hinako Terauchi

A DISSERTATION

Submitted to
Michigan State University
in partial fulfillment of the requirements
for the degree of

Microbiology and Molecular Genetics – Doctor of Philosophy

2024

ABSTRACT

In United States alone, more than 1 in 4 children are diagnosed with some form of allergy, yet the exact etiology of allergy development in childhood is unknown. Many factors have been associated with this rise in such disorders including genetics, epigenetics, environmental toxins and particulates, as well as the microbiota. The host microbiome has been associated with a multitude of human and animal diseases, disorders, and conditions. Its involvement in the atopic and autoimmune disorders is an every-growing field of new knowledge. In this work, I explore the effect of the gut microbiome on allergy, specifically childhood eczema and asthma, using samples and data collected from the Isle of Wight allergy study cohort as well as a fecal-transplanted humanized microbiota mouse models. In addition, measured specific gut metabolites that were significant in distinguishing between the pathology phenotypes in both study sets will be discussed. In chapter 1, I explored the gut bacterial microbiota of infants in the Isle of Wight allergy study cohort and their association with their development in eczema. We also explored bacterial taxa previously shown in published work to be associated with allergy as agonists or antagonists. Subsequent statistical analyses including random forest and logistic regressions supported these findings and results from logistic regressions provide statistical significance for the association of eczema status at age 3 months with the relative abundance of genus *Veillonella* at that age. In chapter 2, a study conducted using a mouse model of asthma created by fecal transplantation of the infants featured in chapter 1, connection between gut microbiota in infancy and lung baseline responses were studied and supported. In chapter 4, the role of the gut metabolome in the development of allergic phenotype was explored using the samples from both chapters 1 and 2, where it was shown that infants with allergic phenotype have a distinct gut metabolomic profile compared to infants without allergic phenotype; and mice with reduced lung functionality expressed a distinct gut metabolic profiles compared to mice without reduced lung functionality. Overall, these studies confirmed previously associated relationship between specific bacterial taxa and allergy using a unique infant cohort as well as an original mouse model, while also providing new points of interest to further deepen the understanding of the relationship and the interaction between the gut contents and the host's development of allergy.

This thesis is dedicated to:
Lady Thumbelina Buns,
Sir Cornelius Porkbelly,
Princess Anastasia Stroganoff,
And my favorite sister Ayana

TABLE OF CONTENTS

CHAPTER 1: Literature Review	1
REFERENCES.....	15
CHAPTER 2: Predominance of <i>Veillonella</i> and other allergy agonists in 3-month-old infant gut microbiota was associated with development of eczema in early childhood in the Isle of Wight Birth Cohort	23
REFERENCES.....	67
APPENDIX.....	71
CHAPTER 3: Fecal microbiota transplants of three distinct human communities to germ-free mice exacerbated inflammation and decreased lung function in their offspring.....	73
REFERENCES.....	140
APPENDIX.....	152
CHAPTER 4: Metabolomic profiles significantly distinguished in the gut based on expressed allergic phenotypes in eczemic infants and in mouse model of asthma	158
REFERENCES.....	196
CHAPTER 5: Conclusions and future directions	209
REFERENCES.....	216

CHAPTER 1: Literature Review

Allergic diseases and the role of the microbiome

Allergic diseases are immune-mediated disorders mainly caused by IgE-dependent immunological reactions to innocuous environmental antigens called allergens[1]. In affected individuals the site of contact with an allergen determines which clinical manifestations develop such as in the airways, skin, or gastrointestinal tract[1]. Allergy triggered by airway exposures include allergic asthma, allergic rhinitis often called hay fever, and ocular allergy or conjunctivitis. Allergic asthma causes coughing, wheezing, shortness of breath, chest tightness, and difficulty breathing when an affected individual is exposed to allergens in the airways. Allergic rhinitis causes sneezing, nasal congestion, runny nose, and itchy nose, eyes, and/or throat upon exposure. Ocular allergy symptoms are seen in the eyes that become red, itchy, and watery[1]. Allergy frequently triggered by skin exposures include dermatitis, urticaria or hives, and angioedema. Dermatitis has several categories, such as contact dermatitis and atopic dermatitis often referred to as eczema, and the common symptoms are redness, itchiness, and inflamed skin [1]. Allergies triggered by GI exposure include food and drug allergies, where allergic reactions occur upon ingestion of an allergen. These GI allergies manifest as nausea, vomiting, diarrhea, swelling of the lips, tongue, or throat, as well as skin and systemic reactions[1]. The development of allergies has been linked to the gut microbiome, especially that of early infancy[2, 3]. Although the exact etiology is unknown, there has been several studies showing relationship between specific and/or a collection of bacterial species within the gut microbiota[4].

Significance and prevalence of allergic diseases

According to the CDC, in the United States, nearly 1 in 3 adults and more than 1 in 4 children suffers from some form of allergy in 2021[5]. Out of the total of adults in the US, 25.7% have seasonal allergy, 7.3% have eczema, and 6.2% have food allergy[5]. For children, 18.9% have seasonal allergy, 10.8% have eczema, and 5.8% have food allergy[5]. For both adults and children, those identifying as Black, non-Hispanic are more likely to have food allergy compared to other groups, while for seasonal allergies affected individuals were more likely in white, non-Hispanic adults than other racial or ethnic groups[5]. The percentage of those with eczema within the total percentage of those with allergies was higher in children (10.8%) than for adults (7.3%), with the highest percentage of eczema in children aged 6-11 years (12.1%),

then 10.4% in children between the age of 0-5 years, followed by 9.8% in children aged 12-17 years[5].

Development, manifestation, and impact of childhood eczema

Eczema, or atopic dermatitis, is a chronic allergic condition where the majority of cases (60%) develop within the first year of life, with 45% developing during the first 2 to 6 months of life[6]. Although not life-threatening on its own, the symptoms experienced along with common comorbidities, such as sleep disturbances and psychological and mental illnesses, eczema can have great impact on the quality of life of those affected[7]. There have been many reports of sleep disturbances caused by childhood eczema[8-10], as well as comorbidities of psychosocial and mental diseases[11-14], where those with eczema suffered depression and suicidal ideation significantly more than their non-eczemic peers[15].

There are many studies demonstrating significant outcomes that support a genetic disposition for developing eczema, shown by the higher prevalence in children with parental eczema history[16, 17] as well as twin studies[18, 19]. Thereafter, additional molecular genetic studies have identified several chromosomal loci as well as specific genes associated with eczema[20]. The most notable, and well studied gene is the filaggrin (*FLG*) gene, which plays a key role in epidermis differentiation[20]. There also has been associations of multiple Single Nucleotide Polymorphisms (SNPs) in immune genes involved in allergic inflammation, such as interleukin(*IL*)4, *IL*5, and *IL*13[20]. However, as with many complex immune diseases, eczema development cannot be fully explained by host genetic predispositions alone.

Eczema prevalence increased in industrialized nations in recent decades[21], suggesting the existence of external, environmental factors driving the development of this allergic disease. One of the extensively studied environmental factors associated with eczema is environmental tobacco smoke. However, while smoking has stronger associations with lower airway diseases, association with eczema is not as consistent[22]. Many of the studies examining the association of eczema and environmental tobacco smoke, especially those that produced contradicting results, measured levels of cotinine, a by-product of nicotine formed within the body, in bodily fluids[23-25]. A different study examined the skin barrier function instead of cotinine levels, where they found an association with environmental tobacco smoke and eczema[26]. This suggested in cases of eczema that environmental tobacco smoke may be directly interacting with

the skin where the disease manifests.

There are other associations for other environmental factors influencing the development of eczema, especially in industrialized nations where a clear molecular mechanism has yet to be identified. However, when focusing on those societies within higher areas of eczema prevalence in industrialized nations, it has been observed that eczema is more common in urban areas than in rural areas[27, 28]. In addition, having multiple siblings[29, 30], early daycare attendance, and co-habitation with a dog[27] have been identified to reduce the likelihood of a child developing eczema and other allergies. In contrast, children in higher socioeconomic households were seen to have higher prevalence of eczema[31], although this finding may be influenced by the availability of healthcare access[32]. Composition of the gut microbiome has also been associated with development of childhood eczema [4, 33].

The current clinical consensus for children diagnosed with eczema is that most will “outgrow” this condition as they age[34]. However, for those that do not, they are more likely to develop more persistent eczema, and/or additional allergic diseases, such as allergic asthma, in a phenomenon referred to as “atopic march”[34]. Atopic march is a natural progression of allergic diseases typically starting from atopic dermatitis or eczema, that progresses from infancy into childhood typically into food allergy, asthma, and allergic rhinitis[35].

Development, manifestation, and impact of childhood asthma

The allergic disease frequently developed as the later part of atopic march is asthma. Asthma is a chronic airway disease affecting 8.0% of adults and 6.5% of children in the US[36]. It is a disease that is often difficult to diagnose in the early years of childhood[37, 38] and its development has been associated with pre-existing eczema in children[34] and co-morbidity with eczema in adults[39]. In 2017, there were an estimated 1.6 million visits to the emergency department along with 183,000 hospitalizations attributable to asthma in the US alone[40]. Asthma prevalence was higher in those identifying as non-Hispanic Black, non-Hispanic multiple-race, and Puerto Rico persons, with asthma attacks more prevalent in children and adult women, and many racial ethnic groups with highest mortality in adult, female, and Black persons[40].

Hallmark phenotypes of asthma are airway hyperresponsiveness (AHR) and inflammation of the airway, both leading to the excessive narrowing of the airways that

contribute to the difficulty of breathing[41]. Although AHR can exist in non-asthmatic disease such as chronic obstructive pulmonary disease (COPD)[42], it is still a key feature used clinically to diagnose a patient with asthma[41]. In a clinical setting, the extent of AHR is measured to deliver a more accurate diagnosis of asthma as well as to monitor the disease severity and progression as part of bronchial provocation tests (BPTs)[41]. There are two major ways of administering BPTs: indirect and direct. In an indirect BPT, bronchial constriction is mediated by a stimulus that elicits bronchoconstriction, such as exercises and allergens[41]. In direct BPT, a bronchial constriction is induced using a pharmacological agonist directly acting on airway smooth muscle receptors, such as methacholine or histamine[41].

The mechanisms and the exact etiology of AHR and asthma development is still unknown, yet there are currently multiple studies that have indicated factors associated with the development of asthma, one of which is host genetics. Several SNPs have been identified to be potential risk factors for developing asthma in childhood[43, 44], including a variation in the *FLG* gene that was also associated with childhood eczema development[45]. In addition to the coded genetic variations, epigenetic factors, specifically DNA methylation events, have also been identified to play a role[46-48], suggesting a molecular mechanisms for how the environmental factors like cigarette smoke[49] could influence asthma development on a genetic level. Other environmental factors that have been associated with childhood asthma development include but are not limited to, early daycare attendance, livestock contact, cohabitation with a dog, endotoxins, diet, and gut and airway microbiome[50-55].

Education of the early immune system

The phenomenon of atopic march suggests the importance of immune system development during early life. A large portion of innate and adaptive immune system education commences at birth with the rush of exposure to environmental antigens; many of these exposures are bacterial cells from the birth canal, parental contact, and food and environmental sources that will become commensal residents of the gut microbiota[56]. However, some immune education has been observed prenatally [57, 58]. Inflammatory cytokines and memory responses can be produced by the immune cell population as early as the second trimester[57-59]. In addition, during mid-gestation, it was observed that viable bacteria in human fetal intestines can influence memory T cell activation, expand fetal lymph node T cells, and reduce

inflammatory cytokine production[59].

Despite prenatal immune activities, innate immunity is impaired during the neonatal stage immediately following birth. Antibody responses along with Type 1 T cells are weak. Early T cell responses are also skewed toward Foxp3⁺ CD25⁺ regulatory T cells via T cell responses directed against the mother's alloantigens[60]. As the neonate develops and is exposed to foreign antigens, both innate and mature immune responses increasingly mature to provide better protection from infectious agents. During these periods, T cells may be activated toward a Type 2 response, a hallmark immune response in allergies, including eczema and allergic asthma[56, 61].

Effects of the microbiome on allergies

An adult human body is estimated to carry about 38 trillion bacterial cells on and in the body, with large and small intestines carrying the greatest burden of all the body parts[62]. Considering that an adult human body is estimated to be made of 30 trillion cells[62], there is no question that such a collection of 38 trillion bacterial cells could have multitudes of effects on the host human body. The “gut microbiota,” referring to the microbiota existing in the gastrointestinal (GI) tract, has been a leading interest in regards to its effect on the host body due to the sheer volume of the microbes that reside in the intestines. The term gut microbiome is also used but refers specifically to the gut microbiota and all of its genetic elements in a more inclusive definition. The gut microbiome has been linked to myriad pathologies and diseases in humans, including but not limited to obesity, Crohn's disease, Inflammatory Bowel Disease (IBD), diabetes, and various allergic diseases like food allergy, eczema, and asthma[63]. The exact molecular mechanisms of how the gut microbiota mediates such a wide array of diseases and conditions are still not fully understood. However, in case of allergic disease development, there is growing agreement that the gut microbiome composition exerts significant affects during the first year of life when the immune system is developing[54, 55]. Atopy, eczema, and food allergy can develop during infancy, and while many children do recover as they age, other children later develop additional allergic diseases such as asthma; a phenomenon described as “atopic/allergic march”[52, 53]. Because 27% of the child population in the US have been diagnosed with atopic, allergic, and autoimmune disorders[64] an in depth review as of 2021 indicated that more scrutiny of the role of the gut microbiota in development of allergic disorders

is needed.

Human Studies linking the microbiome to development of allergy

A number of studies have shown relationships between particular gut microbiota and the development of allergy, especially during the period of early immune development[3, 65]. In a study by Jones et al. focused on detecting characteristics of allergy development and identifying interventions they observed that older children with peanut allergies were less likely to be successfully desensitized compared to their younger cohort[3], indicating the importance of immune development in earlier age. Moreover, the importance of the gut microbiota in the development of food allergies was displayed in an animal study where fecal transfer from an infant with cow's milk allergy to germ-free mice resulted in an anaphylactic response in the mice to cow's milk antigen [65].

Several specific microbial taxa have been associated with the development of allergic diseases. We are calling these putative allergy agonists, while taxa associated with protection from allergy have also been identified. In terms of the microbiome members during the early neonatal stage of life, the phyla *Proteobacteria*, and genera *Acinetobacter*, *Enterococcus*, and *Lactobacillus* were found to be in lower abundance in neonates with positive allergic sensitizations, while having higher abundance of *Bacteroidaceae* and *Bifidobacterium catenulatum* was associated with lack of allergic manifestations[4]. Higher abundance of *Bacteroidaceae*, *Clostridaceae*, and *Enterobacteriaceae*, and lower abundance of *Lactobacillaceae* has also been observed in neonates with eczema[4].

Although asthma cannot be fully diagnosed in neonates, some association of specific neonatal microbial members have been made utilizing wheeze phenotype for having higher abundance of *B fragilis*, *C coccoides*, and *C difficile*, all of which are anaerobes, and a lower abundance of *Staphylococcus aureus*[4]. Intestinal microbial diversity has had mixed observations in its association with allergy development with some studies showing significance and others not[4].

Mouse models of allergy

Animal models are created and used based on the comparative medicine principle[66], and have been used to further the understanding of biology as early as 6th BCE in ancient Greece.

However, the use and development of modern animal models, such as genetically inbred mice, with focus on reproducibility did not enter the field of biomedical research until the 1940s[67, 68]. The most commonly used species today are rodents[69], however many other species are also been used including but not limited to: dogs, rabbits, birds, ruminants, horses, fish, frogs, monkeys, cats, reptiles, squid, crabs, bees, chimpanzees, hamsters, sea slugs, pigs, nematodes, fruit flies, and protozoans[66]. The animal species to use is selected based on the purpose and functionality that fits the objective of the study[70, 71], and it is required that they replicate the physiological and pathological processes while containing biological, anatomical, functional, and/or genetic similarities to the research topic target, frequently humans[71, 72].

In studying allergic asthma in humans, there have been many studies successfully developing and using murine models[73]. Mice do not naturally develop asthma[74], thus requiring a sensitization protocol with an allergen in order to mimic the allergic asthma phenotypes commonly seen in humans[73, 75]. The two main ways of inducing asthma, specifically airway characteristics such as AHR and airway inflammations, are by acute or chronic allergen challenges[73, 75]. Development of acute challenge model is done by multiple administration of allergen along with an adjuvant to promote Th2 responses, with sensitization periods typically lasting less than 2 weeks[73]. In contrast, chronic challenge models are developed by exposing mice to lower doses of allergen for longer periods of sensitization, typically up to 12 weeks[73]. Acute challenge models are capable of producing clinical asthma's key features such as elevated levels of IgE, airway inflammation, AHR, and epithelial hypertrophy[73]. The limitation lies in the fact that an acute challenge model is short-term in nature while clinical asthma is often chronic in humans. Humans with chronic asthma experience chronic inflammation of the airway walls and subsequent airway remodeling, both of which are absent in an acute challenge model[73]. Despite its limitations, acute challenge models have been used to produce supporting evidence of allergic asthma's Th2-mediation, the role of T cells in allergic response, and the role of eosinophils in AHR development[73]. Chronic challenge models were created to address some of the issues of acute challenge models. It also is capable of producing clinical asthma's key features such as Th2-dependent allergic inflammation, allergen-dependent sensitization, and AHR, in addition to airway remodeling, a chronic pathology absent in the acute challenge models[73]. However, it also has its limitations as it expresses some features not seen in human asthma such as lung inflammation not restricted to the airways, as

well as the lack of development of increased airway smooth muscle lesions nor lung parenchymal and vascular remodeling[73, 76]. Both acute and chronic models have their benefits and limitations, thus caution and understanding of one's study objective are vital.

The common allergens used during the sensitization period are ovalbumin (OVA), house dust mites (HDM), cockroach extracts, and *Aspergillus*[73, 75]. OVA is a protein derived from chicken egg that induces a robust allergic pulmonary inflammation in laboratory mice[73]. The use of OVA is very wide-spread in asthmatic mouse models[77], however, it is an allergen that has very little role in human allergic asthma, leading to the use of a more clinically relevant allergens such as HDM, cockroach extracts, and *Aspergillus*[73]. Both HDM and cockroach exposure has been identified as being risk factors for allergic predisposition in children with asthma[78], with HDM allergy considered to be the most frequent of the inhalant allergies[79], making this preparation a more clinically translatable choices to use as sensitizing allergens.

Murine models have also been used in studying the effect of the gut microbiome on the allergic disease phenotypes[80-82]. In one study by Herbst et al, they observed that germ-free mice developed an upregulation of allergic airway inflammation along with increase in Th2-associated cytokines and IgE production, both of which was associated with allergy in humans[82]. Their findings were also supported in a study by Cahenzli et al, where an increase in serum IgE levels was also observed in germ-free mice, which also developed systemic anaphylaxis[81]. They also observed that systemic anaphylaxis was prevented in mice raised with a specific pathogen-free microbiota[81]. The elevation in IgE was also observed in a study where mice were treated with antibiotics to ablate their commensal gut microbiota by antibiotic treatment[80].

In addition to studying the lack of the gut microbiota, a "humanized" mouse model has been created to reproduce the effect of specific gut microbiota compositions on disease development. This has been done by performing fecal transplantation on either germ-free, or antibiotic treated mice[83]. In mice, fecal microbiota transplantation is performed to model the effect of specific microbiome species or compositions related to human diseases[83-86]. Fecal-transplant as a method has existed as a treatment option for humans and was first proposed in 1958 as a treatment for different intestinal and extraintestinal diseases[87]. In human clinical settings, fecal microbiota transplantation (FMT) has been approved for, and successfully used in treating *Clostridium difficile* infections[88], and is currently being explored and studied for

treatment of other diseases linked to the gut microbiome, such as inflammatory bowel disease[89, 90] and ulcerative colitis[91]. Although observed to be effective, FMT does display some safety issues mostly stemming from the current lack of understanding of the effect of a gut microbiome long-term[92]. FMT materials are filtered and screened for transmissible pathogens, however, longer term effects of having a new microbiota such as its effect on phenotype transmission of obesity and metabolic disorders[92]. FMT has yet to receive marketing approval from the US Food and Drug Administration (FDA), and FDA currently are working assiduously to encourage efforts to provide defined and safe FMT[92].

The production of microbial metabolome in the gut

As part of the digestive process of food, animals with a digestive tract utilize mechanical digestions and chemical digestions[93]. While mechanical digestion involves movements of the digestive system like chewing with teeth or intestinal movements, chemical digestion involves breakdown of food materials with “chemicals” with very low or high pH or abrasive enzymes such as stomach acid or bile acid[93]. The consumed food moves through the digestive tract and gets broken down into its component compounds that enables absorption through the intestinal epithelium[93]. The gut microbiota contributes to further breakdown of the consumed food, producing vital nutrients that the host can then uptake[94]. What the host consumes as food becomes the main source of nutrients for the microbes that reside in the host digestive system. Members of the gut microbiota uptake available food particles traveling through the GI tract, utilize these compounds for their metabolism, and produce metabolites or by-products that other microbial community members can utilize[94]. It is the collection of these secreted metabolites that contributes to the building of, and the maintaining of, what is referred to as the gut metabolome.

Microbes consuming each other’s metabolic products within the gut, or within any environmental proximity, is called cross-feeding[95]. Bacterial cross-feeding of metabolites has been shown to be ecologically stable and increases the genotypic diversity within the community[96]. The metabolites directly used in central metabolism such as sugars, and metabolites requiring biosynthesis or uptake that are essential nutrients, such as amino acids and vitamins, are the two main categories of microbially produced metabolites within the cross-feeding networks[95]. Cross-feeding for metabolites in central metabolism occurs in trophic

levels, starting with primary degraders that breaks down complex polysaccharides that get utilized by primary fermenters in glycolysis to produce by-products used by secondary fermenters producing short-chain fatty acids[95]. Molecular hydrogen get produced by primary and secondary fermenters during this process, which gets used by sulfate reducing bacteria, methanogens, and acetogens as electron donor[95]. The trophic level organization of microbial cross-feeding within the gut allows for a better structure for the complex interactions between the members of the microbiota. The resulting food web allows one to focus on specific interactions of interest within this community.

Beyond the utilization of microbially produced metabolites within the microbial community, some metabolites have been identified as hugely beneficial and often vital to the human host's health. The most notable example being the provision of vitamin K and vitamin B groups from members of the gut microbiota[97]. It has also been observed that bacterial microbiota helps to digest dietary carbohydrates, proteins, and polyphenols, as well as host-produced bile acids in humans[98]. It is through this process that many bacterial metabolites that have been associated with host immune modulation are produced.

Bacterial metabolites and allergic disease development

Processing of dietary carbohydrates is done through bacterial fermentation, resulting in production of short chain fatty acids (SCFAs) and gases[98]. Acetate, butyrate, and propionate are the SCFAs most abundant in human feces[98], and have been associated with eliciting anti-inflammatory properties in the host [99]. Generally speaking, *Bacteroidetes* members tend to produce acetate and propionate efficiently, while *Firmicutes* members tend to produce butyrate[100]. Several host immune and gut epithelial cell receptors for SCFAs have been identified, suggesting their involvement in host immune system modulation[33]. High levels of acetate has been associated with protection from food allergy[101], and childhood asthma and wheeze[2, 102, 103]. Presence of abundant butyrate and propionate have also been associated with protection from wheeze and asthma[102, 104].

Bile acids gets secreted by the liver to help with digestion of lipids and have also been associated with allergic phenotypes. Bile acids prior to microbial processing are called conjugated bile acids, and unconjugated bile acids are bile acids that went through the post-processing by the intestinal microbiome. Conjugated bile acids have been associated with

protection in asthma[105, 106], and unconjugated bile acids, a product of microbial metabolism, has also been associated with protection in allergic responses[107, 108] as well as wheeze and childhood asthma[109]. Tryptophan is another bacterial metabolite produced in the digestive system that has been associated with protection from allergic asthma[110-112]. This metabolite has been shown to bind to and stimulate upregulation of the Aryl Hydrocarbon receptor on the surface of many cells in the gastrointestinal tract and other organs during these beneficial responses[113]. With the existence of host-beneficial bacterial metabolites, it is only logical that the opposite, host-detrimental bacterial metabolites also exist. Most acute and well-studied secreted bacterial products are those of human pathogens. Many human-pathogenic bacterial species will secrete some metabolic products with toxic properties to the host that then induce the disease phenotype in the host. Some notable examples of human pathogen toxins include lipopolysaccharide, a metabolic endotoxin produced by gram-negative bacteria, as well as cytotoxic and mitochondriotoxic metabolites produced by *Streptomyces* species[114].

In contrast to pathogen-produced toxic metabolites, bacterial metabolites that induce the onset and the development of allergic diseases have not been made clear. Allergic disease development involves a complex layer of education and activation of immune cells, which includes a wide array of bacterial orders and families, each having their own set of receptors, signals, and functions that are still being uncovered today. Some of the bacterial metabolites reported to be associated with the development of allergy include sphingolipids that have been shown to be active in inducing food allergy[105] and 12, 13-diHOME in childhood allergic asthma[115, 116]. 12,13-diHOME produced by bacterial epoxide hydrolase genes, and was observed that increase in expression of the said gene was associated with an increase in the likelihood of developing atopy, eczema, and asthma during childhood[116]

Histamine is a molecule produced by host immune cells known to elicit Type 2 inflammatory responses. It is produced mainly by mast cells and basophils and is a hallmark of allergic responses. Histamine is stored in cytoplasmic granules within these cells along with other amines such as serotonin, proteases, proteoglycans, cytokines, chemokines and angiogenic factors. Although there are several triggering stimuli, a key mechanism for granule release in mast cells is IgE binding to FcεRI receptors on their surface that are subsequently cross-linked by allergen that can occur in several configurations[117]. This cross linking leads to anaphylactic degranulation producing an immediate type I hypersensitivity. This results in many of the cardinal features of allergy mentioned previously and including vasodilation, increased permeability and smooth muscle

contraction, Histamine has also been observed to be produced via bacterial decarboxylation of amino acids in digestion[118].

Specific aims

The incidence of atopic and autoimmune disorders have been on the rise in industrialized nations[5, 24]. The exact cause and mechanism for this rise in incidence have yet to be clearly determined. However, many factors have been associated with this rise in such disorders including host genetics and epigenetics, exposure to environmental toxins and particulates, bacterial breakdown of ingested dietary materials, as well as exposures to the microbiota in lungs and gut[7, 23, 29, 36, 49, 51, 52, 119].

Currently, the host microbiome has been associated with a multitude of human and animal diseases, disorders, and conditions, and its involvement in the atopic and autoimmune disorders is an ever-growing field of new knowledge. One leading hypothesis is that the microbiota encountered at the start of life determines such outcomes, because it is responsible for initiating early-life immune system development. However, the exact molecular mechanism is still undetermined, but there have been two main hypotheses that have been argued based on current data. One hypothesis is that specific microbe(s) within the host microbiome interacts with the host immune system to trigger the development of allergy. The second hypothesis is that host associated microbes produce and excrete specific metabolite(s) that are taken up by the host to interact with the immune system, leading to allergy development.

The **long-term goal** of these studies was to determine how gut microbiota and metabolome compositions could affect the development of allergic diseases. My **overarching hypothesis** was that there exists a specific composition of both the microbiome and the metabolome in the gut that mediates the development of allergic diseases. To test this hypothesis, the **short-term goal** was to describe and compare the bacterial gut microbiome of infants with allergic eczema to those without. Then, to utilize fecal microbiota from these infants to create an animal model of allergic vs. non-allergic gut microbiota by fecal transplantation to further study the mechanisms of the effect of gut microbiome and metabolome composition on allergic phenotype.

Specific Aim 1: Identify the differences in early gut microbiota between infants with allergic phenotypes and infants without allergic phenotypes

Hypothesis: Composition of the early gut microbiota is associated with development of eczema and/or atopy in infants.

Specific Aim 2: Examine the role of human infant allergy-associated bacterial taxa in development of allergy phenotype in a mouse model of asthma

Hypothesis: Enterobacteriaceae-dominant gut microbiota from eczemic infants will cause increased T helper 2 (Type 2) inflammation and decreased lung function after house dust mite antigen (HDM) exposure in transplanted mice, while Bacteroidaceae-dominant gut microbiota from non-eczemic infants will be protective.

Specific Aim 3: Investigate key differences in gut metabolome based on expressed allergic phenotypes

Hypothesis 3a: Human infants with eczema express distinct set of metabolites in the gut compared to those without eczema.

Hypothesis 3b: Mice treated with an allergen (House Dust Mites) express a distinct set of metabolites in the gut compared to mice with sham treatment.

Hypothesis 3c: Mice with a human-derived gut microbiota from infants with eczema have increased airway hyper-responsiveness and express a distinct set of metabolites in the gut compared to the mice with conventional gut microbiota with observed dampened airway hyper-responsiveness.

Chapter 2 entitled “***Veillonella* and other allergy agonists in 3-month-old infant gut microbiota were associated with development of eczema in early childhood**” shows the results from Specific Aim 1 (page 23). Chapter 3 entitled “***Fecal microbiota transplants of three distinct human communities to germ-free mice exacerbated inflammation and decreased lung function in their offspring***” shows the results of Specific Aim 2 (page 72). Chapter 4 entitled “***Metabolomic profiles significantly distinguished in the gut based on expressed allergic phenotypes in eczemic infants and in mouse model of asthma***” shows the results from Specific Aim 3 (page 155). Finally, Chapter 5 discusses the overall conclusions and next steps for future studies (page 202).

REFERENCES

1. Tanno LK, Calderon MA, Goldberg BJ, Akdis CA, Papadopoulos NG, Demoly P. Categorization of allergic disorders in the new World Health Organization International Classification of Diseases. *Clin Transl Allergy*. 2014;4:42.
2. CDC NCfHS. More Than a Quarter of U.S. Adults and Children Have at Least One Allergy. 2023.
3. Bieber T. Atopic dermatitis. *N Engl J Med*. 2008;358(14):1483-94.
4. Chan Ho Na JC, Eric L. Simpson. Quality of Life and Disease Impact of Atopic Dermatitis and Psoriasis on Children and Their Families. *Children*. 2019;6(12)(133).
5. Camfferman D, Kennedy JD, Gold M, Martin AJ, Lushington K. Eczema and sleep and its relationship to daytime functioning in children. *Sleep Med Rev*. 2010;14(6):359-69.
6. Chamlin SL, Mattson CL, Frieden IJ, Williams ML, Mancini AJ, Cella D, et al. The price of pruritus: sleep disturbance and cosleeping in atopic dermatitis. *Arch Pediatr Adolesc Med*. 2005;159(8):745-50.
7. Stores G, Burrows A, Crawford C. Physiological sleep disturbance in children with atopic dermatitis: a case control study. *Pediatr Dermatol*. 1998;15(4):264-8.
8. Holm EA, Wulf HC, Stegmann H, Jemec GB. Life quality assessment among patients with atopic eczema. *Br J Dermatol*. 2006;154(4):719-25.
9. Absolon CM, Cottrell D, Eldridge SM, Glover MT. Psychological disturbance in atopic eczema: the extent of the problem in school-aged children. *Br J Dermatol*. 1997;137(2):241-5.
10. Mitchell AE, Fraser JA, Morawska A, Ramsbotham J, Yates P. Parenting and childhood atopic dermatitis: A cross-sectional study of relationships between parenting behaviour, skin care management, and disease severity in young children. *Int J Nurs Stud*. 2016;64:72-85.
11. Daud LR, Garralda ME, David TJ. Psychosocial adjustment in preschool children with atopic eczema. *Arch Dis Child*. 1993;69(6):670-6.
12. Patel KR, Immaneni S, Singam V, Rastogi S, Silverberg JI. Association between atopic dermatitis, depression, and suicidal ideation: A systematic review and meta-analysis. *J Am Acad Dermatol*. 2019;80(2):402-10.
13. Wadonda-Kabondo N, Sterne JA, Golding J, Kennedy CT, Archer CB, Dunnill MG, et al. Association of parental eczema, hayfever, and asthma with atopic dermatitis in infancy: birth cohort study. *Arch Dis Child*. 2004;89(10):917-21.
14. Matsuoka S, Nakagawa R, Nakayama H, Yamashita K, Kuroda Y. Prevalence of specific allergic diseases in school children as related to parental atopy. *Pediatr Int*. 1999;41(1):46-51.
15. Schultz Larsen F. Atopic dermatitis: a genetic-epidemiologic study in a population-based twin sample. *J Am Acad Dermatol*. 1993;28(5 Pt 1):719-23.
16. Larsen FS, Holm NV, Henningsen K. Atopic dermatitis. A genetic-epidemiologic study in a population-based twin sample. *J Am Acad Dermatol*. 1986;15(3):487-94.
17. Biagini Myers JM, Khurana Hershey GK. Eczema in early life: genetics, the skin barrier, and lessons learned from birth cohort studies. *J Pediatr*. 2010;157(5):704-14.

18. Williams H, Flohr C. How epidemiology has challenged 3 prevailing concepts about atopic dermatitis. *J Allergy Clin Immunol.* 2006;118(1):209-13.
19. Wahn U. Wahn, U. "The immunology of fetuses and infants: What drives the allergic march. *Allergy.* 2000;55(7):591-9.
20. Wang IJ, Hsieh WS, Wu KY, Guo YL, Hwang YH, Jee SH, et al. Effect of gestational smoke exposure on atopic dermatitis in the offspring. *Pediatr Allergy Immunol.* 2008;19(7):580-6.
21. Schafer T, Dirschedl P, Kunz B, Ring J, Uberla K. Maternal smoking during pregnancy and lactation increases the risk for atopic eczema in the offspring. *J Am Acad Dermatol.* 1997;36(4):550-6.
22. Kramer U, Lemmen CH, Behrendt H, Link E, Schafer T, Gostomzyk J, et al. The effect of environmental tobacco smoke on eczema and allergic sensitization in children. *Br J Dermatol.* 2004;150(1):111-8.
23. LL. Muizzuddin N MK, Vallon P, Maes D. . Effect of cigarette smoke on skin. *J Soc Cosmet Chem.* 1997;48(5):235-42.
24. Flohr C, Pascoe D, Williams HC. Atopic dermatitis and the 'hygiene hypothesis': too clean to be true? *Br J Dermatol.* 2005;152(2):202-16.
25. McNally NJ, Williams HC, Phillips DR, Strachan DP. Is there a geographical variation in eczema prevalence in the UK? Evidence from the 1958 British Birth Cohort Study. *Br J Dermatol.* 2000;142(4):712-20.
26. McKeever TM, Lewis SA, Smith C, Collins J, Heatlie H, Frischer M, et al. Siblings, multiple births, and the incidence of allergic disease: a birth cohort study using the West Midlands general practice research database. *Thorax.* 2001;56(10):758-62.
27. Karmaus W, Botezan C. Does a higher number of siblings protect against the development of allergy and asthma? A review. *J Epidemiol Community Health.* 2002;56(3):209-17.
28. Williams HC, Strachan DP, Hay RJ. Childhood eczema: disease of the advantaged? *BMJ.* 1994;308(6937):1132-5.
29. Pickett KE, Wilkinson RG. Income inequality and health: a causal review. *Soc Sci Med.* 2015;128:316-26.
30. McKenzie C, Tan J, Macia L, Mackay CR. The nutrition-gut microbiome-physiology axis and allergic diseases. *Immunol Rev.* 2017;278(1):277-95.
31. Zimmermann P, Messina N, Mohn WW, Finlay BB, Curtis N. Association between the intestinal microbiota and allergic sensitization, eczema, and asthma: A systematic review. *J Allergy Clin Immunol.* 2019;143(2):467-85.
32. Irvine AD, Mina-Osorio P. Disease trajectories in childhood atopic dermatitis: an update and practitioner's guide. *Br J Dermatol.* 2019;181(5):895-906.
33. Prevention CfDca. Asthma, Most Recent National Asthma Data 2021. 2023.
34. Yang CL, Gaffin JM, Radhakrishnan D. Question 3: Can we diagnose asthma in children under the age of 5 years? *Paediatr Respir Rev.* 2019;29:25-30.

35. Cave AJ, Atkinson LL. Asthma in preschool children: a review of the diagnostic challenges. *J Am Board Fam Med.* 2014;27(4):538-48.
36. Silverberg JI, Hanifin JM. Adult eczema prevalence and associations with asthma and other health and demographic factors: a US population-based study. *J Allergy Clin Immunol.* 2013;132(5):1132-8.
37. Pate CA ZH, Qin X, Johnson C, Hummelman E, Malilay J. Asthma Surveillance — United States, 2006–2018. 2021.
38. Brannan JD, Loughheed MD. Airway hyperresponsiveness in asthma: mechanisms, clinical significance, and treatment. *Front Physiol.* 2012;3:460.
39. Postma DS, Kerstjens HA. Characteristics of airway hyperresponsiveness in asthma and chronic obstructive pulmonary disease. *Am J Respir Crit Care Med.* 1998;158(5 Pt 3):S187-92.
40. Ruan Z, Shi Z, Zhang G, Kou J, Ding H. Asthma susceptible genes in children: A meta-analysis. *Medicine (Baltimore).* 2020;99(45):e23051.
41. Schaubberger EM, Ewart SL, Arshad SH, Huebner M, Karmaus W, Holloway JW, et al. Identification of ATPAF1 as a novel candidate gene for asthma in children. *J Allergy Clin Immunol.* 2011;128(4):753-60 e11.
42. Ziyab AH, Karmaus W, Zhang H, Holloway JW, Steck SE, Ewart S, et al. Allergic sensitization and filaggrin variants predispose to the comorbidity of eczema, asthma, and rhinitis: results from the Isle of Wight birth cohort. *Clin Exp Allergy.* 2014;44(9):1170-8.
43. Chen S, Mukherjee N, Janjanam VD, Arshad SH, Kurukulaaratchy RJ, Holloway JW, et al. Consistency and Variability of DNA Methylation in Women During Puberty, Young Adulthood, and Pregnancy. *Genet Epigenet.* 2017;9:1179237X17721540.
44. Zhang H, Tong X, Holloway JW, Rezwan FI, Lockett GA, Patil V, et al. The interplay of DNA methylation over time with Th2 pathway genetic variants on asthma risk and temporal asthma transition. *Clin Epigenetics.* 2014;6(1):8.
45. Soto-Ramirez N, Arshad SH, Holloway JW, Zhang H, Schaubberger E, Ewart S, et al. The interaction of genetic variants and DNA methylation of the interleukin-4 receptor gene increase the risk of asthma at age 18 years. *Clin Epigenetics.* 2013;5(1):1.
46. Yousefi M, Karmaus W, Zhang H, Ewart S, Arshad H, Holloway JW. The methylation of the LEPR/LEPROT genotype at the promoter and body regions influence concentrations of leptin in girls and BMI at age 18 years if their mother smoked during pregnancy. *Int J Mol Epidemiol Genet.* 2013;4(2):86-100.
47. Mukherjee AB, Zhang Z. Allergic asthma: influence of genetic and environmental factors. *J Biol Chem.* 2011;286(38):32883-9.
48. von Mutius E. Environmental factors influencing the development and progression of pediatric asthma. *J Allergy Clin Immunol.* 2002;109(6 Suppl):S525-32.
49. O'Dwyer DN, Dickson RP, Moore BB. The Lung Microbiome, Immunity, and the Pathogenesis of Chronic Lung Disease. *J Immunol.* 2016;196(12):4839-47.
50. Kozik AJ, Huang YJ. The microbiome in asthma: Role in pathogenesis, phenotype, and response to treatment. *Ann Allergy Asthma Immunol.* 2019;122(3):270-5.

51. Martinez FD, Guerra S. Early Origins of Asthma. Role of Microbial Dysbiosis and Metabolic Dysfunction. *Am J Respir Crit Care Med.* 2018;197(5):573-9.
52. Stokholm J, Blaser MJ, Thorsen J, Rasmussen MA, Waage J, Vinding RK, et al. Maturation of the gut microbiome and risk of asthma in childhood. *Nat Commun.* 2018;9(1):141.
53. Simon AK, Hollander GA, McMichael A. Evolution of the immune system in humans from infancy to old age. *Proc Biol Sci.* 2015;282(1821):20143085.
54. Halkias J, Rackaityte E, Hillman SL, Aran D, Mendoza VF, Marshall LR, et al. CD161 contributes to prenatal immune suppression of IFN γ -producing PLZF $^{+}$ T cells. *J Clin Invest.* 2019;129(9):3562-77.
55. Mishra A, Lai GC, Yao LJ, Aung TT, Shental N, Rotter-Maskowitz A, et al. Microbial exposure during early human development primes fetal immune cells. *Cell.* 2021;184(13):3394-409 e20.
56. Rackaityte E, Halkias J, Fukui EM, Mendoza VF, Hayzelden C, Crawford ED, et al. Viable bacterial colonization is highly limited in the human intestine in utero. *Nat Med.* 2020;26(4):599-607.
57. Mold JE, Venkatasubrahmanyam S, Burt TD, Michaelsson J, Rivera JM, Galkina SA, et al. Fetal and adult hematopoietic stem cells give rise to distinct T cell lineages in humans. *Science.* 2010;330(6011):1695-9.
58. Romagnani S. Immunologic influences on allergy and the TH1/TH2 balance. *J Allergy Clin Immunol.* 2004;113(3):395-400.
59. Sender R, Fuchs S, Milo R. Revised Estimates for the Number of Human and Bacteria Cells in the Body. *PLoS Biol.* 2016;14(8):e1002533.
60. Clemente JC, Ursell LK, Parfrey LW, Knight R. The impact of the gut microbiota on human health: an integrative view. *Cell.* 2012;148(6):1258-70.
61. Statistics NCfH. Allergies and Hay Fever, United States, 2023. Hyattsville, Maryland; 2023.
62. Jones SM, Kim EH, Nadeau KC, Nowak-Wegrzyn A, Wood RA, Sampson HA, et al. Efficacy and safety of oral immunotherapy in children aged 1-3 years with peanut allergy (the Immune Tolerance Network IMPACT trial): a randomised placebo-controlled study. *Lancet.* 2022;399(10322):359-71.
63. Feehley T, Plunkett CH, Bao R, Choi Hong SM, Cullen E, Belda-Ferre P, et al. Healthy infants harbor intestinal bacteria that protect against food allergy. *Nat Med.* 2019;25(3):448-53.
64. Jota Baptista CV, Faustino-Rocha AI, Oliveira PA. Animal Models in Pharmacology: A Brief History Awarding the Nobel Prizes for Physiology or Medicine. *Pharmacology.* 2021;106(7-8):356-68.
65. Ericsson AC, Crim MJ, Franklin CL. A brief history of animal modeling. *Mo Med.* 2013;110(3):201-5.
66. Makowska IJ, Weary DM. A Good Life for Laboratory Rodents? *ILAR J.* 2021;60(3):373-88.

67. Robinson NB, Krieger K, Khan FM, Huffman W, Chang M, Naik A, et al. The current state of animal models in research: A review. *Int J Surg*. 2019;72:9-13.
68. Dominguez-Oliva A, Hernandez-Avalos I, Martinez-Burnes J, Olmos-Hernandez A, Verduzco-Mendoza A, Mota-Rojas D. The Importance of Animal Models in Biomedical Research: Current Insights and Applications. *Animals (Basel)*. 2023;13(7).
69. Swearingen JR. Choosing the right animal model for infectious disease research. *Animal Model Exp Med*. 2018;1(2):100-8.
70. Nials AT, Uddin S. Mouse models of allergic asthma: acute and chronic allergen challenge. *Dis Model Mech*. 2008;1(4-5):213-20.
71. Taube C, Dakhama A, Gelfand EW. Insights into the pathogenesis of asthma utilizing murine models. *Int Arch Allergy Immunol*. 2004;135(2):173-86.
72. Seyyede Masoume Athari EMN, Seyyed Shamsadin Athari. Animal model of allergy and asthma; protocol for researches. *Protocol Exchange*. 2019.
73. Wenzel S, Holgate ST. The mouse trap: It still yields few answers in asthma. *Am J Respir Crit Care Med*. 2006;174(11):1173-6; discussion 6-8.
74. Kumar RK, Herbert C, Foster PS. The "classical" ovalbumin challenge model of asthma in mice. *Curr Drug Targets*. 2008;9(6):485-94.
75. Huss K, Adkinson NF, Jr., Eggleston PA, Dawson C, Van Natta ML, Hamilton RG. House dust mite and cockroach exposure are strong risk factors for positive allergy skin test responses in the Childhood Asthma Management Program. *J Allergy Clin Immunol*. 2001;107(1):48-54.
76. Panzner P, Vachova M, Vlas T, Vitovcova P, Brodska P, Maly M. Cross-sectional study on sensitization to mite and cockroach allergen components in allergy patients in the Central European region. *Clin Transl Allergy*. 2018;8:19.
77. Stefka AT, Feehley T, Tripathi P, Qiu J, McCoy K, Mazmanian SK, et al. Commensal bacteria protect against food allergen sensitization. *Proc Natl Acad Sci U S A*. 2014;111(36):13145-50.
78. Cahenzli J, Koller Y, Wyss M, Geuking MB, McCoy KD. Intestinal microbial diversity during early-life colonization shapes long-term IgE levels. *Cell Host Microbe*. 2013;14(5):559-70.
79. Herbst T, Sichelstiel A, Schar C, Yadava K, Burki K, Cahenzli J, et al. Dysregulation of allergic airway inflammation in the absence of microbial colonization. *Am J Respir Crit Care Med*. 2011;184(2):198-205.
80. Wang Y, Zhang Z, Liu B, Zhang C, Zhao J, Li X, et al. A study on the method and effect of the construction of a humanized mouse model of fecal microbiota transplantation. *Front Microbiol*. 2022;13:1031758.
81. Shimbori C, De Palma G, Baerg L, Lu J, Verdu EF, Reed DE, et al. Gut bacteria interact directly with colonic mast cells in a humanized mouse model of IBS. *Gut Microbes*. 2022;14(1):2105095.

82. Park JC, Im SH. Of men in mice: the development and application of a humanized gnotobiotic mouse model for microbiome therapeutics. *Exp Mol Med*. 2020;52(9):1383-96.
83. Wrzosek L, Ciocan D, Borentain P, Spatz M, Puchois V, Hugot C, et al. Transplantation of human microbiota into conventional mice durably reshapes the gut microbiota. *Sci Rep*. 2018;8(1):6854.
84. Eiseman B, Silen W, Bascom GS, Kauvar AJ. Fecal enema as an adjunct in the treatment of pseudomembranous enterocolitis. *Surgery*. 1958;44(5):854-9.
85. Kumar V, Fischer M. Expert opinion on fecal microbiota transplantation for the treatment of *Clostridioides difficile* infection and beyond. *Expert Opin Biol Ther*. 2020;20(1):73-81.
86. Aroniadis OC, Brandt LJ. Fecal microbiota transplantation: past, present and future. *Curr Opin Gastroenterol*. 2013;29(1):79-84.
87. Weingarden AR, Vaughn BP. Intestinal microbiota, fecal microbiota transplantation, and inflammatory bowel disease. *Gut Microbes*. 2017;8(3):238-52.
88. Leonardi I, Paramsothy S, Doron I, Semon A, Kaakoush NO, Clemente JC, et al. Fungal Trans-kingdom Dynamics Linked to Responsiveness to Fecal Microbiota Transplantation (FMT) Therapy in Ulcerative Colitis. *Cell Host Microbe*. 2020;27(5):823-9 e3.
89. Dhamoon JJPAS. *Physiology, Digestion*. Treasure Island, FL: StatPearls Publishing; 2023.
90. Oliphant K, Allen-Vercoe E. Macronutrient metabolism by the human gut microbiome: major fermentation by-products and their impact on host health. *Microbiome*. 2019;7(1):91.
91. Culp EJ, Goodman AL. Cross-feeding in the gut microbiome: Ecology and mechanisms. *Cell Host Microbe*. 2023;31(4):485-99.
92. Germerodt S, Bohl K, Luck A, Pande S, Schroter A, Kaleta C, et al. Pervasive Selection for Cooperative Cross-Feeding in Bacterial Communities. *PLoS Comput Biol*. 2016;12(6):e1004986.
93. Hill MJ. Intestinal flora and endogenous vitamin synthesis. *Eur J Cancer Prev*. 1997;6 Suppl 1:S43-5.
94. Rowland I, Gibson G, Heinken A, Scott K, Swann J, Thiele I, et al. Gut microbiota functions: metabolism of nutrients and other food components. *Eur J Nutr*. 2018;57(1):1-24.
95. Kim CH. Immune regulation by microbiome metabolites. *Immunology*. 2018;154(2):220-9.
96. Macfarlane S, Macfarlane GT. Regulation of short-chain fatty acid production. *Proc Nutr Soc*. 2003;62(1):67-72.
97. Tan J, McKenzie C, Vuillermin PJ, Goverse G, Vinuesa CG, Mebius RE, et al. Dietary Fiber and Bacterial SCFA Enhance Oral Tolerance and Protect against Food Allergy through Diverse Cellular Pathways. *Cell Rep*. 2016;15(12):2809-24.
98. Depner M, Taft DH, Kirjavainen PV, Kalanetra KM, Karvonen AM, Peschel S, et al. Maturation of the gut microbiome during the first year of life contributes to the protective farm effect on childhood asthma. *Nat Med*. 2020;26(11):1766-75.

99. Arrieta MC, Stiemsma LT, Dimitriu PA, Thorson L, Russell S, Yurist-Doutsch S, et al. Early infancy microbial and metabolic alterations affect risk of childhood asthma. *Sci Transl Med*. 2015;7(307):307ra152.
100. Thorburn AN, McKenzie CI, Shen S, Stanley D, Macia L, Mason LJ, et al. Evidence that asthma is a developmental origin disease influenced by maternal diet and bacterial metabolites. *Nat Commun*. 2015;6:7320.
101. Roduit C, Frei R, Ferstl R, Loeliger S, Westermann P, Rhyner C, et al. High levels of butyrate and propionate in early life are associated with protection against atopy. *Allergy*. 2019;74(4):799-809.
102. Crestani E, Harb H, Charbonnier LM, Leirer J, Motsinger-Reif A, Rachid R, et al. Untargeted metabolomic profiling identifies disease-specific signatures in food allergy and asthma. *J Allergy Clin Immunol*. 2020;145(3):897-906.
103. Nakada EM, Bhakta NR, Korwin-Mihavics BR, Kumar A, Chamberlain N, Bruno SR, et al. Conjugated bile acids attenuate allergen-induced airway inflammation and hyperresponsiveness by inhibiting UPR transducers. *JCI Insight*. 2019;4(9).
104. Willart MA, van Nimwegen M, Grefhorst A, Hammad H, Moons L, Hoogsteden HC, et al. Ursodeoxycholic acid suppresses eosinophilic airway inflammation by inhibiting the function of dendritic cells through the nuclear farnesoid X receptor. *Allergy*. 2012;67(12):1501-10.
105. Yamazaki K, Suzuki K, Nakamura A, Sato S, Lindor KD, Batts KP, et al. Ursodeoxycholic acid inhibits eosinophil degranulation in patients with primary biliary cirrhosis. *Hepatology*. 1999;30(1):71-8.
106. Turi KN, McKennan C, Gebretsadik T, Snyder B, Seroogy CM, Lemanske RF, Jr., et al. Unconjugated bilirubin is associated with protection from early-life wheeze and childhood asthma. *J Allergy Clin Immunol*. 2021;148(1):128-38.
107. van der Sluijs KF, van de Pol MA, Kulik W, Dijkhuis A, Smids BS, van Eijk HW, et al. Systemic tryptophan and kynurenine catabolite levels relate to severity of rhinovirus-induced asthma exacerbation: a prospective study with a parallel-group design. *Thorax*. 2013;68(12):1122-30.
108. Hu Y, Chen Z, Jin L, Wang M, Liao W. Decreased expression of indolamine 2,3-dioxygenase in childhood allergic asthma and its inverse correlation with fractional concentration of exhaled nitric oxide. *Ann Allergy Asthma Immunol*. 2017;119(5):429-34.
109. Unuvar S, Erge D, Kilicarslan B, Gozukara Bag HG, Catal F, Girgin G, et al. Neopterin Levels and Indoleamine 2,3-Dioxygenase Activity as Biomarkers of Immune System Activation and Childhood Allergic Diseases. *Ann Lab Med*. 2019;39(3):284-90.
110. Finkelstein RA, Norris HT, Dutta NK. Pathogenesis Experimental Cholera in Infant Rabbits. I. Observations on the Intraintestinal Infection and Experimental Cholera Produced with Cell-Free Products. *J Infect Dis*. 1964;114:203-16.
111. Scheutz F, Teel LD, Beutin L, Pierard D, Buvens G, Karch H, et al. Multicenter evaluation of a sequence-based protocol for subtyping Shiga toxins and standardizing Stx nomenclature. *J Clin Microbiol*. 2012;50(9):2951-63.

112. Schiavo G, Rossetto O, Santucci A, DasGupta BR, Montecucco C. Botulinum neurotoxins are zinc proteins. *J Biol Chem.* 1992;267(33):23479-83.
113. Fujimura KE, Sitarik AR, Havstad S, Lin DL, Levan S, Fadrosch D, et al. Neonatal gut microbiota associates with childhood multisensitized atopy and T cell differentiation. *Nat Med.* 2016;22(10):1187-91.
114. Levan SR, Stamnes KA, Lin DL, Panzer AR, Fukui E, McCauley K, et al. Elevated faecal 12,13-diHOME concentration in neonates at high risk for asthma is produced by gut bacteria and impedes immune tolerance. *Nat Microbiol.* 2019;4(11):1851-61.
115. Gould HJ, Wu YB. IgE repertoire and immunological memory: compartmental regulation and antibody function. *Int Immunol.* 2018;30(9):403-12.
116. Sanchez-Jimenez F, Ruiz-Perez MV, Urdiales JL, Medina MA. Pharmacological potential of biogenic amine-polyamine interactions beyond neurotransmission. *Br J Pharmacol.* 2013;170(1):4-16.

CHAPTER 2: Predominance of *Veillonella* and other allergy agonists in 3-month-old infant gut microbiota was associated with development of eczema in early childhood in the Isle of Wight Birth Cohort

This chapter is from a manuscript submitted for publication:

Hinako Terauchi, Julia A. Bell, Yu Jiang, Hongmei Zhang, Phillip T. Brooks, Samantha T. Waite, John W. Holloway, Wilfried Karmaus, Susan L. Ewart, Syed Hasan Arshad, Linda S. Mansfield. Predominance of *Veillonella* and other allergy agonists in 3-month-old infant gut microbiota was associated with development of eczema in early childhood in the Isle of Wight Birth Cohort, In Review for PLOS ONE

Abstract

Mounting evidence suggests that exposure to microbially-rich environments in infancy reduces risk for allergy and asthma and that gut microbiota influence maturation of immune function in early life. We hypothesized that particular compositions of the early gut microbiota are associated with development of eczema and/or atopy in infants. Fecal samples from 3-month-old infants were analyzed using 16S V4 rRNA gene Illumina Amplicon sequencing to characterize gut microbiome in an ongoing multigenerational prospective longitudinal study of newborns (Isle of Wight 3rd generation birth cohort). Children were assessed for eczema, wheeze, and atopy up to age 3 years. Eczema was classified as “None” for no eczema ever, “Intermediate” for 1-3 positive diagnoses, and “Persistent” for >4 positive diagnoses. We tested for associations of bacterial taxa profiles with risk of eczema and how this was modified by the age of the child. We also tested for associations of particular bacterial taxa and predicted metabolites with eczema outcomes. A bacterial taxon of the genus *Veillonella* was associated with a diagnosis of eczema in infants at 3 months of age (Random Forest analysis followed by logistic regression $P=0.036$). Principal components analysis (PCA) showed that allergy-associated taxa, *Bifidobacterium*, *Escherichia-Shigella*, *Lachnospiraceae*, *Veillonella* and *Bacteroides* contributed most to the separation between infants with and without eczema in the ordination. Neighbor joining data showed *Escherichia-Shigella*, *Bacteroides_b* and *Veillonella* taxa were in highest relative abundance in decreasing order among the allergy-agonists. Canonical Correspondence Analysis (CCA) showed that eczema and atopy were correlated and associated with allergy agonists *Lachnospira*, *Haemophilus*, *Veillonella*, and *Escherichia-Shigella*. Allergy antagonists *Lactobacillus* (two OTUs), *Ruminococcus* (two OTUs), and *Bifidobacterium_ambiguous_taxon* were associated with absence of eczema and atopy. Children with “Intermediate” eczema with 1-3 positive diagnoses had fecal microbiota more similar to those who never developed eczema during the study period than to those who had a consistent positive diagnosis of eczema persisting for the majority of the study period. Eczema was also associated with atopy ($p=0.031$, Fischer’s exact test), but no other clinical factor examined had a significant association with development of eczema. We identified a candidate bacterial genus, *Veillonella*, along with previously allergy-associated bacterial taxa with a significant risk of eczema in the first 3 years of age in this birth cohort and showed there are differences in the fecal microbiome associated with the severity and persistence of eczema symptoms over the first 3 years of life.

Introduction

Significant increase in incidence of atopic and autoimmune disorders have been documented recently in industrialized nations [120]. Mounting evidence suggests that exposure to microbially-rich environments in infancy reduces risk for allergy and asthma [121, 122] and that gut microbiota influences maturation of immune function in early life [123]. Yet, a recent meta-analysis of probiotic supplementation of infants demonstrated small effects on eczema and none on airway allergies [124]. Thus, knowledge gaps limit usefulness of currently known probiotics to prevent allergy.

The most pressing knowledge gap concerns the influence of gut microbiota in the critical window of immune development during the neonatal period. Despite strong evidence for a common mucosal immune system where pathogen stimulations of gut associated lymphoid tissues affect adaptive immune responses in lungs [125], studies revealing gut microbiota-immune system interactions in allergy are limited. Effects of gut-lung or gut-skin microbiome interactions are even less studied. Eczema, a skin condition of itchy rashes, often appears in early childhood preceding other atopic/allergic disease development such as asthma, a sequence described as the atopic march [126, 127]. Decreases in gut microbiota diversity in early life have been linked to development of asthma [128, 129] and atopic dermatitis [81], but specific causative bacteria taxa remain unknown.

Education of the innate and adaptive immune systems begins at birth with exposure to environmental antigens, many of which are intestinal commensal bacteria [56]. Neonatal infants have impaired innate immunity and weak Type 1 T cell and antibody responses. In this early period, infants have T cell responses directed against the mother's alloantigens that skew their early responses toward Foxp3⁺ CD25⁺ regulatory T cells [60]. Foreign antigen activation of these neonatal T cells can result in Type 2 immunity, which exacerbates allergy [56]. Risks imposed by an immature immune system and pathogen exposures wane as innate and adaptive responses mature, facilitated by diverse balanced bacterial populations. We expect this neonatal period is a window when infants may be predisposed toward allergy when microbial exposures fail to establish a stable commensal community accompanied by appropriate immune system maturation.

Our overarching hypotheses are that gut microbiota impacts risk of childhood allergic disease due to (1) early exposures to pathogens or pathogenic microbiomes, (2) shifts in microbiome

composition with lack of or removal of probiotic members, or (3) presence of specific metabolic products. We addressed our hypotheses using the Isle of Wight (IOW) multi-generation birth cohort to evaluate effects of gut microbiome on allergic outcomes. This is a unique population-based study integrating two consecutive extensively-characterized birth-cohorts: parents born in 1989-1990 (IOW F1) and their children born since 2010 (3rd generation IOW F2). Benefits of this cohort include longitudinal assessments and detailed clinical outcomes related to allergy, which exists at proportions between 30-40% in this study population [130-132]. The approach was to conduct 16S rRNA gene sequencing of fecal microbiota in children born to cohort participants to determine if associations exist between early gut microbiota and development of several allergic manifestations with a main focus on eczema.

Methods

Study cohort and experimental

Influence of gut microbiome composition on allergic outcomes of eczema, recurrent wheeze, and atopy was examined in the IOW F2 birth cohort. Fecal samples were collected from 60 children at 3 months of age by either their parents or the local nurse. Children were assessed for eczema, wheeze, and atopy at 3, 6, 12, and 36 months of age[132] from Jul, 2010 until Oct, 2017. To define microbial patterns associated with triggering or protection from allergies, fecal samples were analyzed using 16S rRNA gene sequencing. Children were recruited into the “Third Generation Study” under ethics approval numbers 09/H0504/129 (22 December 2019), 14/SC/0133 (22 December 2019), and 14/SC/1191 (15 November 2016) from the University of Southampton. The data analysis was carried out without the knowledge of the identity of the infants.

Sample collection

Fecal samples were collected from 60 children at 3 months of age from their diapers either at the time of their visit to the clinic, or at a later date at their home by a visiting nurse.

Samples were each placed into a sterile container, stored on ice during transport, then stored at -80°C for prolonged storage. Each sample was coded to protect the patient identity and their clinical status, then shipped on dry ice to Michigan State University where it was stored at -80°C until processed for DNA isolation, and only opened in an anaerobic hood to preserve strict anaerobes.

Clinical assessments

Children were assessed for their health and clinical status at ages 0, 3, 6, 12, 24, and 36 months at the local clinic by the clinician using International Study of Asthma and Allergy in Childhood (ISAAC) questionnaires (Table 2.1) [18-20]. At 3, 6, 12, 24, and 36 months, eczema and wheeze diagnoses were made based on the ISAAC questionnaire answers. Skin prick test (SPT) was performed at 12 and 36 months to test for atopy.

Eczema status was defined as answering: (1) YES to either (i) “ever have itchy rash coming and going for at least 6 months” (not valid at 3 or 6 months of age), (ii) “rash or eczema that has lasted at least 7 days or more,” or (iii) “ever eczema” (not valid at 3 months), and (2) YES to “the rash was itchy,” and (3) YES to “affected the folds of elbows, behind knees, in front of ankles, on cheeks or around neck, ears, or eyes.” “No eczema” was defined as “never presence of an itchy rash.”

Recurrent wheeze was documented as three or more separate episodes of wheeze in the last 12 months based on the Global Initiative for Asthma, Global Strategy for Asthma Management and Prevention [133].

Skin prick testing (SPT) to 10 common allergens (house dust mite, grass pollen, tree pollen, cat, dog, *Alternaria alternata*, cow’s milk, egg, peanut, and cod) using standardized extracts was conducted at 12 and 36 months of age [134]. A diagnosis of atopy was made when one or more SPT was positive (wheal \geq 3mm above negative control) at either timepoint.

Table 2.1 Longitudinal study design with assessments and samples collected from children of the Isle of Wight third generation birth cohort. At 3, 12, and 36 months, children were examined for severity of eczema using SCORAD[135]. Skin prick testing was performed at 12 and 36 months of age. Validated questionnaires based on the template from the International Study of Asthma and Allergy in Childhood [136] were administered at 3, 6, 12, 24, and 36 months of age (Table 2.1) [137-139].

SAMPLING AND ASSESSMENTS	BIRTH	3 MO.	6 MO.	12 MO.	24 MO.	36 MO.
ISAAC Questionnaires (family history, feeding, smoking, pets, respiratory infections, socioeconomic class, housing characteristics, farm living, exposure to pollutants) (refs 51, 52-54)	x	x	x	x	x	x

Table 2.1 (cont'd)

Pregnancy complications and birth characteristics	X					
Height, weight, BMI	X	X		X	X	X
Urine cotinine		X		X		X
Skin prick tests (atopy diagnosis)				X		X
Genetics, genome-wide DNA-methylation	X					
Microbiome from stool		X		X		X
Eczema and wheeze diagnosis based on ISAAC		X	X	X	X	X
Eczema severity using SCORAD (ref 50)		X		X		X
Medical records scrutiny (antibiotic use, other drugs, infections, physician diagnosed asthma and allergy, treatment given, chest infections)	X	X	X	X	X	X

Isolation of bacterial DNA from infant fecal samples

DNA was isolated from 500mg each of infant fecal sample using the FastDNA SPIN Kit for stool (MP Biomedicals, Solon, OH) according to the manufacturer's protocol. 60 fecal samples were frozen at -80°C prior to processing. Out of the 60, 2 samples did not contain enough fecal material to obtain adequate quality DNA and thus were excluded from further analysis from this point forward. The extracted DNA was checked for concentration and purity using the NanoDrop Spectrophotometer (ThermoFisher Scientific, Inc., Waltham, MA) immediately after isolation, then confirmed using Qubit (ThermoFisher Scientific, Inc., Waltham, MA). The extracted DNA solutions were adjusted for their concentration to be similar among the samples, then validated for presence of 16S V4 region by PCR[140]. All reagents used in the isolation process were tested in the same manner to ensure against the undesired incorporation of environmental bacteria in our microbiome samples, and sterile bacterial 16S rRNA gene DNA-free water was used as a negative control throughout.

16S rRNA gene sequencing and analysis

Isolated DNA samples were submitted to be sequenced for the V4 region of 16S rRNA gene using Illumina MiSeq at the Michigan State University, Research Technology Support Facility

Genomics Core. All microbiome analyses were processed along with the mock communities (HM-782D, BEI) used as a positive control, and the DNA-free water as a negative control for estimation of sequence error. At the time of processing initial data analysis, the data were blinded for all clinical outcomes. Once raw, demultiplexed sequence reads were returned, they were processed through the QIIME2 (version 2019.1) pipeline [141]. At this time, 2 additional samples were removed due to their very low numbers of sequence reads, resulting in total of 56 samples. Within QIIME2, Deblur [142] was used for denoising and vsearch [143] was used for operational taxonomic units (OTU) clustering. The Silva (release 128) database was used to identify taxa at 97% similarity. The processed sequence data were then exported to a local drive where remaining data processing was done in Python and statistical analysis was performed in R, which used open-source packages, vegan (version 2.5-7), factoextra (version 1.0.7), and pheatmap (version 1.0.12).

Isolation and identification of *E. coli* from eczemic infants using Matrix-assisted laser desorption/ionization-time of flight (MALDI-TOF)

Fecal materials from infants with eczema with enough remaining material were streaked on MacConkey agar using aseptic technique for isolation of aerobic bacteria, specifically to isolate for the most abundant agonist taxa readily culturable, *E. coli*. Bacterial growth from the initial fecal materials was re-streaked for isolation on MacConkey agar plates several times until pure single-colony isolates were obtained. Isolated colonies were then submitted to the Veterinary Diagnostic Laboratory at Michigan State University to be identified using MALDI-TOF[144].

PAPRICA analysis

PAPRICA (version 0.5) analysis pipeline was used to predict metabolic output and enzymatic activities based on phylogenetic placement using 16S rRNA gene sequence data [26, 27]. The output from PAPRICA analysis was further analyzed in R and Python. The package pheatmap (version 1.0.12) was used to produce the heatmap (Figures 2.5A, 2.9A) with complete Euclidean clustering and factoextra (version 1.0.7) was used to visualize the result of the principal components analysis (PCA) calculation.

Statistical Analysis

Grouping of eczema diagnosis for analyzing cumulatively and individually

The microbiome analyses were done using two different approaches to clinical categorization

and grouping. Analysis Approach 1 took the cumulative counts of positive eczema diagnosis from a total of 5 time points (3, 6, 12, 24, and 36 months). Those with 4 to 5 instances of positive eczema diagnosis were grouped as having “Persistent” eczema. Those with 1 to 3 instances of positive eczema diagnosis were grouped as “Intermediate” eczema, and those with 0 instances were grouped as “None” for never having eczema. Analysis Approach 2 focused the analysis at a finer level by taking the eczema diagnosis at each individual timepoint of 3, 6, and 12 months. For each time point, the diagnosis was categorized as either “yes” for having a positive eczema diagnosis or “no” for not having an eczema diagnosis.

Analysis of associations between eczema and other allergic conditions

Fischer’s Exact test (VassarStats; <http://vassarstats.net/>) was used to determine if significant differences occurred between observed and expected frequencies between categorical variables of eczema diagnosis (persistent: ≥ 4 diagnoses, intermediate: 1-3 diagnoses, none: 0 diagnosis) and presence or absence of each variable individually: atopy (positive SPT), wheeze, breastfeeding, and antibiotic treatment. In the extended study focused on individual time points (Table 2.2), associations of bacterial taxa with eczema diagnoses of None, intermediate with 1-3 diagnoses, and persistent with 4 or more diagnoses were explored. In all analyses, statistical significance was defined as $p \leq 0.05$. If applicable, corrections for multiple comparisons were made.

Ordination and clustering analyses of microbiotas

PAST software (V4.03) was used to analyze 16S rRNA gene sequence, eczema, and atopy data. Canonical Correspondence Analysis (CCA) was performed to analyze the microbiota data using two clinical factors: eczema, atopy and wheeze. Neighbor joining clustering was used to classify the microbiota data without the influence of the clinical outcomes. Groups identified by neighbor-joining analysis were further analyzed using similarity percentage (SIMPER), analysis of similarity (ANOSIM) and non-parametric multivariate analysis of variance (PERMANOVA). Welch’s unequal variance t-tests were performed for allergy-associated OTU’s with Holm-Sidak correction for multiple comparisons.

Random Forest Analysis

Random Forest, a decision tree-based method, was used to identify specific OTU’s with the highest potential to correctly classify childhood eczema status. The R function *randomForest* was applied to conduct the analyses [145]. An importance value for each OTU was extracted

from the analysis and the top five OTUs with the highest importance values were selected for subsequent analyses. The selected OTUs were further examined using logistic regressions on their association with eczema. The SAS 9.4 procedure PROC LOGISTIC [146] was applied for this purpose and a statistical testing with a p-value of 0.05 or smaller was deemed statistically significant.

Results

Note - For all of the microbiome results, the conversion of OTU numbers to the bacterial taxa can be found in Supplemental Table 2.1.

Overview (Allergic Outcomes and Microbiota Sequencing)

Clinical data at each assessment (3, 6, 12, 24, and 36 months of age) was available for all 56 children who provided fecal samples that were analyzed. Four DNA samples of the 60 extracted were removed for technical reasons – see below. 17 of the 56 children had no instance of positive eczema diagnosis in the first 36 months of life, while the remaining 39 had at least one instance of positive eczema diagnosis. Of these, 18 were classified as having “Persistent” eczema, defined as having 4 to 5 instances of positive eczema diagnosis out of 5 total allergy assessment visits that occurred at 3, 6, 12, 24, and 36 months of age. 21 were classified as having “Intermediate” eczema, defined as having 1 to 3 instances of positive eczema diagnosis out of 5 allergy assessment visits (Fig 2.1.A). Data on the allergic outcomes of eczema, atopy, and wheeze as well as the potentially related histories of breastfeeding and antibiotic use in these 56 infants appear in Table 2.2.

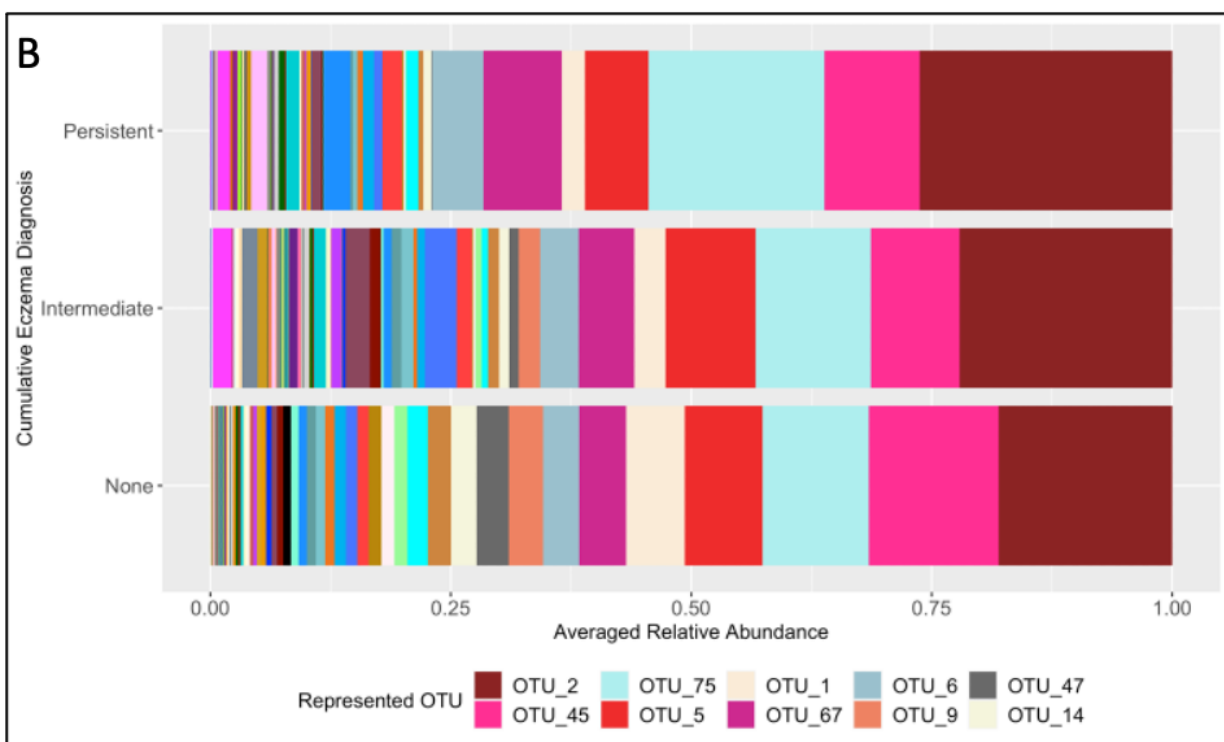
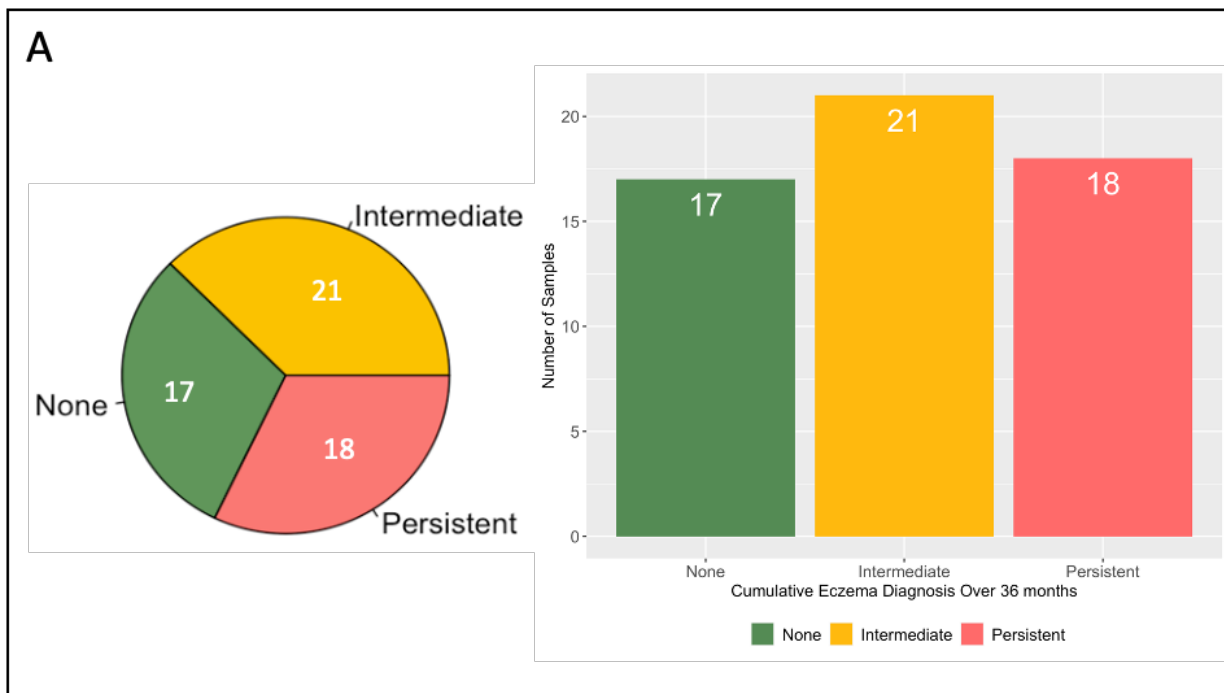


Figure 2.1 Breakdown of the sample population by eczema diagnosis. (A) Grouping based on the cumulative count of positive eczema diagnosis over five time points across the first 36 months of life. The diagnoses were made at 3, 6, 12, 24, and 36 months of age. Persistent group is defined as having 4 to 5 instances, Intermediate group is defined as having 1

Figure 2.1 (cont'd)

to 3 instances, and “None” group is defined as having 0 instances of positive eczema diagnosis over the time period. Out of the total 56 samples analyzed, 18 were categorized into Persistent group, 21 into Intermediate group, and 17 were categorized into “None” group. (B) Bacterial taxa as OTU relative abundances in the fecal samples of infants grouped by their eczema diagnosis: Persistent (4-5 diagnosis instances), Intermediate (1-3 diagnosis instances), and “None” (0 diagnosis instances). Each OTU follows the naming connotation of “OTU_#”, where # represents some numerical integer assigned to each unique OTU. All OTU’s represented as a block of unique color for all 3 eczema diagnosis groupings. The width of each block corresponds to the relative percentage of each OTU.

Wheeze was assessed for all children at ages 3, 6, 12, 24, and 36 months (Table 2.2). No association was found between wheeze and eczema using the none, intermediate, and persistent categories for eczema and “never wheeze” or “ever wheeze” categories ($P=0.1193$, Fisher’s exact test). For additional testing, ten children were classified as having “Persistent” wheeze, defined as having 4 or 5 positive diagnoses of wheeze; 33 were classified as having “Intermediate” wheeze, defined as having one to three positive diagnoses of wheeze; and 13 had no evidence of wheeze at any point. No association was found between wheeze and eczema using the none, intermediate, and persistent categories for wheeze as well as eczema ($P=0.1884$, Fisher’s exact test).

Skin prick testing (SPT) was performed at 12 and 36 months to assess for atopy. Out of 56 children, 11 tested positive at least once, and 4 were not tested. Of 18 children with “Persistent” eczema, 9 were diagnosed with atopy (Table 2.2). Fisher’s exact test for the three eczema categories and “never atopy” and “ever atopy” categories was significant ($P=0.0003$). Pairwise comparisons were made with Fisher’s exact test; the no eczema vs persistent eczema and intermediate eczema vs persistent eczema comparisons were significant after Holm-Sidak correction for multiple comparisons ($P=0.0031$ and $P=0.0212$, respectively). The “no eczema” vs “intermediate eczema” comparison was not significant ($P=0.4922$).

Breastfeeding and antibiotic use were also evaluated with Fisher’s exact test using the three eczema categories and categories “never breastfed” and “ever breastfed” (for even 1 day) and “no antibiotic treatment” and “ever antibiotic treatment” (range, 1 to 3 times), respectively. Neither result was significant ($P=0.1561$ for breastfeeding; $P=1.0$ for antibiotic treatment).

Table 2.2 Allergic characteristics of the cohort based on clinical assessments, questionnaires, and testing.

No. Infants	Eczema Diagnoses	Ever Wheeze	Skin Prick positive	Ever Breast Fed	Ever Antibiotics
17	None, No Eczema	10 (59%)	0 (0%)	12 (70%)	4 (24%)
21	Intermediate Eczema ¹	17 (81%)	2 (10%)	13 (62%)	5 (24%)
18	Persistent Eczema ²	16 (89%)	9 (50%)	16 (89%)	4 (22%)
39	Intermediate or Persistent Eczema	33 (85%)	11 (28%)	29 (74%)	9 (23%)

¹“Intermediate” eczema defined as positive diagnosis of eczema at one to three time points.

²“Persistent” eczema defined as 4 or 5 diagnoses of eczema.

Microbiota sequencing of fecal samples from 3 month old infants

Out of 60 total samples collected, 2 were removed from the study due to not meeting DNA quality standards for sequencing as a result of an insufficient amount of fecal material. DNA was successfully isolated from the remaining 58 samples. Once ensured for concentration and quality by NanoDrop, Qubit, and PCR, the DNA samples were submitted for sequencing of the 16S rRNA gene V4 hyper-variable region using Mi-Seq Illumina amplicon sequencing. An additional 2 samples were removed after sequencing for insufficient read depth, resulting in a total of 56 samples used in this study.

Analysis: Approach 1

Microbiota composition at 3 months showed major overlap when grouped by cumulative eczema status

For the first analysis, 3 groups were created based on the cumulative count of positive eczema diagnosis instances over the first 36 months. Each child received clinical assessments at ages 3, 6, 12, 24, and 36 months. Counting each occurrence of positive eczema diagnosis as “1,” each sample was categorized as having A) “Persistent” eczema, B) “Intermediate” eczema, or C) “None”, or no eczema. If an infant had a total of 4 to 5 instances of positive eczema diagnosis out of the 5 total clinical assessment time points, it was categorized as having “Persistent” eczema. If an infant had 1 to 3 instances, it was categorized as having “Intermediate” eczema. All infants having 0 instances of eczema across all 5 assessment points were categorized as “None”. Out of the 56 samples, 18 were categorized as having “Persistent” eczema, 21 as having

“Intermediate” eczema, and 17 as “None”, or no eczema (Fig 2.1A).

Taxa relative abundance showed overall similarities, with the least variability in higher abundance taxa and more variability in lower abundance taxa (Fig 2.2)

Averaged relative abundance of each OTU with its assigned bacterial taxa based on 16S rRNA gene sequence results are shown as stacked bar charts for the 3 cumulative eczema groupings (Fig 1B). Overall, all 3 groups share the same most highly abundant OTU’s, all at slight differences from one another. OTU_2 (genus *Bifidobacterium*) was in highest abundance across all 3 groups, followed by OTU_45 (family *Lachnospiraceae*, genus unknown) and OTU_75 (Genus *Escherichia-Shigella*), then OTU_5 (genus *Bacteroides*). OTU_45 was highest in “None” (no eczema) which also had the lowest abundance of OTU_75 compared to the other 2 groups, as opposed to “Persistent” eczema, which had the lowest OTU_45 relative abundance and highest OTU_75 relative abundance. A similar pattern was seen for OTU_1 and OTU_67; the “Persistent” eczema group had the highest relative abundance of OTU_67 (genus *Veillonella*) while having lowest relative abundance of OTU_1 (genus *Bifidobacterium*, *ambiguous taxa*). “None” (no eczema) had the opposite where the relative abundance of OTU_67 was the lowest and OTU_1 was highest amongst the 3 groups. When looking at the relative abundance of OTU’s subgrouped by their Family levels, regardless of their overall relative abundance, some families of bacteria had more members present while some only had one or two (Fig 2). Family *Lachnospiraceae* had the greatest number of OTU’s of 21, followed by family *Ruminococcaceae*, which had 11 OTU’s, then *Clostridiaceae*, *Enterobacteriaceae*, and *Veillonellaceae*, which all had 4 OTU’s. Other Families either had 3, 2, or 1 OTU’s. Within Families, typically there was a single OTU that had higher relative abundance than any other OTU’s of that Family, except for *Clostridiaceae*. In *Lachnospiraceae*, OTU_45 (genus unknown) overshadowed in their relative abundance compared to other OTU’s of its Family. In *Ruminococcaceae*, OTU_48 (genus *Faecalibacterium*) stood out as having the highest relative abundance, but only in the “Persistent” eczema group. In *Enterobacteriaceae*, OTU_75 (genus *Escherichia-Shigella*) was in much higher relative abundance than the other 3 OTU’s. In *Veillonellaceae*, OTU_67 (genus *Veillonella*) was in highest relative abundance, and some OTU’s were completely lacking in some of the groups while being present in another. OTU_64 (genus *Megamonas*) and OTU_65 (genus *Megasphaera uncultured*), which were at lower

relative abundance, were also only present in the “Persistent” group, and not present in both “Intermediate” and “None” eczema groups. Another OTU in *Veillonellaceae* Family, OTU_66 (genus *Megasphaera*) was present in both “Persistent” and “Intermediate” eczema, but not present in “None” (no eczema). Families *Bacteroidaceae*, *Bifidobacteriaceae*, *Prevotellaceae*, and *Streptococcaceae* all had 2 OTU’s identified that belonged to their family, with one of them being at much higher relative abundance than the other. In *Bacteroidaceae*, OTU_5 (genus *Bacteroides uncultured*) was overall higher in relative abundance across all 3 groups than OTU_6 (genus *Bacteroides*). In *Bifidobacteriaceae*, OTU_2 (genus *Bifidobacterium*) was overall higher in relative abundance than OTU_1 (genus *Bifidobacterium ambiguous taxa*). In *Prevotellaceae*, OTU_9 (genus *Prevotella.9*) was present in all 3 groups, while OTU_10 (genus *Prevotellaceae NK3b31 group*) was only present in “Intermediate” group. In *Streptococcaceae*, OTU_19 (genus *Streptococcus*) was at much higher relative abundance across all 3 groups compared to OTU_18 (genus *Lactococcus*). *Lactobacillaceae* had OTU_16 (genus *Lactobacillus uncultured*) that was in highest relative abundance across all 3 groups and all 3 OTU’s in the “None” eczema group, but it was much lower in abundance in other 2 groups. OTU_17 (genus *Lactobacillus*) instead showed its presence across all 3 groups and was only lower than another OTU within this Family in the “None” eczema group. *Clostridiaceae*, which was mentioned as being an exception, had both OTU_21 (genus *Clostridium sensu stricto 1 uncultured*) and OTU_22 (genus *Clostridium sensu stricto 1*) as the OTU’s that was consistently in higher abundance than other OTU’s across all 3 groups.

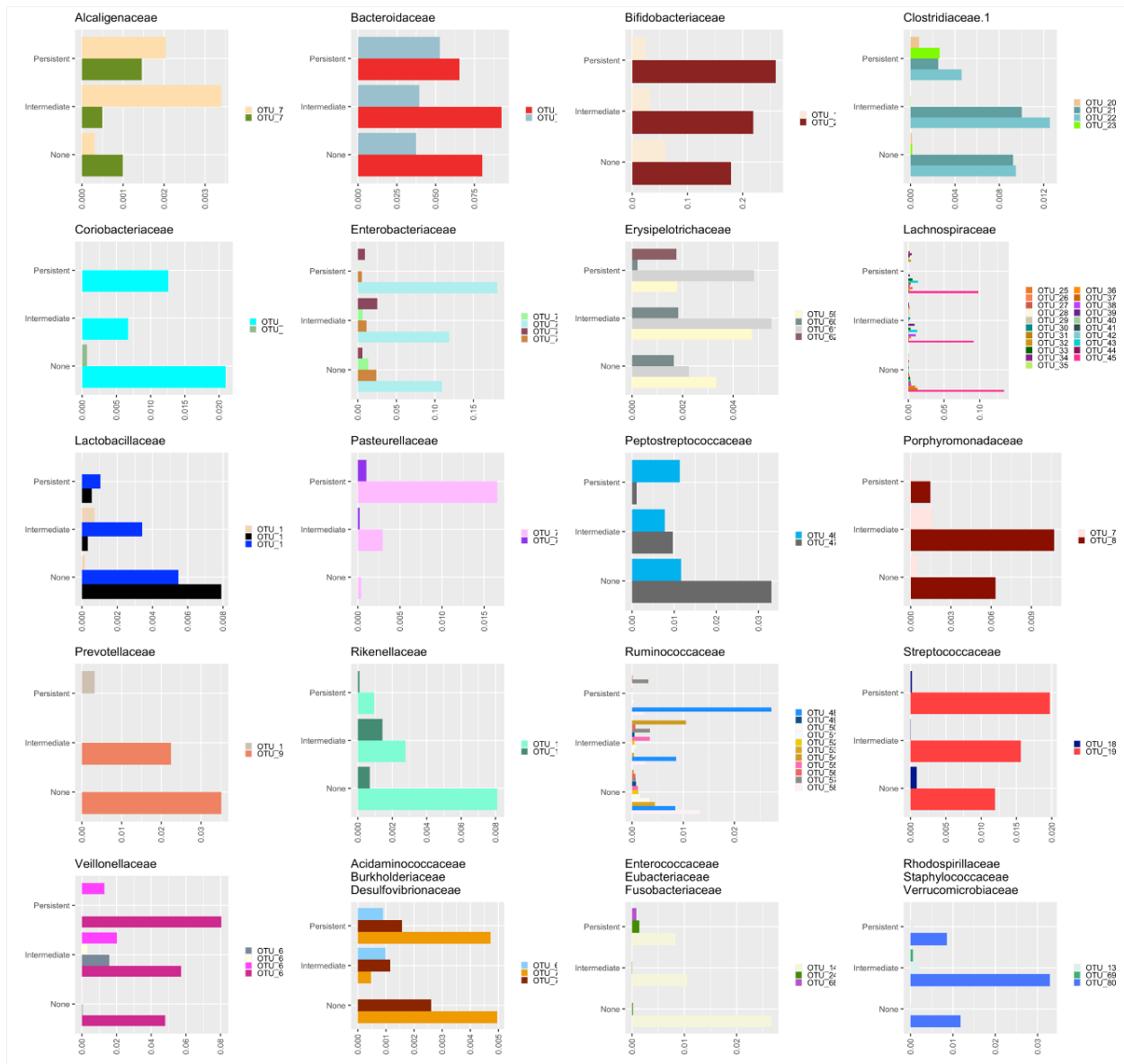


Figure 2.2 Relative abundances of OTUs separated and grouped at the Family level of each bacterial taxon. Each unique color represents a unique OTU, which are grouped by their eczema diagnosis: “Persistent” (4-5 diagnosis instances), “Intermediate” (1-3 diagnosis instances), and “None” (0 diagnosis instances).

Principal Components Analysis (PCA) overlapped “Intermediate” and “None” eczema groups almost completely, and both had slightly less overlap with the “Persistent” group. PCA was used to visualize the spread of the microbiota data based on the 3 cumulative eczema diagnosis groupings. In the PCA bi-plot with all three groups, the first dimension explained 27.7% and the second dimension explained 14.5% of the spread of the data (Fig 2.3A). The 95%

confidence ellipses were not distinct from one another, showing great overlaps amongst all three groups. Out of 3, “None” and “Intermediate” eczema showed the most overlaps, while “None” and “Persistent” eczema showed the least. The variables most responsible for the spread were OTU_2 (genus *Bifidobacterium*), OTU_75 (genus *Escherichia-Shigella*), OTU_45 (family *Lachnospiraceae*), OTU_67 (family *Veillonellaceae*), and OTU_5 (genus *Bacteroides uncultured*) in order of importance (Fig 2.3A). When visualized with just the “None” and “Persistent” eczema, the 95% confidence ellipses still showed great overlaps, however there were some distinction along the 1st dimension, represented as the x-axis (Fig 2.3B). The first dimension contributed 27.9% of the spread of the data, while the second dimension contributed 16.6%. The variables most responsible for the spread of the data were OTU_2 (genus *Bifidobacterium*), OTU_75 (genus *Escherichia-Shigella*), OTU_45 (family *Lachnospiraceae*), OTU_67 (family *Veillonellaceae*), and OTU_5 (genus *Bacteroides*) in order of importance (Fig 2.3C-D).

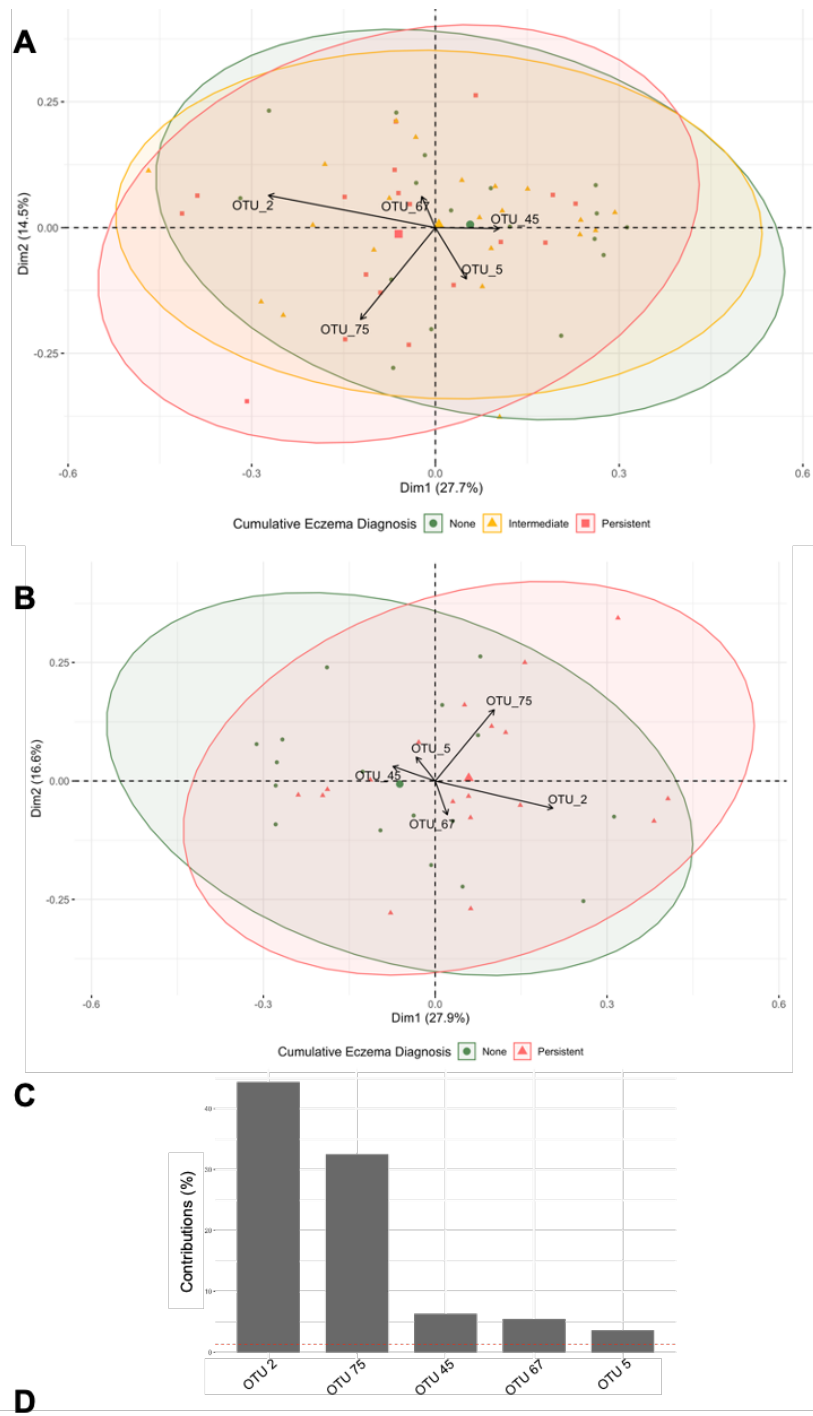


Figure 2.3 Principal Components Analysis (PCA) of bacterial taxa relative abundance

Figure 2.3 (cont'd)

data.(A) PCA grouped by all 3 eczema diagnosis groupings (“Persistent” in orange, “Intermediate” in green, “None” in blue). The top 6 most contributing OTUs (variables) are represented by black arrows. The length and direction of each arrow represents the weight and direction of its contributions. (B) PCA of the same data with only the 2 most extreme eczema diagnosis groupings (“Persistent” in orange, “None” in blue). Black arrows represent the top 5 most contributing OTUs (variables). (C) Bar plot of the percentage of contribution of each of the top 5 most contributing taxa. (D) Keys for the identities of the top 5 most contributing taxa represented in B and C. NaN stands for undefined taxa.

Similarity Percentage (SIMPER) analysis showed that the “None” (no eczema) group had more similar microbiota composition to “Intermediate” eczema than to “Persistent” eczema

SIMPER analysis showed that the OTU compositions in the “None” (no eczema diagnosis) group was most similar to that of “Intermediate” eczema (1-3 positive diagnosis) than to “Persistent” eczema (4-5 positive diagnosis) (Fig 2.4.A). There were many OTU’s that were similar in their relative abundance across the three groups, for both high (shown in red) and low (shown in dark blue) abundance levels. However, there were also a number of OTU’s that showed difference in their relative abundance across the three allergy groupings. Most notable were those in phylum *Firmicutes*. Many members of this phylum showed higher relative abundance in “Persistent” eczema compared to the “None” (no eczema) group. A few members of the *Proteobacteria* also showed the same pattern of having the highest relative abundance in the “Persistent” eczema group.

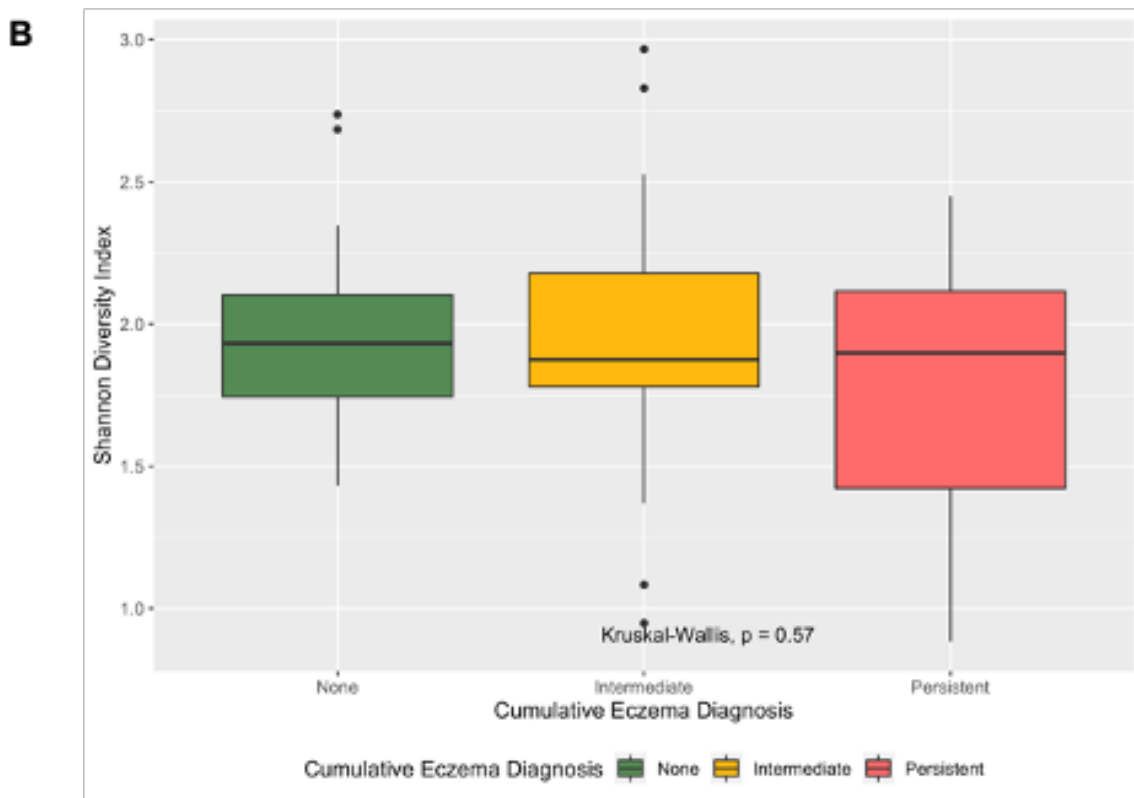
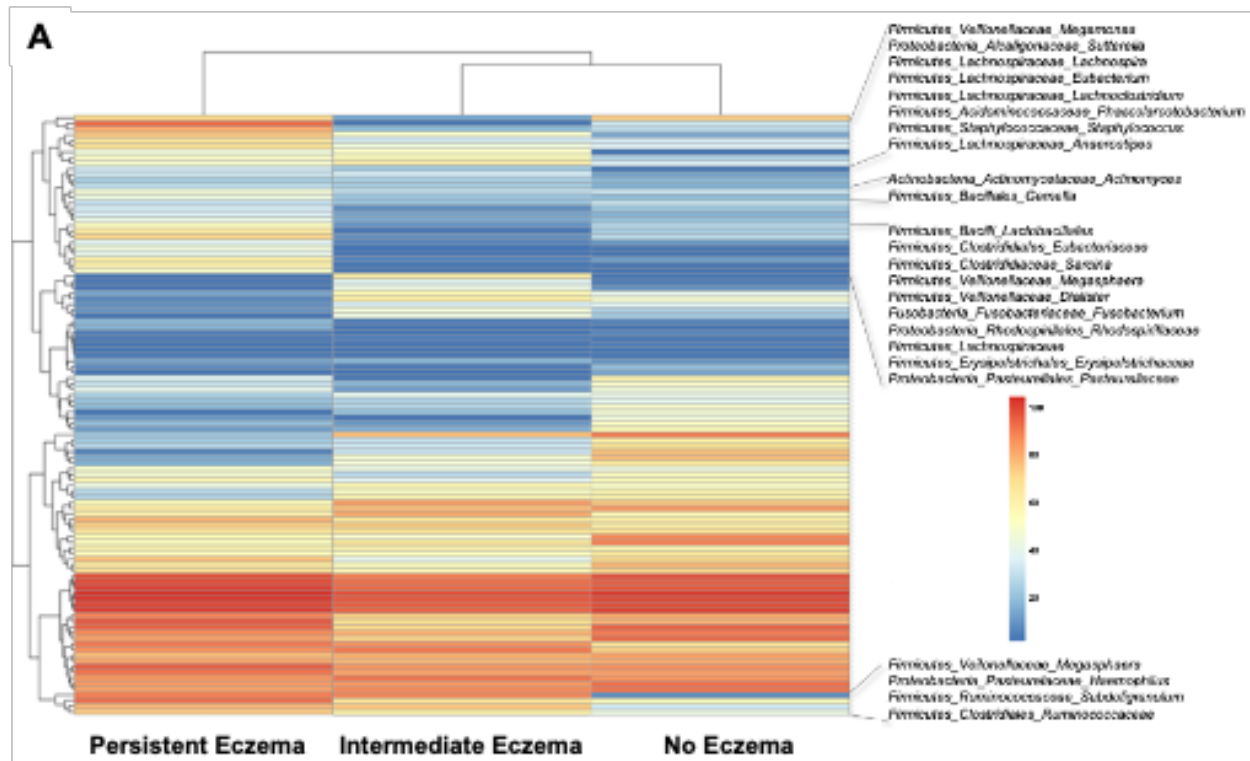


Figure 2.4 (A) Heatmap representations of SIMPER (SIMilarity PERcentage) analysis using relative abundance values of each taxa grouped by the 3 eczema diagnosis groupings.

Figure 2.4 (cont'd)

(“Persistent”: left, “Intermediate”: middle, “None” (labeled as ‘No Eczema’: right). Each cell represents the relative abundance by color, with dark blue being lowest and red color being highest. The dendrogram on the top represents the SIMPER result showing that “Intermediate” and “None” groupings were more similar to each other than to the “Persistent” group. (B) Shows the **Shannon Diversity Index using the OTU data grouped by the 3 eczema diagnoses** (“None”: left in green, “Intermediate”: middle in yellow, “Persistent”: right in red). The mean differences between the 3 groups were not statistically significant ($p=0.57$, Kruskal-Wallis).

Alpha diversity calculated using the Shannon Alpha Diversity Index showed no significant difference amongst all three groups

Shannon diversity index accounts for both richness and evenness to assign a value to explain the level of alpha diversity of a community. The mean differences between the three groups were not statistically significant ($p=0.57$, Kruskal-Wallis). The “None” group had 2 outliers while having the smallest range around its mean. “Intermediate” eczema had 4 outliers and had a slightly greater range around its mean. “Persistent” eczema had no outliers but showed the greatest range around its mean (Fig 2.4B).

Metabolic potentials were not distinguishable between the three groups as inferred using PAPERICA (Pathway Prediction by phylogenetic Placement)

The result of 16S rRNA gene sequencing were fed into PAPERICA software to obtain inferred metabolic pathway potentials of each sample. Each sample were clustered for its inferred relative abundance of metabolic pathway potentials using the complete Euclidean method, forming a dendrogram on the left side of the heatmap (Fig 2.5A). Each of the samples were labeled with their respective group based on their cumulative positive eczema diagnosis count. Clustering showed no distinction amongst the samples based on the eczema grouping, showing an evenly mixed spread. There was one cluster that was most distinct from the rest containing five samples, 3 of which belonged to “None”, 1 to “Intermediate”, and 1 to “Persistent” eczema. This group also showed most the distinguishable pattern on the heatmap representing the relative abundance of each pathway ranging from lowest (dark blue) to highest (red). However,

PCA analysis of the predicted metabolome results also showed great overlaps of 95% confidence ellipses between the groupings. The “None” group showed the largest area of spread, followed by “Persistent” eczema, and then “Intermediate” eczema, which had the tightest spread

(Fig 2.5B). The first dimension represented on the x-axis accounted for 45% of the spread, and the second dimension along the y-axis accounted for 16.8% of the spread.

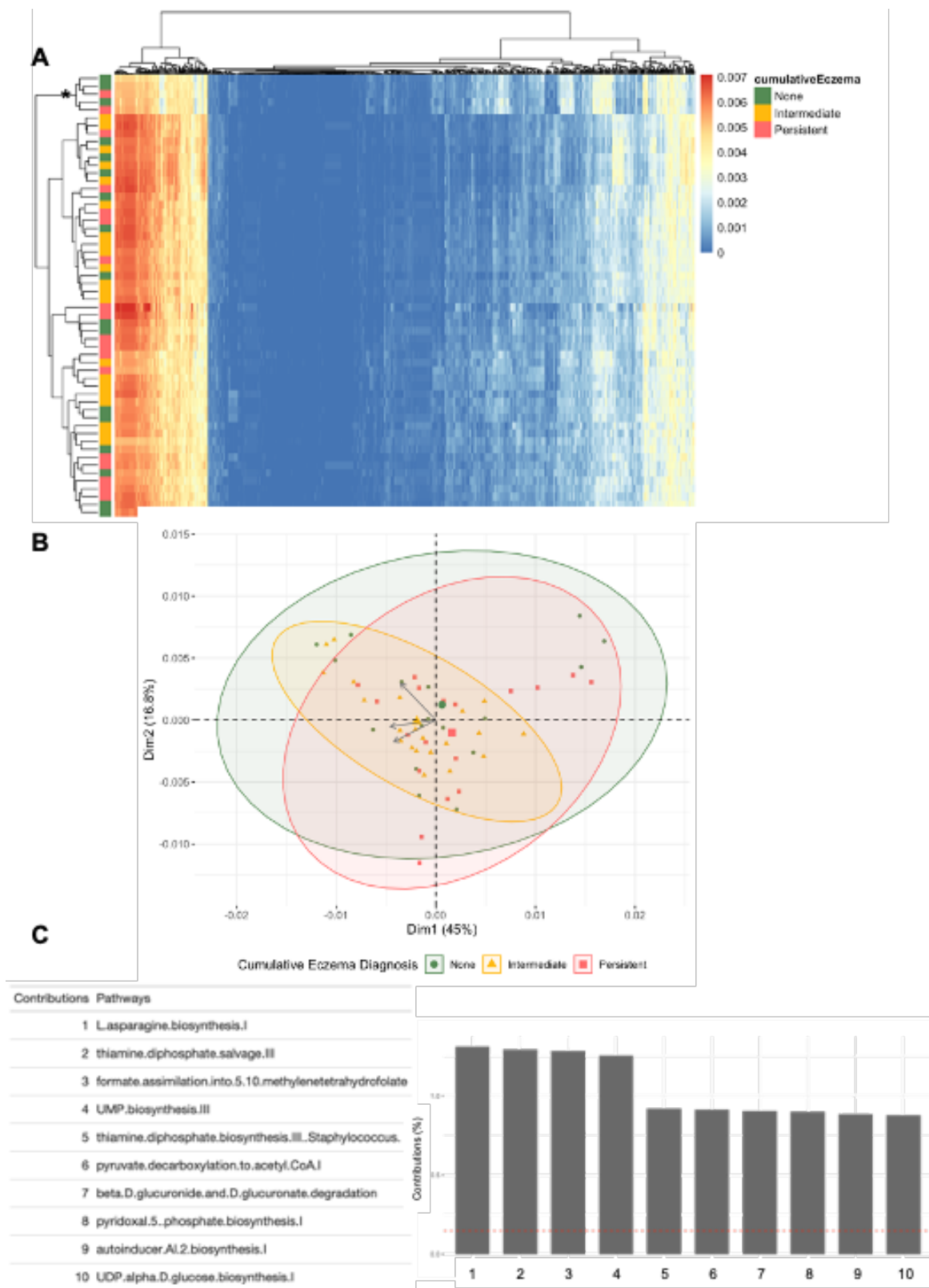


Figure 2.5 PAPERICA analysis results of inferred metabolic pathway potentials based on 16S rRNA gene sequence data. (A) Heatmap of the relative abundance of each of the inferred

Figure 2.5 (cont'd)

metabolic pathways for each sample. The color gradient of each of the cells goes from red (high abundance) to dark blue (low abundance). Each sample is represented as a row and identified for its eczema diagnosis grouping by the color ribbon (red = Persistent, yellow = Intermediate, green = None). The dendrograms used the complete clustering method. (B) Shows the PCA of each sample using the PAPRICA pathways results and grouped by the 3 eczema diagnosis groupings. (C) Shows the top 10 most contributing variables (predicted metabolic pathways) in the spread of data in the PCA shown in (B). The metabolic pathways are shown in decreasing order from 1 – most contributing, to 10 – least contributing of the top 10, with a key to the names of each pathway by numbered ranks. * - Indicates the most distinct cluster.

Analysis: Approach 2

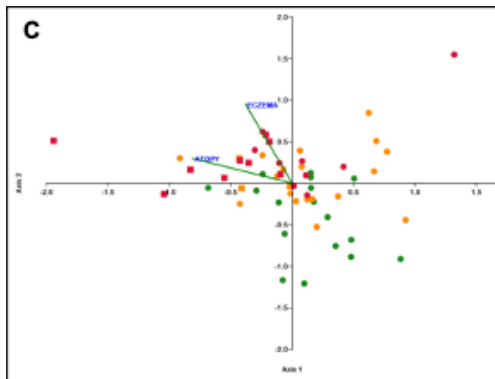
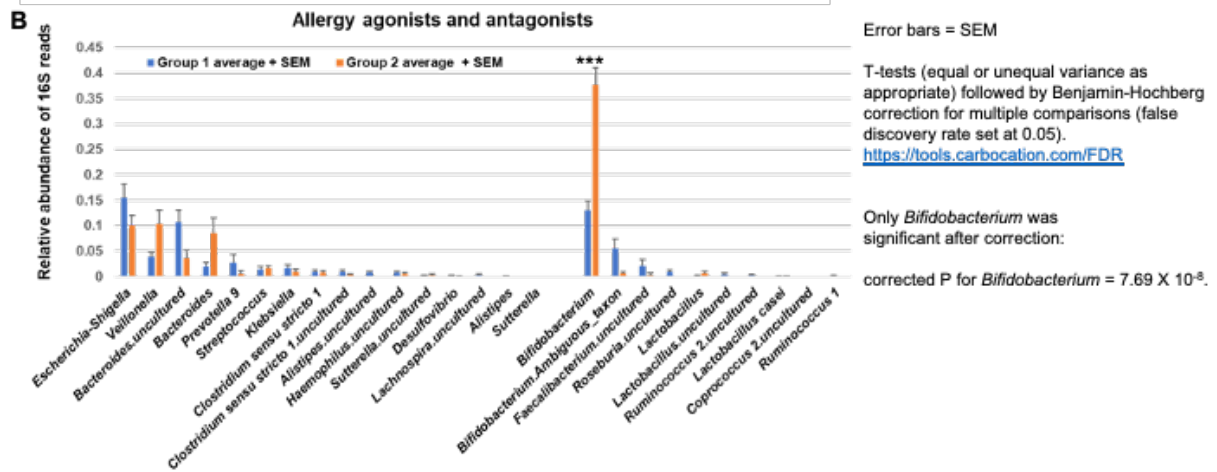
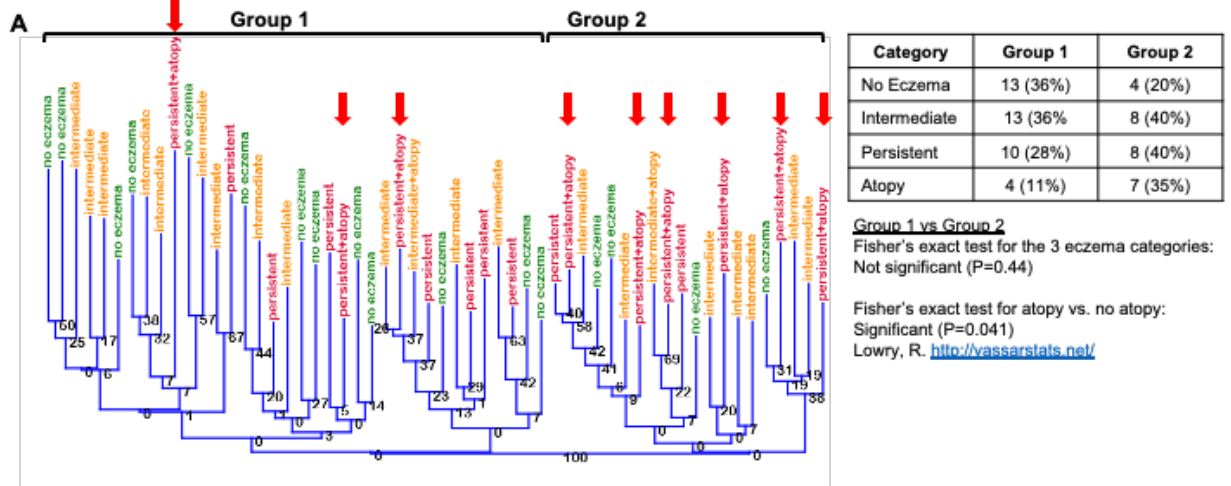
Overview of Analyses from Approach 2

Although there was little differentiation between the microbiotas of infants at the three eczema diagnosis levels as broadly assessed by PCA, SIMPER analysis indicated that the compositions of those diagnosis groups did differ in their levels of several taxa, including taxa associated with allergy in the literature. Furthermore, taxa associated with allergy, hereafter termed allergy agonists were major contributors to the ordinations. Therefore, we performed further analyses to elucidate the possible effects of these differences. First, (1) we performed neighbor-joining clustering of the full data table (all samples, all taxa) to explore whether samples could be separated into distinct clusters based on the bacterial community composition at 3 months of age alone, without respect to allergy diagnoses. Second, (2) we hypothesized that analysis of individual bacterial taxa and groups of taxa implicated as allergy agonists in previous studies would reveal patterns associated with allergy in this population. Next, (3) we hypothesized that addition of another allergic diagnoses, atopy, would strengthen the correlation found between allergic manifestation and the microbiota. And finally, (4) we hypothesized that analysis of the influence of the early gut microbiota on eczema diagnosis at individual early assessment times would provide evidence of the importance of the early gut microbiota on the pattern of eczema development and confirm the importance of presence of individual taxa.

(1) Two distinct microbiota groups emerged using neighbor-joining analysis

Neighbor joining clustering using the Bray Curtis similarity measure with 1000 bootstrap replications was performed on the microbiota data (Figure 2.6, Panel A). This analysis is blind to

allergy phenotype – eczema, atopy, both eczema and atopy, or neither. Two groups with 100% bootstrap support emerged from the analysis where Group 2 containing 20 samples had a preponderance of infants with eczema (85%) and Group 1 containing 36 samples was more evenly divided between infants with no eczema at any time point (39% in that group) and infants with eczema including “Intermediate” and “Persistent”(61% of the samples in that group). In addition, the proportion of infants with atopy diagnoses was higher in group 2 than in group 1; 14% (5 of 36) of the infants in Group 1 had atopy diagnoses, while 30% (6 of 20) of the infants in group 2 had atopy diagnoses. The compositions of the microbiotas in the two groups differed significantly, which was confirmed with one-way PERMANOVA with Bray Curtis similarity ($P \leq 0.0001$).



Category	Upper right quadrant	Lower right quadrant	Upper left quadrant	Lower left quadrant
No eczema	3	8	1	5
Intermediate	6	6	5	4
Persistent	4	2	11	1
Intermediate with atopy	0	0	1	1
Persistent with atopy	0	0	8	1

Fisher's exact P = 0.0108; X² not valid; some expected cells <5
Vasavada, N. 2016. <https://astatna.com/FisherTest/>

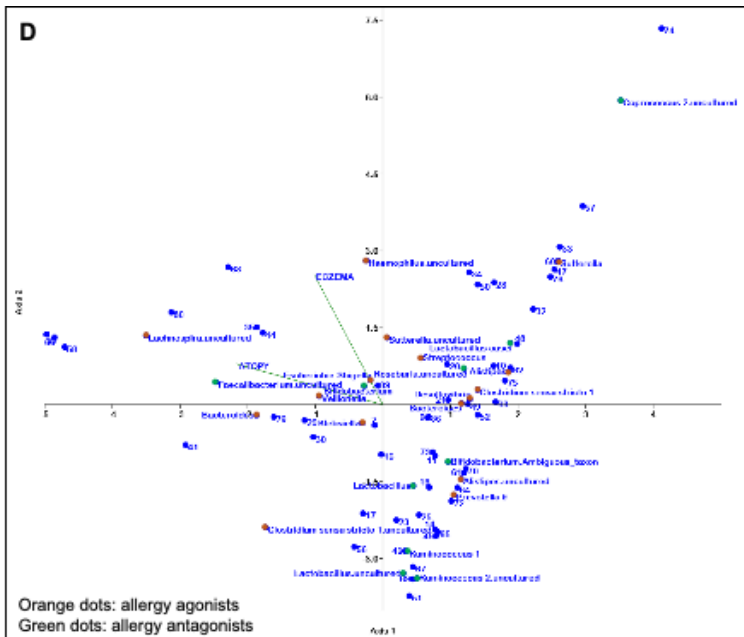


Figure 2.6 Neighbor-joining and Canonical Correspondence analyses.

Figure 2.6 (cont'd)

Panel A. Neighbor-joining. Relative abundances of all taxa; Bray Curtis/1000 bootstraps. Green text indicates the “None” eczema diagnoses, orange text indicates “Intermediate” with 1-3 eczema diagnoses; and red text indicates “Persistent” eczema with 4-5 eczema diagnoses. Red arrows indicate “Persistent” eczema with one or two diagnoses of atopy. **Panel B. Allergy agonists and antagonists in neighbor-joining groups: mean \pm SEM.** Average relative abundances of taxa are shown. Mann-Whitney rank test for equality of medians for each taxon was used followed by Holm-Bonferroni correction for multiple comparisons (*, $P \leq 0.05$; **, $P \leq 0.005$; ***, $P \leq 0.0005$). **Panel C. CCA samples.** Relative abundances of all taxa; factors = total observations of eczema (0-5) and total observations of atopy (0-2). Symbols: square - infant that had at least one atopy diagnosis; dot - infant that did not have atopy; green – “None” eczema (0 eczema diagnoses), orange – “Intermediate” eczema (1-3 eczema diagnoses), and red – “Persistent” eczema (4-5 eczema diagnoses). **Panel D. CCA: taxa.** Relative abundances of all bacterial taxa; Factors = total observations of eczema (0-5) and total observations of atopy (0-2). The taxa named have been associated with allergy in the literature. The plot was truncated to improve visibility; outlying taxa are not shown and their XY coordinates on the full plot are given in the lower left and lower right corners.

(2) Groups defined by neighbor-joining had significant differences in the relative abundances of some bacterial taxa previously associated with allergy development

Multiple studies have implicated a number of bacterial taxa associated with either development or prevention of allergy. Twenty-six such bacterial taxa detected in the infant samples are represented in Table 2.3; 15 of these bacterial taxa have been identified as allergy agonists, and 11 identified as allergy antagonists [2, 55, 81, 82, 102, 147-152].

Table 2.3 Allergy agonists and antagonists detected in the infant samples.

Allergy Agonists	Allergy Antagonists
<i>Alistipes a</i> uncultured	<i>Bifidobacterium</i>
<i>Alistipes b</i>	<i>Bifidobacterium</i> ambiguous
<i>Bacteroides a</i> uncultured	<i>Coprococcus 2</i> uncultured
<i>Bacteroides b</i>	<i>Faecalibacterium</i> uncultured
<i>Clostridium sensu stricto 1 a</i>	<i>Lachnospira</i> uncultured
<i>Clostridium sensu stricto 1 b</i> uncultured	<i>Lactobacillus a</i>
<i>Desulfovibrio</i>	<i>Lactobacillus b</i> uncultured
<i>Escherichia-Shigella</i>	<i>Lactobacillus casei</i>
<i>Haemophilus</i> uncultured	<i>Roseburia</i> uncultured
<i>Klebsiella</i>	<i>Ruminococcus 1</i>
<i>Prevotella 9</i> uncultured	<i>Ruminococcus 2</i> uncultured
<i>Streptococcus</i> uncultured	
<i>Sutterella a</i> uncultured	
<i>Sutterella b</i>	
<i>Veillonella</i> uncultured	

The relative abundances of some members of this subset of allergy-associated taxa were significantly different between the two groups identified using neighbor joining clustering (Figure 2.6, Panel B). The *Escherichia-Shigella* taxon was in highest relative abundance among the allergy-agonists while *Bifidobacterium* was highest amongst the allergy antagonists. In the allergy agonist group, *Bacteroides_b* and *Veillonella* were in higher relative abundance in Group 2, while *Bacteroides_a* was higher in Group 1. In the allergy antagonist group, *Bifidobacterium* that was present at the highest relative abundance was seen to be higher in average relative abundance for Group 2, while *Bifidobacterium_ambiguous* taxon was higher in Group 1.

(3) Eczema and atopy considered together lead to differentiation of microbiotas of infants by Canonical Correspondence Analysis (CCA)

Epidemiological associations have been made between the presence of one or more allergic manifestations in infancy and early childhood and subsequent development of asthma [2].

Because there was a significant association between eczema and atopy in our dataset (Fisher's exact test, $P = 0.0311$), we then asked whether consideration of the two factors together would strengthen the correlation found between allergy and the microbiota [153]. CCA was used to analyze the separation of the microbiota data using the factors atopy and eczema. The two factors were the total number of eczema diagnoses over the five assessment time points (range 0-5) for each individual and the individual's total number of atopy diagnoses obtained by skin prick tests at 12 and 24 months of age (range 0-2).

Samples (Figure 2.6, Panel C) and taxa (Figure 2.6, Panel D) are shown in separate plots for clarity. The infants are designated in Figure 2.6C as having no eczema (green; $N = 17$), intermediate eczema (orange; $N = 21$), or persistent eczema (red; $N=18$). Square symbols indicate at least one positive atopy diagnosis; dots indicate no atopy. The taxa named in Figure 2.6D have been associated with allergy in the literature. The two factors, eczema and atopy, exhibited correlation, contributed approximately equally to the outcome of the analysis, and together separated most infants with "Intermediate" or "Persistent" eczema (lower two quadrants) from most infants with "None" eczema (upper two quadrants). Infants with atopy fell mainly in the lower left quadrant. Allergy-associated taxa, both agonists and antagonists, were distributed through all quadrants of the plot. Allergy antagonists *Lactobacillus* (two OTUs), *Ruminococcus* (two OTUs), and *Bifidobacterium_ambiguous* taxon were particularly prominent in the upper quadrants, while allergy agonists *Lachnospira*, *Haemophilus*, *Veillonella*, and *Escherichia-Shigella* were prominent in the lower quadrants. The plot was truncated to improve visibility; outlying taxa not shown and their XY coordinates on the full plot are given in the lower left and lower right corners.

Analysis: Approach 3

Further examination of the association between the microbiota composition at 3 months of age with eczema diagnosis status at each time point over the first year of life.

Eczema diagnosis given at 3, 6, and 12 months was used to group, then to analyze the microbiota composition of infants at 3 months of age

To further investigate the effect of microbiota composition at infancy on eczema development, we used the individual instances of eczema diagnosis made at 3, 6, and 12 months of age in

addition to the cumulative diagnosis count. Assessments performed at 24 and 36 months were excluded due to a large number of missing values that would cause high uncertainty in inferences. All samples were grouped as either “having a positive eczema diagnosis at the time indicated as “Eczema”, or “having a negative eczema diagnosis at the time” indicated as “No Eczema”. At 3 months of age, out of 56 infants, 18 infants received a positive diagnosis of “Eczema” and 38 infants were categorized as “No Eczema” (Fig 2.7A). At 6 months of age, the number of infants with a positive “Eczema” diagnosis increased to 30 and the remaining 26 were deemed as “No Eczema”. At 12 months of age, 29 infants were diagnosed as having “Eczema” while 27 were diagnosed as “No Eczema”.

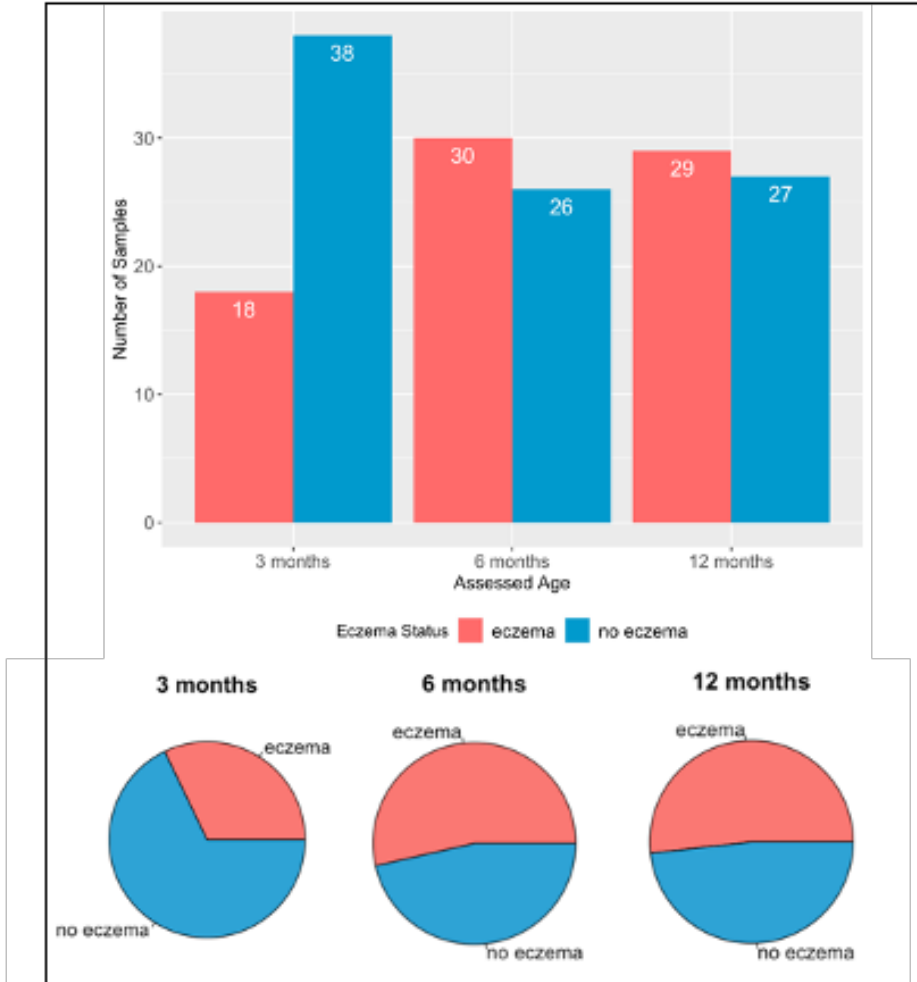
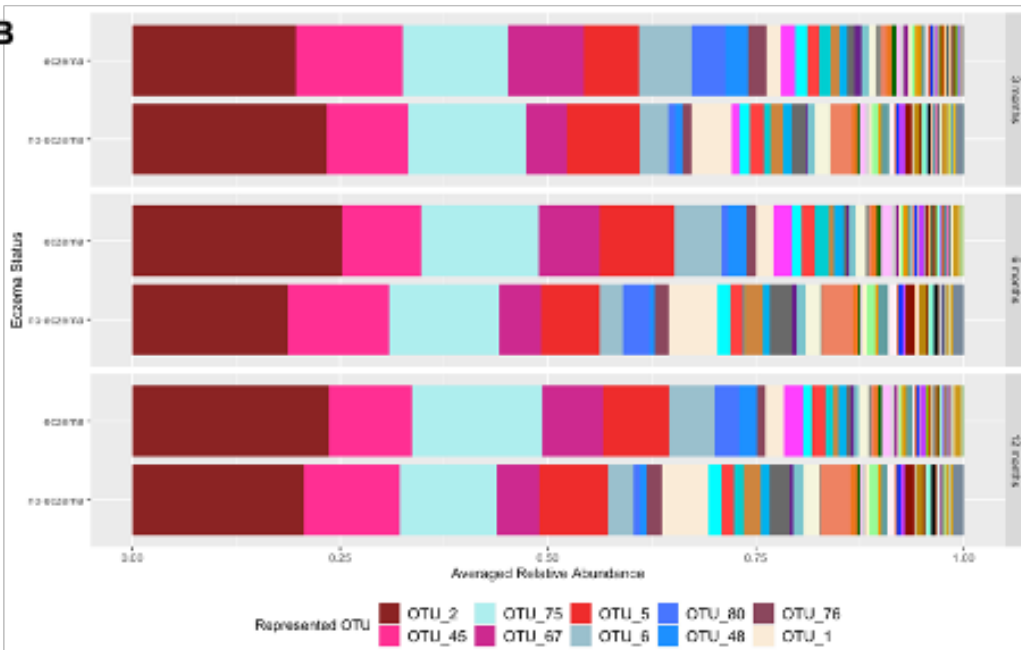
A**B**

Figure 2.7 Breakdown of the sample population based on their eczema diagnosis.

Figure 2.7 (cont'd)

(A) Grouping based on positive or negative diagnosis of eczema at each time point of allergy assessment. Out of the 56 samples analyzed, at 3 months of age, 18 were diagnosed as positive and 38 were diagnosed as negative. At 6 months of age, 30 were diagnosed as positive and 26 as negative. At 12 months of age, 29 were diagnosed as positive and 27 as negative for eczema. (B) Bacterial taxa as OTU relative abundances in the fecal samples of infants (collected at 3 months) grouped by their eczema diagnosis made at 3, 6, and 12 months (“eczema” or “no eczema”). All OTU’s represented as a block of unique color for both eczema diagnosis at each 3 ages.

Taxa relative abundance showed overlapping patterns as the cumulative eczema count grouping for highly abundant OTU’s, while showed opposite patterns in lowly abundance OTU’s (Figs 2.7 and 2.8)

Averaged relative abundance of each OTU with its assigned bacterial taxa based on 16S rRNA gene sequence results are shown as stacked bar charts for both “Eczema” and “No eczema” diagnosis groups at 3, 6, and 12 months. All 6 groups shared similar compositions for their most highly abundant OTU’s, while showing more variation within less abundant OTU compositions.

OTU_2 (genus *Bifidobacterium*) was the most highly abundant at more consistent percentage across all groups. OTU_45 (family *Lachnospiraceae*) and OTU_75 (genus *Escherichia-Shigella*) were the next most highly abundant OTUs in all groups, except for “Eczema” group at 3 months, where OTU_67 (genus *Veillonella*) was in higher relative abundance. OTU_45 was more consistent in their relative abundance between the “Eczema” and the “No eczema” groups along with OTU_75 at 3, 6, and 12 months. OTU_67 was in higher abundance in “Eczema” groups at all 3 time points, but the difference was largest at 3 months.

For lower relative abundance OTU’s, the similar trend of having select few OTU within each taxonomic family at higher relative abundance than the rest stayed true. In family *Lachnospiraceae*, OTU_45 (genus unknown) overshadowed in its relative abundance compared to the rest of the OTU’s as it did in the cumulative eczema count grouping. In family *Ruminococcaceae*, OTU_48 (genus *Faecalibacterium*) was in much higher abundance than any other OTU’s of the family as seen in cumulative eczema count grouping. It was in much higher relative abundance in the “eczema” group at 3, 6, and 12 months. In *Enterobacteriaceae* family, OTU_75 (genus *Escherichia-Shigella*), which was also one of the most highly abundant OTU and was the OTU in higher abundance than other members of the family. It was the same case in *Veillonellaceae*, where OTU_67 (genus *Veillonella*) was highest within the Family, while being

one of the most highly abundant OTU overall. Out of the lesser abundant OTU's within *Veillonellaceae*, OTU_64 (genus *Megamonas*) was consistently in higher abundance in the “No eczema” groups across all 3 time points. OTU_65 (genus *Megasphaera uncultured*), which was only present in the cumulative “Persistent” eczema group, was in highest abundance in the “No eczema” group at 3 months, then appearing in “Eczema” group at 6, then 12 months. OTU_66 (genus *Megasphaera*) appeared in both the “Eczema” and “No eczema” group at 3 months and was minimal in “No eczema” groups in 6 and 12 months. In *Bacteroidaceae* family, the relative abundance of OTU_5 (genus *Bacteroides uncultured*) was less distinct from each other compared to that when using the cumulative eczema count grouping. OTU_5 was still higher than OTU_6 (genus *Bacteroides*) for both diagnoses at 3 months but had an even distribution of relative abundance in the 12 month group. OTU_6 showed consistently higher relative abundance amongst the “Eczema” group.

Bifidobacteriaceae showed a pattern that was more consistent with the cumulative grouping, where OTU_2 (genus *Bifidobacterium*) was in much higher relative abundance across the groups compared to OTU_1 (genus *Bifidobacterium ambiguous taxa*). In *Prevotellaceae*, OTU_9 (genus *Prevotella.9*) was in higher relative abundance than OTU_10 (genus *Prevotellaceae NK3b31 group*) overall, and much higher in “No eczema” groups. OTU's in family *Streptococcaceae* followed the pattern in cumulative grouping where OTU_19 (genus *Streptococcus*) was at much higher relative abundance across all the groups compared to OTU_18 (genus *Lactococcus*). *Lactobacillaceae* had OTU_16 (genus *Lactobacillus uncultured*) that was consistently in higher abundance in the “No eczema” group in all 3 ages. OTU_17 (genus *Lactobacillus*) was in higher abundance than OTU_15 (genus *Lactobacillus casei species*) and got skewed in relative abundance pattern going from being about even within 3 months grouping, to much higher in “No eczema” within 6 and 12 months grouping. *Clostridiaceae* had OTU_21 (genus *Clostridium sensu stricto 1 uncultured*) and OTU_22 (genus *Clostridium sensu stricto 1*) that were higher relative abundance overall compared to the cumulative grouping. However, OTU_23 (genus *Sarcina*) was at higher relative abundance in the “Eczema” group at 12 months.

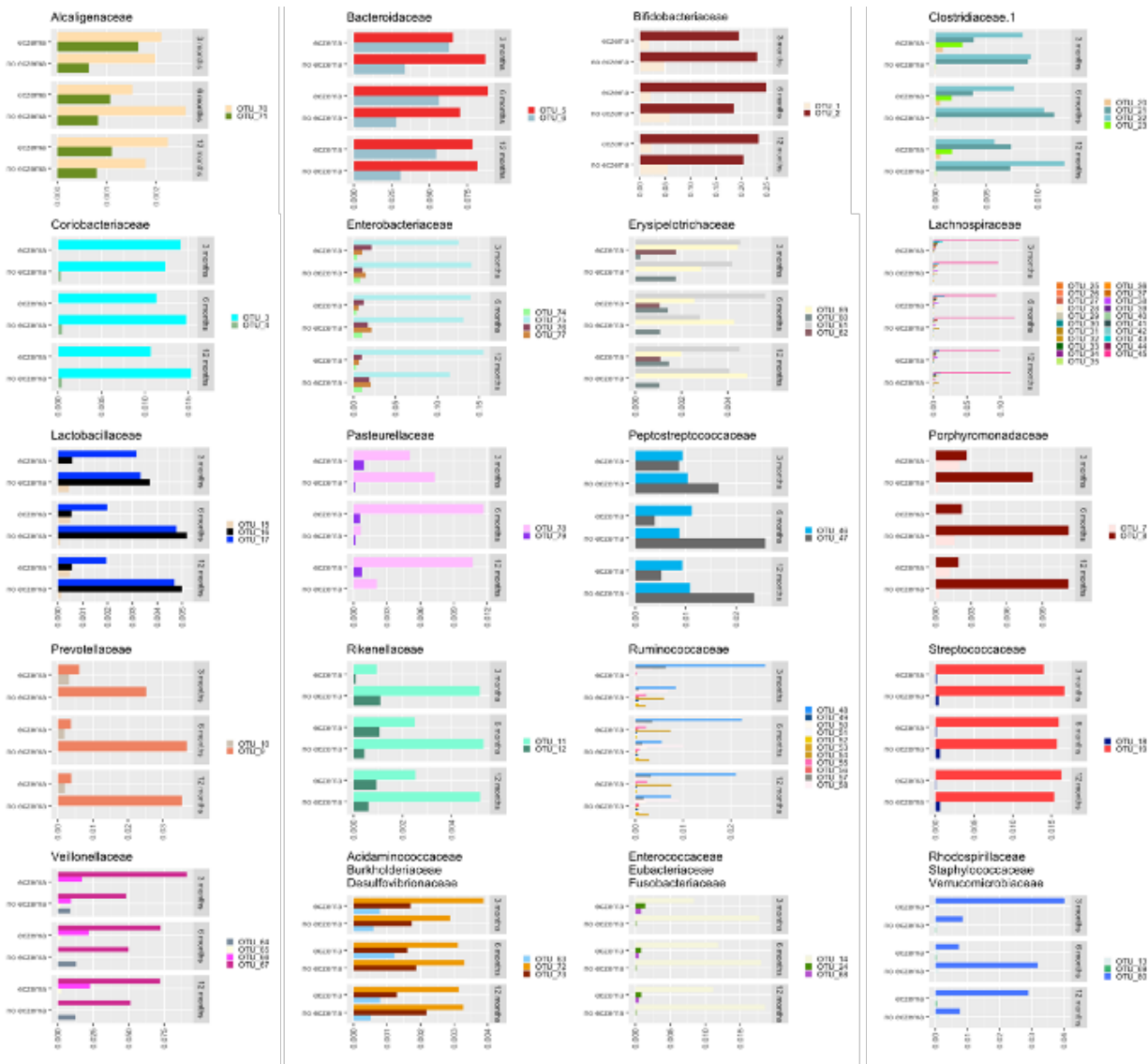


Figure 2.8 Comparisons of specific bacterial taxa in infants with eczema or no eczema. Bacterial taxa are from fecal samples of infants (collected at 3 months) that are shown as OTU relative abundances and grouped by their eczema diagnosis made at 3, 6, and 12 months of age. Bacterial taxa are shown at the family level of taxonomic rank.

Principal Components Analysis (PCA) showed varying overlaps between the 2 eczema statuses at 3, 6, and 12 months of age

PCA was used to visualize the spread of the microbiota data based on their OTU compositions, with 95% confidence ellipses representing the eczema diagnosis grouping (Fig 2.9). The first dimension explained 27.7% and the second dimension explained 14.5% of variation in the data. The top contributing variables are the same OTU's as they were in cumulative grouping. In PCA

visualized using eczema diagnosis at 3 months of age, the 95% confidence ellipse representing the “eczema” group was narrower than that of “no eczema” group, leaving 4 samples in “no eczema” group and 1 in “eczema” group outside of its ellipse (Fig 2.9A). When visualized with groupings by eczema diagnosis at 6 months, the 95% confidence ellipse for “no eczema” group increased in size to include additional samples that sat outside of its range with 3 months grouping. In addition, “eczema” ellipse changed shape to leave out 3 samples now belonging in “eczema” group (Fig 2.9B). With diagnosis at 12 months grouping, “no eczema” ellipse increased its size even more, including all samples. The “eczema” 95% confidence ellipse now contained all the samples belonging to its grouping (Fig 2.9C).

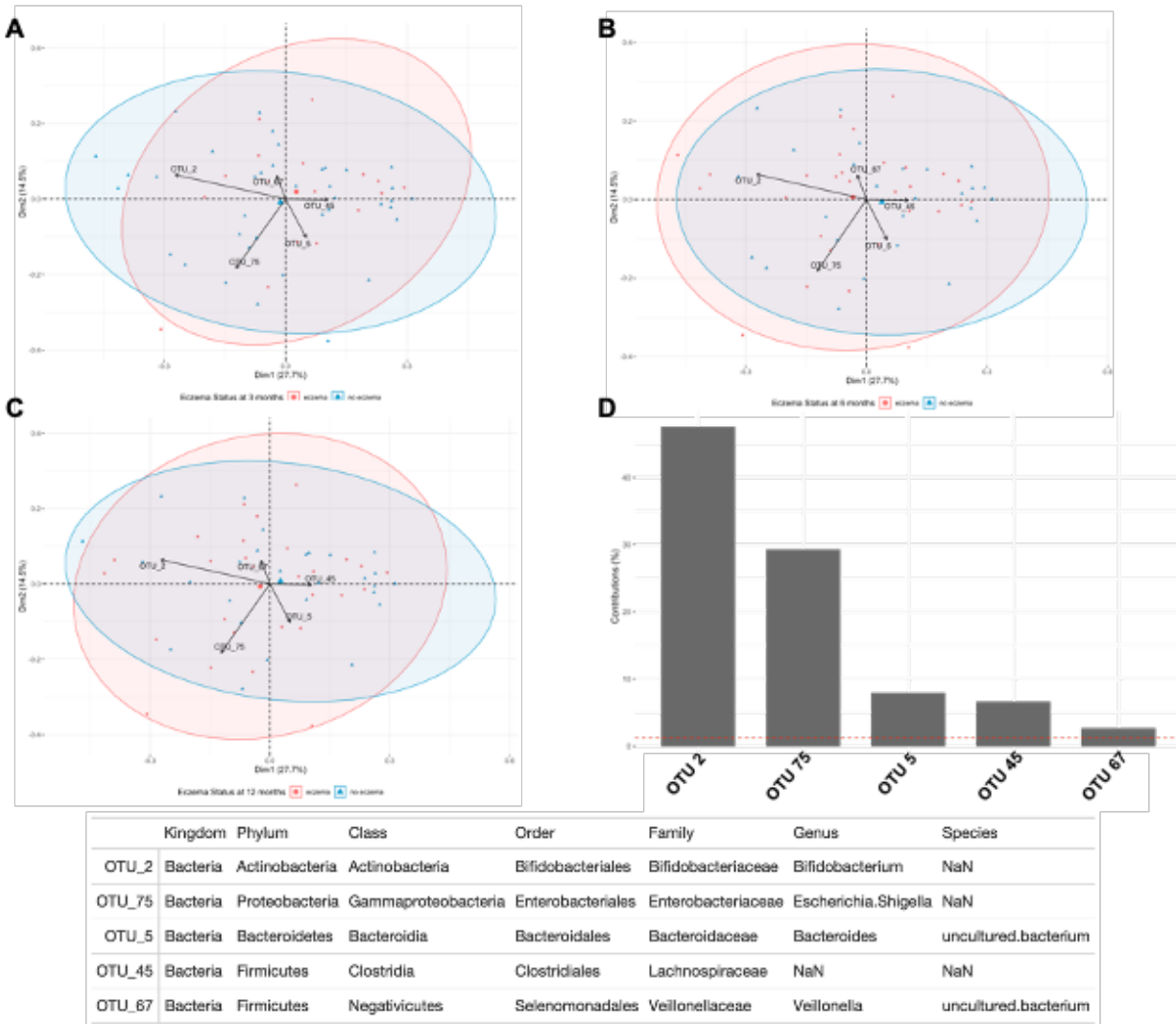


Figure 2.9 PCA of bacterial taxa relative abundance data and the percentage of contribution of each of the top 5 most contributing taxa for each of the ages. (A) made at 3

Figure 2.9 (cont'd)

months of age. The black arrows represent the top 5 most contributing OTUs (variables). (B) PCA and its top 5 made at 6 months of age. (C) PCA grouped by the eczema diagnosis made at 12 months of age. (D) top 5 contributing OTU's for the spread of PCA in (A) – (C).

Alpha diversity calculated using Shannon Diversity Index was not significant for any time point

Shannon Diversity Index was calculated on microbiota compositions grouped by individual eczema diagnosis at 3, 6, and 12 months. Using eczema diagnosis at 3 months, the difference in the Shannon diversity index between those diagnosed with eczema (“Eczema”) and those without eczema (“No eczema”) were not statistically significant ($p=0.54$, Kruskal-Wallis). Grouping by eczema diagnosis made at 6 months, the mean difference was also not statistically significant ($p=0.86$, Kruskal-Wallis). When grouped by eczema diagnosis made at 12 months, the mean difference was still not statistically significant ($p=0.59$, Kruskal-Wallis)(Fig 2.10A).

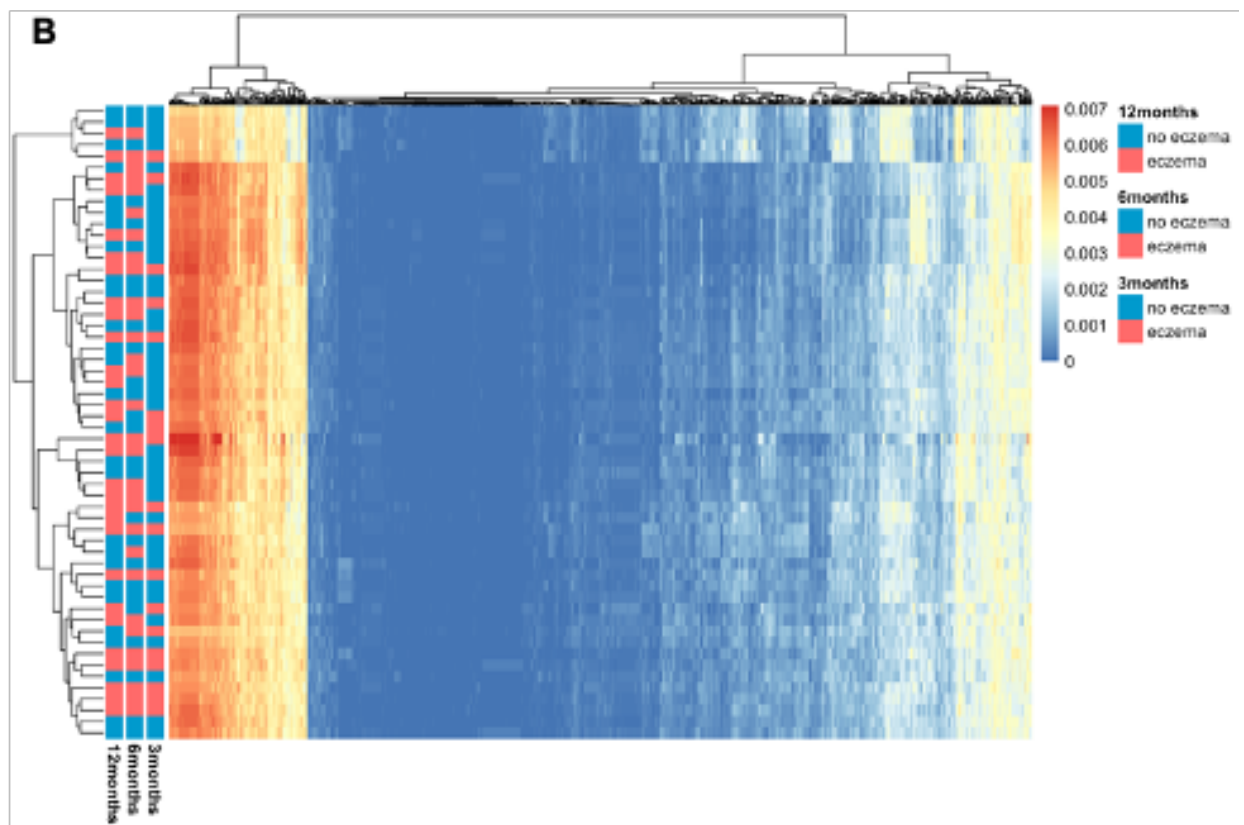
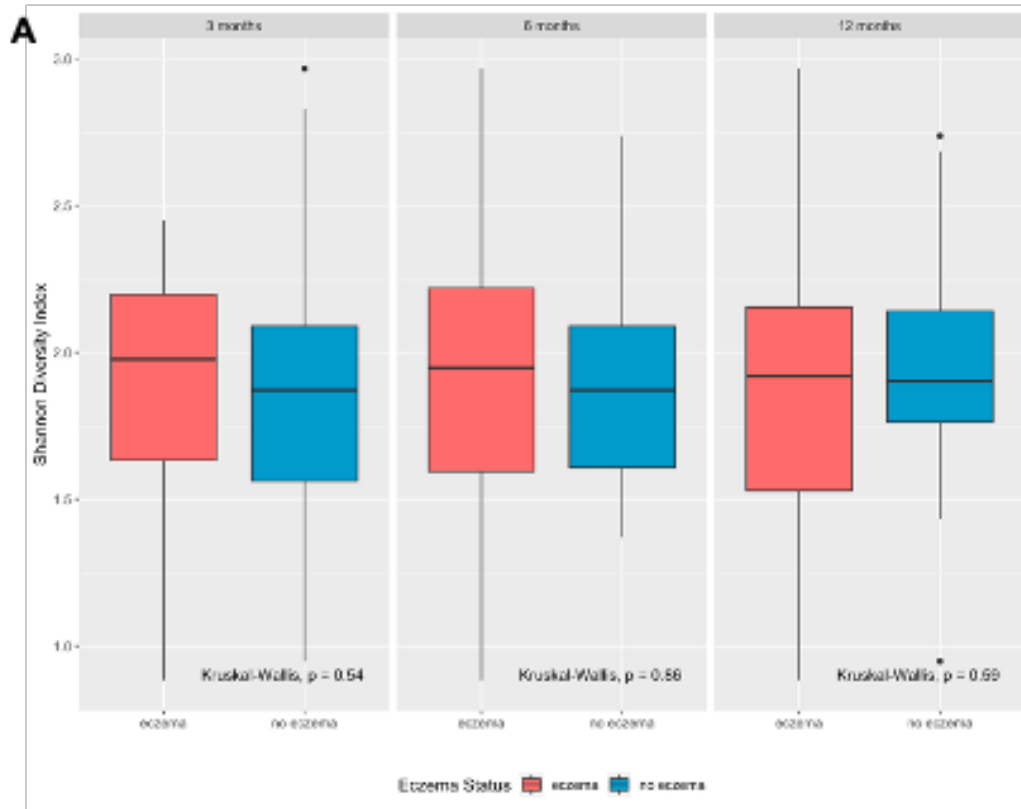


Figure 2.10 (A) Shannon Diversity Index using the OTU data grouped by the eczema

Figure 2.10 (cont'd)

Diagnosis. (“eczema”: red, “no eczema”: blue) at 3, 6, and 12 months of age. The mean differences were not statistically significant for all 3 time points (3 months: $p=0.54$, 6 months: $p=0.86$, 12 months: $p=0.59$; Kruskal-Wallis). (B) **PAPRICA analysis results of inferred metabolic pathway potentials based on 16S rRNA gene sequence bacterial taxa data.**

Heatmap of the relative abundance of each of the inferred metabolic pathways for each sample. The color gradient of each of the cells goes from red (high abundance) to dark blue (low abundance). Each sample is represented as a row and identified for its eczema diagnosis grouping by the color ribbon for each of the 3 time points (red = “eczema”, blue = “no eczema”). The dendrograms used complete clustering method.

Metabolic potentials as inferred using PAPRICA (PATHway Prediction by phylogenetic plAcement) were not distinguishable between groups

The inferred metabolic pathway potentials obtained using PAPRICA software was re-analyzed using the individual eczema diagnosis status grouping at 3, 6, and 12 months. When clustering each sample based on its composition of inferred pathway potential relative abundances using Euclidean method, there were no clear separation of those in “eczema” grouping or “no eczema” grouping on the dendrogram (Fig 2.10B).

Random Forest analysis followed by logistic regression showed statistically significant association between OTU_67 (genus *Veillonella*) and eczema status at 3 months of age

This analysis used an eczema diagnosis defined as answering: (1) YES to (i) “ever have itchy rash coming and going for at least 6 months” (not valid at 3 or 6 months of age), (ii) “rash or eczema that has lasted at least 7 days or more,” or (iii) “ever eczema” (not valid at 3 months), and (2) YES to “the rash was itchy,” and (3) YES to “affected the folds of elbows, behind knees, in front of ankles, on cheeks or around neck, ears, or eyes.” “No eczema” was defined as “never presence of an itchy rash.”

The method of random forest was applied to select OTUs potentially associated with eczema at different ages. The R function *randomForest* was run on the microbiota composition and the eczema status at 3, 6, and 12 months to examine their potential associations. Using 10-fold cross validation, the average accuracy for predicting eczema status based on constructed forests were 80%, 63%, 68%, and 60%, indicating a close connection between microbiota composition at 3 months and the eczema status at 3 months. Five top OTUs out of 15 OTU’s that received the

highest importance values in random forest analysis (Fig 2.11) were further analyzed using logistic regressions. Out of the 5 OTU's analyzed, OTU_67(genus *Veillonella*) showed a statistically significant association with eczema status at 3 months of age (Odds ratio=2.42 for every 10% of increase in relative abundance, p=0.036) after adjusting for offspring gender. Additional associations between OTU_67 and eczema status at other ages were tested using the same model (Table 2.3).

Table 2.3 Estimated odds ratios, 95% confidence intervals, and p-values for the association of *Veillonella* with eczema status at different ages.

	Odds ratio (for every 10% of increase in relative abundance)	95% Confidence Interval		P-values
		2.50%	97.50%	
Month 3	2.42	1.16	6.17	0.036
Month 6	1.91	0.98	4.37	0.085
Month 12	1.10	0.54	2.09	0.774

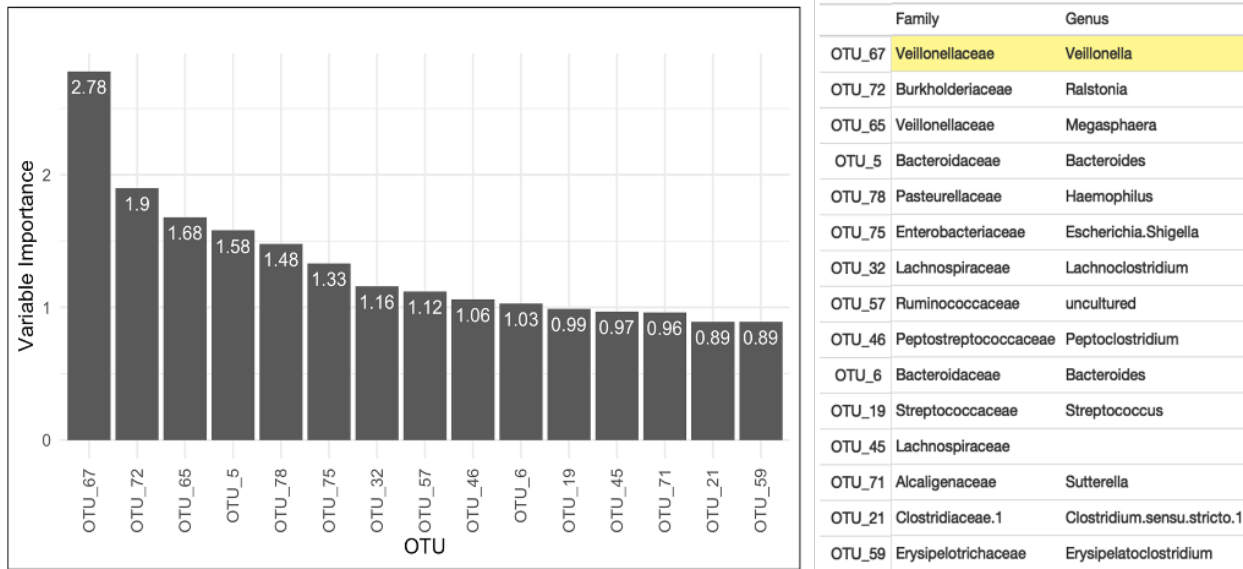


Figure 2.11 Top 15 variable importance from Random Forest analysis. OTU_67, belonging in the *Veillonella* genus was the highest.

Discussion

Samples and data from 56 children of the Isle of Wight Birth Cohort third generation were used to address the hypothesis that a particular composition of the early gut microbiota is associated with development of eczema and/or atopy in infants. Of these, 17 of 56 children were graded as “None” for eczema status in the first 36 months of their life, while the remaining 39 had at least one instance of positive eczema diagnosis. Eighteen had “Persistent” eczema, while 21 were classified with “Intermediate” eczema. This study established an association between *Veillonella* and other allergy agonists in infant gut microbiota at 3 months of age with risk of developing eczema from 1 to 3 years of age in children of the Isle of Wight Birth Cohort.

In the initial family level analysis of the three eczema categories “None” no eczema, “Intermediate” eczema and “Persistent” eczema, there were differences between microbiotas of infants in these three categories. PCA analysis at the OTU level showed considerable overlap; however four known allergy-associated taxa were major contributors to separation of points along major axis 1 (*Bifidobacterium*, *Escherichia-Shigella*, *Prevotella*, and *Veillonella*). Furthermore, SIMPER analysis indicated that the compositions of those clinical groupings did differ in their levels of several taxa, including taxa associated with allergy in the literature. Moreover, bacterial taxa previously associated with allergy, termed allergy agonists, were major contributors to the ordinations. This suggested that analyzing OTU abundance associations would be better served by testing for associations with known allergy agonists or allergy antagonists. These results led us to perform additional analyses via neighbor-joining and canonical correspondence.

Our first approach employed neighbor-joining clustering of the full data table (all samples, all taxa) to explore whether samples could be separated into distinct clusters based on the bacterial community composition at 3 months of age alone, without respect to allergy diagnoses. Neighbor-joining clustering, which does not take eczema category into account, indicated the presence of two strongly separated clusters of microbiotas with 100% bootstrap support. The compositions of the microbiotas in these groups differed significantly by one-way PERMANOVA with Bray Curtis similarity ($P \leq 0.0001$) and one, Group 2, had higher proportions of infants with eczema and atopy. These groups differed markedly in the levels of some allergy-associated taxa (*Escherichia-Shigella*, *Veillonella*, two *Bacteroides* OTUs, *Bifidobacterium*, and *Bifidobacterium_ambiguous* taxon). The *Bifidobacterium* OTU was the most important and the

Escherichia-Shigella OTU the 2nd most important taxa contributing to the dissimilarity between neighbor-joining Group 1 and Group 2 (SIMPER).

In the second approach, we hypothesized that analysis of individual bacterial taxa and groups of taxa implicated as allergy agonists in previous studies would reveal patterns associated with allergy in this population. After analysis, we accepted this hypothesis because groups defined by neighbor-joining had significant differences in the relative abundances of some bacterial taxa previously associated with allergy development. The *Escherichia-Shigella* taxon was in highest relative abundance among the allergy-agonists while *Bifidobacterium* was highest amongst the allergy antagonists. In the allergy agonist group, *Bacteroides* and *Veillonella* were in higher relative abundance in Group 2 with the preponderance of infants with eczema, while *Bacteroides_a* was higher in Group 1. In the allergy antagonist group, *Bifidobacterium* that was present at the highest relative abundance was seen to be higher in average relative abundance for Group 2, while *Bifidobacterium_ambiguous* taxon was higher in Group 1.

In our third approach, we hypothesized that addition of atopy would strengthen the correlation found between eczema and the microbiota. Here, CCA showed that the two factors, eczema and atopy were correlated, contributed approximately equally to the outcome of the analysis, and together separated most infants with “Intermediate” or “Persistent” eczema from most infants with “None” eczema (upper two quadrants) in the ordination plot. These outcomes were associated with the allergy agonists *Lachnospira*, *Haemophilus*, *Veillonella*, and *Escherichia-Shigella*. Conversely, allergy antagonists *Lactobacillus* (two OTUs), *Ruminococcus* (two OTUs), and the *Bifidobacterium_ambiguous* taxon were associated with absence of eczema and atopy. Thus, eczema and atopy considered together by CCA lead to substantial improvements in distinguishing which bacterial taxa of the fecal microbiotas of infants correlated with an allergic clinical presentation. The CCA result confirmed the contributions of both eczema and atopy and the correlation between them.

Finally, in a fourth approach we hypothesized that analysis of the influence of the early gut microbiota on eczema diagnosis at individual early assessment times would provide evidence of the importance of the early gut microbiota on the pattern of eczema development and confirm the importance of key individual taxa. Here, Random Forest analysis followed by logistic regression showed a statistically significant association between *Veillonella* and eczema status at 3 months of age. Taken together, our results support that infants with “Persistent” eczema in the first three

years of life represent a group where the genera *Lachnospira*, *Haemophilus*, *Veillonella*, and *Escherichia-Shigella* acted as a risk microbiome and *Bifidobacterium* and *Bacteroides* acted in a protective manner. Interestingly, in no instance did diversity of the microbiota have impact on susceptibility to allergy in these studies. These results provide evidence for a relationship between microbiota composition at 3 months and development of allergy, particularly for allergy-associated taxa, and justified exploration of the time factor in eczema development.

The next step in assigning allergy agonist status to these bacterial taxa is to culture and identify them at the isolate level and conduct Koch's postulates for validation. While connections between allergy and *Escherichia* have been made previously, we note that *Escherichia-Shigella*, notably *Escherichia coli* contains a wide array of pathotypes within its species that are unidentifiable by 16S rRNA gene sequencing. *Escherichia coli* has been directly isolated and identified from the fecal samples of infants belonging to all eczema diagnosis categories[154]. In this study, we identified two *E. coli* isolates by culture and MALDI-TOF from children with "Persistent" eczema. In further studies we isolated a human-derived *E. coli* strain LM715-1 from a mouse given a fecal microbiota transplant from three of these infants from the third generation Isle of Wight Birth Cohort diagnosed with "Persistent" eczema. We characterized *E. coli* LM715-1 based on Illumina whole genome sequencing and multilocus sequence typing (MLST) using a scheme of seven housekeeping genes; *aspC*, *clpX*, *fadD*, *icdA*, *lysP*, *mdh*, and *uidA* as described previously[155]. Based on this Achtman MLST scheme[156], *E. coli* LM715-1 belonged to sequence type ST141 lineage B2 and predicted serotype O2:H6, which is most often assigned to uropathogenic *E. coli*. We also searched metadata of isolates related to ST141 *E. coli* strains in the EnteroBase dataset containing 235,990 *E. coli* strains, which also supported the classification of this strain as uropathogenic [157]. Given that the infant it was derived from and the mouse that it was transplanted to did not show discernible disease, we assigned it commensal status. However, this outcome supports the goal of characterizing more of these identified agonists for their molecular roles in mediating allergy. Eczemic infant bacterial communities will be tested using molecular Koch's postulates for underlying mechanisms in a mouse model of allergic airway disease.

This study indicated an association between eczema status at 3 months of age and the relative abundance of genus *Veillonella* in infant fecal content at that age. This association was statistically significant at $P=0.036$ using logistic regression, following a random forest analysis

that assigned the highest variable importance value to OTU_67: genus *Veillonella*. Genus *Veillonella*, represented as OTU_67 in this study, was consistently one of the OTU's in higher relative abundance overall. *Veillonella* is an anaerobic, gram-negative bacterial genus regarded as a commensal member of the oral and GI tract microbiome [158]. Although commensal, there are some species within the genus that have been identified to cause cavities and periodontal diseases, and there are recorded cases of meningitis and bacteremia [159, 160]. While there is not yet any direct causal link found between *Veillonella spp.* and human diseases and conditions relating to allergies, multiple microbiome studies have found an association indicating that this genus may be playing a role in human allergy development, specifically eczema and asthma [55, 161-163]. These authors found an association between an increased abundance of *Veillonella spp.* and asthma by the age of 5 [55, 162], allergic rhinitis at 6 years of age [161], and eczema in infants [163]. These findings all align with our findings associating increased abundance of *Veillonella spp.* with positive eczema diagnosis in infants. The infants from which our samples came are still enrolled in the cohort to continue receiving clinical analysis as they age. We expect the infants with increased *Veillonella spp.* content and positive eczema diagnosis to be at a higher risk of developing more allergic diseases, such as asthma and allergic rhinitis, in the coming years.

This study established the association between positive eczema diagnosis in infancy and the previously allergy-related bacterial taxa including *Bifidobacterium*, *Escherichia-Shigella*, *Prevotella*, and *Veillonella spp.* in the fecal microbiota of infants residing on the Isle of Wight and highlighted the value of having both cross-sectional clinical information and a longitudinal clinical trajectory to better assess relationships between the microbiome and allergy. More work is needed to further identify the microbial taxa identities to derive species-level associations, which will allow us to study potential molecular mechanisms in which these members of the microbiota are exacerbating eczema in infants. Further, analysis of actual metabolites will also allow for insight in the collective effect of bacterial microbiota that may surpass the individual taxonomic effects. We also wait on the clinical outcomes of the individuals in the cohort as they age to re-assess our prediction of continued and/or increased severity in allergic diagnosis, for example development of asthma. In the meantime, we have transplanted fecal material from selected individuals in this cohort into germ-free mice to develop a mouse model in which to test Koch's postulates for causation in the pathogenesis of eczema and allergy.

The Isle of Wight cohort provides a population with high rates of allergy and asthma that have been closely followed over three generations. Its strength lies in the consistency of the enrolled population and the minimal uprooting of enrolled families from the island, as well as the relatively small size of the island itself. These factors allow for frequent clinical assessments paired with longitudinal data collection as shown in the previous 2 generations. On the other hand, it also means that the sample size of our cohort is smaller. In developing strong statistical associations, large sample size is always preferred. This limited the options for statistical analyses and forced us to consider other factors that may be influencing our results. Throughout our study, we focused not only on statistical significance but also the detection of qualitative trends across analyses to alleviate the effects of a smaller sample size. We also explored bacterial taxa previously shown in published work to be associated with allergy as agonists or antagonists. Subsequent statistical analyses including random forest and logistic regressions supported these findings and results from logistic regressions provide statistical significance for the association of eczema status at age 3 months with the relative abundance of genus *Veillonella* at that age.

Funding

These studies were funded with federal funds from the National Institute of Allergy and Infectious Diseases, National Institutes of Health, Department of Health and Human Services, under Grant No. R21AI121748-01A1, Defining the role of the early infant microbiota in mediating allergic outcomes associated with asthma in a mouse model to Linda S. Mansfield, Susan L. Ewart and S. Hasan Arshad. The 3rd generation cohort recruitment was supported by R01AI091905. Matching support for the mouse colony, sequencing supplies and salary was provided by the Albert C. and Lois E. Dehn Chair Endowment and a University Distinguished Professor Endowment to Linda S. Mansfield. Matching support for 16S rRNA gene sequencing was provided through a discretionary funding initiative grant to Linda S. Mansfield from the College of Veterinary Medicine and the Office of the Senior Vice President for Research and Innovation of Michigan State University.

Availability of data and materials

All summarized data is presented within this manuscript “Predominance of *Veillonella* and other allergy agonists in 3-month-old infant gut microbiota was associated with development of

eczema

in early childhood in the Isle of Wight Birth Cohort”. The 16S rRNA gene dataset is available through the DRYAD database and is available for use upon publication.

Ethics approvals

Children were recruited into the “Third Generation Study” under written ethics approval numbers 09/H0504/129 (22 December 2019), 14/SC/0133 (22 December 2019), and 14/SC/1191 (15 November 2016) from the National Research Ethic committees in the UK under the supervision of S. Hasan Arshad, MBBS, DM, FRCP.

REFERENCES

1. Stiemsma LT, Turvey SE. Asthma and the microbiome: defining the critical window in early life. *Allergy Asthma Clin Immunol.* 2017;13:3.
2. Riedler J, Braun-Fahrlander C, Eder W, Schreuer M, Waser M, Maisch S, et al. Exposure to farming in early life and development of asthma and allergy: a cross-sectional survey. *Lancet.* 2001;358(9288):1129-33.
3. Ege MJ, Mayer M, Normand AC, Genuneit J, Cookson WO, Braun-Fahrlander C, et al. Exposure to environmental microorganisms and childhood asthma. *N Engl J Med.* 2011;364(8):701-9.
4. Olszak T, An D, Zeissig S, Vera MP, Richter J, Franke A, et al. Microbial exposure during early life has persistent effects on natural killer T cell function. *Science.* 2012;336(6080):489-93.
5. Zuccotti G, Meneghin F, Aceti A, Barone G, Callegari ML, Di Mauro A, et al. Probiotics for prevention of atopic diseases in infants: systematic review and meta-analysis. *Allergy.* 2015;70(11):1356-71.
6. Ichinohe T, Pang IK, Kumamoto Y, Peaper DR, Ho JH, Murray TS, et al. Microbiota regulates immune defense against respiratory tract influenza A virus infection. *Proc Natl Acad Sci U S A.* 2011;108(13):5354-9.
7. Spergel JM, Paller AS. Atopic dermatitis and the atopic march. *J Allergy Clin Immunol.* 2003;112(6 Suppl):S118-27.
8. von Kobyletzki LB BC, Hasselgren M, Larsson M, Lindström CB, Svensson Å. Eczema in early childhood is strongly associated with the development of asthma and rhinitis in a prospective cohort. *BMC Dermatol.* 2012;12(11).
9. Abrahamsson TR, Jakobsson HE, Andersson AF, Bjorksten B, Engstrand L, Jenmalm MC. Low diversity of the gut microbiota in infants with atopic eczema. *J Allergy Clin Immunol.* 2012;129(2):434-40, 40 e1-2.
10. Abrahamsson TR, Jakobsson HE, Andersson AF, Bjorksten B, Engstrand L, Jenmalm MC. Low gut microbiota diversity in early infancy precedes asthma at school age. *Clin Exp Allergy.* 2014;44(6):842-50.
11. Cahenzli J, Koller Y, Wyss M, Geuking MB, McCoy KD. Intestinal microbial diversity during early-life colonization shapes long-term IgE levels. *Cell Host Microbe.* 2013;14(5):559-70.
12. Simon AK, Hollander GA, McMichael A. Evolution of the immune system in humans from infancy to old age. *Proc Biol Sci.* 2015;282(1821):20143085.
13. Mold JE, Venkatasubrahmanyam S, Burt TD, Michaelsson J, Rivera JM, Galkina SA, et al. Fetal and adult hematopoietic stem cells give rise to distinct T cell lineages in humans. *Science.* 2010;330(6011):1695-9.
14. Tariq SM, Matthews SM, Hakim EA, Stevens M, Arshad SH, Hide DW. The prevalence of and risk factors for atopy in early childhood: a whole population birth cohort study. *J Allergy Clin Immunol.* 1998;101(5):587-93.

15. Arshad SH, Holloway JW, Karmaus W, Zhang H, Ewart S, Mansfield L, et al. Cohort Profile: The Isle Of Wight Whole Population Birth Cohort (IOWBC). *Int J Epidemiol*. 2018;47(4):1043-4i.
16. Arshad SH, Patil V, Mitchell F, Potter S, Zhang H, Ewart S, et al. Cohort Profile Update: The Isle of Wight Whole Population Birth Cohort (IOWBC). *Int J Epidemiol*. 2020;49(4):1083-4.
17. Becker AB AE. Asthma guidelines: the Global Initiative for Asthma in relation to national guideline. *Curr Opin Allergy Clin Immunol*. 2017;17(2):99-103.
18. Sadeghnejad A KW, Davis S, Kurukulaaratchy RJ, Matthews S, Arshad SH. Raised cord serum immunoglobulin E increases the risk of allergic sensitisation at ages 4 and 10 and asthma at age 10. *Thorax*. 2004;59(11):936-42.
19. Severity scoring of atopic dermatitis: the SCORAD index. Consensus Report of the European Task Force on Atopic Dermatitis. *Dermatology*. 1993;186(1):23-31.
20. Asher MI, Keil U, Anderson HR, Beasley R, Crane J, Martinez F, et al. International Study of Asthma and Allergies in Childhood (ISAAC): rationale and methods. *Eur Respir J*. 1995;8(3):483-91.
21. Patil VK, Holloway JW, Zhang H, Soto-Ramirez N, Ewart S, Arshad SH, et al. Interaction of prenatal maternal smoking, interleukin 13 genetic variants and DNA methylation influencing airflow and airway reactivity. *Clin Epigenetics*. 2013;5(1):22.
22. Soto-Ramirez N, Karmaus W, Zhang H, Davis S, Agarwal S, Albergottie A. Modes of infant feeding and the occurrence of coughing/wheezing in the first year of life. *Journal of human lactation : official journal of International Lactation Consultant Association*. 2013;29(1):71-80.
23. Karmaus W, Dobai AL, Ogbuanu I, Arshad SH, Matthews S, Ewart S. Long-term effects of breastfeeding, maternal smoking during pregnancy, and recurrent lower respiratory tract infections on asthma in children. *J Asthma*. 2008;45(8):688-95.
24. Brooks PT, Brakel KA, Bell JA, Bejcek CE, Gilpin T, Brudvig JM, et al. Transplanted human fecal microbiota enhanced Guillain Barre syndrome autoantibody responses after *Campylobacter jejuni* infection in C57BL/6 mice. *Microbiome*. 2017;5(1):92.
25. Hall M, Beiko RG. 16S rRNA Gene Analysis with QIIME2. *Methods Mol Biol*. 2018;1849:113-29.
26. Amir A, McDonald D, Navas-Molina JA, Kopylova E, Morton JT, Zech Xu Z, et al. Deblur Rapidly Resolves Single-Nucleotide Community Sequence Patterns. *mSystems*. 2017;2(2).
27. Rognes T, Flouri T, Nichols B, Quince C, Mahe F. VSEARCH: a versatile open source tool for metagenomics. *PeerJ*. 2016;4:e2584.
28. Santos T, Capelo JL, Santos HM, Oliveira I, Marinho C, Goncalves A, et al. Use of MALDI-TOF mass spectrometry fingerprinting to characterize *Enterococcus* spp. and *Escherichia coli* isolates. *J Proteomics*. 2015;127(Pt B):321-31.

29. Team RC. R: A Language and Environment for Statistical Computing. Vienna, Austria: R Foundation for Statistical Computing; 2020. URL <https://www.R-project.org/>.
30. SAS Institute Inc. SAS and all other SAS Institute Inc. product or service names are registered trademarks or trademarks of SAS Institute Inc. C, NC, USA.
31. Sbihi H, Boutin RC, Cutler C, Suen M, Finlay BB, Turvey SE. Thinking bigger: How early-life environmental exposures shape the gut microbiome and influence the development of asthma and allergic disease. *Allergy*. 2019;74(11):2103-15.
32. Arrieta MC, Stiemsma LT, Dimitriu PA, Thorson L, Russell S, Yurist-Doutsch S, et al. Early infancy microbial and metabolic alterations affect risk of childhood asthma. *Sci Transl Med*. 2015;7(307):307ra152.
33. Bisgaard H, Hermansen MN, Buchvald F, Loland L, Halkjaer LB, Bonnelykke K, et al. Childhood asthma after bacterial colonization of the airway in neonates. *N Engl J Med*. 2007;357(15):1487-95.
34. Hilty M, Burke C, Pedro H, Cardenas P, Bush A, Bossley C, et al. Disordered microbial communities in asthmatic airways. *PLoS One*. 2010;5(1):e8578.
35. Lal CV, Travers C, Aghai ZH, Eipers P, Jilling T, Halloran B, et al. The Airway Microbiome at Birth. *Sci Rep*. 2016;6:31023.
36. Depner M, Taft DH, Kirjavainen PV, Kalanetra KM, Karvonen AM, Peschel S, et al. Maturation of the gut microbiome during the first year of life contributes to the protective farm effect on childhood asthma. *Nat Med*. 2020;26(11):1766-75.
37. Herbst T, Sichelstiel A, Schar C, Yadava K, Burki K, Cahenzli J, et al. Dysregulation of allergic airway inflammation in the absence of microbial colonization. *Am J Respir Crit Care Med*. 2011;184(2):198-205.
38. Lynch SV, Wood RA, Boushey H, Bacharier LB, Bloomberg GR, Kattan M, et al. Effects of early-life exposure to allergens and bacteria on recurrent wheeze and atopy in urban children. *J Allergy Clin Immunol*. 2014;134(3):593-601 e12.
39. Penders J, Gerhold K, Stobberingh EE, Thijs C, Zimmermann K, Lau S, et al. Establishment of the intestinal microbiota and its role for atopic dermatitis in early childhood. *J Allergy Clin Immunol*. 2013;132(3):601-7 e8.
40. Stokholm J, Blaser MJ, Thorsen J, Rasmussen MA, Waage J, Vinding RK, et al. Maturation of the gut microbiome and risk of asthma in childhood. *Nat Commun*. 2018;9(1):141.
41. Louisa Owens IAL, Guicheng Zhang, Stephen Turner & Peter N Le Souëf. Prevalence of allergic sensitization, hay fever, eczema, and asthma in a longitudinal birth cohort. *Journal of Asthma and Allergy*. 2018;11:173-80.
42. Ta LDH, Chan JCY, Yap GC, Purbojati RW, Drautz-Moses DI, Koh YM, et al. A compromised developmental trajectory of the infant gut microbiome and metabolome in atopic eczema. *Gut Microbes*. 2020;12(1):1-22.
43. Sher AA, VanAllen ME, Ahmed H, Whitehead-Tillery C, Rafique S, Bell JA, et al. Conjugative RP4 Plasmid-Mediated Transfer of Antibiotic Resistance Genes to Commensal and Multidrug-Resistant Enteric Bacteria In Vitro. *Microorganisms*. 2023;11(1).

44. Jolley KA, Bray JE, Maiden MCJ. Open-access bacterial population genomics: BIGSdb software, the PubMLST.org website and their applications. *Wellcome Open Res.* 2018;3:124.
45. Zhou Z, Alikhan NF, Mohamed K, Fan Y, Agama Study G, Achtman M. The Enterobase user's guide, with case studies on Salmonella transmissions, Yersinia pestis phylogeny, and Escherichia core genomic diversity. *Genome Res.* 2020;30(1):138-52.
46. Könönen E. 250 - Anaerobic Cocci and Anaerobic Gram-Positive Nonsporulating Bacilli. 8 ed. John E. Bennett RD, Martin J. Blaser, editor 2015.
47. Berenger BM, Chui L, Borkent A, Lee MC. Anaerobic urinary tract infection caused by Veillonella parvula identified using cystine-lactose-electrolyte deficient media and matrix-assisted laser desorption ionization-time of flight mass spectrometry. *IDCases.* 2015;2(2):44-6.
48. Ito Y, Nakayama H, Niitsu Y, Kaneko N, Otsuka M, Sawada Y, et al. The first case of Veillonella atypica bacteremia in a patient with renal pelvic tumor. *Anaerobe.* 2022;73:102491.
49. Andréanne Morin CGM, Casper-Emil T. Pedersen, Jakob Stokholm, Bo L. Chawes, Ann-Marie Malby Schoos, Katherine A. Naughton, Jonathan Thorsen, Martin S. Mortensen, Donata Vercelli, Urvish Trivedi, Søren J. Sørensen, Hans Bisgaard, Dan L. Nicolae, Klaus Bønnelykke, Carole Ober. Epigenetic landscape links upper airway microbiota in infancy with allergic rhinitis at 6 years of age. *Journal of Allergy and Clinical Immunology.* 2020;146(6):1358-66.
50. Salameh M, Burney Z, Mhaimed N, Laswi I, Yousri NA, Bendriss G, et al. The role of gut microbiota in atopic asthma and allergy, implications in the understanding of disease pathogenesis. *Scand J Immunol.* 2020;91(3):e12855.
51. Zheng H, Liang H, Wang Y, Miao M, Shi T, Yang F, et al. Altered Gut Microbiota Composition Associated with Eczema in Infants. *PLoS One.* 2016;11(11):e0166026.

APPENDIX

Table 2.4 OUT number to taxa conversion table.

S1 Table. OTU number to Taxa Conversion Table						
OTU Number	Phylum	Class	Order	Family	Genus	Species
OTU_1	Actinobacteria	Actinobacteria	Bifidobacteriales	Bifidobacteriaceae	<i>Bifidobacterium.Ambiguous_taxa</i>	NaN
OTU_2	Actinobacteria	Actinobacteria	Bifidobacteriales	Bifidobacteriaceae	<i>Bifidobacterium</i>	NaN
OTU_3	Actinobacteria	Coriobacteria	Coriobacteriales	Coriobacteriaceae	<i>Collinsella</i>	uncultured.bacterium
OTU_4	Actinobacteria	Coriobacteria	Coriobacteriales	Coriobacteriaceae	<i>Enterorhabdus</i>	uncultured.bacterium
OTU_5	Bacteroidetes	Bacteroidia	Bacteroidales	Bacteroidaceae	<i>Bacteroides</i>	uncultured.bacterium
OTU_6	Bacteroidetes	Bacteroidia	Bacteroidales	Bacteroidaceae	<i>Bacteroides</i>	NaN
OTU_7	Bacteroidetes	Bacteroidia	Bacteroidales	Porphyromonadaceae	<i>Dysgonomonas</i>	NaN
OTU_8	Bacteroidetes	Bacteroidia	Bacteroidales	Porphyromonadaceae	<i>Parabacteroides</i>	NaN
OTU_9	Bacteroidetes	Bacteroidia	Bacteroidales	Prevotellaceae	<i>Prevotella.9</i>	uncultured.bacterium
OTU_10	Bacteroidetes	Bacteroidia	Bacteroidales	Prevotellaceae	<i>Prevotellaceae.NK3B31.group</i>	uncultured.bacterium
OTU_11	Bacteroidetes	Bacteroidia	Bacteroidales	Rikenellaceae	<i>Alistipes</i>	uncultured.bacterium
OTU_12	Bacteroidetes	Bacteroidia	Bacteroidales	Rikenellaceae	<i>Alistipes</i>	NaN
OTU_13	Firmicutes	Bacilli	Bacillales	Staphylococcaceae	<i>Staphylococcus</i>	NaN
OTU_14	Firmicutes	Bacilli	Lactobacillales	Enterococcaceae	<i>Enterococcus</i>	NaN
OTU_15	Firmicutes	Bacilli	Lactobacillales	Lactobacillaceae	<i>Lactobacillus</i>	<i>Lactobacillus.casei</i>
OTU_16	Firmicutes	Bacilli	Lactobacillales	Lactobacillaceae	<i>Lactobacillus</i>	uncultured.bacterium
OTU_17	Firmicutes	Bacilli	Lactobacillales	Lactobacillaceae	<i>Lactobacillus</i>	NaN
OTU_18	Firmicutes	Bacilli	Lactobacillales	Streptococcaceae	<i>Lactococcus</i>	NaN
OTU_19	Firmicutes	Bacilli	Lactobacillales	Streptococcaceae	<i>Streptococcus</i>	uncultured.bacterium
OTU_20	Firmicutes	Clostridia	Clostridiales	Clostridiaceae.1	<i>Clostridium.sensu.stricto.13</i>	NaN
OTU_21	Firmicutes	Clostridia	Clostridiales	Clostridiaceae.1	<i>Clostridium.sensu.stricto.1</i>	uncultured.bacterium
OTU_22	Firmicutes	Clostridia	Clostridiales	Clostridiaceae.1	<i>Clostridium.sensu.stricto.1</i>	NaN
OTU_23	Firmicutes	Clostridia	Clostridiales	Clostridiaceae.1	<i>Sarcina</i>	uncultured.bacterium
OTU_24	Firmicutes	Clostridia	Clostridiales	Eubacteriaceae	NaN	NaN
OTU_25	Firmicutes	Clostridia	Clostridiales	Lachnospiraceae	<i>Anaerostipes</i>	uncultured.bacterium
OTU_26	Firmicutes	Clostridia	Clostridiales	Lachnospiraceae	<i>Anaerostipes</i>	NaN
OTU_27	Firmicutes	Clostridia	Clostridiales	Lachnospiraceae	<i>Blautia</i>	uncultured.bacterium
OTU_28	Firmicutes	Clostridia	Clostridiales	Lachnospiraceae	<i>Coprococcus.2</i>	uncultured.bacterium
OTU_29	Firmicutes	Clostridia	Clostridiales	Lachnospiraceae	<i>Dorea</i>	NaN
OTU_30	Firmicutes	Clostridia	Clostridiales	Lachnospiraceae	<i>Fusicatenibacter</i>	NaN
OTU_31	Firmicutes	Clostridia	Clostridiales	Lachnospiraceae	<i>Hungateella</i>	NaN
OTU_32	Firmicutes	Clostridia	Clostridiales	Lachnospiraceae	<i>Lachnoclostridium</i>	uncultured.organism
OTU_33	Firmicutes	Clostridia	Clostridiales	Lachnospiraceae	<i>Lachnoclostridium</i>	NaN
OTU_34	Firmicutes	Clostridia	Clostridiales	Lachnospiraceae	<i>Lachnospira</i>	uncultured.bacterium
OTU_35	Firmicutes	Clostridia	Clostridiales	Lachnospiraceae	<i>Lachnospiraceae.NK4A136.group</i>	uncultured.bacterium
OTU_36	Firmicutes	Clostridia	Clostridiales	Lachnospiraceae	<i>Lachnospiraceae.NK4A136.group</i>	NaN
OTU_37	Firmicutes	Clostridia	Clostridiales	Lachnospiraceae	<i>Lachnospiraceae.UCG.004</i>	NaN
OTU_38	Firmicutes	Clostridia	Clostridiales	Lachnospiraceae	<i>Roseburia</i>	uncultured.bacterium
OTU_39	Firmicutes	Clostridia	Clostridiales	Lachnospiraceae	<i>Sellimonas</i>	uncultured.bacterium
OTU_40	Firmicutes	Clostridia	Clostridiales	Lachnospiraceae	<i>Tyzzerella.3</i>	uncultured.bacterium
OTU_41	Firmicutes	Clostridia	Clostridiales	Lachnospiraceae	<i>.Eubacterium..elgens.group</i>	NaN
OTU_42	Firmicutes	Clostridia	Clostridiales	Lachnospiraceae	<i>.Eubacterium..hallii.group</i>	uncultured.bacterium
OTU_43	Firmicutes	Clostridia	Clostridiales	Lachnospiraceae	<i>.Ruminococcus..torques.group</i>	uncultured.bacterium
OTU_44	Firmicutes	Clostridia	Clostridiales	Lachnospiraceae	<i>.Ruminococcus..torques.group</i>	NaN

Table 2.4 (cont'd)

S1 Table. OTU number to Taxa Conversion Table						
OTU Number	Phylum	Class	Order	Family	Genus	Species
OTU_45	Firmicutes	Clostridia	Clostridiales	Lachnospiraceae	NaN	NaN
OTU_46	Firmicutes	Clostridia	Clostridiales	Peptostreptococcaceae	Peptoclostridium	uncultured.bacterium
OTU_47	Firmicutes	Clostridia	Clostridiales	Peptostreptococcaceae	NaN	NaN
OTU_48	Firmicutes	Clostridia	Clostridiales	Ruminococcaceae	Faecalibacterium	uncultured.bacterium
OTU_49	Firmicutes	Clostridia	Clostridiales	Ruminococcaceae	Ruminiclostridium.5	uncultured.bacterium
OTU_50	Firmicutes	Clostridia	Clostridiales	Ruminococcaceae	Ruminiclostridium.5	uncultured.organism
OTU_51	Firmicutes	Clostridia	Clostridiales	Ruminococcaceae	Ruminococcaceae.UCG.013	uncultured.bacterium
OTU_52	Firmicutes	Clostridia	Clostridiales	Ruminococcaceae	Ruminococcus.1	NaN
OTU_53	Firmicutes	Clostridia	Clostridiales	Ruminococcaceae	Ruminococcus.2	uncultured.bacterium
OTU_54	Firmicutes	Clostridia	Clostridiales	Ruminococcaceae	Subdoligranulum	uncultured.bacterium
OTU_55	Firmicutes	Clostridia	Clostridiales	Ruminococcaceae	.Eubacterium..coprostanoligenes.group	uncultured.bacterium
OTU_56	Firmicutes	Clostridia	Clostridiales	Ruminococcaceae	uncultured	uncultured.bacterium
OTU_57	Firmicutes	Clostridia	Clostridiales	Ruminococcaceae	uncultured	NaN
OTU_58	Firmicutes	Clostridia	Clostridiales	Ruminococcaceae	NaN	NaN
OTU_59	Firmicutes	Erysipelotrichia	Erysipelotrichales	Erysipelotrichaceae	Erysipelatoclostridium	NaN
OTU_60	Firmicutes	Erysipelotrichia	Erysipelotrichales	Erysipelotrichaceae	Erysipelotrichaceae.UCG.003	uncultured.bacterium
OTU_61	Firmicutes	Erysipelotrichia	Erysipelotrichales	Erysipelotrichaceae	.Clostridium..innocuum.group	NaN
OTU_62	Firmicutes	Erysipelotrichia	Erysipelotrichales	Erysipelotrichaceae	NaN	NaN
OTU_63	Firmicutes	Negativicutes	Selenomonadales	Acidaminococcaceae	Phascolarctobacterium	uncultured.bacterium
OTU_64	Firmicutes	Negativicutes	Selenomonadales	Veillonellaceae	Megamonas	uncultured.bacterium
OTU_65	Firmicutes	Negativicutes	Selenomonadales	Veillonellaceae	Megasphaera	uncultured.bacterium
OTU_66	Firmicutes	Negativicutes	Selenomonadales	Veillonellaceae	Megasphaera	NaN
OTU_67	Firmicutes	Negativicutes	Selenomonadales	Veillonellaceae	Veillonella	uncultured.bacterium
OTU_68	Fusobacteria	Fusobacteria	Fusobacteriales	Fusobacteriaceae	Fusobacterium	NaN
OTU_69	Proteobacteria	Alphaproteobacteria	Rhodospirillales	Rhodospirillaceae	uncultured	NaN
OTU_70	Proteobacteria	Betaproteobacteria	Burkholderiales	Alcaligenaceae	Sutterella	uncultured.bacterium
OTU_71	Proteobacteria	Betaproteobacteria	Burkholderiales	Alcaligenaceae	Sutterella	NaN
OTU_72	Proteobacteria	Betaproteobacteria	Burkholderiales	Burkholderiaceae	Ralstonia	NaN
OTU_73	Proteobacteria	Deltaproteobacteria	Desulfovibrionales	Desulfovibrionaceae	Desulfovibrio	NaN
OTU_74	Proteobacteria	Gammaproteobacteria	Enterobacteriales	Enterobacteriaceae	Citrobacter	NaN
OTU_75	Proteobacteria	Gammaproteobacteria	Enterobacteriales	Enterobacteriaceae	Escherichia.Shigella	NaN
OTU_76	Proteobacteria	Gammaproteobacteria	Enterobacteriales	Enterobacteriaceae	Klebsiella	NaN
OTU_77	Proteobacteria	Gammaproteobacteria	Enterobacteriales	Enterobacteriaceae	NaN	NaN
OTU_78	Proteobacteria	Gammaproteobacteria	Pasteurellales	Pasteurellaceae	Haemophilus	uncultured.bacterium
OTU_79	Proteobacteria	Gammaproteobacteria	Pasteurellales	Pasteurellaceae	NaN	NaN
OTU_80	Verrucomicrobia	Verrucomicrobiae	Verrucomicrobiales	Verrucomicrobiaceae	Akkermansia	uncultured.bacterium

CHAPTER 3: Fecal microbiota transplants of three distinct human communities to germ-free mice exacerbated inflammation and decreased lung function in their offspring

This chapter is from a manuscript submitted for publication:

Ivon Moya Uribe, Hinako Terauchi, Julia A. Bell, Alexander Zanetti, Sanket Jantre, Marianne Huebner, S. Hasan Arshad, Susan L. Ewart, Linda S. Mansfield. Fecal microbiota transplants of three distinct human communities to germ-free mice exacerbated inflammation and decreased lung function in their offspring, In review for mBio. (Co-First authors)

Abstract

Lack of appropriate microbial exposure in early life has emerged as a key factor explaining explosive rise in allergies and autoimmune diseases [1, 2], yet little is known about effects of gut microbiota on postnatal immune development. We hypothesized that *Enterobacteriaceae*-dominant gut microbiota from eczemic infants would cause increased T helper 2 (Type 2) inflammation and decreased lung function after house dust mite antigen (HDM) exposure in transplanted mice, while *Bacteroidaceae*-dominant gut microbiota from non-eczemic infants would be protective. Mixed fecal slurries from 3-month-old infants of the Isle of Wight 3rd generation birth cohort designated “Infant A” (eczema positive) and “Infant B” (eczema negative) were transplanted into germ-free C57BL/6 mice. Infant A and B offspring were used to test effects of specific microbiotas on allergic airway disease with and without HDM compared to C57BL/6 mice with mouse microbiota (Mouse negative control) and with adult human-derived microbiota (Adult C positive control). Infant A and B microbiotas were successfully transplanted, maintained initial levels of diversity, and passed to offspring largely unchanged. Baseline lung mechanics (without methacholine [MCh]) for mice with three human-derived microbiotas were significantly different from Mouse microbiota controls in both non-allergic (PBS treated) and allergic (HDM treated) mice. Respiratory system resistance (Rrs) was increased ($p < 0.05$ to $p < 0.01$) and respiratory system compliance (Crs) was decreased ($p < 0.05$ to $p < 0.01$) in mice carrying all three human microbiotas. Measures of airway hyperresponsiveness (AHR) showed higher estimated means of peak Rrs and peripheral airway resistance (G) with each unit increase of MCh for mice carrying Infant A, Infant B or Adult C microbiota compared to Mouse negative controls; differences were significant only in Infant B mice ($p < 0.0119$). Differences between microbiotas were mainly due to increases in resistance in smaller airways and in tissue resistance. HDM treatment significantly elevated IL-4, eosinophils, lung inflammation and mucus cell metaplasia and decreased macrophages and lung function ($p < 0.05$) in mice of all microbiotas. Human-derived microbiotas produced distinct features. Infant B and Adult C mice had significantly elevated basal levels of total IgE compared to negative controls ($p < 0.05$), while Infant A mice did not. In human-derived microbiota mice given HDM, only Adult C mice had significantly elevated IL-5 and IL-13 ($p < 0.05$). HDM treated Adult C and Infant B mice had significantly elevated neutrophils ($p < 0.05$), while HDM treated Infant A mice had significantly elevated lymphocytes ($p < 0.01$). Allergy agonists were

abundant in human-derived microbiotas compared to mouse microbiotas, while allergy antagonists were numerous in mouse microbiotas and low in human-derived microbiotas. Pro-inflammatory taxa were abundant in human-derived microbiotas and low or absent in mouse microbiotas, while anti-inflammatory taxa were abundant in mouse microbiotas and few in human-derived microbiotas.

Importance

Data support multiple proinflammatory allergy agonists functioning in a community-wide fashion to impair lung function in the absence of antagonistic anti-inflammatory taxa. The structure of these human-derived microbiotas played an important role in determining the characteristics of these varied allergic responses and the resulting lung impairment, yet all three human-derived microbiotas had detrimental effects on lung function even in the absence of the allergen. Using a comparative approach, we showed that composition of gut microbiota can alter innate/immune regulation in the gut-lung axis to increase baseline responses and the risk of allergic sensitization.

Introduction

Asthma is a chronic airway disease characterized by inflammation and airway hyper-responsiveness (AHR) with a prevalence of 7.9% in the US population [164]. It is the most common chronic condition among children worldwide according to WHO and may be preceded by eczema, wheeze or atopy [38]. The exact etiology of asthma is yet unknown, however, multiple factors have been associated with its development, such as genetics, mode of birth, childhood setting, early animal exposures, use of antibiotics, and, more recently, composition of the gut and lung microbiota [44-49, 131, 137, 147, 165-168]. AHR, a cardinal feature of asthma, is a state in which the airways constrict excessively in response to either a direct stimulus (e.g. histamine, methacholine) that acts directly on receptors of the airway smooth muscle (ASM) or an indirect stimulus (e.g. allergen)[41]. AHR can be present in both allergic and non-allergic asthmatic patients and is associated with other diseases such as chronic obstructive pulmonary disease [42, 169]. The degree of AHR in asthma is correlated with disease severity, often precedes asthma in children, and is a main therapeutic target for the management of exacerbated symptoms [170]. Yet mechanisms underlying AHR are heterogeneous and include genetic

factors, ASM alterations, airway extracellular matrix component remodeling, and airway inflammation [170, 171]. Hyperresponsiveness is characterized by functional changes in airway resistance and lung elastic properties; these changes are commonly assessed by measuring lung function [170].

Specific microbiota or microbes have been linked to the pathogenesis of allergies, including asthma, eczema, and food allergies [63]. Development of the respiratory microbiota depends heavily on exposures during the first few hours of life onward, which are dependent upon delivery mode, early environment, and infections among other factors [2, 172, 173]. In one study, tracheal aspirates soon after birth showed dominant *Firmicutes* and *Proteobacteria* with presence of *Actinobacteria* and *Bacteroidetes* [150]. Bisgaard et al. showed that in 1 month-old infants, bacterial colonization of the hypopharyngeal region of the airway with *Streptococcus pneumoniae*, *Haemophilus influenzae*, or *Moraxella catarrhalis* was associated with later development of asthma [148]. In the lower respiratory tract, *Proteobacteria*, including those of the genera *Haemophilus*, *Moraxella* and *Neisseria*, were over-represented in asthma patients compared to non-asthmatic volunteers [149].

Studies on the gut-lung axis have examined the role of gut microbiota on allergic airway disease. Reduced diversity of fecal bacterial microbiota in infants at 1 or 12 months of age was associated with increased risk of allergic sensitization, allergic rhinitis, and peripheral blood eosinophilia at 5 years [174]. Penders and colleagues examined the composition of the infant fecal microbiota in association with development of atopic dermatitis and food allergy. They found that increased *Clostridium* cluster I prevalence at ages 5 and 13 weeks was positively associated with development of atopic dermatitis [152]. Likewise, increased risk of asthma at 5 years was found to be significantly associated with increased abundance of *Veillonella* and decreased abundance of *Roseburia*, *Alistipes* and *Flavonifractor* in fecal microbiota at 1 year of age when compared to children without an asthma diagnosis [55]. Lack of protective taxa have also been implicated in asthma pathogenesis. Lynch *et al.* studied early life house dust exposures and showed that abundant *Firmicutes* and *Bacteroidetes* bacteria reduced asthma risk in the inner-city high asthma prevalence Urban Environment and Childhood Asthma cohort [151]. Arrieta et al. showed that decreased abundance of the genera *Lachnospira*, *Veillonella*, *Faecalibacterium*, and *Rothia* and both associated decreases in fecal acetate and dysregulation of enterohepatic metabolites occurred in children who developed asthma [2]. Depner and colleagues

demonstrated that the protective effect of farm exposures in reducing asthma prevalence was partially mediated by maturation of the gut microbiota in the first year of life; protection was correlated with bacterial taxa predicted to produce butyrate and increased abundance of genes encoding butyryl-CoA:acetate-CoA-transferase [102]. Bacterial taxa contributing to these protective effects included *Roseburia* and *Coproccoccus*. These studies strongly suggest that microbiota composition influences allergic susceptibility.

Mouse models also support the role of early life microbiota in modulating allergic sensitization [80-82]. Herbst et al showed that upregulation of allergic airway inflammation occurred in germ-free mice and could be reversed by colonizing the mice with specific pathogen free commensal gut microbiota in early life at least 4 weeks before sensitizing mice to ovalbumin [82]. In a related study, germ-free mice and those with low-diversity gut microbiota developed greatly elevated serum IgE levels and increased mast-cell-surface-bound IgE leading to exaggerated oral ovalbumin-induced systemic anaphylaxis [81]. This effect could be prevented by active colonization with mouse specific pathogen free microbiota during a critical time window in early life. In limited-flora gnotobiotic mice, Stefka and colleagues determined that specific *Clostridia* within the gut microbiota regulated innate lymphoid cell function and intestinal epithelial permeability by an innate lymphoid cell-3 (ILC3) and IL-22-dependent mechanism to protect against allergen sensitization [80]. Moreover, mice fed house dust from homes with dogs exhibited significantly reduced bronchial responsiveness and lung inflammation after both allergic challenge and inoculation with respiratory syncytial virus [175]. Despite these studies, knowledge gaps still exist regarding the specific taxa and mechanisms in early childhood by which the gut microbiota influences development of asthma and allergic diseases [176].

Our long-term goal is to determine the role of the early infant microbiota in providing resistance or enhancing susceptibility to allergic diseases. To discover bacterial taxa associated with allergic disease or protection from it in an early trial, we conducted 16S rRNA gene sequencing of fecal samples of 60 infants at 3 months of age and tested clinical indicators of allergy over the first three years of life in an ongoing prospective longitudinal study of the offspring of the well-characterized Isle of Wight (IOW) birth cohort [131]. Infants that harbored low diversity microbial communities with increased abundance of *Escherichia coli/Shigella* had higher risk for eczema, while high diversity microbial communities with high *Bacteroides* abundance were associated with protection against eczema. As eczema often precedes asthma,

these results suggested the possibility of a relationship between the microbiota and asthma [177]. We hypothesized that offspring of mice transplanted with *Escherichia coli/Shigella/Bifidobacterium* enriched microbiotas from infants with persistent eczema would develop allergic inflammation and have a lower threshold to methacholine (MCh)-induced AHR when sensitized to house dust mite antigen (HDM) and, conversely, mice without these taxa but with high levels of *Bacteroides* spp. would be protected. Selected fecal samples from infants with persistent eczema and from infants with no discernible allergic manifestations were transplanted into germ-free C57BL/6 mice. Offspring from germ-free mice transplanted with microbiota from healthy young adults (Adult C) demonstrated a Type 2 immune bias to *Campylobacter jejuni* in our previous study and served in this study as a positive control for AHR after HDM sensitization [140]. Using these three types of transplanted mice and conventional mouse microbiota negative control mice that were all of the same C57BL/6 genetic background, we conducted a study to link early microbiota composition to development of allergic hyperresponsiveness with and without exposure to HDM. Our objectives in these studies were 1) to provide proof-of-concept for transplanted human microbiota mouse models of allergic asthma and 2) to study mechanisms underlying microbial effects on infant allergy related to the Isle of Wight birth cohort participants.

Results

Selection of infant fecal microbiotas for transplant (Figure 3.1)

Fecal samples from sixty 3-month-old infants were analyzed in a preliminary trial in an ongoing multigenerational prospective longitudinal study of newborns (Isle of Wight third generation birth cohort) using 16S rRNA gene sequencing to examine the association of bacterial taxa profiles with risk of eczema [131]. Three-month-old infants harboring a fecal microbiota with increased abundance of *Escherichia coli-Shigella* and *Bifidobacterium* had higher risk for eczema at 1–3 years based on SIMPER (similarity percentage) analysis of bacterial taxa OTUs, while infants with higher abundance of fecal *Bacteroides* were non-eczemic (Figure 3.1A). Representative fecal samples from infants with and without eczema were selected for transplant into mice based on the 16S rRNA gene sequencing analysis (Figure 3.1B), canonical correspondence analysis (CCA), and SIMPER results. Four samples with elevated *Enterobacteriaceae* that were also closely grouped in the CCA were selected and designated as

Infant A microbiota (Figure 3.1B). All of these fecal samples had high levels of *Escherichia/Shigella* and low levels of *Bacteroides* 16S sequence reads, and these infants had eczema diagnosed at 4 or 5 time points between 3 and 36 months of age. Likewise, three fecal samples with high levels of *Bacteroides* reads from infants with no evidence of eczema or other allergic responses were selected and designated as Infant B microbiota (Figure 3.1B). Fecal samples were handled in an anaerobic chamber, mixed in equal volumes and stored for transplant at minus 80°C.

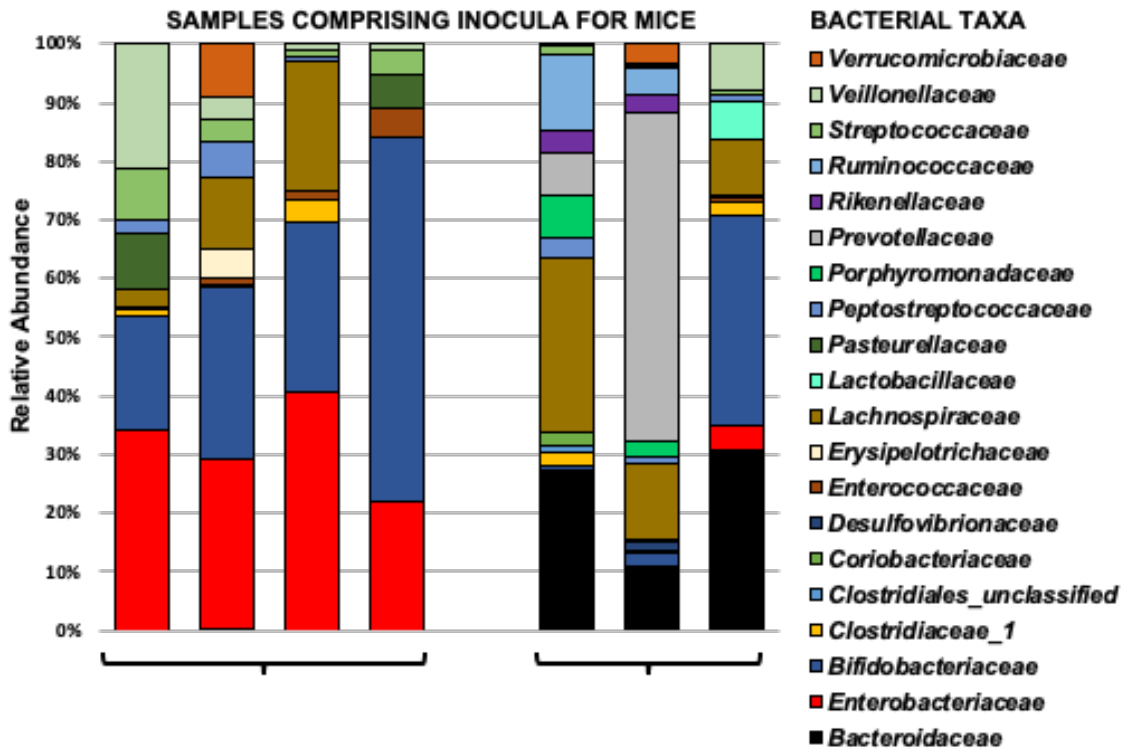
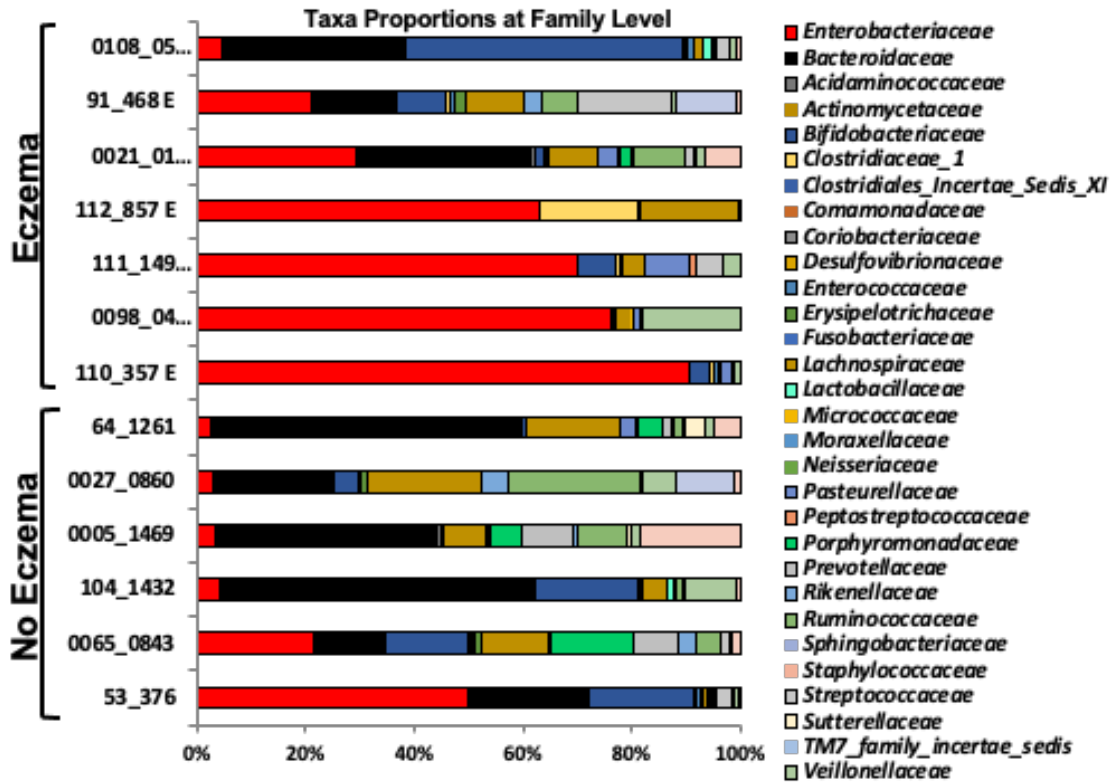


Figure 3.1 Relative abundance of fecal bacterial taxa in Isle of Wight 3-month-old infants. A) Taxa proportions in eczemic and non-eczemic infant samples. B) Infant samples used to inoculate germ free mice.

Fecal Microbiota Transplantation (FMT) of inocula and experimental mice

Transplant procedure and starting inocula (Figure 3.2)

Mixed fecal slurries from Isle of Wight 3-month-old infants with persistent eczema designated “Infant A” and without eczema designated “Infant B” were transplanted into germ-free mice via oral gavage. First and second-generation offspring of transplanted mice were used to conduct two experiments to test the effects of Infant A and B microbiotas on enhancing allergic airway disease after HDM exposure. Individual mouse-to-mouse variation in the three human-derived fecal communities was minimal (Figure 3.2A). Mice with mouse microbiota were only slightly more variable in this regard (Figure 3.2A). Principal components analysis (PCA) showed that all four microbiotas in mice were distinct (Figure 3.2B). PCA comparing human-derived Infant A, Infant B and Adult C microbiotas showed that all three human-derived microbiotas were distinct (Figure 3.2C). Bacterial taxa contributing to separation in dimension 1 of the PCA of all four microbiotas and accounting for 72% of the variance between Infant A, Infant B, Adult C and Mouse microbiotas included *Bacteroides* uncultured, *Bacteroidales* S24.7 uncultured, and *Faecalibacterium*, while those contributing to dimension 2 and accounting for 8.1% of the variance were *Bacteroides* uncultured, *Lachnospiraceae*, *Bacteroidales* S24.7, *Faecalibacterium*, *Alistipes* and *Bacteroides* (Figure 3.2B). Bacterial taxa contributing to separation in dimension 1 of the PCA of the three transplanted microbiotas and accounting for 42.5% of the variance between Infant A, Infant B, and Adult C microbiotas included *Bacteroides* uncultured, *Alistipes*, *Bacteroides* and *Coprobacter*, while those contributing to dimension 2 and accounting for 21.5% of the variance were *Lachnospiraceae* and *Alistipes* (Figure 3.2C). The dendrogram based on UPGMA analysis of mice in experiment 1 showed that experimental mice with the same microbiota given either Dulbecco’s Phosphate Buffered Saline (PBS) or HDM (Figure 3.2D) grouped with their similar microbiotas post treatment. These results showed that experimental treatment with HDM allergen did not cause large shifts in the microbiota.

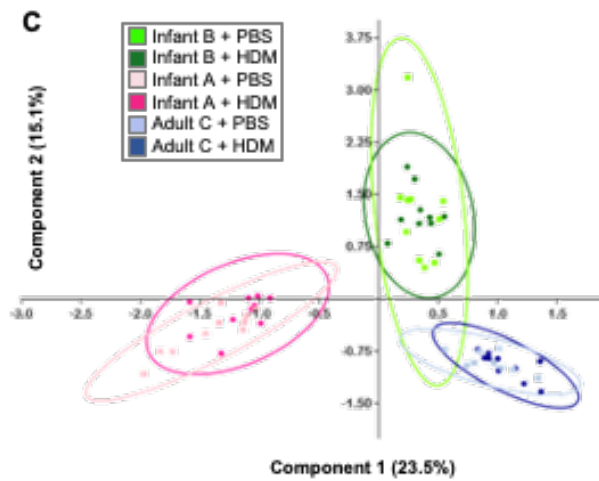
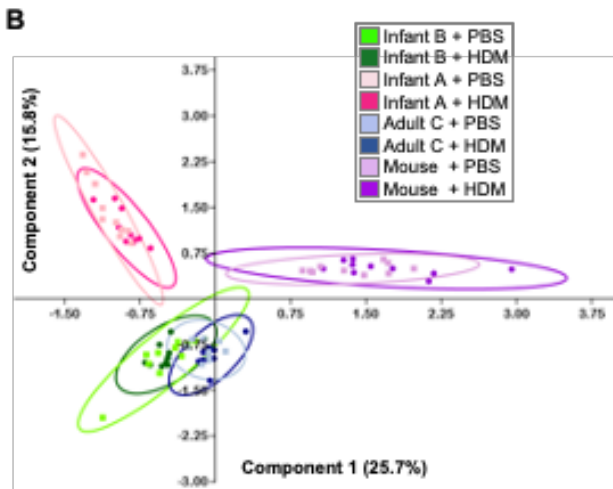
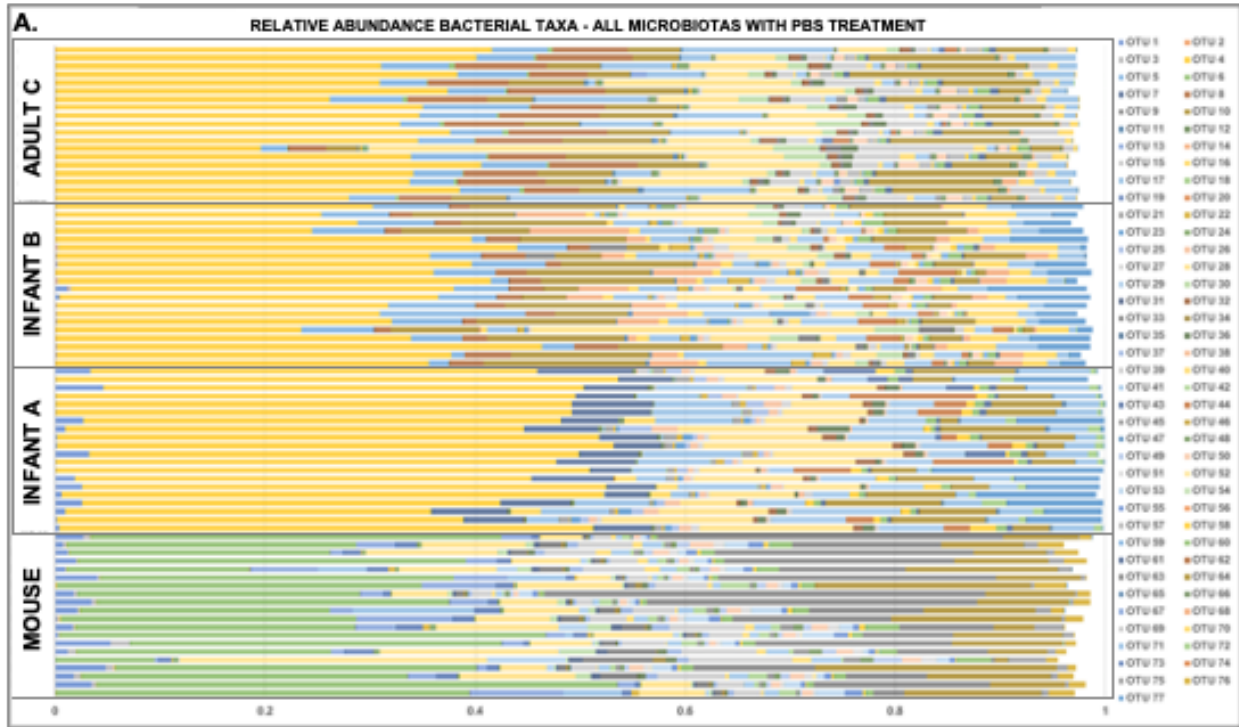
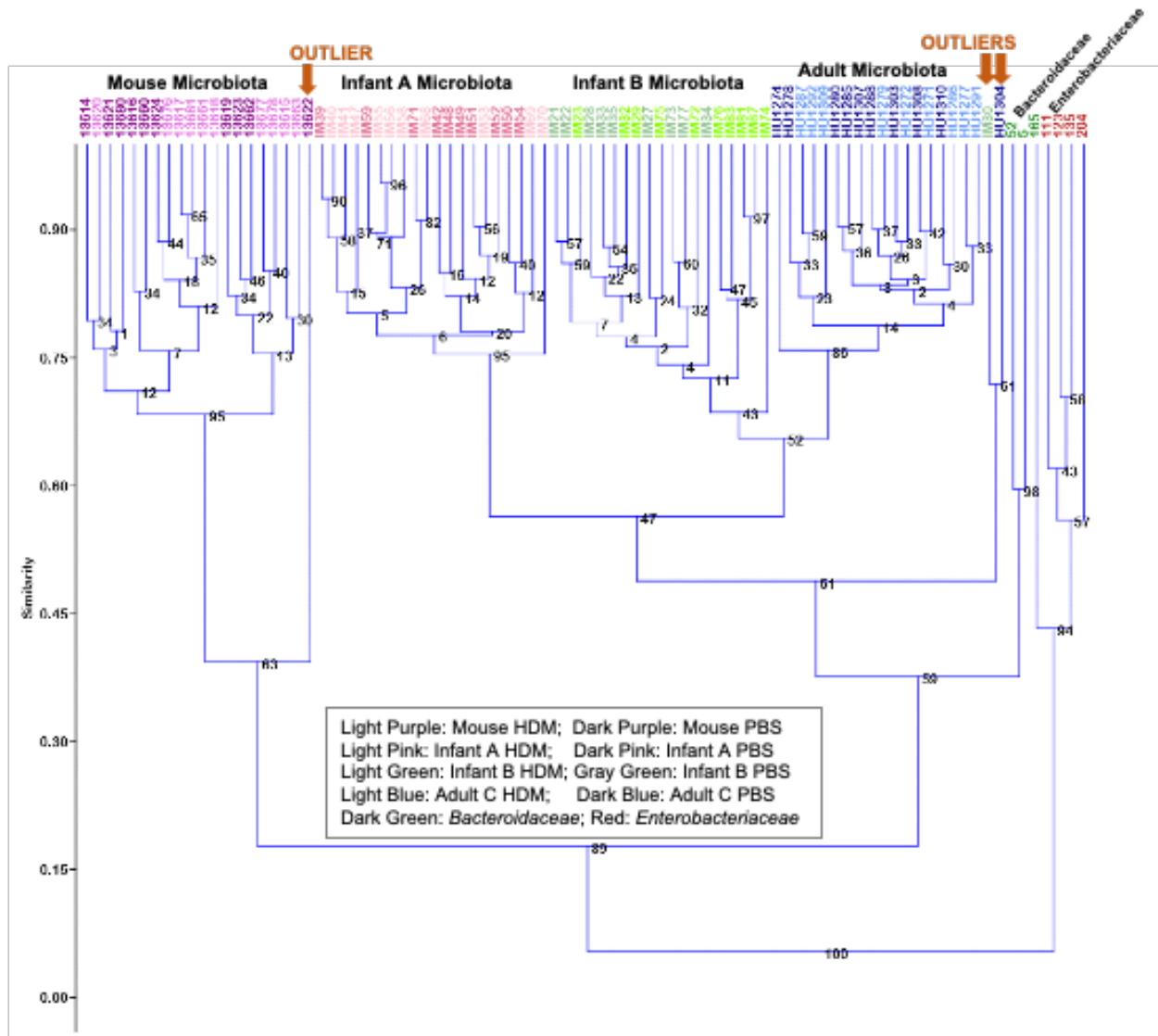


Figure 3.2 Comparisons of 16S rRNA gene sequencing of all mouse groups. (A) shows relative taxa abundance of mice in all experimental groups, showing Adult C, Infant A, Infant B and Mouse microbiotas. (B) Principal components analysis (PCA) of Infant A, Infant B, Adult C and Mouse microbiota bacterial taxa abundance. (C) PCA of Infant A, Infant B and Adult C human-derived microbiota bacterial taxa abundance. (D) UPGMA clustering with Bray Curtis similarity index with 1000 bootstrap replications of all mouse samples and *Enterobacteriaceae* or *Bacteroidaceae* dominant inocula showing clustering by microbiota groups. Treatment of mice with phosphate buffered saline (PBS) or house dust mite (HDM) did not produce recognizable differences in fecal bacterial taxa. Outliers are shown with arrows.

Figure 3.2 (cont'd)



Outcome of inocula transfer to Infant A and B mice after stabilization, adaptation to mouse diet, and breeding (Figure 3.3A).

Microbiota that remained in transplanted mice were passed to the offspring largely unchanged although abundances of bacterial taxa were altered and some taxa did not persist (Figure 3.3A). For example, Infant A mice did not retain *Ruminiclostridium* or *Mollicutes* taxa that were at very low abundance in the inoculum. SIMPER analysis was used to determine the contribution of each taxon to the observed similarity (or dissimilarity) between samples (Figure 3.3A and B). When considering the higher abundance taxa in the Infant A inoculum, we found that

Bifidobacterium, *E. coli-Shigella*, *Lachnospiraceae*, *Roseburia*, *Peptoclostridium* and *Streptococcus* transferred to mice and decreased in abundance, while *Clostridium sensu stricto*, *Akkermansia*, *Desulfovibrio*, *Peptostreptococcaceae* and *Veillonella* transferred and increased in abundance. When considering the higher abundance taxa in the Infant B inoculum, we found that *Bifidobacterium*, *Bacteroides*, *E. coli-Shigella*, *Lachnospiraceae*, *Prevotella*, *Peptoclostridium* and *Streptococcus* transferred to mice and decreased in abundance, while uncultured *Bacteroides*, *Lachnospiraceae* NK4A136, *Alistipes*, *Clostridium sensu stricto*, *Akkermansia*, *Sutterella*, *Peptostreptococcaceae*, uncultured *Lachnospiraceae*, *Lachnoclostridium* and *Christensenellaceae* R-7 transferred and increased in abundance. The remainder of the taxa in Infant A and B inocula transferred to mice and remained at similar abundances.

Comparison of transplanted human-derived community compositions (Figure 3.3B)

The human-derived microbiotas were largely distinct. Bacterial taxa present in the three human-derived communities but absent in the mouse communities included *Akkermansia*, *Parasutterella*, *Sutterella*, *Peptostreptococcaceae* and *Lachnoclostridium*. An uncultured *Bacteroides* taxon was elevated in all three human-derived microbial communities but not present in mice with mouse microbiota. An OTU identified as *Escherichia-Shigella* was abundant in Infant A, present at very low levels in Infant B, and undetectable in Adult C human-derived microbiotas. *Bifidobacterium* and *Akkermansia* were more abundant in Infant A than in Infant B mice. One bacterial taxon in Infant A mice that did not appear in Infant B mice was *Coprobacter*. Several taxa were more abundant in Infant B than Infant A mice, including *Alistipes*, *Parabacteroides*, *Lactobacillus*, *Parasutterella* uncultured, *Sutterella*, a member of the family *Lachnospiraceae*, *Roseburia*, *Ruminiclostridium* and *Blautia*. Further, Infant A mice had *Klebsiella* that was not present in the other microbiotas. Bacterial taxa present in Adult C microbiotas and not present in either Infant microbiota included *Lactobacillus*, *Parasutterella* and a member of the *Clostridiales* vadinBB60 group. Thus, there were bacterial taxa shared between microbiotas and those that were distinct to each microbiota studied.

Bacterial Taxa	Inocula Groups		Microbiota Groups in Mice				Major Loadings on Indicated PCA axes	
	Enterobacteriaceae Inoculum	Bacteroides Inoculum	Infant A	Infant B	Adult C	Mouse	4 Microbiota Groups	3 Human-derived Microbiota Groups
Bacteroidetes_Bacteroidia_Bacteroidales_Bacteroidaceae_Bacteroides_uncultured	0.000991	0.125	0.489	0.344	0.341	0.00029	1, 2	1
Bacteroidetes_Bacteroidia_Bacteroidales_Bacteroidales_S24-7_group_uncultured	0.000317	0.000102	1.88E-05	2.74E-05	0.00304	0.312	1, 2	
Firmicutes_Erysipelotrichia_Erysipelotrichales_Erysipelotrichaceae_Faecalibaculum_uncultured	0.00017	0.000187	3.28E-05	4.13E-05	3.02E-05	0.158	1, 2	
Firmicutes_Clostridia_Clostridiales_Lachnospiraceae_Lachnospiraceae_NK4A136_group_uncultured	0.000101	0.00403	0.097	0.0622	0.108	0.0893	2	2
Bacteroidetes_Bacteroidia_Bacteroidales_Rikenellaceae_Alistipes_uncultured	5.61E-05	0.0303	4.31E-05	0.102	0.0599	4.53E-05	2	1, 2
Actinobacteria_Actinobacteria_Bifidobacteriales_Bifidobacteriaceae_Bifidobacterium	0.331	0.116	0.012	0.000762	1.49E-05	0.0186		
Firmicutes_Erysipelotrichia_Erysipelotrichales_Erysipelotrichaceae_Turicibacter_uncultured	0.000142	0.000332	0.059	0.0348	0.0794	0.102		
Bacteroidetes_Bacteroidia_Bacteroidales_Bacteroidaceae_Bacteroides	3.60E-05	0.0902	3.29E-05	0.0556	0.0562	1.58E-05	2	1
Firmicutes_Clostridia_Clostridiales_Clostridiaceae_1_Clostridium_sensu_stricto_1_uncultured	0.00377	0.00961	0.0434	0.0408	0.049	0.0142		
Bacteroidetes_Bacteroidia_Bacteroidales_Porphyromonadaceae_Parabacteroides	4.18E-05	0.0321	2.02E-05	0.027	0.0749	6.26E-06		
Proteobacteria_Gammaproteobacteria_Enterobacteriales_Enterobacteriaceae_Escherichia-Shigella	0.287	0.00772	0.00793	4.96E-05	4.44E-06	3.97E-05		
Firmicutes_Clostridia_Clostridiales_Lachnospiraceae	0.1	0.106	0.0495	0.0298	0.0107	0.0133		
Verrucomicrobia_Verrucomicrobiae_Verrucomicrobiales_Verrucomicrobiaceae_Akkermansia_uncultured	0.0122	0.0131	0.0405	0.0404	1.94E-05	2.00E-05		
Bacteroidetes_Bacteroidia_Bacteroidales_Porphyromonadaceae_Coprobacter_uncultured	0.000177	1.73E-05	0.0614	2.45E-05	1.04E-05	5.68E-06		1
Firmicutes_Clostridia_Clostridiales_Lachnospiraceae_uncultured	1.01E-05	0.000111	0.00259	0.00653	0.0329	0.042		
Proteobacteria_Deltaproteobacteria_Desulfuovibrionales_Desulfuovibrionaceae_Desulfuovibrio	0.000588	0.021	0.0347	0.0202	0.0171	1.64E-05		
Proteobacteria_Betaproteobacteria_Burkholderiales_Alcaligenaceae_Sutterella	0	0.00249	6.53E-06	0.0368	0.00865	0		
Firmicutes_Bacilli_Lactobacillales_Lactobacillaceae_Lactobacillus	0	0.0349	9.45E-06	0.0307	1.91E-05	8.79E-06		
Firmicutes_Bacilli_Lactobacillales_Lactobacillaceae_Lactobacillus_uncultured	0.000109	0	2.37E-06	4.84E-06	0.000778	0.0351		
Firmicutes_Clostridia_Clostridiales_Peptostreptococcaceae	0.00643	0.00405	0.0206	0.0169	0.00183	6.05E-06		
Firmicutes_Clostridia_Clostridiales_Lachnospiraceae_Lachnospiraceae_UCG-001_uncultured	3.03E-05	1.73E-05	6.49E-06	0.0154	0.018	0.00773		
Firmicutes_Clostridia_Clostridiales_Lachnospiraceae_Roseburia_uncultured	0.0012	0.0179	8.30E-06	0.00609	0.00389	0.0168		
Bacteroidetes_Bacteroidia_Bacteroidales_Prevotellaceae_Prevotella_9_uncultured	0	0.0803	8.54E-06	0.00319	0	3.99E-06		
Firmicutes_Clostridia_Clostridiales_Ruminococcaceae_Ruminiclostridium_9_uncultured	1.15E-05	0.00221	0	0.00572	0.0116	0.0117		
Firmicutes_Clostridia_Clostridiales_Peptostreptococcaceae_Peptoclostridium_uncultured	0.0259	0.0181	0.00688	0	0.0109	0		
Firmicutes_Bacilli_Lactobacillales_Streptococcaceae_Streptococcus_uncultured	0.0546	0.00671	0.000794	1.10E-05	1.86E-06	0		
Firmicutes_Clostridia_Clostridiales_Ruminococcaceae_Ruminococcaceae_UCG-014_uncultured	0	0	0	0	4.32E-06	0.0153		Relative Abundance
Firmicutes_Negativicutes_Selenomonadales_Veillonellaceae_Veillonella_uncultured	0.0402	0.0285	0	8.12E-06	0	2.47E-06		5.00E-01
Firmicutes_Clostridia_Clostridiales_Clostridiales_vadinBB60_group_uncultured	0	0.000336	0	9.69E-05	0.000243	0.0148		2.50E-01
Firmicutes_Clostridia_Clostridiales_Lachnospiraceae_uncultured	5.93E-05	0.0028	3.64E-06	0.011	0.00539	0.00626		1.20E-01
Proteobacteria_Betaproteobacteria_Burkholderiales_Alcaligenaceae_Parasutterella	0	0	1.71E-06	2.13E-06	0.015	0		6.13E-02
Proteobacteria_Betaproteobacteria_Burkholderiales_Alcaligenaceae_Parasutterella_uncultured	0	0	3.58E-06	0.0124	0.0026	0		3.06E-02
Firmicutes_Clostridia_Clostridiales_Lachnospiraceae_Lachnoclostridium_uncultured	0	0.000774	0.0101	0.00715	0.000451	0		1.53E-02
Tenericutes_Mollicutes_Mollicutes_RF9	8.65E-06	0	0	0	0.00012	0.0133		7.66E-03
Firmicutes_Clostridia_Clostridiales_Christensenellaceae_Christensenellaceae_R-7_group	1.51E-05	0.000613	0.00595	0.00871	6.26E-06	2.49E-06		0.00E+00

Bacterial Taxa	INFANT A	INFANT B	ADULT	MOUSE	Relative Abundance
Bacteroidetes:D_2_Bacteroidia:D_3_Bacteroidales:D_4_Bacteroidaceae:D_5_Bacteroides:D_6_uncultured	0.489	0.344	0.341	0.00029	
Bacteroidetes:D_2_Bacteroidia:D_3_Bacteroidales:D_4_Bacteroidales_S24-7_group:D_5_uncultured_bacterium:D_6	1.88E-05	2.74E-05	0.00304	0.312	
Firmicutes:D_2_Erysipelotrichia:D_3_Erysipelotrichales:D_4_Erysipelotrichaceae:D_5_Faecalibaculum:D_6_uncultured	3.28E-05	4.13E-05	3.02E-05	0.158	
Bacteroidetes:D_2_Bacteroidia:D_3_Bacteroidales:D_4_Rikenellaceae:D_5_Alistipes:D_6_uncultured_bacterium	4.31E-05	0.102	0.0599	4.53E-05	
Firmicutes:D_2_Clostridia:D_3_Clostridiales:D_4_Lachnospiraceae:D_5_Lachnospiraceae_NK4A136_group:D_6_uncultured	0.097	0.0622	0.108	0.0893	
Firmicutes:D_2_Erysipelotrichia:D_3_Erysipelotrichales:D_4_Erysipelotrichaceae:D_5_Turicibacter:D_6_uncultured	0.059	0.0348	0.0794	0.102	
Firmicutes:D_2_Clostridia:D_3_Clostridiales:D_4_Clostridiaceae_1:D_5_Clostridium_sensu_stricto_1:D_6_uncultured	0.0434	0.0408	0.049	0.0142	
Bacteroidetes:D_2_Bacteroidia:D_3_Bacteroidales:D_4_Porphyromonadaceae:D_5_Parabacteroides;	2.02E-05	0.027	0.0749	6.26E-06	
Bacteroidetes:D_2_Bacteroidia:D_3_Bacteroidales:D_4_Bacteroidaceae:D_5_Bacteroides;	3.29E-05	0.0556	0.0562	1.58E-05	
Verrucomicrobia:D_2_Verrucomicrobiae:D_3_Verrucomicrobiales:D_4_Verrucomicrobiaceae:D_5_Akkermansia:D_6_uncultured	0.0405	0.0404	1.94E-05	2.00E-05	
Bacteroidetes:D_2_Bacteroidia:D_3_Bacteroidales:D_4_Porphyromonadaceae:D_5_Coprobacter:D_6_uncultured	0.0614	2.45E-05	1.04E-05	5.68E-06	
Firmicutes:D_2_Clostridia:D_3_Clostridiales:D_4_Lachnospiraceae:D_5_uncultured:D_6_uncultured	0.00259	0.00653	0.0329	0.042	
Firmicutes:D_2_Clostridia:D_3_Clostridiales:D_4_Lachnospiraceae;	0.0495	0.0298	0.0107	0.0133	
Proteobacteria:D_2_Deltaproteobacteria:D_3_Desulfuovibrionales:D_4_Desulfuovibrionaceae:D_5_Desulfuovibrio	0.0347	0.0202	0.0171	1.64E-05	
Proteobacteria:D_2_Betaproteobacteria:D_3_Burkholderiales:D_4_Alcaligenaceae:D_5_Sutterella	6.53E-05	0.0368	0.00865	0	
Firmicutes:D_2_Bacilli:D_3_Lactobacillales:D_4_Lactobacillaceae:D_5_Lactobacillus:D_6_uncultured	2.37E-06	4.84E-06	0.000778	0.0351	
Firmicutes:D_2_Clostridia:D_3_Clostridiales:D_4_Peptostreptococcaceae;	0.0206	0.0169	0.00183	6.05E-06	
Firmicutes:D_2_Bacilli:D_3_Lactobacillales:D_4_Lactobacillaceae:D_5_Lactobacillus;	9.45E-06	0.0307	1.91E-05	8.79E-06	
Actinobacteria:D_2_Actinobacteria:D_3_Bifidobacteriales:D_4_Bifidobacteriaceae:D_5_Bifidobacterium	0.012	0.000762	1.49E-05	0.0186	
Firmicutes:D_2_Clostridia:D_3_Clostridiales:D_4_Lachnospiraceae:D_5_Lachnospiraceae_UCG-001:D_6_uncultured	6.49E-06	0.0154	0.018	0.00773	
Firmicutes:D_2_Clostridia:D_3_Clostridiales:D_4_Lachnospiraceae:D_5_Roseburia:D_6_uncultured	8.30E-06	0.00609	0.00389	0.0168	
Firmicutes:D_2_Clostridia:D_3_Clostridiales:D_4_Ruminococcaceae:D_5_Ruminiclostridium_9:D_6_uncultured	0	0.00572	0.0116	0.0117	
Firmicutes:D_2_Clostridia:D_3_Clostridiales:D_4_Ruminococcaceae:D_5_Ruminococcaceae_UCG-014:D_6_uncultured	0	0	4.32E-06	0.0153	
Firmicutes:D_2_Clostridia:D_3_Clostridiales:D_4_Clostridiales_vadinBB60_group:D_5_uncultured_bacterium:D_6	0	9.69E-05	0.000243	0.0148	
Proteobacteria:D_2_Betaproteobacteria:D_3_Burkholderiales:D_4_Alcaligenaceae:D_5_Parasutterella	1.71E-06	2.13E-06	0.015	0	
Firmicutes:D_2_Clostridia:D_3_Clostridiales:D_4_Lachnospiraceae:D_5_uncultured;	3.64E-06	0.011	0.00539	0.00626	
Proteobacteria:D_2_Betaproteobacteria:D_3_Burkholderiales:D_4_Alcaligenaceae:D_5_Parasutterella:D_6_uncultured	3.58E-06	0.0124	0.0026	0	
Tenericutes:D_2_Mollicutes:D_3_Mollicutes_RF9;	0	0	0.00012	0.0133	0.5
Firmicutes:D_2_Clostridia:D_3_Clostridiales:D_4_Lachnospiraceae:D_5_Lachnoclostridium:D_6_uncultured	0.0101	0.00715	0.000451	0	0.25
Firmicutes:D_2_Clostridia:D_3_Clostridiales:D_4_Christensenellaceae:D_5_Christensenellaceae_R-7_group	0.00595	0.00871	6.26E-06	2.49E-06	0.125
Proteobacteria:D_2_Gammaproteobacteria:D_3_Enterobacteriales:D_4_Enterobacteriaceae:D_5_Escherichia-Shigella	0.00793	4.96E-05	4.44E-06	3.97E-05	0.0625
Proteobacteria:D_2_Gammaproteobacteria:D_3_Enterobacteriales:D_4_Enterobacteriaceae:D_5_Klebsiella	0.00011	0	0	0	0.03125
Proteobacteria:D_2_Gammaproteobacteria:D_3_Pasteurellales:D_4_Pasteurellaceae:D_5_Haemophilus:D_6_uncultured	4.81E-05	7.38E-06	4.20E-06	0	0.0156
Firmicutes:D_2_Negativicutes:D_3_Selenomonadales:D_4_Veillonellaceae:D_5_Veillonella:D_6_uncultured	0	8.12E-06	0	2.47E-06	0.0078
					0

Figure 3.3 Average relative abundance of all bacterial taxa. (A) Heatmap of taxa collectively

Figure 3.3 (cont'd)

contributing 90% of differences in SIMPER analysis and having high loadings in the principal components analysis for the inocula (*Enterobacteriaceae-enriched*, *Bacteroidaceae-enriched*), the human-derived microbiota (Infant A, Infant B and Adult C), and mouse microbiota. B) SIMPER analysis of 90% of cumulative bacterial taxa from mice transplanted with Infant A, Infant B and Adult C human-derived fecal microbiota compared to mouse microbiota. Top of Table shows taxa contributing 90% of difference in SIMPER; Taxa contributing <90% of difference are shown below black line.

Comparison of microbiota diversity in four microbiotas (Figure 3.4A)

Analysis of the diversity of the four microbial communities showed that 3 of 4 communities were diverse and that the transplanted Infant communities retained the diversity seen in the donor samples (Figure 3.4A)[140, 178]. Shannon alpha diversity analyses were not significantly different between donor Infant A inoculum and Infant A mice and between donor Infant B inoculum and Infant B mice (Figure 3.4A). However, the Infant A donor inoculum and the Infant A mouse microbiotas were significantly decreased in diversity compared to the Infant B inoculum, Infant B mouse microbiota, Adult C mouse microbiota and the control mice carrying mouse microbiota (Figure 3.4A).

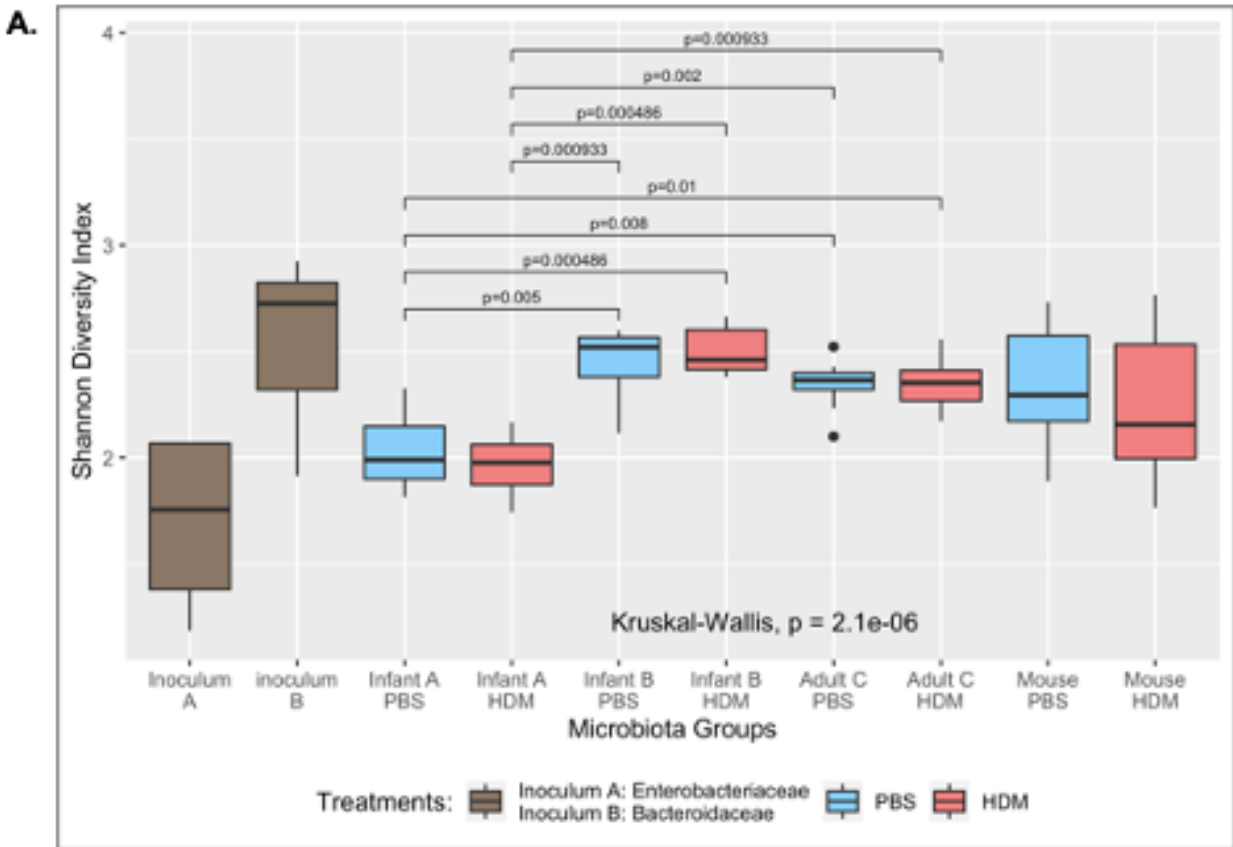


Figure 3.4 Characteristics of bacterial taxa in mouse models. (A) Shannon alpha diversity Index performed on operational taxonomic units from *Enterobacteriaceae* inoculum, *Bacteroidaceae* inoculum, Infant A mice given phosphate buffered saline and house dust mite, Infant B mice given phosphate buffered saline and house dust mite, Adult C mice given phosphate buffered saline and house dust mite, and conventional mouse microbiota mice given phosphate buffered saline and house dust mite. *Enterobacteriaceae* inoculum and Infant A mice given phosphate buffered saline and house dust mite had significantly lower diversity than all of the other groups. (B) abundant in human-derived microbiotas compared to mouse microbiotas (Panel 1), while allergy antagonists were numerous in mouse microbiotas and low in human-derived microbiotas (Panel 2). Pro-inflammatory taxa were abundant in human-derived microbiotas and low or absent in mouse microbiotas (Panel 3), while anti-inflammatory taxa were abundant in mouse microbiotas and few in human-derived microbiotas (Panel 4). Panels C-F show average relative abundance of bacterial taxa grouped according to the four microbiotas Infant A, Infant B, Adult C, and Mouse. Grouped by abundance as (C) high abundance, (D) medium abundance, (E) Low abundance and (F) lowest abundance. Each graph shows the taxa displayed in that chart (see keys). Note that many taxa are found only in the human-derived or the mouse microbiota.

Figure 3.4 (cont'd)

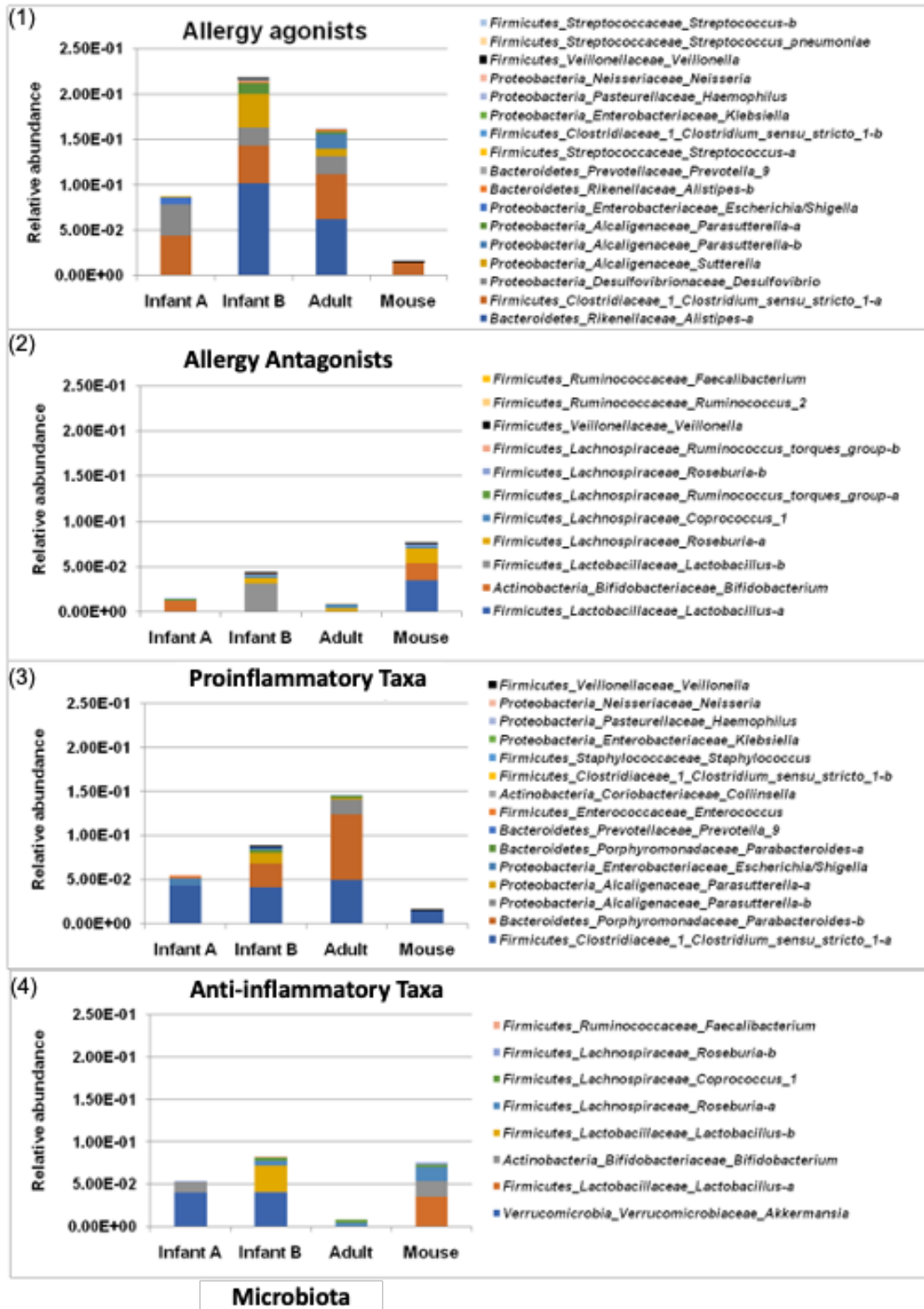
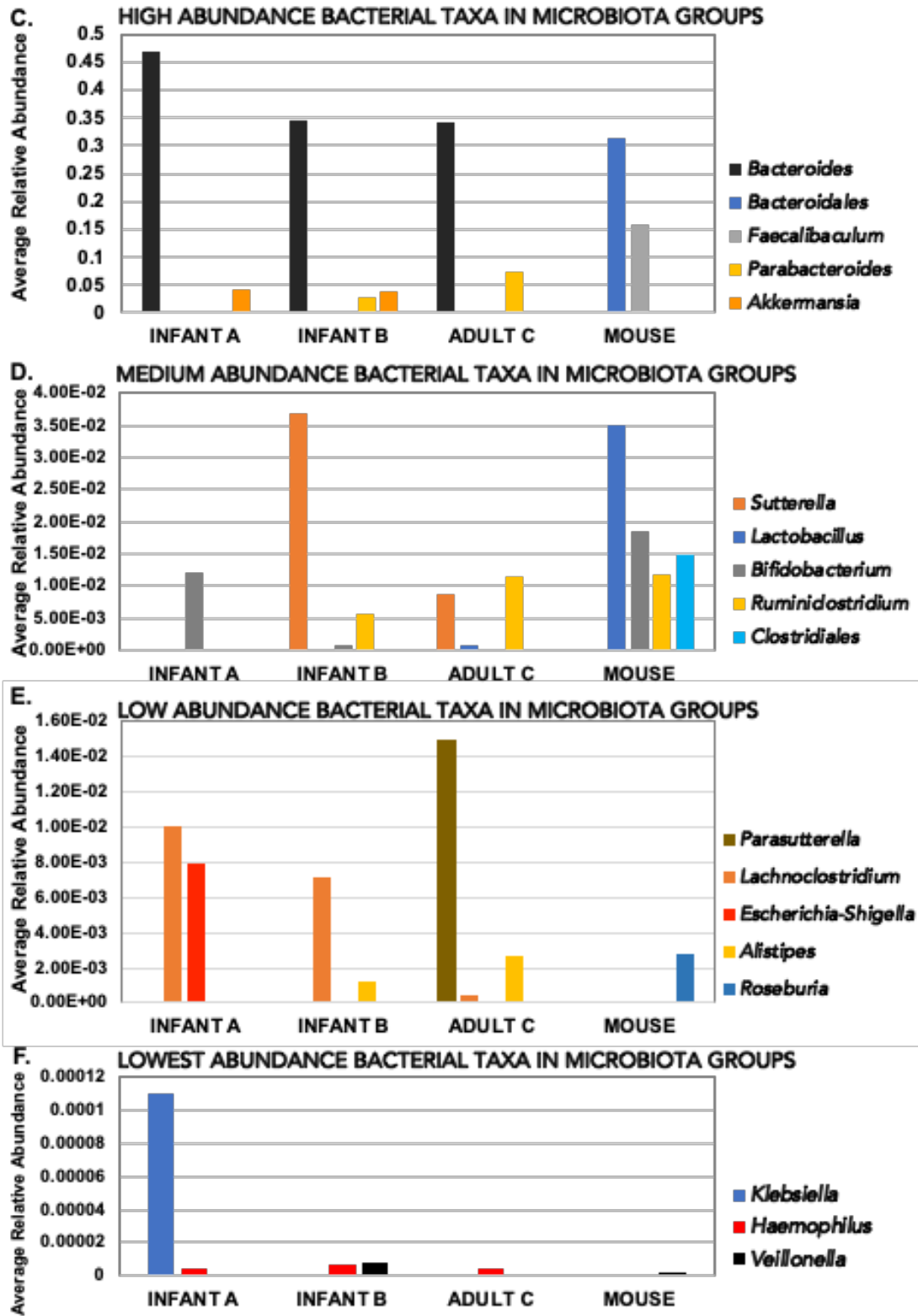


Figure 3.4 (cont'd)



Allergy agonists/antagonists and pro-/anti-inflammatory bacterial taxa in experimental mice (Figure 3.4B)

We also considered the average relative abundance of bacterial taxa known to act as allergy agonists or antagonists and those known to be proinflammatory or anti-inflammatory in human-derived versus mouse microbiotas (Figure 3.4B). The total fraction of allergy agonists was greater in the human-derived microbiotas than in the mouse microbiotas (Figure 3.4B, panel 1; Table 3.1). There were greater numbers of individual agonist taxa than antagonist taxa detected in the entire dataset. The situation in the conventional mouse microbiota was reversed—allergy agonistic taxa were in smaller proportions and fewer in number of individual taxa, while allergy antagonistic taxa were in greater total proportions and there were more individual taxa (Figure 3.4B, panel 2; Table 3.1). The relative total proportions of allergy agonist taxa reflect the trends in relative severities of lung function responses in the mice with human-derived microbiotas (Figure 3.6).

The average relative abundance of pro- and anti- inflammatory taxa had somewhat different patterns; however, there were still more individual pro-inflammatory taxa than individual anti-inflammatory taxa detected in the entire dataset (Figure 3.4B, panels 3 and 4). The human-derived microbiotas had more pro-inflammatory taxa than the mouse-adapted microbiotas and each human-derived microbiota had particular proinflammatory taxa present or in greater abundance than in the others (Table 3.2). Of these, only the uncultured *Bacteroides* and *Haemophilus* were found in all three communities (Figures 3.4B, 3.4C, 3.4F). Infant A mice carried more *E. coli-Shigella* (Figure 3.4E). Infant B and Adult C had one proinflammatory taxon in common, *Parabacteroides* OTU59 (Figure 3.4C). Adult C had higher levels of *Parasutterella* OTUs (Figure 3.4E). Adult C microbiota mice had the largest difference in total proportions and total numbers of pro- and anti-inflammatory taxa, with abundant pro-inflammatory taxa (Figure 3.4B, panels 3 and 4; Table 3.2). The outcomes in the protected mice with mouse microbiota were reversed with regard to pro- and anti-inflammatory taxa (Figure 3.4B, panels 3 and 4).

Table 3.1 Bacterial taxa found in Infant A, Infant B, Adult C and Mouse microbiotas known to act as allergy agonists or antagonists based on published studies [2, 55, 80-82, 102, 147-152].

ALLERGY AGONISTS	Infant A	Infant B	Adult C	Mouse
<i>Streptococcus pneumonia</i>	1	1	1	0
<i>Moraxella catarrhalis</i>	0	0	0	0
<i>Neisseria</i>	0	0	0	0
<i>Veillonella</i>	0	1	0	0
<i>Clostridium cluster I</i>	1	1	1	1
<i>Desulfovibrio</i>	1	1	1	0
<i>Sutterella</i>	0	1	1	0
<i>Parasutterella</i>	0	0	1	0
<i>Escherichia coli/Shigella</i>	1	0	0	0
<i>Klebsiella</i>	1	0	0	0
<i>Haemophilus</i>	1	1	1	0
<i>Prevotella</i>	0	1	0	0
<i>Alistipes</i>	0	1	1	0
Total Agonist Taxa	6	8	7	1

ALLERGY ANTAGONISTS	Infant A	Infant B	Adult C	Mouse
<i>Clostridia (Clostridiales)</i>	0	0	0	1
<i>Lachnospira</i>	1	1	1	1
<i>Veillonella</i>	1	0	0	0
<i>Faecalibacterium</i>	0	0	0	1
<i>Rothia mucilaginosa</i>	0	0	0	0
<i>Roseburia</i>	0	1	1	1
<i>Ruminococcus, Coprococcus</i>	0	0	0	1
<i>Lactobacillus</i>	0	1	0	1
<i>Bifidobacteria</i>	1	0	0	1
Total Antagonist Taxa	3	3	2	6

Table 3.2 Bacterial taxa found in Infant A, Infant B, Adult C and Mouse microbiotas known to function in a proinflammatory or antiinflammatory manner in acute of chronic diseases based on published studies [2, 55, 80-82, 102, 147-152]. Data represents presence absence values. Microbiotas were scored as 1 if a particular taxa was present and 0 if it was not present.

PROINFLAMMATORY TAXA	Infant A	Infant B	Adult C	Mouse
<i>Clostridia/C. perfringens/C. difficile</i>	1	1	1	1
<i>Collinsella</i>	0	1	1	0
<i>Enterobacter aerogenes</i>	0	0	0	0
<i>Enterococci</i>	1	0	0	0
<i>Escherichia coli/Shigella OTU42</i>	1	1	0	0
<i>Haemophilus</i>	1	1	1	0
<i>Klebsiella</i>	1	0	0	0
<i>Moraxella</i>	0	0	0	0
<i>Morganella morganii</i>	0	0	0	0
<i>Neisseria</i>	0	0	0	0
<i>Parabacteroides OTU59</i>	0	1	1	0
<i>Parasutterella OTU26</i>	0	1	1	0
<i>Prevotella</i>	0	1	0	0
<i>Staphylococcus aureus</i>	0	0	0	0
<i>Veillonella</i>	0	1	0	0
Total Proinflammatory Taxa	5	8	5	1

ANTI-INFLAMMATORY TAXA	Infant A	Infant B	Adult C	Mouse
<i>Akkermansia muciniphila</i>	1	1	0	0
<i>Bacteroides</i>	1	1	1	0
<i>Bifidobacterium OTU 18</i>	1	0	0	1
<i>Coprococcus eutactus</i>	0	1	0	1
<i>Faecalibacterium prausnitzii</i>	0	0	0	0
<i>Lactobacillus</i>	0	0	0	1
<i>Lactobacillus uncultured OTU 7</i>	0	0	0	1
<i>Roseburia OTU</i>	0	1	0	1
<i>Roseburia OTU</i>	0	0	0	1
Total Anti-Inflammatory Taxa	3	4	1	6

Mouse microbiota composition potentially modulating immune responses

While all four microbiotas had some taxa with bioinformatic evidence of potentially anti-inflammatory taxa, the mouse microbiota had more of these genera and they were more abundant (Figure 3.4B panel 2 and panel 4, 4D, 4E, Tables 3.1 and 3.2). Known anti-inflammatory taxa present in the mouse microbiotas and absent or at exquisitely low amounts in the three human-derived communities were members of the order *Bacteroidales*, *Faecalibacterium*, *Lactobacillus*, *Roseburia*, and a member of the order *Clostridiales* (Figure 3.4B-F). A member of the family *Ruminococcaceae* was another anti-inflammatory taxon present in the mouse microbiotas and absent in the human-derived communities except for a few reads in Adult C (Figure 3.3A and B).

Measurement of lung function in mice with human microbiotas after HDM sensitization

A protocol was developed with the goal of devising an allergen-exposure that would induce a moderate level of allergic response and decline in lung function, such that we could test for components of the microbiota that either increased or decreased the response to allergens (Table 3.3). A 2-week exposure using 30-50 ug HDM delivered intranasally in PBS was found to be most appropriate for our purposes. Lung function was assessed in terms of resistance, compliance and elastance of the respiratory system, as well as Newtonian resistance, tissue resistance and tissue elastance. We used C57BL/6 mice because they have been shown to exhibit modest AHR responses to HDM that could be exacerbated by other factors such as microbiota. Measurements at peak responses of resistance (Rrs in cmH₂O.s/ml), compliance (Crs in ml/cmH₂O), elastance (Ers in cmH₂O/ml), tissue elastance (H in, cmH₂O/ml), tissue damping (G in cmH₂O/ml), and conducting airway (Newtonian) resistance (Rn in cmH₂O.s/ml) for each methacholine dose for PBS and HDM treatment groups produced usable data for all mice tested to assess airway hyperresponsiveness (Supplemental Tables 3.1 and 3.2).

Table 3.3 Design for Experiment 1 shows the four gut microbiotas used and the number (N) of male (M) and female (F) mice in each group of microbiota and treatment combination.

Each group was treated with phosphate buffered saline (PBS) control or house dust mite (HDM) extract intranasally on Days 0, 2, 5, 7, 9, and 12. On Day 14, several phenotypes were assessed. Specifically, lung function measurements were taken using flexiVent over the course of increasing doses of aerosolized methacholine. Thereafter, bronchoalveolar lavage, blood, lung, and gastrointestinal samples were collected. The design for experiment 2 was exactly the same as in experiment 1, except that we used only mice carrying Infant B or Infant A microbiota and mice with Adult C and Mouse microbiota were not used.

Microbiota	Treatment	N & sex	Treatments administered ¹						Phenotype
			Day 0	Day 2	Day 5	Day 7	Day 9	Day 12	
Mouse Control	PBS	5M, 5F	25 ul	30 ul	30 ul	30 ul	30 ul	30 ul	Day 14
Mouse Control	HDM	5M, 5F	50 ug	30 ug	30 ug	30 ug	30 ug	30 ug	Day 14
Infant A	PBS	5M, 5F	25 ul	30 ul	30 ul	30 ul	30 ul	30 ul	Day 14
Infant A	HDM	5M, 5F	50 ug	30 ug	30 ug	30 ug	30 ug	30 ug	Day 14
Infant B	PBS	3M, 3F	25 ul	30 ul	30 ul	30 ul	30 ul	30 ul	Day 14
Infant B	HDM	5M, 5F	50 ug	30 ug	30 ug	30 ug	30 ug	30 ug	Day 14
Adult C	PBS	5M, 5F	25 ul	30 ul	30 ul	30 ul	30 ul	30 ul	Day 14
Adult C	HDM	5M, 5F	50 ug	30 ug	30 ug	30 ug	30 ug	30 ug	Day 14

¹All HDM extract administered in 0.2 ml volume of PBS.

Human-derived microbiota modifies baseline pulmonary function in mice (Experiment 1)

Before analyzing the effects of allergen exposure on airway hyperresponsiveness using MCh, we found that baseline lung mechanics for mice with all three human microbiotas were significantly different from the controls carrying mouse microbiota in both non-allergic (treated with PBS) and allergic (treated with HDM) mice (Figure 3.5). Baseline mechanics corresponds to values taken before any MCh was administered. Overall, respiratory system resistance (Rrs), which includes contributions from the conducting and peripheral airways, the lung tissue, and the chest wall, was increased in mice carrying all 3 human microbiotas (Figure 3.5A). Respiratory system compliance (Crs), which describes the ease with which the respiratory system can be expanded, was decreased (Figure 3.5B), and respiratory system elastance (Ers), which represents the elastic

stiffness of the respiratory system, was increased in mice carrying human microbiotas compared to the controls carrying mouse microbiota (Figure 3.5G). These findings indicate an overall decrease in lung function in mice carrying human microbiotas compared to mice carrying control mouse microbiota.

The effects of microbiota on baseline respiratory mechanics were also seen when the mechanics of the large airways and smaller peripheral airways and tissue were examined. For tissue and peripheral airway resistance (G), mice with all 3 human microbiotas had higher values than mice with mouse microbiota, and this increment was significant for 2 experimental groups: non-allergic (treated with PBS) mice with Adult C human microbiota when compared to those with control mouse microbiota with the same treatment, and allergic (treated with HDM) mice with Infant A microbiota when compared to those with mouse microbiota with the same treatment (Figure 3.5H). For tissue elastance (H), which represents tissue stiffness, mice with Infant B and Adult C human microbiotas had significantly higher values compared to mice with control microbiota, and this increase was seen both in HDM- and PBS-treated mice (Figure 3.5I,L). Conversely, Newtonian Resistance (Rn), which represents mainly the resistance of the large conducting airways, was shown to be significantly increased for mice with Infant A and Adult C microbiota treated with PBS when compared to mice carrying mouse microbiota with the same treatment (Figure 3.5C). These results indicate that mice carrying any of the three human microbiotas had different lung mechanics at baseline characterized by overall greater lung stiffness and airway resistance and decreased compliance compared to mice carrying mouse microbiota. No significant differences were found in lung measurements between the PBS- or HDM-treated mice carrying different human microbiotas when compared to each other (Figures 3.5D, E, F, J, K, L). The treatment with HDM caused no significant increase at baseline when compared to PBS treatment (mice that did not receive HDM) for any of the microbiotas, with the exception of mouse microbiota, where the group challenged with HDM had significantly lower values of compliance when compared to the group carrying the same microbiota but given PBS treatment (Figure 3.5B, E).

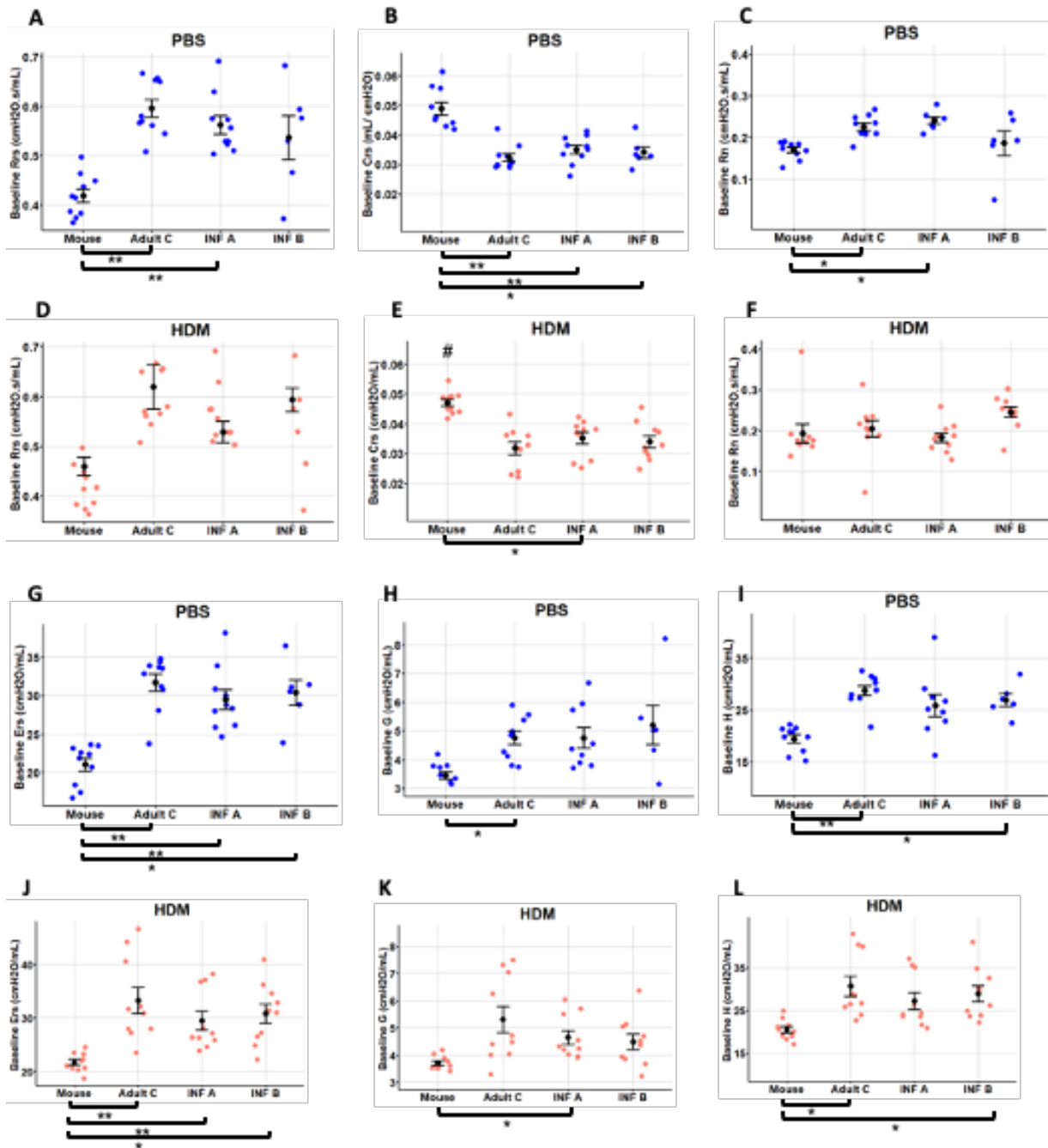


Figure 3.5 Lung baseline mechanics for mice with all three human microbiotas were significantly different from the controls carrying mouse microbiota. Data shows examination of baseline lung mechanics for (A,D) total airway resistance Rrs, (B,E) total airway compliance Crs, (C,F) central airway resistance Rn, (G,J) tissue elastance Ers, (H,K) peripheral airways and tissue damping G, and (I,L) tissue elastance H for mice treated with PBS or HDM. Data represent mean \pm SE from 10 mice per group. Data analyzed with Kruskal Wallis with Mann-Whitney for pairwise comparisons. * $p < 0.05$. ** $p < 0.01$. # $p < 0.05$ compared to same microbiota with different treatment.

Airway hyperresponsiveness (AHR) (Experiment 1)

After recording baseline lung mechanics, methacholine (MCh), a muscarinic agonist, was given at increasing doses via nebulization to evaluate AHR in the context of both allergic and non-allergic conditions. Methacholine induces bronchoconstriction by acting directly on muscarinic receptors of the airway smooth muscle. The methacholine test is a sensitive tool to confirm or exclude a diagnosis of asthma [179]. AHR in these experiments was measured in the context of changes in lung function by assessing respiratory parameters and analyzing their dose response curves. To account for the differences observed at baseline between mice carrying different microbiotas, a general linear mixed model (GLMM)(See Methods) was used to analyze the observed data and generate predicted dose response curves (Supplemental Tables 3.1 and 3.2).

Based on the results of the GLMM the effect of an increase in dose of MCh (levels = 0,12.5,25,50,100 mg/mL) on the total airway resistance (Rrs) parameter, which represents total respiratory constriction, was different for the microbiota groups ($\chi^2 = 9.1195, p = 0.0277$)(Figure 3.6A, Table 3.4). There was a 0.0059 ± 0.0019 cmH₂O.s/mL increase in the peak Rrs value for mice with Infant B microbiota over mice with mouse microbiota for each 1 mg/mL increase in MCh. Refer to the observed values of Rrs, Crs, Peak Rn, G, Ers and H collected for each experimental group at each MCh dose as shown in Supplemental Figure 3.1.

Table 3.4 Linear mixed effects model for respiratory system resistance (Rrs) data: type III sum of squares and contrasts corresponding to significant categorical variables. *P-values adjusted with Tukey method; significant values are bolded.

Variable	χ^2 – statistic	Degrees of freedom	P-value
Intercept	30.4520	1	0.0000
Log(Baseline_Rrs)	353.3577	1	0.0000
Dose	0.4688	1	0.4935
Microbiota	1.7320	3	0.6298
Treatment	1.2579	1	0.2621
Dose*Microbiota	9.1195	3	0.0277*
Estimates of dose effects for microbiota groups			
	Estimate	Standard Error	95% Conf. Interval (Slope)
Mouse	0.0009	0.0013	(-0.0016,0.0033)
Human Adult	0.0039	0.0014	(0.0012,0.0067)
Infant A	0.0049	0.0016	(0.0019,0.0080)
Infant B	0.0067	0.0019	(0.0031,0.0104)
Contrasts of dose effects between different microbiota groups			
	Estimate	Standard Error	P-value
Human Adult - Mouse	0.0031	0.0016	0.2365
Infant A - Mouse	0.0041	0.0017	0.0778
Infant B - Mouse	0.0059	0.0019	0.0119*
Infant A - Human Adult	0.0010	0.0018	0.9433
Infant B - Human Adult	0.0028	0.0020	0.4813
Infant B - Infant A	0.0018	0.0020	0.7900

When examining the resistance of the conducting larger airways versus the peripheral smaller airways and tissue compartments, which are represented by Newtonian Resistance (Rn)(Figure 3.6C) and tissue resistance (G)(Figure 3.6B, Table 3.5), respectively, we observed that the differences in resistance between the microbiotas were mostly due to the increase in resistance in smaller airways and in tissue peak resistance. The effect of an increase in the dose of MCh was different for the microbiota groups ($\chi^2 = 11.8434, p = 0.0079$)(Figure 3.6, Table 3.5), while the same effect in resistance of the larger airways showed no significant difference between the microbiota groups ($\chi^2 = 2.1436, p = 0.5432$)(Figure 3.6C). Specifically, for the AHR observed in the smaller airways and tissue, mice with Infant B microbiota had a 0.0320 ± 0.0125 cmH₂O/mL increase in the peak G value (Tissue resistance) over mice with mouse microbiota for each 1 mg/mL increase in MCh, corresponding to a 0.4 % increase with each unit (Figure 3.6B; Table 3.5). Even though we observed higher estimated means of peak Rrs and G with each

unit increase of MCh for mice carrying Infant A or Adult C microbiota when compared to mouse microbiota, these differences were not significant (Figure 3.6A and B; Table 3.4, Table 3.5).

Table 3.5 Linear mixed effects model for tissue damping (G) data: type III sum of squares and contrasts corresponding to significant categorical variables. *P-values adjusted with Tukey method; significant values are bolded.

Variable	χ^2 – statistic	Degrees of freedom	P-value
Intercept	30.8900	1	0.0000
Log(Baseline_G)	198.4985	1	0.0000
Dose	13.5011	1	0.0002
Microbiota	10.1044	3	0.0177*
Treatment	5.1657	1	0.0230*
Dose*Microbiota	11.8434	3	0.0079**
Estimates of dose effects for microbiota groups			
	Estimate	Standard Error	95% Conf. Interval (Slope)
Mouse	0.0234	0.00641	(0.0108,0.0360)
Human Adult	0.0396	0.00837	(0.0231,0.0560)
Infant A	0.0429	0.00855	(0.0261,0.0597)
Infant B	0.0715	0.01059	(0.0507,0.0924)
Contrasts of dose effects between different microbiota groups			
	Estimate	Standard Error	P-value
Human Adult - Mouse	0.01620	0.0100	0.3722
Infant A - Mouse	0.01953	0.0101	0.2145
Infant B - Mouse	0.04816	0.0117	0.0003**
Infant A - Human Adult	0.00333	0.0110	0.9905
Infant B - Human Adult	0.03196	0.0125	0.0528
Infant B - Infant A	0.02864	0.0124	0.0972

Airway hyperresponsiveness in mice carrying humanized microbiotas was also characterized by an overall increased in stiffness or Respiratory elastance (Ers) of the respiratory system (Figure 3.6D; Table 3.6) and, as expected, a decrease in its reciprocal, lung compliance (Crs)(Figure 3.6E; Table 3.7). The effect of an increase in dose of methacholine on peak Ers and bottom Crs values was different for the microbiota groups ($\chi^2 = 9.1195, p = 0.0277$ and $\chi^2 = 9.4158, p = 0.0242$, respectively)(Figures 3.6D and E, Tables 3.6 and 3.7). Once again, mice

with Infant B microbiota had the highest estimated means of peak Ers with each unit increase of MCh, and there was a 0.1520 ± 0.0450 cmH₂O/mL increase in the peak Ers value for mice with infant B microbiota over mice with mouse microbiota for each 1 mg/mL increase in MCh, corresponding to a 0.31% increase with each unit, which was significant ($p = 0.0045$) (Figure 3.6D; Table 3.6). Mice with Infant B microbiota also showed the highest estimated means for peak tissue elastance (H) values, an indicator of airway closure, where there was a 0.0528 ± 0.0272 cmH₂O/mL increase in the peak H value over mice with mouse microbiota for each 1 mg/mL increase in MCh, corresponding to a 30% increase compared to mice with Mouse microbiota ($p = 0.0051$) (Figure 3.6F, Table 3.8).

Table 3.6 Linear mixed effects model for respiratory system elastance (Ers) data: type III sum of squares and contrasts corresponding to significant categorical variables. *P-values adjusted with Tukey method.

Variable	χ^2 – statistic	Degrees freedom	of P-value
Intercept	0.1265	1	0.7221
Log(Baseline_Ers)	551.8094	1	0.0000
Dose	3.2407	1	0.0718
Microbiota	5.8657	3	0.1183
Treatment	5.4813	1	0.0192 *
Dose*Microbiota	11.1608	3	0.0109 *
Estimates of dose effects for microbiota groups			
	Estimate	Standard Error	95% Conf. Interval
Mouse	0.0477	0.0270	(-0.00541,0.101)
Human Adult	0.1042	0.0306	(0.04402,0.164)
Infant A	0.1131	0.0321	(0.04984,0.176)
Infant B	0.1997	0.0378	(0.12544,0.274)
Contrasts of dose effects between different microbiota groups			
	Estimate	Standard Error	P-value
Human Adult - Mouse	0.05648	0.0397	0.4864
Infant A - Mouse	0.06534	0.0405	0.3729
Infant B - Mouse	0.15202	0.0450	0.0045**
Infant A - Human Adult	0.00886	0.0423	0.9968
Infant B - Human Adult	0.09554	0.0466	0.1717
Infant B - Infant A	0.08668	0.0469	0.2523

Table 3.7 Linear mixed effects model for respiratory system compliance (Crs) data: type III sum of squares and contrasts corresponding to significant categorical variables. *P-values adjusted with Tukey method.

Variable	χ^2 – statistic	Degrees of freedom	P-value
Intercept	0.4009	1	0.52661
Log(Baseline_Crs)	536.6499	1	0.00000
Dose	2.4957	1	0.11416
Microbiota	6.8176	3	0.07795
Treatment	4.3851	1	0.03625*
Dose*Microbiota	9.4158	3	0.02424*
Estimates of dose effects for microbiota groups			
	Estimate	Standard Error	95% Conf. Interval
Mouse	-0.00003	0.0000178	(-0.00006, 0.000006)
Human Adult	-0.00007	0.0000166	(-0.00010, -0.00004)
Infant A	-0.00006	0.0000161	(-0.00009, -0.00002)
Infant B	-0.00010	0.0000168	(-0.00010, -0.00006)
Contrasts of dose effects between different microbiota groups			
	Estimate	Standard Error	P-value
Human Adult - Mouse	-0.0000424	0.0000236	0.2772
Infant A - Mouse	-0.0000277	0.0000230	0.6245
Infant B - Mouse	-0.000069	0.0000235	0.0186*
Infant A - Human Adult	0.0000147	0.0000222	0.9110
Infant B - Human Adult	-0.0000266	0.0000227	0.6447
Infant B - Infant A	-0.0000413	0.0000220	0.2402

Table 3.8 Linear mixed effects model for tissue elastance (H) data: type III sum of squares and contrasts corresponding to significant categorical variables. *P-values adjusted with Tukey method.

Variable	χ^2 – statistic	Degrees of freedom	P-value
Intercept	24.7364	1	0.0000
Log(Baseline_H)	460.5645	1	0.0000
Dose	6.3121	1	0.0111 *
Microbiota	6.9794	3	0.0726
Treatment	11.2480	1	0.0008 ***
Dose*Microbiota	10.3063	3	0.0161 *
Estimates of dose effects for microbiota groups			
	Estimate	Standard Error	95% Conf. Interval
Mouse	0.0403	0.0162	(0.0083,0.0722)
Human Adult	0.0888	0.0196	(0.0503,0.1274)
Infant A	0.0750	0.0183	(0.0390,0.1109)
Infant B	0.1277	0.0210	(0.0864,0.1691)
Contrasts of dose effects between different microbiota groups			
	Estimate	Standard Error	P-value
Human Adult - Mouse	0.0485	0.0251	0.2150
Infant A - Mouse	0.0347	0.0240	0.4723
Infant B - Mouse	0.0875	0.0262	0.0051**
Infant A - Human Adult	-0.0139	0.0262	0.9519
Infant B - Human Adult	0.0389	0.0282	0.5129
Infant B - Infant A	0.0528	0.0272	0.2144

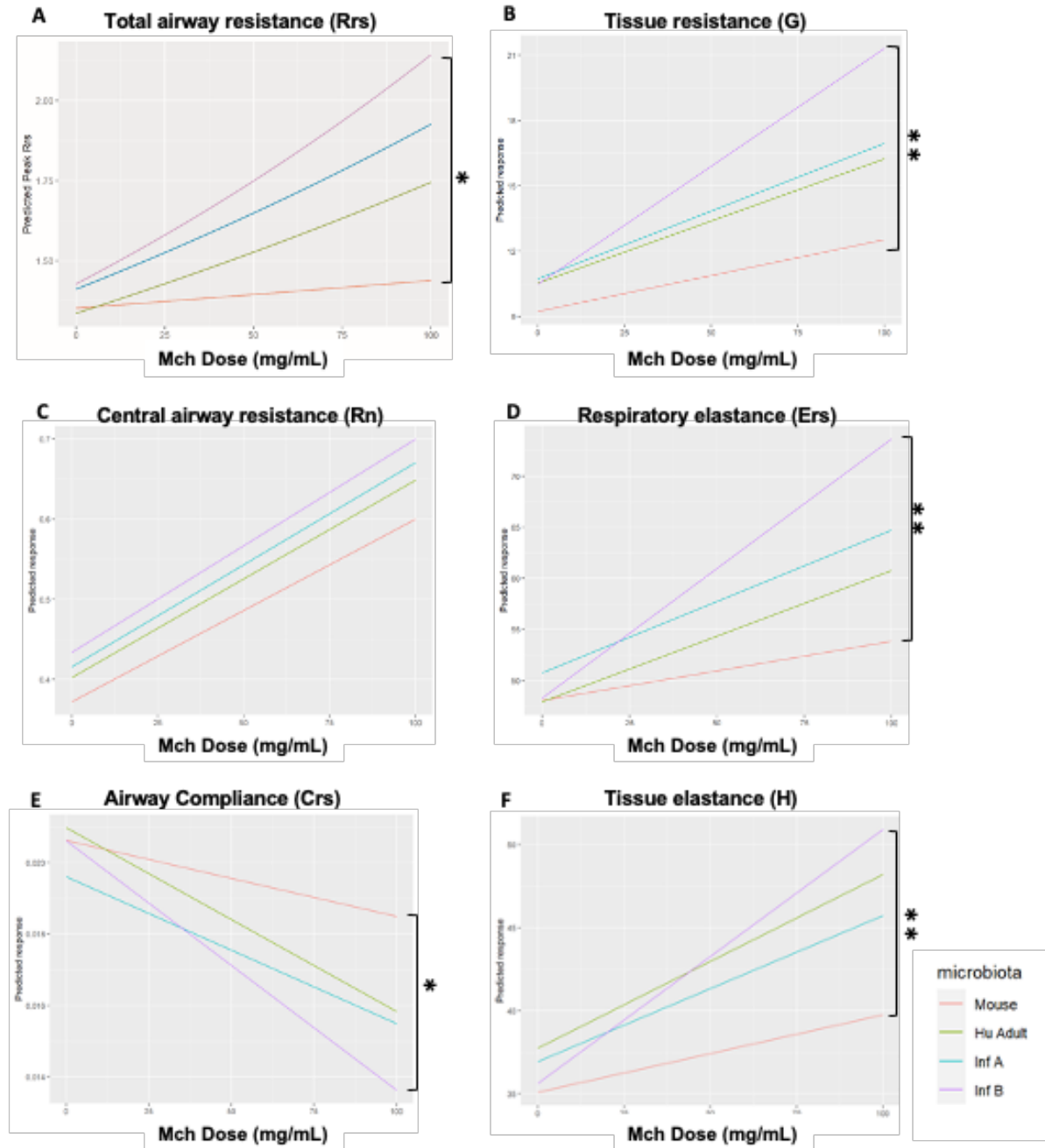


Figure 3.6 Mice carrying Infant B microbiota showed increased airway hyperresponsiveness after methacholine challenge compared to mice with control microbiota. Lines represent predicted change in peak value of lung function for each unit increase of methacholine (MCh) using a general linear mixed (GLM) model for the corresponding microbiota. Data represented on each line include mice from both PBS and HDM treatment groups for A) Total airway resistance, B) Tissue resistance, C) Central airway resistance, D) Respiratory elastance, E) Airway compliance, and F) Tissue elastance. Pairwise comparisons were used to compare slopes. *p < 0.05. **p < 0.01.

While peak Rrs in mice treated with HDM had a higher estimated mean at each dose of MCh compared to mice treated with PBS, the effect of treatment with HDM was not statistically significant ($p = 0.2621$, Figure 3.7A; Table 3.4), and the same pattern was observed for peak Rn values (Figure 3.7B). In contrast, peak G, Ers, Crs, and H values in mice treated with HDM had higher estimated means at each dose of MCh when compared to PBS-treated mice, and these increases were statistically significant (Figure 3.7C-F and Tables 3.5-3.8). Despite these findings, the effect of HDM treatment was not different between microbiotas. Thus, treatment with HDM did decrease lung function, as expected, but its effect did not vary among mice with the different human-derived microbiotas or between mice with any of the human-derived microbiotas and those with mouse microbiota. Collectively, these data suggest early gut microbiota composition plays an important role in determining baseline characteristics of AHR, and that in this study, its effect on AHR was more relevant than the presence or absence of the allergen.

Overall, these results indicate that mice with all 3 humanized microbiotas showed a tendency to increased AHR compared to mice with conventional mouse microbiota. Mice carrying Infant B microbiota showed the highest AHR and had a significant increase in AHR compared to the control group. The differences in AHR between mice carrying Infant B compared to mouse microbiota were characterized by increased resistance of the smaller peripheral airways (G) as well as an increase in airway closure (H), while resistance of the conducting airways (Rn) likely played a lesser role. Additionally, when airway resistance (Rrs) is elevated, as was detected in mice with Infant B microbiota, air can become trapped in the lungs limiting gas exchange resulting in bronchospasms, airway inflammation and increased mucus over time. Finally, the decreases in compliance (Crs) and elastance (Ers) detected here indicates that the lungs were stiffer with a higher than normal elastic recoil. This is expected to require a greater-than-average change in pleural pressure to change the volume of the lungs, thus, increasing the respiratory effort.

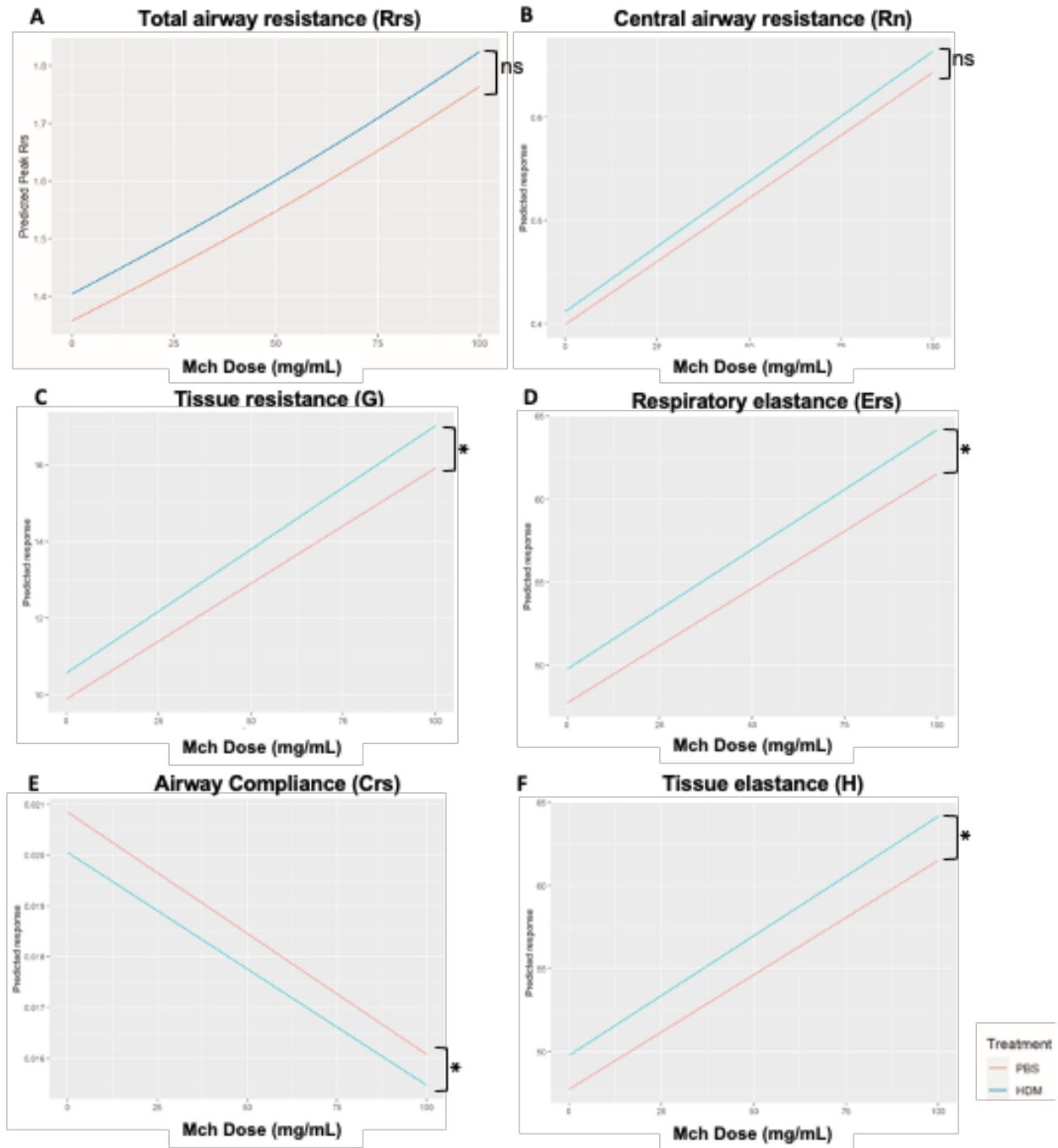


Figure 3.7 Mice treated with HDM had higher estimated means at each dose of MCh but its effect did not vary among the different microbiotas. A general linear mixed model was used to evaluate reactivity to methylcholine (Mch). Lines represent predicted change in peak value of lung function for each unit increase of MCh using a GLM for the corresponding treatment. Data represent the rate of change of (A) total airway resistance, (B) Central airway resistance, (C) Tissue resistance, (D) Respiratory elastance, (E) Airway compliance, and (F) Tissue elastance, relative to dose change of Mch. Red is phosphate buffered saline treated and blue is house dust mite treated. Y axis represents value of the specific lung function in their original scale. Pairwise

Figure 3.7 (cont'd)

comparisons were used to compare slopes. *P < 0.05. **P < 0.01. Data represented on each line include mice from all four microbiotas given the same treatment. Pairwise comparisons were used to compare slopes. *p < 0.05. **p < 0.01.

Effect of sex in baseline mechanics and airway hyperreactivity

No differences were found between male and female baseline values for any of the lung parameters measured, although this study was not designed or powered to specifically determine the effect of sex on airway hyperreactivity. Given these considerations, the main effect of sex was not significant for any of the parameters in our linear mixed models that evaluated AHR.

Mice carrying human or mouse microbiotas had similar histopathologic changes after acute exposure to HDM

Lung tissues and bronchoalveolar lavage fluid (BALF) were obtained to evaluate tissue inflammation, airway remodeling, infiltration of inflammatory immune cells, mucus cell metaplasia and an array of cytokines, including the Th2, Th1 and Th17 families.

Histopathological scoring showed that treatment with HDM increased inflammation in the lungs of mice with all 4 types of microbiotas when compared to their PBS controls (p values were Mouse p=0.003, Adult C p=0.033, Infant A p=0.003, Infant B p=0.038) (Figure 3.8A).

Histopathology scores were highest in Adult C mice given HDM. Inflammation in the lungs was concentrated around mid to small sized airways in HDM-treated mice (Fig. 3.8A).

Proportions of inflammatory cells changed in the BALF in response to HDM treatment in all microbiotas (Figure 3.8B). Mice with the Adult C microbiota given HDM had the greatest increases in eosinophils, lymphocytes and neutrophils. We observed significantly increased numbers of inflammatory cells in the BALF after HDM exposure, mainly an increase in the relative number of eosinophils (Mouse p=0.003, Adult C p=0.005, Infant A p=0.004, Infant B p=0.048), compared to mice carrying the same microbiota but treated with PBS (Figure 3.8C). Adult C and Infant B microbiota mice also had significant increases in neutrophils after HDM treatment when compared to mice given PBS (p<0.01 and p<0.05, respectively)(Figure 3.8C). Infant A microbiota mice had a significant increase of lymphocytes after HDM treatment when compared to mice given PBS (p<0.01)(Figure 3.8C). When comparing mice in all microbiota groups given PBS, no significant differences were found in the percentage of total BALF cells.

Similarly, when comparing mice in all microbiota groups given HDM, no significant differences were found in percentage of total BALF cells.

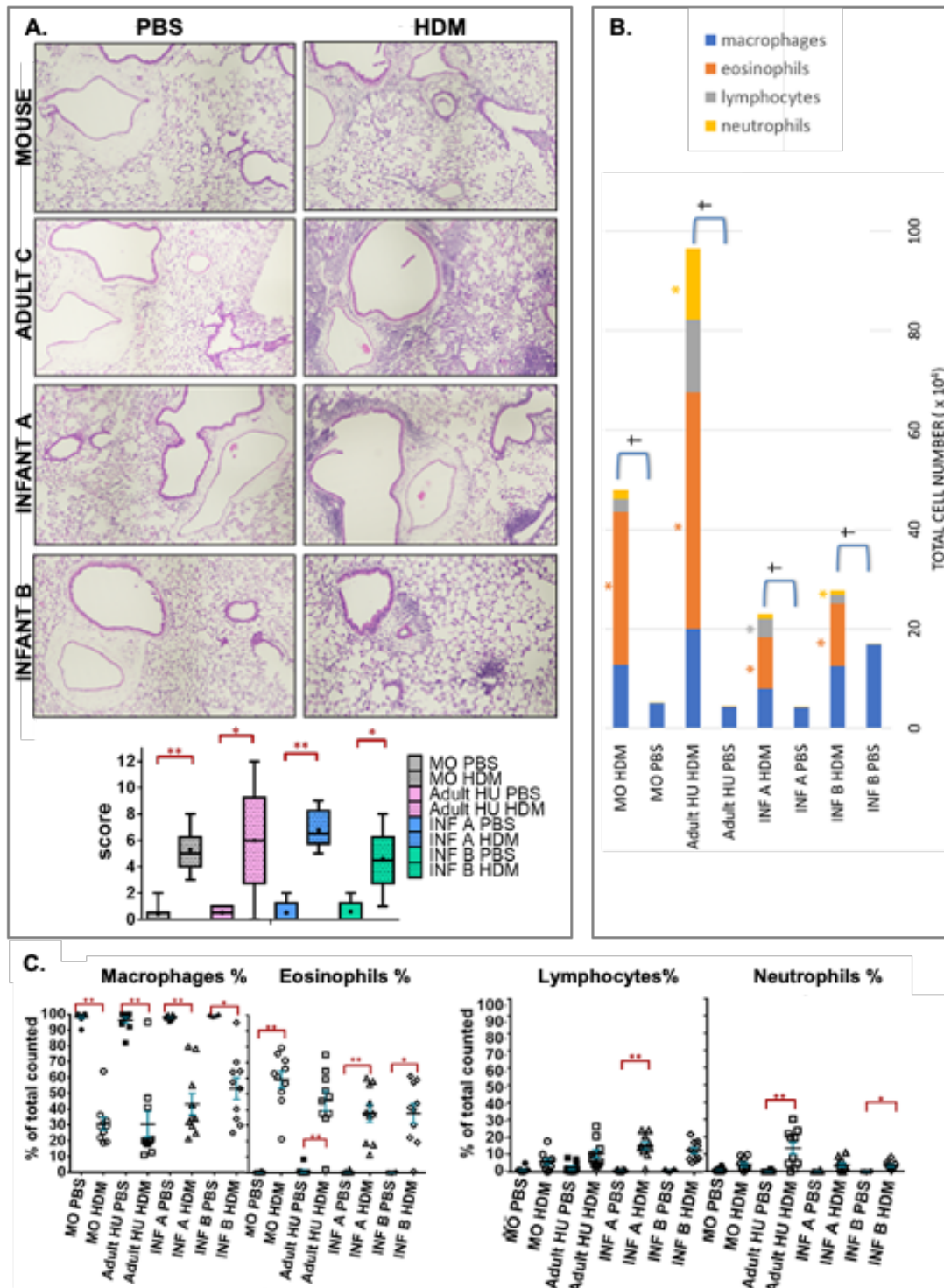
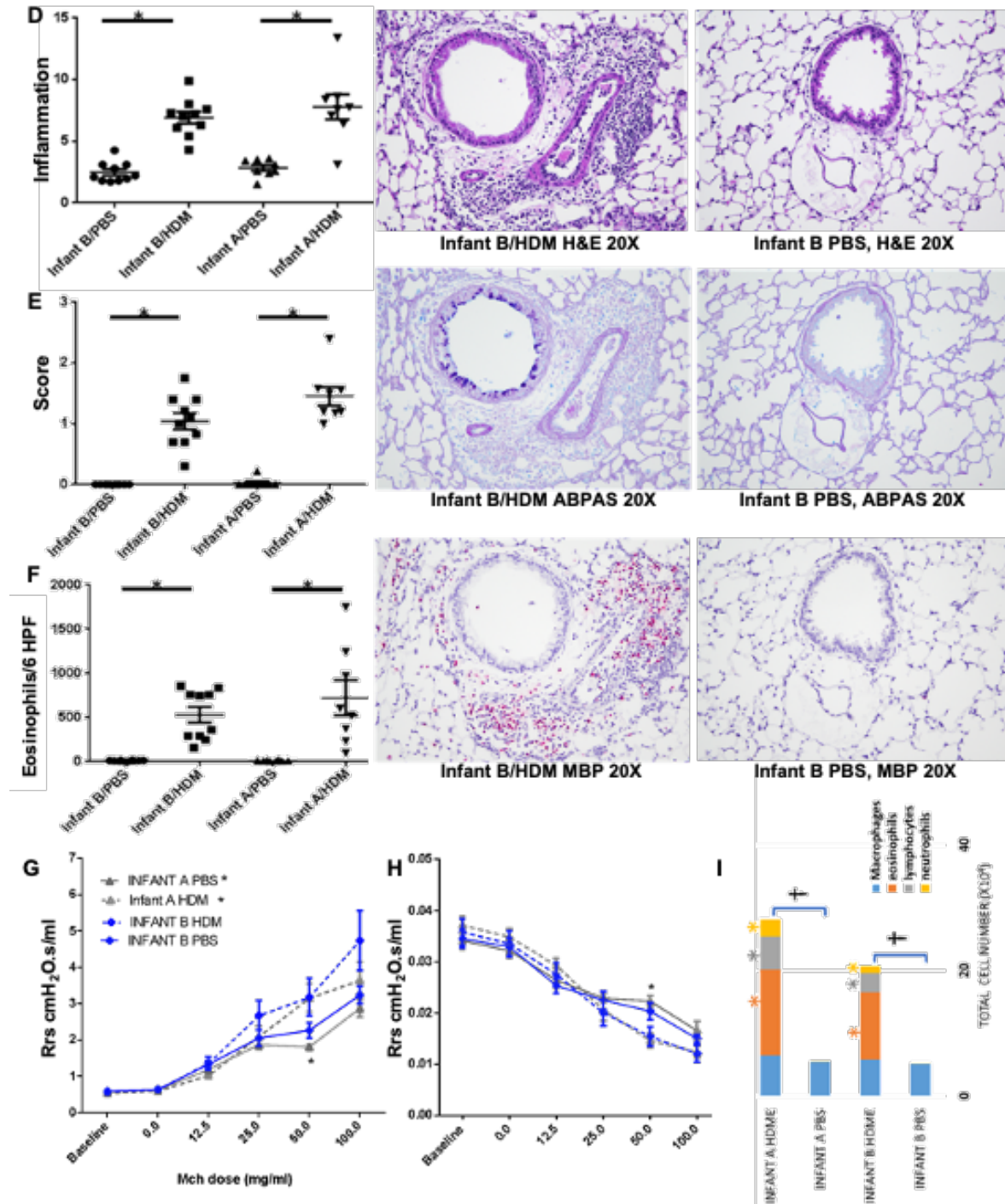


Figure 3.8 Histopathology and bronchoalveolar lavage results. (A – C) A) Lung histology and scores for each group. B) Total cell numbers from bronchoalveolar lavage with

Figure 3.8 (cont'd)

differential cell counts. C) Percentage of total cell count for cell populations in the bronchoalveolar lavage. Data represents mean \pm SE. *P < 0.05. **P < 0.01. Quantification of (D) Inflammation in hematoxylin and eosin stained lung sections, (E) Mucus Cell Metaplasia in Alcian Blue PAS stained lung sections, and (F) Density of Eosinophils on major basic protein stained lung sections. G) Total airway compliance and (H) total airway resistance of mice at baseline and after receiving increasing doses of Mch. (I) stacked bar graphs represent total cell number in BAL with proportions for each cell type in different color based on differential cell count performed in 300 cells per field.



Finally, IL-4 from lung homogenates of mice given HDM was significantly increased compared to those given PBS for mouse, Adult C, infant A and infant B microbiotas (p values=0.047, 0.016, 0.019, 0.035, respectively), while IL-13 was significantly increased for mice with Adult C microbiota given HDM ($p<0.05$) and IL-5 was significantly increased for mice with Mouse and Adult C microbiotas given HDM ($p<0.05$)(Figure 3.9A-C). Other

cytokines showed no differences in their levels neither between mice with the same microbiota give PBS or HDM treatments nor between those with different microbiotas (data not shown). Our results are consistent with an acute allergic airway response to HDM, as seen by the inflammation surrounding airways and blood vessels in the lung accompanied by marked infiltration of eosinophils and increased production of Type 2-associated cytokines. Most of the inflammatory responses were not significantly different between the different microbiotas, but certain cell types and Il-5 and Il-13 cytokines varied according to microbiota.

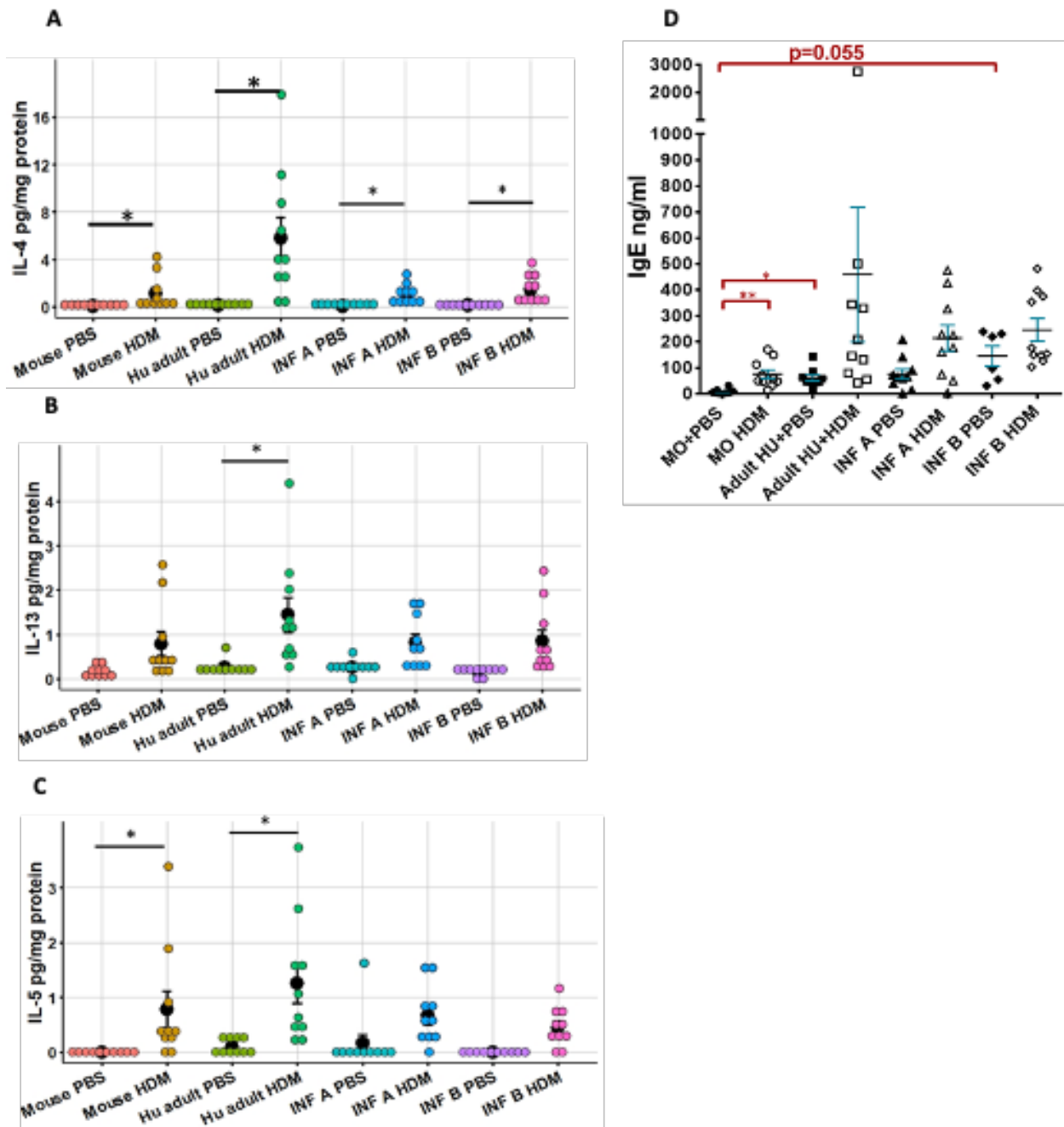


Figure 3.9 Type 2 immune response to HDM in different mice carrying different microbiotas. A) Interleukin-4 cytokine responses measured in lung tissue. B) Interleukin-13 cytokine responses measured in lung tissue. C) Interleukin-5 cytokine responses measured in lung tissue. D) Total immunoglobulin E responses in mice with different microbiotas given phosphate buffered saline or house dust mite allergen. Data represent mean \pm SE from 10 mice per group. Data analyzed with Kruskal Wallis with Mann-Whitney for pairwise comparisons. * $p < 0.05$. ** $p < 0.01$.

Mice with human microbiota developed elevated levels of total serum IgE

Mice with all human-derived microbiotas had overall increased levels of serum total IgE compared to mice with mouse microbiota in both PBS- and HDM-treated conditions (Figure 3.9D). Specifically, mice carrying Adult C human microbiota treated with PBS had significantly higher total serum IgE levels compared to mice carrying Mouse microbiota treated with PBS (p value= 0.007). Also, mice carrying Infant B microbiota given PBS had significantly higher values of total serum IgE compared to mice carrying Mouse microbiota given PBS (p values= 0.055). Infant B microbiota mice given HDM trended to higher levels of IgE compared to Mouse microbiota mice given PBS (p values= 0.062). Only mice carrying Mouse microbiota showed a significant increase in total serum IgE after treatment with HDM compared to the PBS control (p value= 0.009) (Figure 3.9D). This difference between levels of total serum IgE does not reflect a specific HDM-IgE increase since we only observed a few animals with detectable levels of HDM-specific IgE after the two weeks of HDM treatment (Supplemental Figure 3.2). Furthermore, other studies suggest that HDM-specific serum IgE levels require more than 2 weeks of HDM treatment to develop [180]. These results suggest that there is an association of increased total serum IgE with the increased AHR observed in mice carrying human microbiotas, compared to mice carrying mouse microbiota. However, since pretreatment total serum IgE levels were not measured in this experiment, additional work is needed to verify such an association.

Functional alterations in the resistance and elasticity of the respiratory system in mice with human-derived microbiota were associated with increased in total serum IgE levels but not HDM-specific IgE

To determine whether there was an association between eosinophilic infiltrates, lung inflammation, and Th17 and Th2 cytokines with lung function measurements, we evaluated the correlation between the presence of these factors and lung function parameters. A statistically significant moderate to strong positive correlation between overall baseline values for lung resistance and total serum IgE levels was found in all microbiota groups given HDM or PBS (Pearson correlation coefficient for HDM and PBS treated animals were equal to 0.408 and 0.650, respectively). Similar results were found for Total airway compliance (Crs), Total airway elastance (Ers), Tissue resistance (G) and Tissue elastance (H) (Supplemental Table 3.3). When

evaluating these correlations grouped by microbiota, we found that Adult C mice treated with HDM had a significant strong correlation between Rrs and total IgE at baseline, dose 0 mg/ml of Mch, dose 12.5 mg/ml of MCh, and dose 50 mg/ml, and a significant strong correlation between G and total IgE at dose 12.5 mg/ml of Mch. Mice carrying Infant A microbiota treated with PBS showed significant strong correlation between several lung function parameters at both baseline and dose 0 mg/ml of the Mch challenge. Mouse microbiota only had a significant strong correlation between Rrs at baseline and IgE, and only in PBS conditions. Infant B microbiota had no significant correlations between lung function parameters and total IgE. Interestingly, none of the other variables measured in our experiment showed a relevant correlation with lung function, or with each other, when analyzed by Pearson and Spearman correlation. Thus, we did not observe a correlation between the numbers of eosinophils, IL-4 or IL-13 cytokine levels, or lung inflammation with the amount of resistance and compliance lung function values. However, a strong correlation between baseline values (MCh = 0) for lung resistance and compliance and total serum IgE levels was found in two of the 6 groups of mice: those carrying human Adult C microbiota and given HDM treatment, and mice carrying Infant A microbiota and treated with PBS (Figure 3.10).

MICROBIOTA GROUPS	TREATMENT	MICROBIAL ECOLOGY				IMMUNOLOGICAL RESPONSES				LUNG HISTOPATHOLOGY						LUNG FUNCTION IMPAIRMENT																					
		DIVERSITY High (H) or low (L)	NUMBER OF PROINFLAMMATORY TAXA	NUMBER OF ALLERGY AGONISTS	NUMBER OF ANTI-INFLAMMATORY TAXA	NUMBER OF ALLERGY ANTAGONISTS	IL-4 (significant *p < 0.05)	IL-5 (significant *p < 0.05)	IL-13 (significant *p < 0.05)	IgE (significant *p < 0.05)	EOSINOPHILS BAL MEAN CELL COUNT	LYMPHOCYTES BAL MEAN CELL COUNT	NEUTROPHILS BAL MEAN CELL COUNT	MUCUS CELL META PLASIA RANK SCORE (1-3)	LARGE AIRWAY LESION RANK SCORE (1-20)	SMALL AIRWAY LESION RANK SCORE (1-20)	LUNG PARENCHYMA LESION RANK SCORE (1-20)	OVERALL LUNGS RAW SCORE (1-70)	RRS - MCH SIGNIFICANT INCREASE	CRS - MCH SIGNIFICANT DECREASE	LUNG ERS BASELINE	LUNG CRS BASELINE	LUNG RRS BASELINE	LUNG H BASELINE	LUNG G BASELINE	LUNG RN BASELINE	ERS AHR	CRS SIGNIFICANT AHR	RRS SIGNIFICANT AHR	H SIGNIFICANT AHR	G SIGNIFICANT AHR	RN SIGNIFICANT AHR					
Mouse Control	PBS	H	1	1	6	6				47	441	269	-	0	1	1	0																				
Mouse	HDM	H	1	1	6	6	*	*	*	3.0x10 ⁵	2.5x10 ⁴	1.9x10 ⁴	-	11	13	7	53																				
Infant A	PBS	L	5	6	3	3				186	416	115	0	1	2	0	5																				
Infant A	HDM	L	5	6	3	3	*		*	1.0x10 ⁵	3.7x10 ⁴	9709	1.35	19	18	11	68																				
Infant B	PBS	H	8	8	4	3			*	410	701	24	0	3	1	1	6																				
Infant B	HDM	H	8	8	4	3	*			1.2x10 ⁵	1.7x10 ⁴	9223	1.05	13	14	5	46																				
Adult C	PBS	H	5	7	1	2			*	343	1031	40	-	0	1	2	5																				
Adult C	HDM	H	5	7	1	2	*	*	*	4.7x10 ⁵	1.4x10 ⁵	1.4x10 ⁵	-	14	13	12	60																				

Figure 3.10 Summary heatmap showing responses of different microbiota groups given phosphate buffered saline (PBS) or house dust mite (HDM). (A) Summary heatmap shows data driving distinctions between lung function impairments in mice carrying one of four microbiota groups given PBS or HDM treatments and assessed using flexiVent, lung bronchoalveolar lavage cell counts (BAL), lung histopathology scoring and fecal microbiota16S rRNA gene sequencing. Proinflammatory and antiinflammatory taxa categories and agonist and

Figure 3.10 (cont'd)

antagonist categories are ranked scores for presence absence of defined bacteria shown in B and C. Shannon alpha diversity for the four microbiota groups are shown as high (H) or low (L) diversity. ERS is elastance, CRS is compliance, RRS is respiratory resistance, H Is tissue elastance, G is smaller peripheral airways and tissue damping, RN is central airway resistance and AHR is airway hyperresponsiveness. Methacholine (MCH) administration caused significant increases in lung resistance (RRS) and decreases in compliance (CRS) as shown by gray squares. Significant differences between lung baseline mechanics of groups compared to mice with mouse microbiota given PBS are also shown by gray squares. Infant B microbiota mice were the only group that had significantly increased airway hyperresponsiveness after MCH challenge when compared to mice with control microbiota given PBS.

Mice in Experiment 2 had similar responses to those in Experiment 1 (Table 3.9)

To confirm our previous findings that mice with Infant A and Infant B microbiotas were not different in their allergic airway response, we conducted a second experiment with four groups 1) Infant A with PBS, Infant A with HDM, Infant B with PBS and Infant B with HDM. Mice were sensitized to HDM, and MCh challenge given and lung function measured as in experiment 1. We observed no significant differences in lung function at baseline between Infant A or Infant B microbiota mice, given the same treatments. Also, we did not observe a significant difference in responses to increasing doses of Mch or AHR, measured as total airway resistance and compliance (Figure 3.8G and H). Furthermore, baseline lung function values and values taken at different doses of MCh for each microbiota were similar between experiment 1 and experiment 2 for mice in the same treatment group with the same microbiota (Data not shown). As seen in experiment 1, there were no significant differences between AHR responses between mice with the same microbiota treated with HDM and PBS, except for Infant A microbiota at dose 50 mg/ml of MCh, in which the increase in airway resistance and decrease in airway compliance were significantly higher than the PBS treated group (Figure 3.8G and H). Overall similar results from experiments 1 and 2 support the rejection of our hypothesis that Infant B microbiota decreased allergic response compared to Infant A microbiota.

Table 3.9 Comparison of Average \pm SEM values obtained. A) total airway resistance and B) Total airway compliance measurements for similar experimental groups between experiment 1 and experiment 2, at both baseline and at increasing doses of Mch.

A

Experiment		Baseline					
		values	0 mg/ml	12.5 mg/ml	25 mg/ml	50 mg/ml	100 mg/ml
1	Inf B-PBS	0.5512 \pm	0.5795 \pm	1.0437 \pm	1.6699 \pm	2.0632 \pm	2.2268 \pm
		0.0345	0.0371	0.0672	0.1148	0.1552	0.1340
2	Inf B-PBS	0.5881 \pm	0.6421 \pm	1.3302 \pm	2.0525 \pm	2.2647 \pm	3.2423 \pm
		0.0174	0.0187	0.0992	0.2234	0.2107	0.2404
1	Inf B-HDM	0.5989 \pm	0.6544 \pm	1.2302 \pm	2.5534 \pm	3.1823 \pm	6.0280 \pm
		0.0244	0.0324	0.1445	0.4232	0.3079	1.1228
2	Inf B-HDM	0.5711 \pm	0.6334 \pm	1.3573 \pm	2.6771 \pm	3.1805 \pm	4.7392 \pm
		0.0488	0.0519	0.1804	0.4078	0.5177	0.8228
1	Inf A-PBS	0.5523 \pm	0.6127 \pm	1.0951 \pm	1.8097 \pm	1.8817 \pm	3.1757 \pm
		0.0124	0.0221	0.0490	0.1454	0.1277	0.5439
2	Inf A-PBS	0.5647 \pm	0.6226 \pm	1.1888 \pm	1.8694 \pm	1.8123 \pm	2.8665 \pm
		0.0192	0.0172	0.1312	0.1336	0.0531	0.2331
1	Inf A-HDM	0.5361 \pm	0.6037 \pm	1.0237 \pm	2.2247 \pm	2.5345 \pm	2.9607 \pm
		0.0220	0.0361	0.1123	0.5509	0.3490	0.3431
2	Inf A-HDM	0.5393 \pm	0.6040 \pm	1.0292 \pm	2.0994 \pm	3.1587 \pm	3.6473 \pm
		0.0181	0.0202	0.0896	0.2909	0.3845	0.4978

B

Experiment		Baseline					
		values	0 mg/ml	12.5 mg/ml	25 mg/ml	50 mg/ml	100 mg/ml
1	Inf B-PBS	0.0335 \pm	0.0324 \pm	0.0277 \pm	0.0236 \pm	0.0207 \pm	0.0172 \pm
		0.0015	0.0013	0.0008	0.0014	0.0009	0.0012
2	Inf B-PBS	0.0345 \pm	0.0329 \pm	0.0253 \pm	0.0225 \pm	0.0203 \pm	0.0150 \pm
		0.0018	0.0018	0.0014	0.0018	0.0017	0.0009
1	Inf B-HDM	0.0335 \pm	0.0315 \pm	0.0260 \pm	0.0184 \pm	0.0161 \pm	0.0105 \pm
		0.0020	0.0019	0.0013	0.0013	0.0014	0.0016
2	Inf B-HDM	0.0358 \pm	0.0335 \pm	0.0275 \pm	0.0200 \pm	0.0154 \pm	0.0121 \pm
		0.0026	0.0025	0.0023	0.0025	0.0019	0.0017
1	Inf A-PBS	0.0350 \pm	0.0332 \pm	0.0275 \pm	0.0232 \pm	0.0213 \pm	0.0166 \pm
		0.0013	0.0013	0.0012	0.0014	0.0018	0.0019
2	Inf A-PBS	0.0341 \pm	0.0321 \pm	0.0264 \pm	0.0229 \pm	0.0223 \pm	0.0166 \pm
		0.0017	0.0013	0.0016	0.0008	0.0011	0.0018
1	Inf A-HDM	0.0349 \pm	0.0324 \pm	0.0273 \pm	0.0211 \pm	0.0179 \pm	0.0139 \pm
		0.0019	0.0021	0.0026	0.0028	0.0021	0.0018
2	Inf A-HDM	0.0371 \pm	0.0349 \pm	0.0292 \pm	0.0206 \pm	0.0147 \pm	0.0124 \pm
		0.0017	0.0016	0.0014	0.0021	0.0014	0.0012

Once again, lung inflammation was evaluated by total cell counts and differential counts in BALF and by lung histopathology. No differences were found in the amount or type of cell infiltration in the BAL when comparing Infant B to Infant A mice given the same treatment (PBS or HDM)(Figure 3.8I). Again, the amount of cell infiltration increased significantly after HDM treatment for mice with both microbiotas with a predominance of eosinophils over lymphocytes and neutrophils (Figure 8I). Total cell numbers were also similar to what was observed for Infant A and Infant B in experiment 1 (Figure 3.8B). For lung histopathology scoring in experiment 2 we found a significant difference in inflammation between mice with the Infant A microbiota who received PBS inoculations and those with the Infant A microbiota who received HDM inoculations ($p < 0.05$), and between mice with the Infant B microbiota who received PBS inoculations and those with the Infant B microbiota who received HDM inoculations ($p < 0.05$)(Figure 3.8D). No significant differences were observed when comparing the two PBS groups or when comparing the two HDM groups to one another. In the second experiment comparing outcomes in Infant A and B mouse groups, the amount of mucus cell metaplasia in all mice given HDM was increased compared to mice given PBS, but no differences between the microbiotas were found (Figure 3.8E).

Similar to the results for lung inflammation, significant increases were observed when comparing mucus cell metaplasia in HDM treated groups to PBS ($p < 0.05$)(Figure 3.8E). Lastly, significant differences were observed when comparing the density of eosinophils in groups treated with HDM to groups treated with PBS ($p < 0.05$), but not when comparing mice with Infant A microbiota treated with HDM or PBS to mice with Infant B microbiota treated with HDM or PBS, respectively (Figure 3.8F). Overall these results indicate an increase in lung inflammation after treatment with HDM, but no differences were found in the amount of inflammation between the two microbiota groups. Moreover, the difference in findings between experiment 1 and 2 can be explained by the increase in variance among data during experiment 1 and the larger number of experimental groups. Despite this difference we can conclude that the values of Baseline IgE for mice with the same microbiota were similar between the two experiments. The average value of baseline IgE for the Infant A PBS treated group was 39 ng/ml, and for the Infant B PBS group it was 242 ng/ml, which represents similar values when compared to experiment 1 (Figure 3.9, D and E). This shows that mice carrying Infant A or Infant B microbiota maintain their specific IgE phenotype throughout subsequent generations

because the microbiota is passed on essentially unchanged.

Discussion

This study established two new murine models with human-derived fecal microbiota from infants of the Isle of Wight birth cohort to study effects of gut microbiota in asthma pathogenesis

Fecal microbiotas from Infant A eczemic infants and Infant B non-eczemic infants were successfully transplanted to germ-free mice, remained stable, passed to offspring largely unchanged, and maintained a consistent diversity. To evaluate inflammatory allergic responses in airways of mice carrying different microbiotas, we used an induced asthma-like model using HDM, a common allergen associated with human asthma known to generate a Type 2 immune response polarization. This response is characterized by increased T helper 2 cytokines IL-4, IL-5 and IL-13, induction of class switch recombination in activated B cells to IgE; and eosinophilic infiltration into the lungs [181]. Despite having distinct microbiotas, Infant A, Infant B, and Adult C models all had decreased lung function at baseline without any allergen treatment when stimulated with methacholine in a dose-response design. The lung functions we evaluated corresponded to the overall resistance, elastance and compliance of the respiratory system (referred to as Rrs, Ers, and Crs, respectively), central airway resistance (Rn), smaller peripheral airway resistance and tissue damping (G), and tissue elastance (H). Significant increases in Rrs and Rn at baseline were seen in mice with Infant A and Adult C microbiotas. Significant decreases in compliance (Crs) at base line were seen in mice with all human-derived microbiotas, which correlated with modest increases in cellular infiltrates in lungs. These results indicated a direct effect of the human-derived microbiotas in eliciting increased respiratory resistance (Rrs), elastance (Ers), central airway resistance (Rn), tissue damping (G), tissue elastance (H) and decreased lung compliance. When mice were sensitized with HDM, significant differences were seen in lung baseline mechanics in Ers, G, H and decreased compliance (Crs), but the human-derived microbiotas had less effect on Rrs and Rn. Nevertheless, when sensitized with HDM, mice carrying all human-derived microbiotas demonstrated AHR compared to PBS controls with mouse microbiota, but these elevations were statistically significant only in the Infant B mice. All three of these human-derived microbiota models will be useful for studying how acquisition and maturation of the microbiota affects an individual's respiratory mechanics

and immune responses. A great advantage to this comparative approach was using germ-free mice of the single C57BL/6 genotype so that host genetic background is not a consideration. Also, the models were established without using antibiotics to deplete the original microbiota; this procedure eliminates previous microbial influences on the immune response. Further, the offspring we used as experimental mice acquired microbiota vertically and passively from their parents and littermates, similar to how a child would acquire its microbiota from parents and siblings. Because **these microbiotas were vertically transferred largely unchanged to their offspring, they provide replenishable and tractable models for testing effects of the microbiota on allergic airway disease outcomes. Strict exclusion of extraneous microbiota was achieved because mice were maintained in a closed barrier colony with sterile gowning and gloving for handling the mice.** Since most work done on influence of gut microbiota points to an early life effect, using a model where the microbiota establishes and matures naturally before mice are tested for asthmatic responses is an advantage for mimicking the human life course that predisposes to asthma.

In mice with all three human microbiotas we found significant impairment in baseline respiratory mechanics—in the absence of a direct stimulus for bronchoconstriction—when compared to the control mouse microbiota and to healthy non-allergic animals. To our knowledge, this is the first demonstration of impairment of baseline lung function attributed to specific human gut microbiotas. The differences in lung function at baseline between mice carrying human microbiotas versus congenic mice carrying mouse microbiota points towards a direct effect of the gut microbiota on respiratory mechanics. This direct effect may be mediated by the early microbiota during the time of education of the immune system, which subsequently contributes to susceptibility to AHR. This conclusion is strengthened by the findings that lung function parameters from these three models, e.g. tissue elastance versus central airway resistance, did not show the same magnitude of change. In examining the reported results of a recent study by Brown and colleagues examining lung responses to ozone in C57BL/6 mice of from two different vendors with different gut microbiotas, we noticed differences in pulmonary baseline responses even in the absence of ozone [182]. Although the authors don't comment on these data, this result provides another example where changes in baseline respiratory mechanics provoke differences in AHR between mice with different gut microbiotas, reinforcing the idea that

gut microbiota has a direct effect on lung function. Because differences observed at baseline respiratory mechanics within each lung function may mislead one to believe that differences observed at different MCh doses are caused by increased reactivity to MCh or AHR, and not just due to the initial differences found at baseline, we developed a statistical model to evaluate reactivity to MCh while controlling for baseline in order to accurately pinpoint differences in AHR of these mice. Thus, we were able to account for differences at baseline respiratory mechanics when measuring AHR in mice exposed to PBS or HDM. **The significant effects seen here on baseline respiratory mechanics support the idea that investigators should define and control for gut microbiota in studies where lung function parameters are being evaluated.**

Lung function results indicated that mice with all three human-derived microbiotas showed a tendency to increased AHR compared to mouse microbiota after only two weeks of HDM sensitization

Mice with Infant B microbiota showed the highest AHR and had significant increases in AHR compared to the control group. The differences in AHR between mice carrying Infant B compared to mouse microbiota were characterized by increased resistance of the smaller peripheral airways (G) as well as an increased in airway closure (H), while resistance of the conducting airways (Rn) likely play a lesser role. This occurred even before a full adaptive immune response to HDM was present.

When taken together, the BALF cell counts, histopathological scoring, cell-specific staining and cytokine analyses suggest that inflammation, while elevated, appears to be involved but not sufficient to account for the decreased lung function in mice with the three human-derived microbiotas

We observed a pattern of AHR in Infant B microbiota mice that was significantly increased compared to mice carrying the mouse microbiota. Importantly, this phenomenon was observed in the absence of specific HDM-induced inflammatory responses (non-allergic). In HDM-treated mice, those with Adult C and Infant A microbiotas had higher lung histologic scores than mice with mouse microbiota and mice with all human-derived microbiotas had increases in inflammatory cells, mainly surrounding the small airways. However, these responses were not

statistically significant due to large variation in the range of lung inflammation within the groups. Slight elevation of lung inflammation occurred in the PBS-treated human-derived microbiota groups but it was not significant. Likewise, when given PBS, Infant B mice had elevated macrophages in BALF that was not significant. When given HDM, proportions of inflammatory cells increased in the BALF in response to HDM treatment in all microbiotas; mice carrying the Adult C microbiota had the highest numbers of eosinophils, lymphocytes, and neutrophils, but these were not statistically significantly different from mice with other microbiotas. Interestingly, only Adult C and Infant B microbiota mice had significant increases in neutrophils after HDM treatment. In contrast, mice with Infant A microbiota had significant increases in BALF lymphocytes after HDM treatment, not seen in other groups. These specific increases in neutrophils and lymphocytes in BALF likely relate to distinct bacterial exposures. Also, after HDM sensitization, we did see significant increases in mucus cell metaplasia in Infant A and B microbiota mice compared to their PBS controls. When given HDM, mice with all four microbiotas had elevated IL-4 responses. There was a similar trend toward elevated IL-13 in HDM-treated mice for all microbiotas, but only mice with Adult C microbiota had statistically significant elevations. After HDM treatment, IL-5 was elevated in mice with either Mouse or Adult C microbiota, but neither Infant A nor B microbiota mice produced this cytokine at significant levels. We also examined total serum IgE levels in all mice at the time of necropsy. When given HDM, mice with mouse microbiota had significantly elevated total serum IgE. However, two of the human-derived microbiota groups (Adult C and Infant B), had significant elevations when given PBS alone, compared to the mouse PBS control group. In fact, none of the human-derived microbiotas had significantly elevated total serum IgE when given HDM because the background responses in the PBS-treated groups were so high. Levels of HDM-specific serum IgE were not detectable two weeks post sensitization, which was not surprising since adaptive responses take longer to fully develop [180]. Taken together, these data suggest that inflammatory changes alone do not explain the decreased lung function found in mice with human-derived microbiotas. This conclusion is further supported by the presence of lung function decline in the absence of HDM sensitization or in HDM-treated mice only two weeks after sensitization at a time when a full adaptive immune response had not occurred. These studies confirm what has been seen in patients with asthma, where AHR can be present in the absence of significant inflammation [183].

These studies support the concept that multiple allergy agonists and proinflammatory taxa functioned in a community-wide fashion to impair lung function in the absence of antagonistic and anti-inflammatory taxa

The summary heatmap (Figure 3.10A) shows that this concept is strongly supported and that each human-derived microbiota harbored a different constellation of agonists and proinflammatory taxa, which likely lead to the varied allergic and pathologic manifestations measured. Candidate taxa acting as putative allergy agonists in microbiotas 1) Infant A were *Bacteroides*, *Lachnospiraceae*, *Turicibacter*, *Clostridium*, *Escherichia coli/Shigella*, *Coprobacter*, *Lachnoclostridium*, *Klebsiella*, *Haemophilus*, 2) Infant B were *Bacteroides*, *Lachnospiraceae*, *Alistipes*, *Turicibacter*, *Clostridium*, *Parabacteroides*, *Sutterella*, *Parasutterella*, *Haemophilus*, and *Veillonella*, and 3) Adult C were *Bacteroides*, *Lachnospiraceae*, *Turicibacter*, *Parabacteroides*, *Alistipes*, *Ruminiclostridium*, *Sutterella*, *Parasutterella* and *Haemophilus* (Figure 3.10B). Known proinflammatory taxa present in these human-derived microbiotas included *Bacteroides*, *Parabacteroides*, *Akkermansia*, *Sutterella*, *E. coli-Shigella*, *Parasutterella*, *Klebsiella*, *Haemophilus*, and *Veillonella* (Figure 3.10C). Only the uncultured *Bacteroides* sp. and *Haemophilus* were found in all three communities, but none of the proinflammatory taxa mentioned appeared in the protected mouse microbiota. Thus, the pattern of responses in each microbiota correlated to presence of different mixes of agonist and inflammatory taxa. For example, Infant A mice where lung function responses were less than in mice with Infant B and Adult C microbiotas had much smaller proportions of allergy agonists *Alistipes*, *Sutterella*, and *Parasutterella* and a larger proportion of the allergy antagonist *Bifidobacterium*. Also, Infant A microbiotas had much smaller proportions of pro-inflammatory taxa *Parabacteroides* and *Parasutterella* and a larger proportion of anti-inflammatory *Bifidobacterium*. Finally, diversity had no apparent effects as the Infant A microbiota was low diversity and these mice had the lowest positive allergic responses when compared with Infant B and Adult C.

We acknowledge that there **could be single bacterial taxon that exerted large effects because several potential respiratory pathogens were identified, but none that solely explain the data. Thus, our results lead us to reject our hypothesis that *E. coli-Shigella* were the sole responsible agonist taxon, given that this taxon was only present in appreciable amounts in the Infant A microbiota. Another possibility is that metabolites from groups of taxa may act to impair lung function in mice with the human-derived microbiotas, but, if**

so, these metabolites would be different for these three human-derived communities. Because of the complexity of the mixes of allergy agonists/antagonists and pro- and antiinflammatory taxa in the three human-derived microbiotas that were associated with lung function decline, more work is needed to discern whether the metabolites produced by these three human microbiotas could be mainly responsible for these effects or whether specific virulence mechanisms drive the phenomena. Other studies have shown the association of certain gut microbiota compositions, diversity, or metabolites with the presence of allergic airway disease [123, 184]. While mechanisms are not yet known, Olszak et al. showed that microbial exposure during early life has persistent effects on natural killer T cell function [123]. Depner et al. mentioned the association of increased levels of butyrate produced by the microbiota as a potential clue to how specific microbial communities exert an asthma-protective effect [102]. Since butyrate and other metabolic products can be sensed by the vagus nerve as described in the process of Inflammatory bowel disease [185], it is likely that either the presence or absence of certain gut metabolites may have effects on the afferent and efferent nerve output which innervate the airways and chest wall and that travel via the vagus nerve. These nerve terminals are responsible for the degree of airway smooth muscle constriction and AHR, especially in response to increasing doses of MCh, and they exhibit plasticity in early stages of life when certain conditions are met, such an increase in the amount of specific neurotrophins and nerve growth factors.

Known allergy antagonists and antiinflammatory bacterial taxa dominated the mouse microbiota while the number of these genera and their abundances were much lower in the human-derived microbiotas. Allergy antagonists unique to the mouse microbiota included *Clostridia* (*Clostridiales*), *Faecalibacterium*, and *Ruminococcus-Coprococcus*, while *Roseburia*, *Lactobacillus*, and *Bifidobacteria* were in high amounts but also present in one of the human-derived communities. Antiinflammatory bacterial taxa were also found exclusively in the protected mouse microbiota including *Roseburia* and *Lactobacillus* which were distinct OTUs from the same genera seen in Infant B microbiotas. These observations are consistent with the findings of Arrieta and colleagues in children at risk of asthma that were also missing some of these protective taxa (*Lachnospira*, *Veillonella*, *Faecalibacterium*, *Rothia*) [2]. Yet, genera such as *Veillonella* contain both protective and pathogenic species, so more work is needed to determine species specific characteristics of the identified bacterial taxa. Depner et al. showed

that microbial communities with the likelihood of producing butyrate—especially those in children on farms—were the ones associated with the highest protective effect against asthma [102]. They demonstrated that bacterial taxa contributing to protective effects of butyrate included *Roseburia* and *Coprococcus* [102]. In our study *Roseburia* and *Coprococcus* were present in protected mice with mouse microbiota but were also found in similar levels in Infant B and Adult C mice bearing human-derived microbiotas. Moreover, mice with Infant B microbiota hypothesized to be “protective” had decreased lung function and the highest AHR compared to the control mouse microbiota. This may have been due to the shifts in abundance observed in bacterial taxa in the transplanted mice compared to donor infants; all mice were fed a high fiber, low fat diet mouse chow substantially different from the milk and/or formula diet of the infants from whom the transplant inocula were derived. In another study, Trompette et al. found that treatment of mice with the short chain fatty acid (SCFA) propionate led to alterations in bone marrow hematopoiesis that were characterized by enhanced generation of macrophage and dendritic cell (DC) precursors and subsequent seeding of the lungs by DCs with high phagocytic capacity but an impaired ability to promote Type 2 cell effector function [186]. Recognizing our results and these findings, we rejected our hypothesis that a high abundance Bacteroides-enriched gut microbiota from non-eczemic infants was protective in transplanted mice after challenge with HDM. More work is needed to determine if adding back each or all of these organisms could prevent decreases in lung function in mice with human-derived microbiotas.

Thus, lung function declines in mice with what we expected to be a protective Infant B microbiota were clear-cut, but the cause for this outcome was not. We acknowledge it was more difficult to discern impairments in lung function due to a specific microbiota when examining mice sensitized with HDM because increased allergen-associated inflammatory responses were high across all microbiota groups. After HDM treatment, inflammation around the airways caused an overall increase in resistance and tissue stiffness, making subtle differences in respiratory mechanics observed at baseline in the negative control mice harder to detect. However, it is known that HDM has no effect on baseline respiratory mechanics as seen in studies of HDM-treated BALB/c mice [187]. Therefore, this study suggests the AHR differences found between mice carrying the human-derived microbiotas and the control mice are due to a direct effect of the microbiota on airway structural components and potentially airway innervation. Yet, we can’t rule out action by other immune cells known to

influence airway innervation and AHR that were not evaluated such as mast cells [188-191]. Mast cells may provide an intermediary pathway between gut microbiota and lung function responses [191, 192].

Possible limitations

The main limitations identified were high variance within each experimental group especially those groups with human-derived microbiota and the presence of a few outliers for respiratory mechanics, inflammatory responses and specific immune markers measured. This is not surprising when measuring biological variables and may be due to variation in the abundance of bacterial taxa acquired by individual mice from their parents. For example a greater abundance of a proinflammatory/agonist taxon or decreased abundance of anti-inflammatory/antagonist taxon in an individual mouse could cause variation in responses. Another possibility for the variation was that we chose a relatedly short time course of HDM sensitization and challenge. This was chosen to focus specifically on innate responses while capturing some early adaptive response but was not ideal for evaluating peak adaptive immune responses or HDM-specific IgE levels between the mice with different microbiotas such as pointed out by Woo et al. [180]. This variation did impede us from being able to use parametric statistical tools such as ANOVA to evaluate our data. Yet, the same response patterns were found in repeated experiments over generations of mice, which gave us confidence in the results. Furthermore, this variation was not due to age or sex in our experiments. Moreover, we did find a correlation between levels of baseline IgE and baseline lung function responses for compliance and resistance in mice with Infant B and Adult C microbiotas.

In conclusion, our study strongly supports a direct connection between a particular gut microbiota exposure in infancy and lung baseline responses. Because altered lung responses may lead to AHR and therefore to asthma, our study supports the existence of a mechanism through which the gut microbiota can alter the threshold level for developing asthma independently of the level of airway inflammation. Future experiments will focus on determining changes in airway innervation after exposure to a particular microbiota, as well as changes in other immune cells that can be targeted by IgE during development to influence lung mechanics and airway innervation during lung development and maturation. We propose that a risk microbiota

promotes structural and functional changes in the lungs during the developmental period, which exacerbates the overall airway allergic response.

Materials and methods

Laboratory Animals

Mouse experiments followed the guidelines of the National Institutes of Health Guide to the Care and Use of Laboratory Animals. All protocols were reviewed and approved by the Institutional Animal Use and Care Committee of Michigan State University (06/12-107099, 6/15-101-00, and 05/17-091-00). All mice used in these studies were C57BL/6 mice originally obtained from The Jackson Laboratory (Bar Harbor, ME) barrier facility. Mice used had conventional mouse microbiota or human microbiota from 1) 3-month-old infants from the Isle of Wight Birth Cohort [18] or 2) young adults (Adult C)[140, 178]. Mice with human-derived microbiota were offspring of the mice given FMT from Isle of Wight infants. All experiments were conducted with age-matched male and female mice between 8-10 weeks of age. Specific pathogen free breeding colonies for these mice were established on the campus of Michigan State University in facilities free of *Helicobacter*, *Campylobacter*, *Citrobacter rodentium*, *Enterococcus faecalis*, and other known colitis-causing or respiratory pathogens based on testing as previously described [19]. Mice were tested for these bacteria prior to use. Sentinel mice were used in both the conventional and humanized microbiota mouse colonies to monitor for known mouse pathogens at 6-month intervals (IDEXX BioAnalytics, Columbia, MO).

Study cohort and collection of fecal samples from infants

Fecal samples from 3-month-old infants of the Isle of Wight (IOW) third generation birth cohort were used [131]. 60 infants were recruited by obtaining consent from pregnant IOW cohort members and pregnant partners of male cohort members to collect fecal samples and clinical outcome parameters at 3, 6, 12, 24 and 36 months of age. IRB documents and approvals have been published for this study [54]. Fecal samples were collected from diapers by nurses, coded to protect identity and clinical status, and placed into a sterile container at the 3-month visit. If a fecal sample was not available during the clinic visit, nurses arranged a home visit to collect samples. Samples were stored on ice for the short transport, bagged in an anaerobic pouch, and then stored at -80°C until processed. Infant fecal samples for transplant into germ-free mice were selected based on 16S rRNA gene sequencing and correlation with assessments for allergic

disease including eczema, wheeze, atopy and asthma over the 3-year time frame. Thus, all samples used for the FMT of germ-free mice were collected previously [54] and data analyzed to determine which samples to use for transplantation. Fecal samples for transplant were selected based on 1) bacterial taxonomic structure at genus level, 2) ordination using canonical correspondence analysis (CCA), and 3) similarity percentage analysis (SIMPER).

Fecal collection and Illumina 16S rRNA gene sequencing and data analysis to assess which samples to use for FMT

Batches of samples were sent to the Mansfield lab by overnight Federal Express shipping on dry ice. Samples were handled in an anaerobic hood for aliquoting. DNA was isolated from 500 mg of each sample using the FastDNA SPIN Kit for stool (MP Biomedicals, Solon, OH) according to the manufacturer's protocol. Careful attention was given to preventing lab contamination by the operator or within the laminar flow hood. All reagents were validated free of 16S DNA before use. Standard controls (Mock Community, ATCC/BEI) were run alongside samples to control for contamination of the reagents during processing. Qubit analysis (Thermo-Fisher Scientific, Waltham, MA) was performed to determine DNA concentration; 16S rRNA gene PCR was performed to validate the quantity and purity of the DNA samples prior to submission to the Michigan State University Research Technology Support Facility (RTSF) for Illumina MiSeq sequencing. At RTSF, the V4 region of the 16S rRNA gene were amplified by PCR in triplicate using two sets of barcoded primers [58], and the PCR products purified, combined, and sequenced using Illumina MiSeq. In all, 62 samples were submitted for sequencing, including 60 mouse samples, the original fecal slurry used for inoculation of founder mice, and a mock community (HM-782D, BEI) for estimation of sequencing error. PCR products were normalized using an Invitrogen SequalPrep DNA normalization plate and the normalized products pooled. After quality control and quantitation, the pool was loaded on a standard MiSeq v2 flow cell and sequenced with a 500 cycle MiSeq v2 reagent kit (paired-end 250 base pair reads). Base calling was performed by Illumina Real Time Analysis (RTA) v1.18.54 and output of RTA was demultiplexed and converted to FastQ format files with Illumina Bcl2fastq v1.8.4. 109,085 high-quality reads from Illumina sequencing remained - average read number per group: 3896 (min 3245, max 5053).

16S rRNA gene amplicon analysis protocol was performed using QIIME2 (v. 2019.1) version <https://docs.qiime2.org/2019.1/> accessed May 2019. Alignment was accomplished using

the Silva 16S ribosomal gene database [59]. Chimeric sequences and any sequences classified as chloroplast, mitochondria, Archaea, or Eukaryota, were removed from the dataset using UCHIME. Sequences were clustered in Operational Taxonomic Units (OTUs) of 97% sequence identity yielding 128 OTUs. Analyses were performed in PAST 3.07 [60] and R version 4.06 [193]. Following processing of sequences and chimera removal in QIIME2. Groups were sub-sampled at a depth of 3245 reads and grouped using an average neighbor method. Sequence read data has been made available through the DRYAD database under <https://doi.org/10.5061/dryad.xgxd254hs>.

Preparation of the inocula

To preserve all components of the microbiota in its original state, fecal samples and the inocula were handled in an anaerobic hood. Each sample was suspended in 2 ml of Trypticase soy broth. The samples for each microbiota mixture were combined in a single 50 ml conical centrifuge tube. Solids were removed by sedimentation in a sealed tube and removing the supernatant to a sterile tube. Inocula-containing tubes were sealed prior to removal from the anaerobic hood and transported on ice to the containment facility. 200 μ l of inoculum was delivered to each mouse immediately by oral gavage in a laminar flow biological safety cabinet using a 3.5 French red rubber feeding tube attached to a 1 ml syringe. Approximately 0.5 ml of each Infant A and Infant B mix was saved in 2.0 ml cryovials for DNA isolation for sequencing of the inocula.

Fecal Microbiota Transplantation (FMT) of germ-free mice (Figure 3.2)

C57BL/6 germ-free mice were from the same barrier facility at The Jackson Laboratory as the C57BL/6 mice with conventional mouse microbiota. They underwent caesarian rederivation and their offspring were thereafter propagated in the germ-free facility at University of Michigan (Ann Arbor, MI). Germ-free C57BL/6 mice were bred for these studies by University of Michigan. At 7 weeks of age, mice were transported to Michigan State University in sterile shipping containers, immediately placed into a biosafety cabinet and inoculated with the human fecal microbiota by oral gavage. All operators including scientists and animal care personnel gowned and gloved every time mice were handled. Sterile technique was used to prevent transfer of the operators' or environmental microbiota to mice. Five male and 5 female germ-free C57BL/6 mice received a fecal transplant of the Infant A inoculum and 5 male and 5 female mice received the Infant B inoculum.

Mice were observed for clinical signs after fecal transplant twice daily for two weeks.

Then they were placed in breeding pairs according to their microbiota and allowed to breed for at least two breeding cycles to generate mice for a closed colony and to conduct the two experimental studies. Breeding practices were employed to maximize the mixing of the microbiota within a microbiota type: 1) male mice were left with the pregnant female until the offspring were weaned and 2) we randomized the selection of males for females for breeding pairs to eliminate a “family” bias in subsequent generations. Details for Adult C mice were transplanted in a similar manner as previously described [140, 178]. All mice were monitored by a rigorous testing program for mouse pathogens using sentinels and testing by Charles River Laboratories (Wilmington, MA).

Experimental designs for mouse model of allergic airway disease

Experiment 1 Design (Table 3.3)

To address the effect of microbiota on airway allergic responses, 20 mice, from each of the 4 different gut microbiota groups including mouse (control), Infant A, Infant B, and Adult C, were randomly assigned to treatment groups with vehicle (PBS) or HDM as previously described [194]. The outcomes assessed in each of these experiments (airway responsiveness, histopathology scores, BALF cytology, serum immunoglobulins and cytokines) are quantitative measures of allergy that were analyzed as continuous variables.

Age-matched C57BL/6 mice (n=10 per group) were used in all experiments. We used inbred mice housed in a strictly controlled environment and handled in a highly standardized manner, which improves uniformity of the allergy response variables within groups. This uniformity of outcome variables has long been our experience, is widely established in the literature [1, 3-7], and was the basis for our sample size (n= 8 or 10/group). Finally, the sample size was selected based on achieving 83.1% power for broncho-hyperresponsiveness to MCh after HDM treatment. A total of 8 experimental groups (n=10 per group, 5 males and 5 females) were used. At the end of the HDM treatment protocol, data was collected from each mouse to evaluate allergic responses based on lung function and immune responses. Mice that were mis-dosed during the treatment protocol (4 mice in Infant B PBS group), and mice that died during the surgical procedure or during measurement of lung mechanics for lung function were excluded from the analysis.

Experiment 2 Design (Table 3.3)

In order to confirm our previous findings of Infant A and Infant B not being different in their airway's allergic response, we conducted a second experiment. The experimental design was exactly the same as in experiment 1, except that we used only mice carrying Infant B or Infant A microbiota. Experimental design is shown in Table 3.3 recognizing that mice with Adult C and Mouse microbiota were not used. Mice were sensitized to HDM as indicated in experiment 1. Lung function and MCh challenge were obtained as indicated in experiment 1. Once again, lung inflammation was evaluated by total cell counts in BALF and by lung histopathology. Differential cell counts were also performed as described in Experiment 1. For experiment 2, lung histopathology scoring was evaluated in three categories: Inflammation, mucus cell metaplasia and density of eosinophils. We measured mucus cell metaplasia in this experiment as another possible inflammatory marker for the degree of the airway allergic response, with the intention of picking up other differences between responses in mice with Infant A and Infant B microbiota.

Sensitization to allergen

Approximately 10–15 weeks after birth, house dust mite allergen sensitization was initiated (Table 3.3). Mice were inoculated on a schedule such that those receiving allergen were exposed to 50 µg of HDM in 25 µL of Dulbecco's Phosphate Buffered Saline (PBS) on the first day, designated day 0, and 30 µg of HDM in 30 µL of PBS on days 2, 5, 7, 9, and 12 (Table 3.3). Those controls receiving only PBS received equivalent volumes on those days. To perform the sensitization, mice were placed in an induction chamber and given 3% isoflurane through a vaporizer at a rate of 1L/min until non-motile and non-responsive to handling. Mice were then removed from the chamber, held by scruffing, and had 10 µl of the HDM solution or PBS administered intranasally via a pipette. Between each subject the isolation chamber and all gloves were sprayed with 70% ethanol.

Tracheal Cannulation and Respiratory Mechanics Evaluation using flexiVent Analysis

Forty-eight hours after receiving the last dose of HDM or PBS, mice were anaesthetized via a mixture of ketamine (range 80-120 mg/kg), xylazine (range 8-12 mg/kg), and acepromazine (range 5-10 mg/kg) given intraperitoneally. Once movement ceased and mice were non-

responsive to a toe pinch, a ventral midline incision was made over the mid-cervical region from the base of the jaw to the thoracic inlet. The trachea was exposed by blunt dissection, a small incision made in the mid-cervical trachea distal to the larynx, and an 18-gauge beveled cannula was inserted and secured with a ligature. Animals were then ventilated using a flexiVent apparatus (SCIREQ, Montreal, QC) at a frequency of 15000-120 breaths per minute and at a volume of 10 ml/kg body weight at 0.17-0.2 ml/breath. Mice were allowed to exhale passively through an expiratory valve to an end pressure of 4 cm H₂O positive end expiratory pressure. Any animals which displayed respiratory effort during the process were administered an additional 0.1 ml injection of ketamine (range 80-120 mg/kg), xylazine (range 8-12 mg/kg), and acepromazine (range 5-10 mg/kg) given intraperitoneally. To stimulate airway constriction, an allergic challenge of aerosol acetyl- β -methylcholine (MCh, Sigma-Aldrich, St. Louis, MO) was generated through an in-line nebulizer (Aeroneb, SCIREQ, Montreal, QC) that was administered in increasing doses (0.625 to 200 mg/mL) in 10 second dosing intervals with a 3-5-minute break between dosing. Six increasing doses of MCh starting at 0 (PBS), 6.25, 12.5, 25, 50 and 100 mg/ml were delivered. Data were collected for 2 minutes 45 seconds following each methacholine dose in a series of 12 repetitions of the single frequency forced oscillation (SnapShot-150) and complex forced oscillation (Quick Prime) maneuvers as applied by the flexiVent apparatus. Data on pressure and flow was collected throughout and used to determine resistance and compliance of the airways. Responses to increasing methacholine doses were measured within 2m 45s post nebulization using the flexiVent. Single frequency or complex forced oscillations maneuvers were applied by the flexiVent. Volumes and pressures were recorded, and the following parameters measured or derived from those measurements to evaluate lung function including: dynamic resistance of the respiratory system (Rrs), which assesses the resistance to air flow as a function of the extent (level of airway constriction); dynamic compliance of the respiratory system (Crs), which assesses the ability of the lungs to stretch; dynamic elastance (Ers), which assesses lung stiffness; Newtonian resistance (Rn), which assesses central airway resistance constriction; tissue damping (G), which reflects tissue (alveolar) resistance; and alveolar tissue constriction and tissue elastance (H), which reflects tissue (alveolar) elastance (alveolar tissue stiffness).

Bronchoalveolar lavage (BAL) total cell and differential cell counts

To collect BALF, 0.7 to 0.8 ml of sterile saline was slowly instilled through the tracheal catheter. Then, BALF was slowly withdrawn until bubbles appeared, dispensed into a sterile tube and the process repeated. BALF samples were pooled, and total cells counted on a hemocytometer. Following this, 150ul BALF was centrifuged onto slides using a Shandon Cytospin 3 Centrifuge (Marshall Scientific, Hampton, NH) at 40x g for 10 minutes. Slides were air dried, fixed in methanol and stained with Diff Quick stain (Polysciences, Inc., Warrington, PA) for differential counting. Remaining BALF was centrifuged at 465g (=1500 rpm), at 4°C for 15 minutes, supernatants removed and stored at -80°C.

Euthanasia

Mice still under anesthesia from the mechanics evaluation, were euthanized via exsanguination. Mice were wet with 70% ethanol to avoid hair in the incision site, and then a ventral midline incision was made from the xiphoid process to the pubis. Visceral organs were evaluated for gross abnormalities then moved to the side to expose the abdominal aorta. A 1 mL syringe with a 25g needle was used to collect approximately 0.5 mL of blood, after which the vessel was severed to complete exsanguination. The collected blood was transferred into a 0.8 mL lithium heparin separator tube, which was then spun for 15 minutes at 3,500 rpm at 4°C. Serum was then removed and stored in a freezer (-20°C). At this point the thoracic cavity was opened via blunt dissection of the hemi-diaphragms, and complete collapse of the lungs was evaluated before complete removal of the chest wall. Finally, the heart, lung, and trachea were removed as a block.

Lung dissection, fixation, sectioning, and staining

Once BALF was collected, the heart-lung block was removed by dissection with extreme care to prevent nicking of trachea, extrapulmonary bronchi or lung lobes. Lungs were removed from the thoracic cavity attached to the canula and placed on a sheet of dental wax to reduce surface friction. First the right main stem bronchus was ligated using silk-suture and the 4 right lung lobes were removed. The right cranial, middle, and postcaudal lobes were placed into a 2 mL screw-top cryovial and snap frozen in liquid N₂. These lobes were then stored in the -20°C freezer. The right caudal lobe was cut in half and placed into a 2 mL flat bottom tube containing

1.5 mL of RNAlater and placed in a 4°C refrigerator for 24 hours before being moved to a -20°C freezer for future RNA analysis. Next the trachea and left lung lobes were fixed in 10% neutral buffered formalin using an inflation-fixation apparatus. The trachea and lungs were perfused under constant pressure (30 cm of fixative pressure) for 1 hour under 30 cm of fixative pressure. Thereafter lungs were tied off, removed from the apparatus, and stored in a large volume of formalin until further processing.

The fixed left lobes were separated from the trachea by severing the left main stem bronchus using scissors. The lobes were then sectioned on dental wax and sliced transversely into approximately 3 mM sections using a straight razorblade. These sections were placed cut side down into a cassette which was then submerged into 30% ethanol. The specimens were dehydrated, embedded in paraffin, and three sections cut from each block at 4 µm thickness. Sections were then deparaffinized and stained with hematoxylin and eosin (H&E), Alcian blue periodic acid-Schiff (ABPAS), or major basic protein (MBP) by the Investigative Histopathology Laboratory, Division of Human Pathology, Department of Physiology, Michigan State University. Slides were then scanned and digitized using an Olympus VS110 machine and were subsectioned at 20x using Visiomorph Microimager (Visiopharm, Denmark) [195]. In order to score inflammation, slides stained for Hematoxylin and Eosin were assessed. 6 10X fields under were captured using a Nikon DS-F13 camera attached to a Nikon H600L light microscope and stitched together using the NIS-Elements BR 5.02.00 program (Nikon-USA, Melville, NY). Within these fields large airways, small airways, and vasculature were assessed for the layers of inflammatory cells that surrounded each structure at their densest/thickest point. The results for each type of structure were averaged, and then the three resulting values were averaged for an overall 'inflammatory score.

Lung histopathology scoring

The histologic scoring system for the lungs was based on published scoring criteria [196-200]. Our scoring system was based on a meta-analysis of four published protocols and allows for focus on observed lesions by the slide reader. We first noted the number of tissue sections on the slide. Using a battlement pattern for each section, the total number of large airways was recorded. The reader then repeated the battlement pattern evaluating how many of these airways were affected by inflammation. To be considered positive, an airway was required to be cuffed

with closely associated mononuclear cells. Thereafter the large airway(s) with the worst pathology were evaluated to determine the density/thickness of inflammation surrounding the structures. This evaluation was based on the thickness of the layer of inflammatory cells comprising the diameter of the aggregate that was recorded as a ranked score (0-3, none, mild, severe) based on the rubric for those structures. We also noted the diameter of the largest aggregate evaluated. The process was repeated (Steps 1-4) for small airways and for vasculature (Steps 1-4). Thereafter the parenchyma was evaluated for the presence of inflammatory cells not associated with airways or vasculature and a score assigned (0-3, none, mild, severe) for generalized inflammation. Next, a point of 1 was added if focal clusters of inflammatory cells were present within the parenchyma. Finally, a point of 1 was added if there was evidence of obliterated small airways within areas of dense parenchymal inflammation (either focal or generalized). A total score was reached by adding all the points scored to achieve a 'Pathology Grade'. Two independent blinded investigators (LSM, IMU) scored the images based on the consensus scoring system and graded the inflammation score.

Measurement of lung cytokines

The cranial right lung lobes were thawed on ice, weighed and homogenized in Q-mammalian protein kit buffer containing protease inhibitor (QIAGEN Inc. USA), using the TissueLyser II (QIAGEN Inc., Germantown, MD). Homogenates were further centrifuged at 14,000x g for 20 minutes in a microcentrifuge precooled to 4°C, and supernatants (i.e., total protein fractions) were aliquoted into new microcentrifuge tubes precooled to 4°C and stored at -80°C until further analysis. Total protein in mg/ml was measured using the Pierce™ BCA Protein Assay Kit (Thermo Fisher Scientific Inc. Massachusetts, U.S). Cytokines were measured using a commercially available flow cytometry-based, multiplexed, bead assay panel (LEGENDplex Mouse Th Cytokine Panel, BioLegend, San Diego, CA). Just before analysis, aliquoted supernatants of the lung homogenates were thawed on ice and centrifuged at 300 x g for 10 minutes at 4°C to further pellet any debris and ensure clarity. The assay was performed using undiluted supernatant and a V-bottom microplate, according to the manufacturer's instructions. All samples were run in duplicate. Analytes included IFN- γ , TNF- α , IL-2, IL-4, IL-5, IL-6, IL-9, IL-10, IL-13, IL-17A, IL-17F, IL-21, and IL-22. Data were acquired on a BD FACSCanto II flow cytometer and analyzed using the LEGENDplex Data Analysis software, where standard

curves were generated for each analyte. Data are presented as the average of the replicates in pg cytokine/mg of protein.

Total IgE and specific anti-HDM IgE analysis

Plasma samples were aliquoted to avoid repetitive freezing and thawing and stored at -80°C .

Total plasma IgE was measured using BioLegend Mouse IgE ELISA MAX Deluxe Set (BioLegend, Inc. San Diego, CA). Briefly, samples were diluted according to a standardized dilution factor based on results from preliminary assays. Samples that were higher than the limit of detection on the first run were repeated using a higher dilution. Mouse IgE standard was reconstituted in buffer, and six two-fold serial dilutions were performed according to the manufacturer's instructions. All incubation steps with shaking were done at 200 rpm. Capture antibody for mouse IgE was diluted in 1X coating buffer. 100 µL was added to each well of a 96 well plate, and the plate was incubated overnight at 4°C. Plates were washed four times with ELISA wash buffer (20X) (BioLegend, Inc. San Diego, CA) and 200 µL of 1X Assay Diluent A was added to each well for blocking. Plates were incubated for 1 hour at room temperature. Samples were diluted in 1X Assay Diluent A. Plates were washed four times and 100 µL of each sample was added to appropriate wells. Plates were incubated at room temperature with shaking for 2 hours and then washed four times. 100 µL of biotinylated detection antibody (diluted 1:200 in 1X Assay Diluent A) was added to each well and plates were incubated for 1 hour at room temperature with shaking. Plates were washed four times. 100 µL of Avidin-HRP (diluted 1:1000 in 1X Assay Diluent A) was added to each well; then plates were incubated 30 minutes at room temperature with shaking. Plates were washed five times. Wash buffer was allowed to sit for 30-60 seconds between each wash. TMB substrate solution was prepared and 100 µL of substrate solution was added to each well. Plates were then incubated in the dark at room temperature for 15 minutes. 100 µL of stop solution (2 N sulfuric acid) was added to each well and the absorbance was read at 450 nm using a microplate reader. All the samples were run in duplicate. Concentrations were calculated through elisaanalysis.com, using a 4-parameter logistic curve as recommend in the kit instructions. For samples that were repeated on multiple plates, the concentrations were averaged. Data are presented as ng/ml.

For specific HDM-IgE measurement, we used the Mouse Anti-House Dust Mite (HDM) IgE Antibody Assay Kit (Chondrex Inc, Woodinville, WA). Plasma samples were handled as above

and different dilutions were tested in preliminary assays to arrive at a standard dilution of 1:10. All samples were run in duplicates. The assay was performed following the manufacturer kit's instructions. Final concentrations were calculated using a 4-parameter logistic curve through elisaanalysis.com and are presented as the average of the duplicates in ng/ml.

Bacterial DNA isolation from mouse feces

At the time of necropsy, fecal samples were collected, the tubes immediately placed on dry ice, stored at -80°C and later processed for 16S rRNA gene sequencing to assess the fecal microbiota of the mice. DNA was extracted using the FastDNA SPIN Kit stool kit (MP Biomedicals, Solon, OH) following the manufacturer's protocol. Briefly, for each mouse, a single fecal pellet was suspended in 978 µL of sodium phosphate, 122 µL of MT buffer added, and the sample homogenized using a bead beater for 40 seconds. The samples were centrifuged at 14,000 x g for 10 minutes, and the supernatant was then extracted, combined with 250 µL PBS, and centrifuged at 14,000 x g for 5 minutes. The supernatant was again collected and combined with 1 mL of the provided DNA binding matrix. The resulting solution was mixed on a tube vortex for 2 minutes, allowed to resettle, and then 500 µL of supernatant was discarded. The remaining solution was resuspended and then centrifuged 600 µL at a time at 14,000 x g for 1 minute in a Spin Filter tube. The resulting pellet was washed by resuspending in 500 µL of ethanolated SEWS-M and centrifuged at 14,000 x for 1 minute, then again for 2 minutes after disposing of the waste fluid. Samples were then allowed to air dry at room temperature for 5 minutes before being resuspended in 200 µL of DES (DNase/Pyrogen-Free Water) and incubated at 55°C for 15 minutes on a heating block. Samples were then centrifuged at 14,000 x g for 2 minutes, and the filtered liquid was collected for further analysis. The presence of DNA was assessed in all samples using a Nanodrop instrument before being placed in a -80°C freezer for storage.

DNA samples from all mouse fecal samples were validated and processed for 16S rRNA gene sequencing as described for infant fecal samples above. 16S rRNA gene amplicon analysis was performed using QIIME2 (v. 2019.1) as described above for infant fecal samples and microbial ecology data analyzed.

Statistical analysis

Microbial ecology data from 16S rRNA gene sequencing of infant and mouse fecal DNA was

analyzed to determine the richness and evenness of the infant and mouse fecal bacterial communities. Principal Components Analysis (PCA) was performed in R [193] to examine relative compositions of the three human-derived microbiotas (Infant A, Infant B and Adult C), Mouse microbiota and the two Infant inocula A and B. PCA was also performed to examine the relatedness of the three human-derived microbial communities Infant A, Infant B and Adult C microbiotas separately. To examine similarity (dissimilarity) between bacterial taxa in these two sets of groups, we performed a two-way PERMANOVA in PAST 4.03 using the Bray Curtis similarity measure (with microbiota and treatment as factors). Unweighted Pair Groups with Arithmetic Averaging (UPGMA) was performed in PAST 4.03 on samples from all microbiota groups and the Infant A and Infant B inocula using the Bray Curtis similarity measure with 1000 bootstrap replications in PAST version 4.03. For the heat maps, we compared the average relative abundance of the bacterial taxa contributing 90% of the differences in Similarity Percentage calculation (SIMPER; in PAST 4.03) for 1) all samples (Infant A, Infant B and Adult C, Mouse microbiotas and the two Infant inocula A and B) and for 2) the three human-derived microbiotas.

For cytokine analysis, plasma total and specific HDM IgE, differential cell counts and lung histopathology, and lung function measurements are presented as mean \pm standard error. Kruskal-Wallis one way ANOVA statistic was used on PAST 4.02 to compare baseline lung functions for the microbiota groups.

A general linear mixed (GLM) model was used to examine the effects of methacholine (MCh) concentrations, microbiota groups, and treatment assignment on the degree of airway hyperresponsiveness [201]. Outcomes were measurements of the lung function at peak (bottom for Crs) after each MCh dose or after nebulized PBS was delivered (dose 0). The outcomes were included in the model with a logarithmic transformation. Predictors included dose, microbiota, treatment, and the log-transformed baseline values for each dose. Random effects accounted for the repeated measures on each mouse. Mouse microbiota group served as the reference category in microbiota groups, whereas PBS (sham) treatment served as the reference treatment. Interaction terms were included to assess the effect of dose on the peak lung function for each microbiota group. To compare reactivity to increasing doses of MCh, the predicted slopes coefficients from the linear mixed model for each microbiota group were compared using the Tukey test for multiple pairwise comparisons. For each model, we considered a p-value < 0.05 to

indicate a statistical significance. All analyses were conducted using statistical software R version 4.06 using the glmmTMB and lme4 packages [193]. Pearson and Spearman correlation analyses were conducted using the ggpairs and ggally packages in R software.

Acknowledgement

We thank the Investigative Histopathology Laboratory, Division of Human Pathology, Department of Physiology, Michigan State University for their excellent preparation and staining of slides for the project. We thank Neil Hammer for allowing us to use his anaerobic hood for handling the original fecal samples from the infants.

Funding

These studies were funded mainly with federal funds from the National Institute of Allergy and Infectious Diseases, National Institutes of Health, Department of Health and Human Services, under Grant No. R21AI121748-01A1, Defining the role of the early infant microbiota in mediating allergic outcomes associated with asthma in a mouse model. Matching support for the mouse colony, sequencing supplies and salary was provided by the Albert C. and Lois E. Dehn Chair Endowment and a University Distinguished Professor Endowment to Linda S. Mansfield. Matching support for 16S rRNA gene sequencing was provided through a discretionary funding initiative grant from the College of Veterinary Medicine and the Office of the Senior Vice President for Research and Innovation of Michigan State University. Stipend for the author Hinako Terauchi was provided by the College of Veterinary Medicine, Michigan State University.

Availability of data and materials

All data is presented within this manuscript “Fecal microbiota transplants of three distinct human communities to germ-free mice exacerbated inflammation and decreased lung function in their offspring” and is available for use upon publication. Datasets are available through the DRYAD database under <https://doi.org/10.5061/dryad.xgxd254hs>.

Author’s contributions

Ivon Moya Uribe – analyzing lung function and immunological functions of mice based on

stored samples, data analysis, producing the figures and tables, and writing the manuscript.

Hinako Terauchi – Conducting mouse experiments and necropsy procedures, processing of samples for 16S rRNA gene sequencing, validating samples for sequencing, processing sequencing data through the pipeline and data analysis, and writing and review of the manuscript.

Julia A. Bell – assisting with fecal transplant procedure to produce Infant A and B mice, breeding all mice, organizing and conducting mouse experiments and necropsy procedures, data analysis, producing figures and tables and writing and reviewing of the manuscript.

Alexander Zanetti – establishing a ranked scheme based on the literature for histopathology scoring and examining and scoring slides of the lungs for various parameters.

Sanket Jantre – data analysis, writing and reviewing of manuscript

Marianne Huebner – data analysis, writing and reviewing of the manuscript

S. Hasan Arshad – Principal Investigator for the Isle of Wight birth cohort study, medical management of patients, supervision of nursing staff for data and sample collection, and reviewing the manuscript.

Susan L. Ewart – obtaining funding, organizing, and conducting mouse experiments especially lung function studies, necropsy procedures, data analysis, writing and reviewing of the manuscript.

Linda S. Mansfield – obtaining funding, conducting fecal transplant procedures to produce Infant A and B mice, breeding mice, organizing, and conducting mouse experiments and necropsy procedures, reading histopathology slides, data analysis, writing and reviewing of the manuscript.

Competing interests

The authors declare that they have no competing interests.

Ethics approvals

All procedures involving animals were performed in accordance with the recommendations described in the Guide for the Care and Use of Laboratory Animals of the National Institutes of Health under protocols approved by the Michigan State University Institutional Animal Use and Care Committee (approval numbers 06/12-107-00 and 06/15-101-00).

REFERENCES

1. Tanno, L.K., et al., Categorization of allergic disorders in the new World Health Organization International Classification of Diseases. *Clin Transl Allergy*, 2014. **4**: p. 42.
2. Arrieta, M.C., et al., Early infancy microbial and metabolic alterations affect risk of childhood asthma. *Sci Transl Med*, 2015. **7**(307): p. 307ra152.
3. Jones, S.M., et al., Efficacy and safety of oral immunotherapy in children aged 1-3 years with peanut allergy (the Immune Tolerance Network IMPACT trial): a randomised placebo-controlled study. *Lancet*, 2022. **399**(10322): p. 359-371.
4. Zimmermann, P., et al., Association between the intestinal microbiota and allergic sensitization, eczema, and asthma: A systematic review. *J Allergy Clin Immunol*, 2019. **143**(2): p. 467-485.
5. CDC, N.C.f.H.S., More Than a Quarter of U.S. Adults and Children Have at Least One Allergy. 2023.
6. Bieber, T., Atopic dermatitis. *N Engl J Med*, 2008. **358**(14): p. 1483-94.
7. Chan Ho Na, J.C., Eric L. Simpson, Quality of Life and Disease Impact of Atopic Dermatitis and Psoriasis on Children and Their Families. *Children*, 2019. **6**(12)(133).
8. Camfferman, D., et al., Eczema and sleep and its relationship to daytime functioning in children. *Sleep Med Rev*, 2010. **14**(6): p. 359-69.
9. Chamlin, S.L., et al., The price of pruritus: sleep disturbance and cosleeping in atopic dermatitis. *Arch Pediatr Adolesc Med*, 2005. **159**(8): p. 745-50.
10. Stores, G., A. Burrows, and C. Crawford, Physiological sleep disturbance in children with atopic dermatitis: a case control study. *Pediatr Dermatol*, 1998. **15**(4): p. 264-8.
11. Holm, E.A., et al., Life quality assessment among patients with atopic eczema. *Br J Dermatol*, 2006. **154**(4): p. 719-25.
12. Absolon, C.M., et al., Psychological disturbance in atopic eczema: the extent of the problem in school-aged children. *Br J Dermatol*, 1997. **137**(2): p. 241-5.
13. Mitchell, A.E., et al., Parenting and childhood atopic dermatitis: A cross-sectional study of relationships between parenting behaviour, skin care management, and disease severity in young children. *Int J Nurs Stud*, 2016. **64**: p. 72-85.
14. Daud, L.R., M.E. Garralda, and T.J. David, Psychosocial adjustment in preschool children with atopic eczema. *Arch Dis Child*, 1993. **69**(6): p. 670-6.
15. Patel, K.R., et al., Association between atopic dermatitis, depression, and suicidal ideation: A systematic review and meta-analysis. *J Am Acad Dermatol*, 2019. **80**(2): p. 402-410.
16. Wadonda-Kabondo, N., et al., Association of parental eczema, hayfever, and asthma with atopic dermatitis in infancy: birth cohort study. *Arch Dis Child*, 2004. **89**(10): p. 917-21.
17. Matsuoka, S., et al., Prevalence of specific allergic diseases in school children as related to parental atopy. *Pediatr Int*, 1999. **41**(1): p. 46-51.
18. Schultz Larsen, F., Atopic dermatitis: a genetic-epidemiologic study in a population-based twin sample. *J Am Acad Dermatol*, 1993. **28**(5 Pt 1): p. 719-23.

19. Larsen, F.S., N.V. Holm, and K. Henningsen, Atopic dermatitis. A genetic-epidemiologic study in a population-based twin sample. *J Am Acad Dermatol*, 1986. **15**(3): p. 487-94.
20. Biagini Myers, J.M. and G.K. Khurana Hershey, Eczema in early life: genetics, the skin barrier, and lessons learned from birth cohort studies. *J Pediatr*, 2010. **157**(5): p. 704-14.
21. Williams, H. and C. Flohr, How epidemiology has challenged 3 prevailing concepts about atopic dermatitis. *J Allergy Clin Immunol*, 2006. **118**(1): p. 209-13.
22. Wahn, U., Wahn, U. "The immunology of fetuses and infants: What drives the allergic march. *Allergy*, 2000. **55**(7): p. 591-599.
23. Wang, I.J., et al., Effect of gestational smoke exposure on atopic dermatitis in the offspring. *Pediatr Allergy Immunol*, 2008. **19**(7): p. 580-6.
24. Schafer, T., et al., Maternal smoking during pregnancy and lactation increases the risk for atopic eczema in the offspring. *J Am Acad Dermatol*, 1997. **36**(4): p. 550-6.
25. Kramer, U., et al., The effect of environmental tobacco smoke on eczema and allergic sensitization in children. *Br J Dermatol*, 2004. **150**(1): p. 111-8.
26. LL. Muizzuddin N, M.K., Vallon P, Maes D. , Effect of cigarette smoke on skin. *J Soc Cosmet Chem*, 1997. **48**(5): p. 235-242.
27. Flohr, C., D. Pascoe, and H.C. Williams, Atopic dermatitis and the 'hygiene hypothesis': too clean to be true? *Br J Dermatol*, 2005. **152**(2): p. 202-16.
28. McNally, N.J., et al., Is there a geographical variation in eczema prevalence in the UK? Evidence from the 1958 British Birth Cohort Study. *Br J Dermatol*, 2000. **142**(4): p. 712-20.
29. McKeever, T.M., et al., Siblings, multiple births, and the incidence of allergic disease: a birth cohort study using the West Midlands general practice research database. *Thorax*, 2001. **56**(10): p. 758-62.
30. Karmaus, W. and C. Botezan, Does a higher number of siblings protect against the development of allergy and asthma? A review. *J Epidemiol Community Health*, 2002. **56**(3): p. 209-17.
31. Williams, H.C., D.P. Strachan, and R.J. Hay, Childhood eczema: disease of the advantaged? *BMJ*, 1994. **308**(6937): p. 1132-5.
32. Pickett, K.E. and R.G. Wilkinson, Income inequality and health: a causal review. *Soc Sci Med*, 2015. **128**: p. 316-26.
33. McKenzie, C., et al., The nutrition-gut microbiome-physiology axis and allergic diseases. *Immunol Rev*, 2017. **278**(1): p. 277-295.
34. Irvine, A.D. and P. Mina-Osorio, Disease trajectories in childhood atopic dermatitis: an update and practitioner's guide. *Br J Dermatol*, 2019. **181**(5): p. 895-906.
35. Prevention, C.f.D.C.a., Asthma, Most Recent National Asthma Data 2021. 2023.
36. Yang, C.L., J.M. Gaffin, and D. Radhakrishnan, Question 3: Can we diagnose asthma in children under the age of 5 years? *Paediatr Respir Rev*, 2019. **29**: p. 25-30.
37. Cave, A.J. and L.L. Atkinson, Asthma in preschool children: a review of the diagnostic challenges. *J Am Board Fam Med*, 2014. **27**(4): p. 538-48.

38. Silverberg, J.I. and J.M. Hanifin, Adult eczema prevalence and associations with asthma and other health and demographic factors: a US population-based study. *J Allergy Clin Immunol*, 2013. **132**(5): p. 1132-8.
39. Pate CA, Z.H., Qin X, Johnson C, Hummelman E, Malilay J, Asthma Surveillance — United States, 2006–2018, in *MMWR Surveill Summ* 2021. 2021. p. 1-32.
40. Brannan, J.D. and M.D. Lougheed, Airway hyperresponsiveness in asthma: mechanisms, clinical significance, and treatment. *Front Physiol*, 2012. **3**: p. 460.
41. Postma, D.S. and H.A. Kerstjens, Characteristics of airway hyperresponsiveness in asthma and chronic obstructive pulmonary disease. *Am J Respir Crit Care Med*, 1998. **158**(5 Pt 3): p. S187-92.
42. Ruan, Z., et al., Asthma susceptible genes in children: A meta-analysis. *Medicine (Baltimore)*, 2020. **99**(45): p. e23051.
43. Schauberger, E.M., et al., Identification of ATPAF1 as a novel candidate gene for asthma in children. *J Allergy Clin Immunol*, 2011. **128**(4): p. 753-760 e11.
44. Ziyab, A.H., et al., Allergic sensitization and filaggrin variants predispose to the comorbidity of eczema, asthma, and rhinitis: results from the Isle of Wight birth cohort. *Clin Exp Allergy*, 2014. **44**(9): p. 1170-8.
45. Chen, S., et al., Consistency and Variability of DNA Methylation in Women During Puberty, Young Adulthood, and Pregnancy. *Genet Epigenet*, 2017. **9**: p. 1179237X17721540.
46. Zhang, H., et al., The interplay of DNA methylation over time with Th2 pathway genetic variants on asthma risk and temporal asthma transition. *Clin Epigenetics*, 2014. **6**(1): p. 8.
47. Soto-Ramirez, N., et al., The interaction of genetic variants and DNA methylation of the interleukin-4 receptor gene increase the risk of asthma at age 18 years. *Clin Epigenetics*, 2013. **5**(1): p. 1.
48. Yousefi, M., et al., The methylation of the LEPR/LEPROT genotype at the promoter and body regions influence concentrations of leptin in girls and BMI at age 18 years if their mother smoked during pregnancy. *Int J Mol Epidemiol Genet*, 2013. **4**(2): p. 86-100.
49. Mukherjee, A.B. and Z. Zhang, Allergic asthma: influence of genetic and environmental factors. *J Biol Chem*, 2011. **286**(38): p. 32883-9.
50. von Mutius, E., Environmental factors influencing the development and progression of pediatric asthma. *J Allergy Clin Immunol*, 2002. **109**(6 Suppl): p. S525-32.
51. O'Dwyer, D.N., R.P. Dickson, and B.B. Moore, The Lung Microbiome, Immunity, and the Pathogenesis of Chronic Lung Disease. *J Immunol*, 2016. **196**(12): p. 4839-47.
52. Kozik, A.J. and Y.J. Huang, The microbiome in asthma: Role in pathogenesis, phenotype, and response to treatment. *Ann Allergy Asthma Immunol*, 2019. **122**(3): p. 270-275.
53. Martinez, F.D. and S. Guerra, Early Origins of Asthma. Role of Microbial Dysbiosis and Metabolic Dysfunction. *Am J Respir Crit Care Med*, 2018. **197**(5): p. 573-579.
54. Stokholm, J., et al., Maturation of the gut microbiome and risk of asthma in childhood. *Nat Commun*, 2018. **9**(1): p. 141.

55. Simon, A.K., G.A. Hollander, and A. McMichael, Evolution of the immune system in humans from infancy to old age. *Proc Biol Sci*, 2015. **282**(1821): p. 20143085.
56. Halkias, J., et al., CD161 contributes to prenatal immune suppression of IFN γ -producing PLZF⁺ T cells. *J Clin Invest*, 2019. **129**(9): p. 3562-3577.
57. Mishra, A., et al., Microbial exposure during early human development primes fetal immune cells. *Cell*, 2021. **184**(13): p. 3394-3409 e20.
58. Rackaityte, E., et al., Viable bacterial colonization is highly limited in the human intestine in utero. *Nat Med*, 2020. **26**(4): p. 599-607.
59. Mold, J.E., et al., Fetal and adult hematopoietic stem cells give rise to distinct T cell lineages in humans. *Science*, 2010. **330**(6011): p. 1695-9.
60. Romagnani, S., Immunologic influences on allergy and the TH1/TH2 balance. *J Allergy Clin Immunol*, 2004. **113**(3): p. 395-400.
61. Sender, R., S. Fuchs, and R. Milo, Revised Estimates for the Number of Human and Bacteria Cells in the Body. *PLoS Biol*, 2016. **14**(8): p. e1002533.
62. Clemente, J.C., et al., The impact of the gut microbiota on human health: an integrative view. *Cell*, 2012. **148**(6): p. 1258-70.
63. Statistics, N.C.f.H., Allergies and Hay Fever, United States, 2023. 2023: Hyattsville, Maryland.
64. Feehley, T., et al., Healthy infants harbor intestinal bacteria that protect against food allergy. *Nat Med*, 2019. **25**(3): p. 448-453.
65. Jota Baptista, C.V., A.I. Faustino-Rocha, and P.A. Oliveira, Animal Models in Pharmacology: A Brief History Awarding the Nobel Prizes for Physiology or Medicine. *Pharmacology*, 2021. **106**(7-8): p. 356-368.
66. Ericsson, A.C., M.J. Crim, and C.L. Franklin, A brief history of animal modeling. *Mo Med*, 2013. **110**(3): p. 201-5.
67. Laboratory, T.J. Our History. [cited 2023; Available from: <https://www.jax.org/about-us/history#nobel-prizes-et-al>].
68. Makowska, I.J. and D.M. Weary, A Good Life for Laboratory Rodents? *ILAR J*, 2021. **60**(3): p. 373-388.
69. Robinson, N.B., et al., The current state of animal models in research: A review. *Int J Surg*, 2019. **72**: p. 9-13.
70. Dominguez-Oliva, A., et al., The Importance of Animal Models in Biomedical Research: Current Insights and Applications. *Animals (Basel)*, 2023. **13**(7).
71. Swearingen, J.R., Choosing the right animal model for infectious disease research. *Animal Model Exp Med*, 2018. **1**(2): p. 100-108.
72. Nials, A.T. and S. Uddin, Mouse models of allergic asthma: acute and chronic allergen challenge. *Dis Model Mech*, 2008. **1**(4-5): p. 213-20.
73. Taube, C., A. Dakhama, and E.W. Gelfand, Insights into the pathogenesis of asthma utilizing murine models. *Int Arch Allergy Immunol*, 2004. **135**(2): p. 173-86.

74. Seyyede Masoume Athari, E.M.N., Seyyed Shamsadin Athari, Animal model of allergy and asthma; protocol for researches. Protocol Exchange, 2019.
75. Wenzel, S. and S.T. Holgate, The mouse trap: It still yields few answers in asthma. *Am J Respir Crit Care Med*, 2006. **174**(11): p. 1173-6; discussion 1176-8.
76. Kumar, R.K., C. Herbert, and P.S. Foster, The "classical" ovalbumin challenge model of asthma in mice. *Curr Drug Targets*, 2008. **9**(6): p. 485-94.
77. Huss, K., et al., House dust mite and cockroach exposure are strong risk factors for positive allergy skin test responses in the Childhood Asthma Management Program. *J Allergy Clin Immunol*, 2001. **107**(1): p. 48-54.
78. Panzner, P., et al., Cross-sectional study on sensitization to mite and cockroach allergen components in allergy patients in the Central European region. *Clin Transl Allergy*, 2018. **8**: p. 19.
79. Stefka, A.T., et al., Commensal bacteria protect against food allergen sensitization. *Proc Natl Acad Sci U S A*, 2014. **111**(36): p. 13145-50.
80. Cahenzli, J., et al., Intestinal microbial diversity during early-life colonization shapes long-term IgE levels. *Cell Host Microbe*, 2013. **14**(5): p. 559-70.
81. Herbst, T., et al., Dysregulation of allergic airway inflammation in the absence of microbial colonization. *Am J Respir Crit Care Med*, 2011. **184**(2): p. 198-205.
82. Wang, Y., et al., A study on the method and effect of the construction of a humanized mouse model of fecal microbiota transplantation. *Front Microbiol*, 2022. **13**: p. 1031758.
83. Shimbori, C., et al., Gut bacteria interact directly with colonic mast cells in a humanized mouse model of IBS. *Gut Microbes*, 2022. **14**(1): p. 2105095.
84. Park, J.C. and S.H. Im, Of men in mice: the development and application of a humanized gnotobiotic mouse model for microbiome therapeutics. *Exp Mol Med*, 2020. **52**(9): p. 1383-1396.
85. Wrzosek, L., et al., Transplantation of human microbiota into conventional mice durably reshapes the gut microbiota. *Sci Rep*, 2018. **8**(1): p. 6854.
86. Eiseman, B., et al., Fecal enema as an adjunct in the treatment of pseudomembranous enterocolitis. *Surgery*, 1958. **44**(5): p. 854-9.
87. Kumar, V. and M. Fischer, Expert opinion on fecal microbiota transplantation for the treatment of *Clostridioides difficile* infection and beyond. *Expert Opin Biol Ther*, 2020. **20**(1): p. 73-81.
88. Aroniadis, O.C. and L.J. Brandt, Fecal microbiota transplantation: past, present and future. *Curr Opin Gastroenterol*, 2013. **29**(1): p. 79-84.
89. Weingarden, A.R. and B.P. Vaughn, Intestinal microbiota, fecal microbiota transplantation, and inflammatory bowel disease. *Gut Microbes*, 2017. **8**(3): p. 238-252.
90. Leonardi, I., et al., Fungal Trans-kingdom Dynamics Linked to Responsiveness to Fecal Microbiota Transplantation (FMT) Therapy in Ulcerative Colitis. *Cell Host Microbe*, 2020. **27**(5): p. 823-829 e3.

91. Dhamoon, J.J.P.A.S., Physiology, Digestion. 2023, Treasure Island, FL: StatPearls Publishing.
92. Oliphant, K. and E. Allen-Vercoe, Macronutrient metabolism by the human gut microbiome: major fermentation by-products and their impact on host health. *Microbiome*, 2019. **7**(1): p. 91.
93. Culp, E.J. and A.L. Goodman, Cross-feeding in the gut microbiome: Ecology and mechanisms. *Cell Host Microbe*, 2023. **31**(4): p. 485-499.
94. Germerodt, S., et al., Pervasive Selection for Cooperative Cross-Feeding in Bacterial Communities. *PLoS Comput Biol*, 2016. **12**(6): p. e1004986.
95. Hill, M.J., Intestinal flora and endogenous vitamin synthesis. *Eur J Cancer Prev*, 1997. **6 Suppl 1**: p. S43-5.
96. Rowland, I., et al., Gut microbiota functions: metabolism of nutrients and other food components. *Eur J Nutr*, 2018. **57**(1): p. 1-24.
97. Kim, C.H., Immune regulation by microbiome metabolites. *Immunology*, 2018. **154**(2): p. 220-229.
98. Macfarlane, S. and G.T. Macfarlane, Regulation of short-chain fatty acid production. *Proc Nutr Soc*, 2003. **62**(1): p. 67-72.
99. Tan, J., et al., Dietary Fiber and Bacterial SCFA Enhance Oral Tolerance and Protect against Food Allergy through Diverse Cellular Pathways. *Cell Rep*, 2016. **15**(12): p. 2809-24.
100. Depner, M., et al., Maturation of the gut microbiome during the first year of life contributes to the protective farm effect on childhood asthma. *Nat Med*, 2020. **26**(11): p. 1766-1775.
101. Thorburn, A.N., et al., Evidence that asthma is a developmental origin disease influenced by maternal diet and bacterial metabolites. *Nat Commun*, 2015. **6**: p. 7320.
102. Roduit, C., et al., High levels of butyrate and propionate in early life are associated with protection against atopy. *Allergy*, 2019. **74**(4): p. 799-809.
103. Crestani, E., et al., Untargeted metabolomic profiling identifies disease-specific signatures in food allergy and asthma. *J Allergy Clin Immunol*, 2020. **145**(3): p. 897-906.
104. Nakada, E.M., et al., Conjugated bile acids attenuate allergen-induced airway inflammation and hyperresponsiveness by inhibiting UPR transducers. *JCI Insight*, 2019. **4**(9).
105. Willart, M.A., et al., Ursodeoxycholic acid suppresses eosinophilic airway inflammation by inhibiting the function of dendritic cells through the nuclear farnesoid X receptor. *Allergy*, 2012. **67**(12): p. 1501-10.
106. Yamazaki, K., et al., Ursodeoxycholic acid inhibits eosinophil degranulation in patients with primary biliary cirrhosis. *Hepatology*, 1999. **30**(1): p. 71-8.
107. Turi, K.N., et al., Unconjugated bilirubin is associated with protection from early-life wheeze and childhood asthma. *J Allergy Clin Immunol*, 2021. **148**(1): p. 128-138.

108. van der Sluijs, K.F., et al., Systemic tryptophan and kynurenine catabolite levels relate to severity of rhinovirus-induced asthma exacerbation: a prospective study with a parallel-group design. *Thorax*, 2013. **68**(12): p. 1122-30.
109. Hu, Y., et al., Decreased expression of indoleamine 2,3-dioxygenase in childhood allergic asthma and its inverse correlation with fractional concentration of exhaled nitric oxide. *Ann Allergy Asthma Immunol*, 2017. **119**(5): p. 429-434.
110. Unuvar, S., et al., Neopterin Levels and Indoleamine 2,3-Dioxygenase Activity as Biomarkers of Immune System Activation and Childhood Allergic Diseases. *Ann Lab Med*, 2019. **39**(3): p. 284-290.
111. Finkelstein, R.A., H.T. Norris, and N.K. Dutta, Pathogenesis Experimental Cholera in Infant Rabbits. I. Observations on the Intraintestinal Infection and Experimental Cholera Produced with Cell-Free Products. *J Infect Dis*, 1964. **114**: p. 203-16.
112. Scheutz, F., et al., Multicenter evaluation of a sequence-based protocol for subtyping Shiga toxins and standardizing Stx nomenclature. *J Clin Microbiol*, 2012. **50**(9): p. 2951-63.
113. Schiavo, G., et al., Botulinum neurotoxins are zinc proteins. *J Biol Chem*, 1992. **267**(33): p. 23479-83.
114. Fujimura, K.E., et al., Neonatal gut microbiota associates with childhood multisensitized atopy and T cell differentiation. *Nat Med*, 2016. **22**(10): p. 1187-1191.
115. Levan, S.R., et al., Elevated faecal 12,13-diHOME concentration in neonates at high risk for asthma is produced by gut bacteria and impedes immune tolerance. *Nat Microbiol*, 2019. **4**(11): p. 1851-1861.
116. Gould, H.J. and Y.B. Wu, IgE repertoire and immunological memory: compartmental regulation and antibody function. *Int Immunol*, 2018. **30**(9): p. 403-412.
117. Sanchez-Jimenez, F., et al., Pharmacological potential of biogenic amine-polyamine interactions beyond neurotransmission. *Br J Pharmacol*, 2013. **170**(1): p. 4-16.
118. Stiemsma, L.T. and S.E. Turvey, Asthma and the microbiome: defining the critical window in early life. *Allergy Asthma Clin Immunol*, 2017. **13**: p. 3.
119. Riedler, J., et al., Exposure to farming in early life and development of asthma and allergy: a cross-sectional survey. *Lancet*, 2001. **358**(9288): p. 1129-33.
120. Ege, M.J., et al., Exposure to environmental microorganisms and childhood asthma. *N Engl J Med*, 2011. **364**(8): p. 701-9.
121. Olszak, T., et al., Microbial exposure during early life has persistent effects on natural killer T cell function. *Science*, 2012. **336**(6080): p. 489-93.
122. Zuccotti, G., et al., Probiotics for prevention of atopic diseases in infants: systematic review and meta-analysis. *Allergy*, 2015. **70**(11): p. 1356-71.
123. Ichinohe, T., et al., Microbiota regulates immune defense against respiratory tract influenza A virus infection. *Proc Natl Acad Sci U S A*, 2011. **108**(13): p. 5354-9.
124. Spergel, J.M. and A.S. Paller, Atopic dermatitis and the atopic march. *J Allergy Clin Immunol*, 2003. **112**(6 Suppl): p. S118-27.

125. von Kobyletzki LB, B.C., Hasselgren M, Larsson M, Lindström CB, Svensson Å, Eczema in early childhood is strongly associated with the development of asthma and rhinitis in a prospective cohort. *BMC Dermatol*, 2012. **12**(11).
126. Abrahamsson, T.R., et al., Low diversity of the gut microbiota in infants with atopic eczema. *J Allergy Clin Immunol*, 2012. **129**(2): p. 434-40, 440 e1-2.
127. Abrahamsson, T.R., et al., Low gut microbiota diversity in early infancy precedes asthma at school age. *Clin Exp Allergy*, 2014. **44**(6): p. 842-50.
128. Tariq, S.M., et al., The prevalence of and risk factors for atopy in early childhood: a whole population birth cohort study. *J Allergy Clin Immunol*, 1998. **101**(5): p. 587-93.
129. Arshad, S.H., et al., Cohort Profile: The Isle Of Wight Whole Population Birth Cohort (IOWBC). *Int J Epidemiol*, 2018. **47**(4): p. 1043-1044i.
130. Arshad, S.H., et al., Cohort Profile Update: The Isle of Wight Whole Population Birth Cohort (IOWBC). *Int J Epidemiol*, 2020. **49**(4): p. 1083-1084.
131. Becker AB, A.E., Asthma guidelines: the Global Initiative for Asthma in relation to national guideline. *Curr Opin Allergy Clin Immunol*, 2017. **17**(2): p. 99-103.
132. Sadeghnejad A, K.W., Davis S, Kurukulaaratchy RJ, Matthews S, Arshad SH, Raised cord serum immunoglobulin E increases the risk of allergic sensitisation at ages 4 and 10 and asthma at age 10. *Thorax*, 2004. **59**(11): p. 936-942.
133. Severity scoring of atopic dermatitis: the SCORAD index. Consensus Report of the European Task Force on Atopic Dermatitis. *Dermatology*, 1993. **186**(1): p. 23-31.
134. Asher, M.I., et al., International Study of Asthma and Allergies in Childhood (ISAAC): rationale and methods. *Eur Respir J*, 1995. **8**(3): p. 483-91.
135. Patil, V.K., et al., Interaction of prenatal maternal smoking, interleukin 13 genetic variants and DNA methylation influencing airflow and airway reactivity. *Clin Epigenetics*, 2013. **5**(1): p. 22.
136. Soto-Ramirez, N., et al., Modes of infant feeding and the occurrence of coughing/wheezing in the first year of life. *J Hum Lact*, 2013. **29**(1): p. 71-80.
137. Karmaus, W., et al., Long-term effects of breastfeeding, maternal smoking during pregnancy, and recurrent lower respiratory tract infections on asthma in children. *J Asthma*, 2008. **45**(8): p. 688-95.
138. Brooks, P.T., et al., Transplanted human fecal microbiota enhanced Guillain Barre syndrome autoantibody responses after *Campylobacter jejuni* infection in C57BL/6 mice. *Microbiome*, 2017. **5**(1): p. 92.
139. Hall, M. and R.G. Beiko, 16S rRNA Gene Analysis with QIIME2. *Methods Mol Biol*, 2018. **1849**: p. 113-129.
140. Amir, A., et al., Deblur Rapidly Resolves Single-Nucleotide Community Sequence Patterns. *mSystems*, 2017. **2**(2).
141. Rognes, T., et al., VSEARCH: a versatile open source tool for metagenomics. *PeerJ*, 2016. **4**: p. e2584.

142. Santos, T., et al., Use of MALDI-TOF mass spectrometry fingerprinting to characterize *Enterococcus* spp. and *Escherichia coli* isolates. *J Proteomics*, 2015. **127**(Pt B): p. 321-31.
143. Team, R.C., R: A Language and Environment for Statistical Computing. 2020, R Foundation for Statistical Computing: Vienna, Austria.
144. SAS Institute Inc. SAS and all other SAS Institute Inc. product or service names are registered trademarks or trademarks of SAS Institute Inc., C., NC, USA.
145. Sbihi, H., et al., Thinking bigger: How early-life environmental exposures shape the gut microbiome and influence the development of asthma and allergic disease. *Allergy*, 2019. **74**(11): p. 2103-2115.
146. Bisgaard, H., et al., Childhood asthma after bacterial colonization of the airway in neonates. *N Engl J Med*, 2007. **357**(15): p. 1487-95.
147. Hilty, M., et al., Disordered microbial communities in asthmatic airways. *PLoS One*, 2010. **5**(1): p. e8578.
148. Lal, C.V., et al., The Airway Microbiome at Birth. *Sci Rep*, 2016. **6**: p. 31023.
149. Lynch, S.V., et al., Effects of early-life exposure to allergens and bacteria on recurrent wheeze and atopy in urban children. *J Allergy Clin Immunol*, 2014. **134**(3): p. 593-601 e12.
150. Penders, J., et al., Establishment of the intestinal microbiota and its role for atopic dermatitis in early childhood. *J Allergy Clin Immunol*, 2013. **132**(3): p. 601-607 e8.
151. Louisa Owens, I.A.L., Guicheng Zhang, Stephen Turner & Peter N Le Souëf, Prevalence of allergic sensitization, hay fever, eczema, and asthma in a longitudinal birth cohort. *Journal of Asthma and Allergy*, 2018. **11**: p. 173-180.
152. Ta, L.D.H., et al., A compromised developmental trajectory of the infant gut microbiome and metabolome in atopic eczema. *Gut Microbes*, 2020. **12**(1): p. 1-22.
153. Sher, A.A., et al., Conjugative RP4 Plasmid-Mediated Transfer of Antibiotic Resistance Genes to Commensal and Multidrug-Resistant Enteric Bacteria In Vitro. *Microorganisms*, 2023. **11**(1).
154. Jolley, K.A., J.E. Bray, and M.C.J. Maiden, Open-access bacterial population genomics: BIGSdb software, the PubMLST.org website and their applications. *Wellcome Open Res*, 2018. **3**: p. 124.
155. Zhou, Z., et al., The Enterobase user's guide, with case studies on *Salmonella* transmissions, *Yersinia pestis* phylogeny, and *Escherichia* core genomic diversity. *Genome Res*, 2020. **30**(1): p. 138-152.
156. Könönen, E., 250 - Anaerobic Cocci and Anaerobic Gram-Positive Nonsporulating Bacilli. 8 ed. Mandell, Douglas, and Bennett's Principles and Practice of Infectious Diseases, ed. R.D. John E. Bennett, Martin J. Blaser. Vol. 2. 2015.
157. Berenger, B.M., et al., Anaerobic urinary tract infection caused by *Veillonella parvula* identified using cystine-lactose-electrolyte deficient media and matrix-assisted laser desorption ionization-time of flight mass spectrometry. *IDCases*, 2015. **2**(2): p. 44-6.
158. Ito, Y., et al., The first case of *Veillonella atypica* bacteremia in a patient with renal pelvic tumor. *Anaerobe*, 2022. **73**: p. 102491.

159. Andréanne Morin, C.G.M., Casper-Emil T. Pedersen, Jakob Stokholm, Bo L. Chawes, Ann-Marie Malby Schoos, Katherine A. Naughton, Jonathan Thorsen, Martin S. Mortensen, Donata Vercelli, Urvis Trivedi, Søren J. Sørensen, Hans Bisgaard, Dan L. Nicolae, Klaus Bønnelykke, Carole Ober, Epigenetic landscape links upper airway microbiota in infancy with allergic rhinitis at 6 years of age. *Journal of Allergy and Clinical Immunology*, 2020. **146**(6): p. 1358-1366.
160. Salameh, M., et al., The role of gut microbiota in atopic asthma and allergy, implications in the understanding of disease pathogenesis. *Scand J Immunol*, 2020. **91**(3): p. e12855.
161. Zheng, H., et al., Altered Gut Microbiota Composition Associated with Eczema in Infants. *PLoS One*, 2016. **11**(11): p. e0166026.
162. Centers for Disease, C.a.P., Most recent National Asthma Data. 2019 (Last updated May, 2019).
163. Ziyab, A.H., et al., DNA methylation of the filaggrin gene adds to the risk of eczema associated with loss-of-function variants. *J Eur Acad Dermatol Venereol*, 2013. **27**(3): p. e420-3.
164. Ziyab, A.H., et al., Association of filaggrin variants with asthma and rhinitis: is eczema or allergic sensitization status an effect modifier? *Int Arch Allergy Immunol*, 2014. **164**(4): p. 308-18.
165. Arshad, S.H., et al., Cohort Profile Update: The Isle of Wight Whole Population Birth Cohort (IOWBC). *Int J Epidemiol*, 2020.
166. Adami, A.J. and S.J. Bracken, Breathing Better Through Bugs: Asthma and the Microbiome. *Yale J Biol Med*, 2016. **89**(3): p. 309-324.
167. Wu, Z.X., et al., Prenatal and early, but not late, postnatal exposure of mice to sidestream tobacco smoke increases airway hyperresponsiveness later in life. *Environ Health Perspect*, 2009. **117**(9): p. 1434-40.
168. Chapman, D.G. and C.G. Irvin, Mechanisms of airway hyper-responsiveness in asthma: the past, present and yet to come. *Clin Exp Allergy*, 2015. **45**(4): p. 706-19.
169. Ito, J.T., et al., Extracellular Matrix Component Remodeling in Respiratory Diseases: What Has Been Found in Clinical and Experimental Studies? *Cells*, 2019. **8**(4).
170. Biesbroek, G., et al., Early respiratory microbiota composition determines bacterial succession patterns and respiratory health in children. *Am J Respir Crit Care Med*, 2014. **190**(11): p. 1283-92.
171. Teo, S.M., et al., The infant nasopharyngeal microbiome impacts severity of lower respiratory infection and risk of asthma development. *Cell Host Microbe*, 2015. **17**(5): p. 704-15.
172. Bisgaard, H., et al., Reduced diversity of the intestinal microbiota during infancy is associated with increased risk of allergic disease at school age. *J Allergy Clin Immunol*, 2011. **128**(3): p. 646-52 e1-5.
173. Fujimura, K.E., et al., House dust exposure mediates gut microbiome *Lactobacillus* enrichment and airway immune defense against allergens and virus infection. *Proc Natl Acad Sci U S A*, 2014. **111**(2): p. 805-10.

174. Huang, Y.J. and H.A. Boushey, The microbiome in asthma. *J Allergy Clin Immunol*, 2015. **135**(1): p. 25-30.
175. Kong, H.H., et al., Temporal shifts in the skin microbiome associated with disease flares and treatment in children with atopic dermatitis. *Genome Res*, 2012. **22**(5): p. 850-9.
176. Collins, J., et al., Humanized microbiota mice as a model of recurrent *Clostridium difficile* disease. *Microbiome*, 2015. **3**: p. 35.
177. Directors, A.B.o., Guidelines for Methacholine and Exercise Challenge Testing—1999. American Thoracic Society 1999.
178. Woo, L.N., et al., A 4-Week Model of House Dust Mite (HDM) Induced Allergic Airways Inflammation with Airway Remodeling. *Sci Rep*, 2018. **8**(1): p. 6925.
179. Gandhi, V.D., et al., House dust mite interactions with airway epithelium: role in allergic airway inflammation. *Curr Allergy Asthma Rep*, 2013. **13**(3): p. 262-70.
180. Brown, T.A., et al., Early life microbiome perturbation alters pulmonary responses to ozone in male mice. *Physiol Rep*, 2020. **8**(2): p. e14290.
181. Lommatzsch, M., Airway hyperresponsiveness: new insights into the pathogenesis. *Semin Respir Crit Care Med*, 2012. **33**(6): p. 579-87.
182. Ver Heul, A., J. Planer, and A.L. Kau, The Human Microbiota and Asthma. *Clin Rev Allergy Immunol*, 2019. **57**(3): p. 350-363.
183. Bonaz, B., T. Bazin, and S. Pellissier, The Vagus Nerve at the Interface of the Microbiota-Gut-Brain Axis. *Front Neurosci*, 2018. **12**: p. 49.
184. Trompette, A., et al., Gut microbiota metabolism of dietary fiber influences allergic airway disease and hematopoiesis. *Nat Med*, 2014. **20**(2): p. 159-66.
185. Vanoirbeek, J.A., et al., Noninvasive and invasive pulmonary function in mouse models of obstructive and restrictive respiratory diseases. *Am J Respir Cell Mol Biol*, 2010. **42**(1): p. 96-104.
186. Patel, K.R., et al., Mast cell-derived neurotrophin 4 mediates allergen-induced airway hyperinnervation in early life. *Mucosal Immunol*, 2016. **9**(6): p. 1466-1476.
187. Patel, K.R., et al., Targeting acetylcholine receptor M3 prevents the progression of airway hyperreactivity in a mouse model of childhood asthma. *FASEB J*, 2017. **31**(10): p. 4335-4346.
188. Bonvini, S.J., et al., Novel airway smooth muscle-mast cell interactions and a role for the TRPV4-ATP axis in non-atopic asthma. *Eur Respir J*, 2020. **56**(1).
189. Mendez-Enriquez, E. and J. Hallgren, Mast Cells and Their Progenitors in Allergic Asthma. *Front Immunol*, 2019. **10**: p. 821.
190. Traina, G., Mast Cells in Gut and Brain and Their Potential Role as an Emerging Therapeutic Target for Neural Diseases. *Front Cell Neurosci*, 2019. **13**: p. 345.
191. Team, R.C., A language and environment for statistical computing. 2020.

192. Mansfield, L.S., et al., C57BL/6 and congenic interleukin-10-deficient mice can serve as models of *Campylobacter jejuni* colonization and enteritis. *Infect Immun*, 2007. **75**(3): p. 1099-115.
193. Nault, R., et al., Development of a computational high-throughput tool for the quantitative examination of dose-dependent histological features. *Toxicol Pathol*, 2015. **43**(3): p. 366-75.
194. Kujur, W., et al., Caerulomycin A inhibits Th2 cell activity: a possible role in the management of asthma. *Sci Rep*, 2015. **5**: p. 15396.
195. Adami, A.J., et al., Early-life antibiotics attenuate regulatory T cell generation and increase the severity of murine house dust mite-induced asthma. *Pediatr Res*, 2018. **84**(3): p. 426-434.
196. Lee, K.S., et al., Inhibition of phosphoinositide 3-kinase delta attenuates allergic airway inflammation and hyperresponsiveness in murine asthma model. *FASEB J*, 2006. **20**(3): p. 455-65.
197. Kwak, Y.G., et al., Involvement of PTEN in airway hyperresponsiveness and inflammation in bronchial asthma. *J Clin Invest*, 2003. **111**(7): p. 1083-92.
198. Zaiss, M.M., et al., The Intestinal Microbiota Contributes to the Ability of Helminths to Modulate Allergic Inflammation. *Immunity*, 2015. **43**(5): p. 998-1010.
199. McCullagh, P. and J.A. Nelder, *Generalized Linear Models*. Second Edition. 1989, London: Chapman and Hall.

APPENDIX

Supplemental Figures

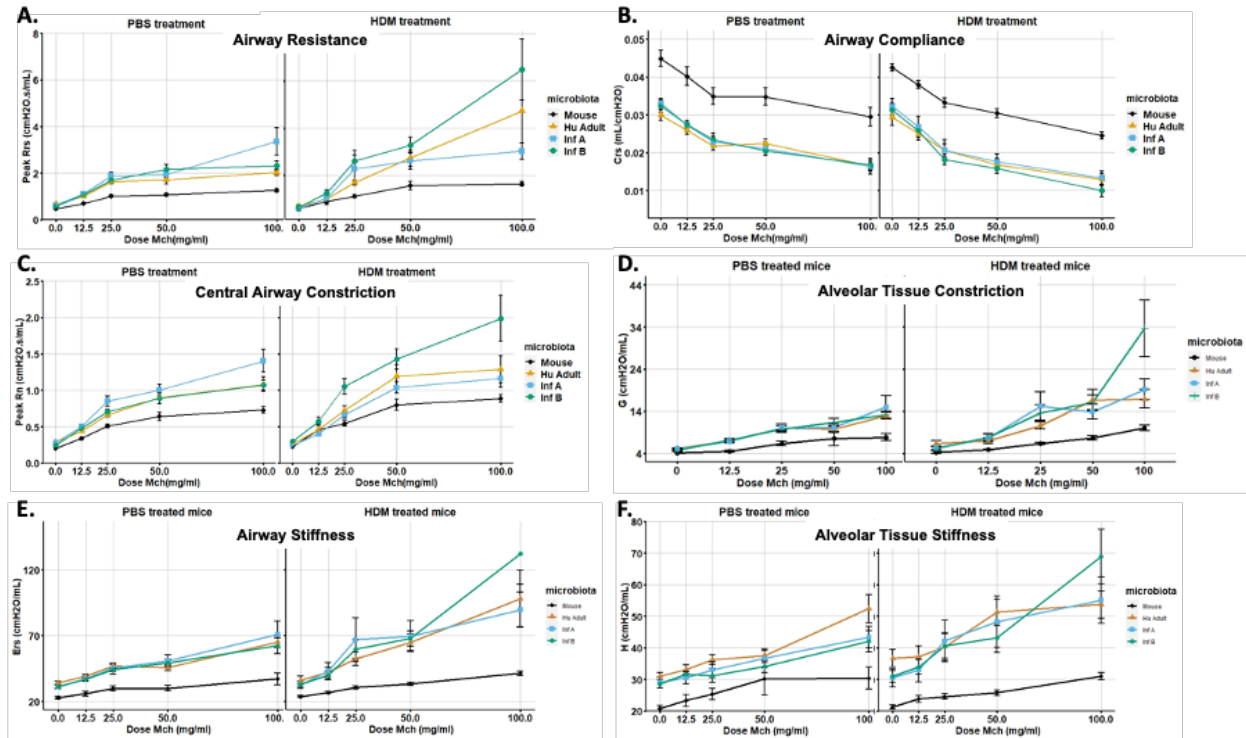


Figure 3.11 Observed peak values for each lung function, at each Mch dose given and separated by treatment. Panel (A) represents total airway resistance. Panel (B) represents total airway compliance. Panel (C) represents microcentral airway constriction, Panel (D) represents alveolar tissue constriction, Panel (E) represents airway stiffness, and Panel (F) represents alveolar tissue stiffness. Data shown as mean \pm SEM (n=10).

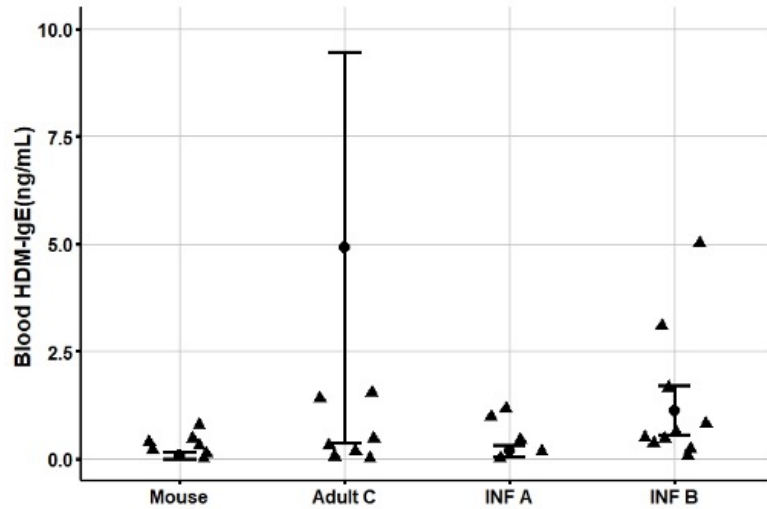


Figure 3.12 Blood HDM-IgE levels in mice treated with HDM for 12 days did not show significant increase. Data represent mean \pm SE from 10 mice per group. Individual values per group are also shown as single data points. Some individual values per group that were equal to 0 ng/ml may overlap with each other in the graph. One value from Adult C group (45.74 ng/ml) is not shown due to being extremely high compared to the rest of the data and was left outside the graphing scale.

Supplemental Tables

Table 3.10 Measurements at peak responses of resistance (Rrs in cmH2O.s/ml), compliance (Crs in ml/cmH2O), elastance (Ers in cmH2O/ml), tissue elastance (H in cmH2O/ml), tissue damping (G in cmH2O/ml), and conducting airway (Newtonian) resistance (Rn in cmH2O.s/ml) for each methacholine dose for phosphate buffered saline (PBS) treatment groups. The peak response is the top three measurements for all parameters except Crs, for which it is the lowest three measurements. $x \pm s$ represents average \pm 1 SD. N is the number of non-missing values.

Lung function parameter	Methacholine dose				
	0 mg/ml (N=36)	12.5 mg/ml (N=36)	25 mg/ml (N=36)	50 mg/ml (N=36)	100 mg/ml (N=36)
Baseline Rrs	0.533 \pm 0.097	†0.562 \pm 0.096 *	†0.853 \pm 0.196	†0.980 \pm 0.243	†1.215 \pm 0.31
Peak Respiratory Resistance (Rrs)	0.59 \pm 0.10	0.96 \pm 0.22	1.54 \pm 0.47	1.67 \pm 0.58	2.27 \pm 1.29
Baseline_Crs	0.0374 \pm 0.0085	†0.0355 \pm 0.007	†0.0316 \pm 0.008	†0.0290 \pm 0.007	†0.0267 \pm 0.007
Peak Respiratory Compliance (Crs)	0.0353 \pm 0.0077	0.0305 \pm 0.0077	0.0260 \pm 0.0074	0.0252 \pm 0.0081	0.0200 \pm 0.0082
Baseline_Ers	27.9 \pm 5.6	†29.4 \pm 5.8	†33.4 \pm 7.2	†36.3 \pm 8.0	†40.2 \pm 10.4
Peak Respiratory Elastance (Ers)	29.5 \pm 5.8	†34.5 \pm 7.4	†41.2 \pm 10.3	†43.2 \pm 12.6	†58.4 \pm 24.2
Baseline_H	25.4 \pm 5.3	†26.4 \pm 5.7	†27.9 \pm 6.3	†30.2 \pm 7.1	†32.6 \pm 10.6
Peak Tissue Elastance (H)	27.3 \pm 5.6	29.5 \pm 6.4	31.5 \pm 7.2	34.6 \pm 10.6	42.1 \pm 13.9
Baseline_G	4.29 \pm 0.85	†4.33 \pm 0.77	†5.48 \pm 1.27	†5.79 \pm 1.38	†7.29 \pm 3.19
Peak Tissue Resistance (G)	4.77 \pm 0.78	6.27 \pm 1.42	8.97 \pm 2.59	9.48 \pm 3.57	12.11 \pm 5.50

Table 3.10 (cont'd)

Baseline_Rn	0.202 ± 0.048	†0.217 ± 0.056	†0.358 ± 0.095	†0.460 ± 0.146	†0.599 ± 0.189
Peak Conducting Airway Resistance (Rn)	0.256 ± 0.051	0.437 ± 0.093	0.679 ± 0.184	0.855 ± 0.253	1.071 ± 0.402

† Baselines for doses 12.5-100 mg/ml of Mch correspond to the last value measured by *flexiVent* at the end of the dose response curve of the preceding dose.

Table 3.11 Measurements at peak responses of resistance (Rrs in cmH₂O.s/ml), compliance (Crs in ml/cmH₂O), elastance (Ers in cmH₂O/ml), tissue elastance (H in, cmH₂O/ml), tissue damping (G in cmH₂O/ml), and conducting airway (Newtonian) resistance (Rn in cmH₂O.s/ml) for each methacholine dose for house dust mite (HDM) treatment groups.

The peak response is the top three measurements for all parameters except Crs, for which it is the lowest three measurements. $x \pm s$ represents average \pm 1 SD. N is the number of non-missing values.

Lung function parameter	Methacholine dose				
	0 mg/ml (N=40)	12.5 mg/ml (N=40)	25 mg/ml (N=40)	50 mg/ml (N=40)	100 mg/ml (N=40)
Baseline_Rrs	0.56 ± 0.11	†0.60 ± 0.13	†0.95 ± 0.35	†1.37 ± 0.67	†1.82 ± 0.85
Peak Respiratory Resistance (Rrs)	0.64 ± 0.21	1.04 ± 0.38	1.93 ± 1.25	2.55 ± 1.14	3.97 ± 3.81
Baseline_Crs	0.0365 ± 0.008 1	†0.0342 ± 0.008 0	†0.0297 ± 0.007 5	†0.0255 ± 0.008 3	†0.0224 ± 0.007 8
Peak Respiratory Compliance (Crs)	0.0339 ± 0.007 6	0.0289 ± 0.007 7	0.0232 ± 0.008 3	0.0202 ± 0.007 8	0.0152 ± 0.007 3
Baseline_Ers	28.8 ± 7.0	†31.1 ± 8.4	†36.3 ± 11.2	†45.0 ± 20.0	†51.9 ± 23.5
Total Respiratory Elastance (Ers)	31.3 ± 8.3	37.9 ± 13.7	52.2 ± 31.6	58.8 ± 27.0	90.3 ± 61.8
Baseline_H	26.6 ± 7.0	†28.4 ± 8.7	†30.5 ± 10.0	†34.4 ± 13.0	†37.7 ± 16.3

Table 3.11 (cont'd)

Peak Tissue Elastance (H)	29.9 ± 8.8	32.0 ± 9.9	37.0 ± 15.2	42.1 ± 18.6	52.2 ± 23.2
Baseline_G	4.6 ± 1.1	†4.8 ± 1.1	†6.1 ± 2.2	†7.8 ± 3.8	†9.9 ± 4.7
Peak Tissue Damping (G)	5.3 ± 1.5	6.8 ± 2.5	11.4 ± 7.0	13.6 ± 6.5	20.0 ± 14.4
Baseline_Rn	0.204 ± 0.062	†0.223 ± 0.061	†0.387 ± 0.150	†0.569 ± 0.197	†0.769 ± 0.338
Peak Conducting Airway Resistance (Rn)	0.260 ± 0.056	0.474 ± 0.180	0.746 ± 0.291	1.115 ± 0.429	1.332 ± 0.719

† Baselines for doses 12.5-100 mg/ml of Mch correspond to the last value measured by *flexiVent* at the end of the dose response curve of the preceding dose.

Table 3.12 Pearson correlation coefficients (ρ) for baselines of each of the lung function parameters versus total serum IgE and separated by treatment. “Corr” value corresponds to the correlation value for all microbiota groups given that specific treatment. (PBS or HDM). Correlation coefficients values separated by microbiota are shown below. A value between 0.3 to 0.5 is considered moderate positive correlation, while a value between 0.5 to 1.0 is considered strong positive correlation. *- indicates correlation test p values that were <0.05. *.- indicates correlation test p values that were <0.1.**

	PBS (ρ)	HDM (ρ)
Total airway resistance (Rrs)	Corr: 0.408* MOUSE: 0.655* ADULT C: 0.409 INFANT A: 0.644 INFANT B: 0.394	Corr: 0.650*** MOUSE: -0.066 ADULT C: 0.772** INFANT A: 0.544 INFANT B: 0.201
Total airway Compliance (Crs)	Corr: -0.326. MOUSE: -0.378 ADULT C: -0.161 INFANT A: -0.565 INFANT B: -0.387	Corr: -0.390* MOUSE: -0.266 ADULT C: -0.467 INFANT A: -0.383 INFANT B: 0.125
Total airway elastance (Ers)	Corr: 0.342* MOUSE: 0.393 ADULT C: 0.160 INFANT A: 0.680. INFANT B: 0.273	Corr: 0.460** MOUSE: 0.266 ADULT C: 0.537 INFANT A: 0.349 INFANT B: -0.214
Central airways resistance (Rn)	Corr: 0.103 MOUSE: 0.347 ADULT C: -0.180 INFANT A: -0.354 INFANT B: 0.300	Corr: 0.339* MOUSE: -0.112 ADULT C: 0.604. INFANT A: 0.282 INFANT B: 0.058
Tissue resistance (G)	Corr: 0.367* MOUSE: 0.246 ADULT C: 0.513 INFANT A: 0.699. INFANT B: -0.078	Corr: 0.423** MOUSE: 0.063 ADULT C: 0.510 INFANT A: 0.416 INFANT B: -0.308
Tissue Elastance (H)	Corr: 0.245 MOUSE: 0.388 ADULT C: -0.185 INFANT A: 0.793* INFANT B: 0.428	Corr: 0.423** MOUSE: 0.063 ADULT C: 0.510 INFANT A: 0.416 INFANT B: -0.308

CHAPTER 4: Metabolomic profiles significantly distinguished in the gut based on expressed allergic phenotypes in eczemic infants and in mouse model of asthma

Abstract

Increasing evidence supports the importance of the role the gut microbiome plays on the development and manifestation of allergic diseases, such as eczema and asthma. In addition to specific bacterial taxa influencing the allergic outcomes of the hosts, various bacterial metabolites have been associated with allergy. We hypothesized that varying gut microbiota, along with varying allergic phenotypes results in a distinguishable metabolome. Two sets of samples were used in this study: fecal samples of 3-months old infants originating from the Isle of Wight 3rd generation cohort, and ceca samples of mouse models of asthma and allergy with three different humanized gut microbiota with predispositions to allergic phenotypes. Untargeted metabolomic profiling utilizing liquid chromatography-mass spectrometry was performed on all samples, and metabolite abundance data was analyzed by experimental groups. Infants with persistent early childhood eczema exhibited a distinct metabolite profile compared with infants without any childhood eczema. Hippuric acid and dihydrocortisol were in significantly lower abundance in infants with persistent eczema in infancy. Mice with humanized gut microbiota with predispositions to allergic response and lowered lung functions had significantly distinguishable metabolite profiles compared to mice with conventional mouse microbiota and dampened allergic response. Mice treated with an allergen (house dust mites) also exhibited number of metabolites significantly distinguishable from mice without allergen exposure, although in less degree than the microbiota differences.

Introduction

Allergic diseases affected nearly third of the adult, and over a quarter children in the U.S. in 2021 according to CDC[5]. The exact underlying mechanisms of allergy development is still unknown, yet many factors has been attributed to aiding in either developing, or preventing of developing allergies that can be categorized in 3 main genres: genetics[20, 43-45, 47], the environment[27, 29, 50, 51], and the microbiome[4, 33, 53-55, 63]. The effect of the microbiome, especially the gut microbiome on allergy has been a fast-growing field in both deepening the understanding of the mechanisms of allergic diseases, as well as the development of novel treatment and prevention of said diseases[55, 80, 124, 202, 203]. Specific bacterial taxa has been associated with the development of allergy such as Higher abundance of *Bacteroidaceae*, *Clostridaceae*, and *Enterobacteriaceae* with neonatal eczema[4], increased risk

of asthma development with *Enterobacteriaceae* abundance[202], and increased *Veillonella* abundance in children with asthma[2, 55, 203]. *Veillonella* abundance was also associated with eczema in early infancy in our previous study of Isle of Wight cohort infants[204]. The molecular mechanisms of how bacterial members of the gut microbiome can influence the host immune system to a point of allergy manifestation is still unknown, yet there are arguments for the microbial metabolites playing such role[33, 99, 203]. Metabolites like short-chain fatty acids(SCFA)[33, 99, 104], both conjugated[105, 106] and unconjugated[107, 108] bile acids, and tryptophan[110-112] have all been associated with protection from allergy. On the opposite end, histamine [118], indole propionate[105], and 12,13-diHOME[116] are examples of bacterial-related metabolites associated with the development of allergy. Histidine was also associated with wheeze in children in a different study[205] Relationship between the gut microbiome and metabolome on allergic phenotype also have been explored using mouse models[80-83].

Our overarching hypothesis was that the allergic phenotype produces distinguishable gut metabolome composition compared to those without allergy. This was explored by performing an untargeted metabolomic profiling on A) infant fecal samples collected at 3 months of age, combined with eczema diagnosis over the first 3 years of their life[204], and B) mice ceca samples of mice with fecal-transplanted, humanized gut microbiota, that were studied for their lung functions and allergic responses upon allergen sensitizations[206]. This set of studies was used to answer our hypothesis that I) human infants with eczema expresses distinct set of metabolites in the gut compared to those without eczema, II) mice with a human-derived gut microbiota from infants with eczema will have an increased airway hyper-responsiveness and express a distinct set of metabolites in the gut compared to the mice with conventional gut microbiota with observed dampened airway hyper-responsiveness, and lastly, III) mice treated with an allergen (house dust mites) will express distinct set of metabolites in the gut compared to mice with sham treatment.

Materials and methods

Human infant study cohort

Influence of gut microbiome composition on allergic outcomes of eczema, recurrent wheeze, and atopy was examined in the IOW F2 birth cohort. Fecal samples were collected from 60 children at 3 months of age by either their parents or the local nurse. Children were assessed for eczema,

wheeze, and atopy at 3, 6, 12, and 36 months of age[132] from July 2010 until October 2017. To define microbial patterns associated with triggering or protection from allergies, fecal samples were analyzed using 16S rRNA gene sequencing at the Michigan State University, Research Technology Support Facility Genomics Core. Children were recruited into the “Third Generation Study” under ethics approval numbers 09/H0504/129 (22 December 2019), 14/SC/0133 (22 December 2019), and 14/SC/1191 (15 November 2016) from the University of Southampton. The data analysis was carried out without knowledge of the identity of the infants. Each infant was categorized in 3 groups based on their eczema diagnoses during the first 3 years of their life: “Persistent” if they had 4-5 positive diagnosis of eczema, “Intermediate” if 1-3 positive diagnosis of eczema, and “None” for never being diagnosed with eczema[204].

Sample collection

Human infant fecal samples

Fecal samples of infants at 3 months of age were collected as described in Terauchi et al[204]. Briefly, fecal samples were collected from 60 children at 3 months of age from their diapers either at the time of their visit to the clinic, or at a later date at their home by a visiting nurse. Samples were each placed into a sterile container, stored on ice during transport, then stored at -80°C for prolonged storage. Each sample was coded to protect the patient identity and their clinical status, then shipped on dry ice to Michigan State University where it was stored at -80°C until processed for DNA isolation, and only opened in an anaerobic hood to preserve strict anaerobes. Of the 56 samples analyzed in the previous study, 31 samples had enough material remaining for this metabolome analysis, and thus were used in this study.

Mouse cecal samples

Total of 80 mice ceca of fecal-transplanted and control C57BL/6 mice were dissected and flash-frozen during necropsy at the time of the experiment as described in Moya-Urbe et al[206]. There were 4 microbiota-based groups with 20 mice each, further divided into either the negative control sham-treated with PBS, or house dust mite (HDM) allergen treated mice evenly, totaling in 8 groups with 10 mice in each group. The 2 experimental microbiota groups were called InfantA and InfantB, both having received a fecal-transplant from infant groups as germ-free mice, where InfantA group received the fecal contents of allergy-prone infants and InfantB group received the fecal contents of infants without allergy. AdultC group was a positive control for

allergy-prone humanized mouse model, having received fecal-transplant of adults that increased the allergic response in mice[140]. Fourth group called “Mouse” was a negative control of mice having never received a fecal-transplant, containing the conventional mouse microbiota. The collected cecum was stored at -80°C in cryovials until processing for this study.

Sample preparation

Human infant fecal samples

Aliquots of the original samples were created in the anaerobic hood using sterile serological loops into sterile cryovials. The sample aliquots were transported and kept on dry ice, until immediately before processing when they were thawed on wet ice. Approximately 30 – 50 mg of the sample were taken from each sample to be processed for mass spectrometry analysis for metabolites using individual sterile serological loops. A method control consisting of the sterile serological loop alone was also added.

Mice cecal content samples

Frozen mice ceca were thawed on wet ice. Inside a laminar flow bacteriological hood, contents were squeezed out of each cecum inside of a sterile Petri dish. This procedure was performed using sterile bacterial serological loops and surgical forceps and scissors sterilized in a bead heater. Each sample was processed individually with a new set of sterile equipment.

Approximately 30 – 50 mg of the cecal contents were processed further for analysis.

Both human infant fecal samples and mice cecal content samples were processed for metabolite extraction simultaneously following the same protocol. Approximately 30-50 mg of each sample content was added to a microcentrifuge tube containing 50 µL of internal standard cocktail.

Internal standard cocktail consisted of: 10 µL of labeled bile acid internal stock solution containing 100 pmol each of glycocholic acid-*d*₄ and glyoursodeoxycholic acid-*d*₄ (Avanti Polar Lipids, Alabaster, AL, USA), [¹³C₁₆]palmitic acid (Toronto Research Chemicals, Toronto, ON, Canada) internal standard stock solution containing 100 pmol, succinic acid-*d*₄ (Sigma-Aldrich) internal standard stock solution containing 500 pmol, phenylalanine-*d*₇ (Toronto Research Chemicals) internal standard stock solution containing 100 pmol, and labeled short-chain fatty acids (SCFA; containing 1.5 µg each of [¹³C]sodium formate, [¹³C₂]sodium acetate, [¹³C₃]sodium propionate, and [¹³C₄]sodium butyrate) internal stock solution, provided by the RTSF Mass Spectrometry and Metabolomics Core at Michigan State University. The sample was

homogenized in ice water ultrasound bath, then 350 μ L of ice-cold HPLC-grade methanol containing 0.1% butylated hydroxytoluene (BHT) was added. After 10 minutes of resting on ice, tubes were vortexed and centrifuged for 10 minutes at 10,000 x g. Supernatant was removed and transferred to the total extract tube to be used for mass spectrometry analysis. Extracts were divided into 5 different tubes to preserve opportunities for additional analyses in the future. Remaining pellet was washed with 200 μ L of ice-cold high-performance liquid chromatography (HPLC)-grade isopropanol, then centrifuged again at 10,000 x g for 10 minutes. Supernatant was combined with the previously removed supernatant, then dried for storage using SpeedVac without the application of heat. Dried samples were stored at -80°C until the day of mass spectrometry analysis.

Metabolite profiling using liquid chromatography-mass spectrometry(LC-MS) on a quadrupole time-of-flight (QToF) mass spectrometer

All samples were re-suspended in initial mobile phase solution used for the LC-MS analysis, which was acetonitrile/10 mM ammonium formate + 10 mM ammonium hydroxide in water (95:5 v/v). Re-suspended samples were transferred to amber glass autosampler vials along with the following controls: “blank” initial mobile phase only control, experimental negative controls, “method” control of sterile serological loop, “pooled” containing a portion of every single sample. Samples were analyzed using electrospray ionization in negative-ion mode on a QToF mass spectrometer (Waters Xevo G2-XS QToF) using an Acquity pump and Waters BEH amide column (2.1 x 100 mm, 1.7 μ m particles). This approach is more likely to detect polar acidic metabolites common in central metabolic pathways than other chromatographic and ionization methods but may miss some neutral lipids. Mobile phase A consisted of 10 mM ammonium formate + 10 mM ammonium hydroxide in water, and acetonitrile/10 mM ammonium formate + 10 mM ammonium hydroxide in water (95:5 v/v) was used as mobile phase B. Total flow rate was set to 0.40 mL/min with column temperature: 40°C. Linear solvent gradient (A/B) was set as: 0.0 min (0/100); 1.0 min (0/100), 10.0 min (40/60); 15.0 min (60/40), 18.0 min (60/40); 18.01 min (0/100); 20.0 min (0/100), followed by a 5-min hold. Data acquisition was set as continuum mode MS^E with dynamic range extension over mass range of m/z 50-1200; sensitivity mode; scan time 0.25 seconds/scan; data acquisition from 0-20 minutes. Lockspray reference was leucine enkephalin, and mass correction was not automatically applied as this correction was

performed during subsequent data processing.

Data analysis

Initial Processing of Mass Spectrometry Raw Data Using ProgenesisQI and EZinfo

Resulting raw data from the Quadrupole Time of Flight (QToF) mass spectrometer were uploaded to the analysis software Progenesis QI (ver 3.0; Waters Corporation). The raw data files were imported, and mass corrected using the signal from the lockspray reference; then peaks underwent retention time alignment using the negative control as a reference. Once aligned, peak picking was performed using the automatic peak picking feature combining signals from a list of adducts that are commonly observed in negative-ion mode electrospray ionization (e.g. $[M-H]^-$, $[M+formate]^-$, $[M+Cl]^-$, $[M-H-H_2O]^-$, and some dimer ions), and signals from the various adducts and naturally-occurring stable isotopes were combined for each compound to yield a single value. Any metabolites with highest abundance mean in blank, method control, or negative controls were removed. This dataset was exported as a CSV document for 2-group comparisons. For ordination analysis in EZinfo, abundances of metabolites were normalized using default parameters and then filtered using thresholds of: Anova p-value ≤ 0.01 , max fold change ≥ 10 , and max abundance $> 10,000$. The processed compound data were then imported into EZinfo version 3.0.2.0 software (Umetrics, Malmö, Sweden) where ordination analyses were performed using both Principal Components Analysis (PCA) and Partial Least Squares-Discriminant Analysis (PLS-DA). The data were log-transformed and scaled (e.g. Pareto scaling) for each comparison made.

2-group comparisons of metabolites

Further manual filtering of the compound abundance data

For analysis of metabolite data between two groups, a five-step filtering process was performed, beginning by using statistical measures of between group differences and fold-change differences between groups. Between-group p-values were calculated by ProgenesisQI software based on the normalized abundance values. Once exported, in step 1, all the metabolites with p-values > 0.05 were removed. In step 2, all metabolites with max foldchange, calculated in Progenesis QI using the normalized abundances, below 2.0 were removed. In step 3, relative mass defect, a measure of fractional hydrogen content[207, 208], was calculated based on the

m/z values using the equation: $\frac{m/z - \text{Integer}(m/z)}{m/z} * 1,000,000$, calculated by rounding the mass down to the lower integer. Then removed all metabolites with relative mass defect above 1200 ppm, as these are usually signals from inorganic salts. In step 4, any metabolites with frequency of zero values across samples above 30% were removed. In step 5, median values using raw abundances per metabolite were calculated. Then the median value ratios between the groups were calculated, then sorted in numerical order.

Statistical analysis of metabolite abundances between 2 groups

Paired Wilcoxon tests were performed to obtain the significance p-values for comparison between 2 test groups for each metabolite, followed by Bonferroni correction for multiple comparisons using rstatix package (ver 0.7.2) in R. Visualization of data was done using packages ggplot2 (ver 3.4.2) and ggpubr (ver0.4.0) in R.

Results

Overall, total of 8688 unique metabolites were measured by mass spectrometry. Thirteen compounds were identified as having highest abundance means in either the blank, method-, or run-control, thus removed, and the remaining 8675 unique metabolites were retained for analyses. Filtering process done for the ordination analyses removed additional 7931 metabolites, retaining 744 total distinct metabolites. For 2-group analyses, additional filtering was performed on the 8675 metabolites, leaving varying number of unique metabolites for each group comparisons as explained for each analysis in the appropriate sections below.

Analyses of Isle of Wight human infant metabolome

Separation of metabolite profiles were clearer between Persistent group and None group than Intermediate group

To reduce the dimensionality of such large data sets, it is useful to visualize the similarities of metabolite profiles between samples. Metabolite abundance data with filtering done in Progenesis QI was processed in EZinfo software for ordination analyses. Principal Component Analysis (PCA) was performed on 744 unique metabolites using three experimental groups created based on the eczema diagnosis during the first 3 years of life (Figure 4.1A). All samples fell within the 95% Hotelling's ellipse in the PCA scores plot, indicating a lack of

outliers (Figure 4.1A). All three groups included in this analysis, Persistent, Intermediate, and None, were not clearly separated by groups in the first two principal components (Figure 4.1A). Partial least squares-discriminant analysis (PLS-DA), a supervised classification method, was performed on the same dataset containing 744 unique metabolites and 3 clinical eczema groups. All samples fell within the scores plot Hotelling's ellipse again, indicating the lack of an outlier (Figure 4.1B). In addition, the groups were seen to be more spread apart in the scores plot but retained overlaps with samples belonging in the None group most present in the upper left quadrant, those in the Intermediate group mostly belonging in the lower right quadrant, and those in the Persistent group falling in between the other two groups (Figure 4.1B).

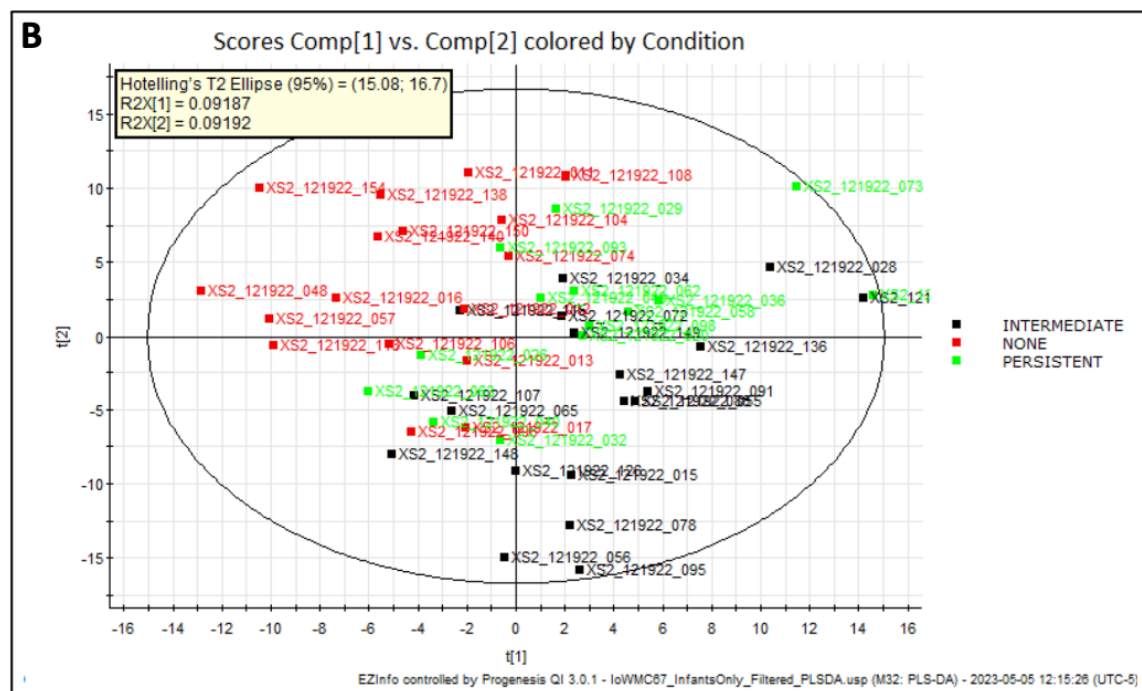
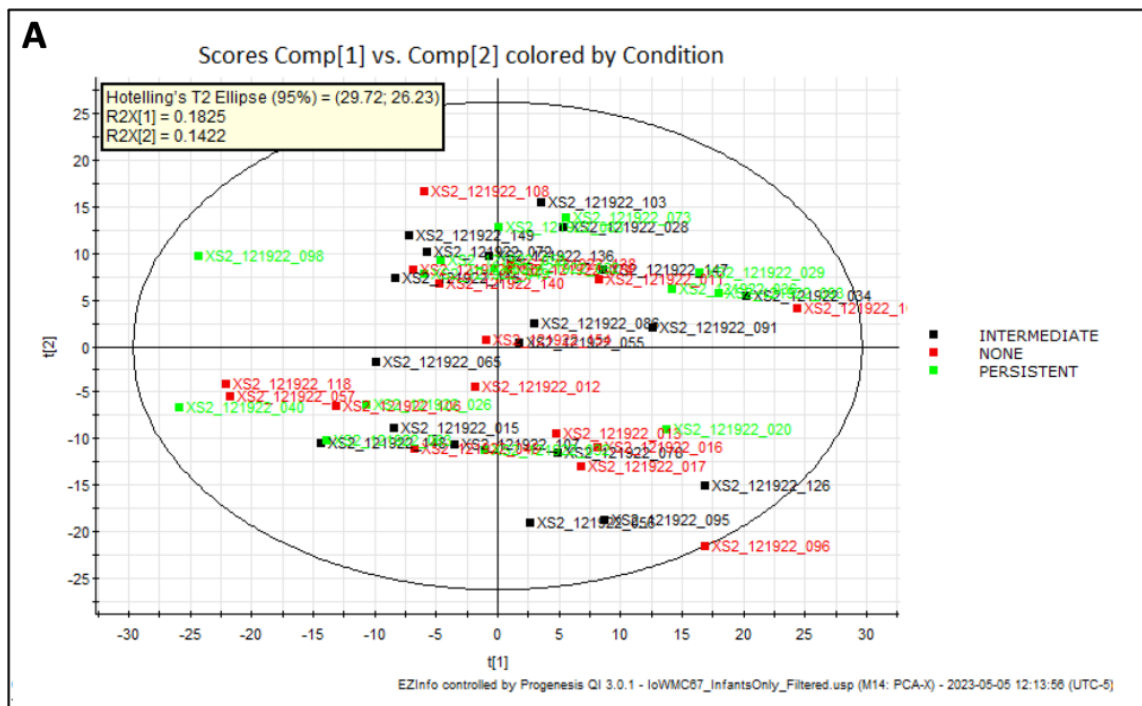


Figure 4.1 Ordination analyses of metabolite abundances in human infant samples grouped by eczema status over the first 3 years of life. Neon lime green color indicates samples that belong in the Persistent eczema group, Red color indicates samples belonging in the None group, and black color indicates samples in the Intermediate eczema group. **(A)**PCA scores plot calculated from abundances of 744 unique metabolites scaled using Unit Variance and log transformed. All samples fell within the Hotelling's ellipse. **(B)** PLS-DA scores plot performed

Figure 4.1 (cont'd)

on 744 unique metabolites using Unit Variance scaling and log transformation. All samples fell within the Hotelling's ellipse.

The PCA and PLS-DA analyses were repeated with just using Persistent and None groups to emphasize the potential differences between the eczema diagnosis by using the two most extreme groups (Figure 4.2). In either case, all samples remained within the scores plot Hotelling's ellipse, and one metabolite was removed due to not being present in either of the groups included in this analysis. PCA showed a separation and some clustering of samples that was not explained by the clinical grouping, as both groups were in either side of the spread (Figure 4.2A). However, in PLS-DA, the separation became clearer with samples in the Persistent group falling mostly within the upper right quadrant, containing samples only in the Persistent group, while lower left quadrant only contained samples in the None group (Figure 4.2B). Upper left and lower right quadrants were shared by samples from both groups, however there was a wider separation between those from different groups (Figure 4.2B).

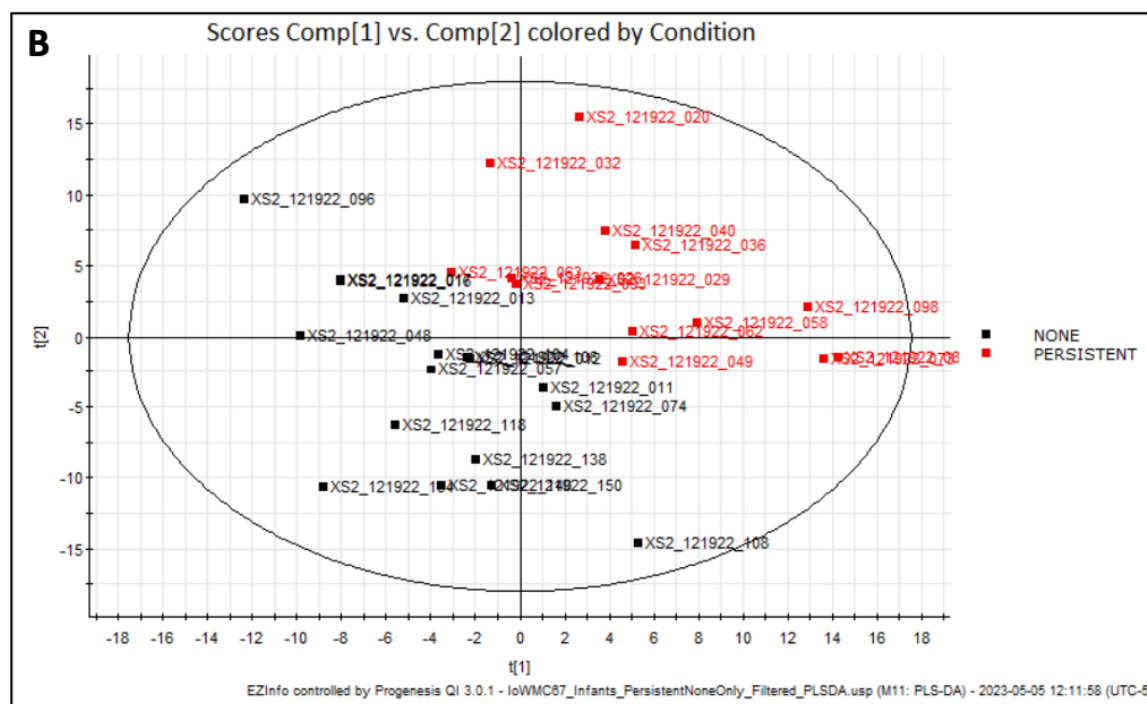
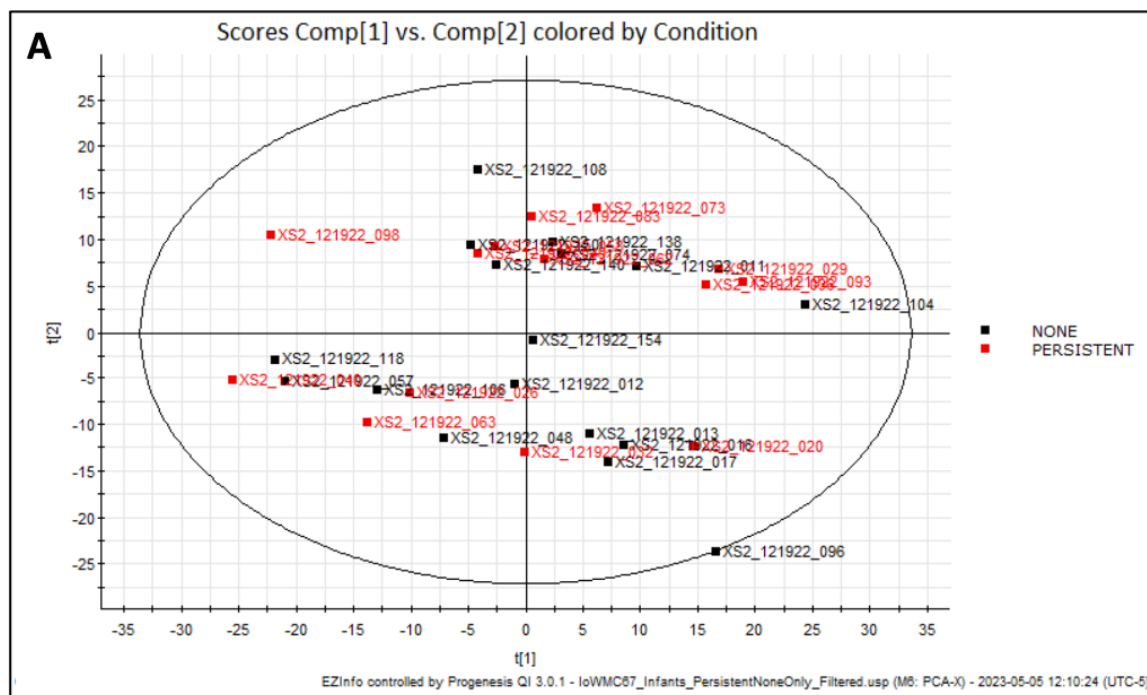


Figure 4.2 Ordination analyses of metabolite abundances in human infant samples grouped by 2 most extreme eczema status over the first 3 years of life. Red color indicates samples in the Persistent eczema group, and black color indicates samples in the None group. (A) PCA scores plot of 743 unique metabolites with their abundances scaled with Unit Variance and log transformed. All samples fell within the Hotelling's ellipse. (B) PLS-DA scores plot of 743 unique metabolites with abundances scaled with Unit Variance and log transformation. All points fell within the Hotelling's space, and samples in Persistent group mostly fell on the upper

Figure 4.2 (cont'd)

right quadrant while samples in the None group fell mostly on the remaining three quadrants.

A collection of metabolites significantly differed in abundances between the Persistent and None groups

To further investigate the differences in the metabolome of those with childhood eczema and those without, abundances of each metabolites were compared and filtered statistically to reveal a group of metabolites that distinguished the two study groups. Upon stringent filtering as described in the methods section, 113 unique metabolites were identified as being most distinguishing between the metabolome of Persistent and None groups. Of 113, 50 metabolites had their re-calculated p-value < 0.05 , suggesting statistically significant difference (data not shown). From the 50 statistically significant metabolites, 39 metabolites were further selected based on the ratios of median values between the Persistent and None group. Eleven metabolites were identified for having both p-value < 0.05 and median ratio of Persistent:None < 0.5 , indicating a significant lower abundance in infants with persistent eczema, and higher abundance in infants who never developed childhood eczema (Figure 4.3A). 28 metabolites were identified for having both p-value < 0.05 and the median ratio of Persistent/None > 2.0 , indicating a significantly higher abundance in the metabolome of infants with persistent eczema and lower abundance in infants without childhood eczema (Figure 4.3B).

Although most of the metabolite identifications were inconclusive using spectral database searches, a few of the metabolites measured in the infant samples were manually annotated. Of the 11 metabolites with significantly higher abundance in the None, or no-eczema, group, metabolite-89 was annotated as hippuric acid and metabolite-9 was annotated as dihydrocortisol. Of the 28 metabolites with significantly higher abundance in Persistent group, metabolite-18 was identified as the tripeptide Asn-Ser-Thr and metabolite-24 as an unknown compound with a formula of $C_{16}H_{26}N_6O_5$ based on high resolution mass analysis.

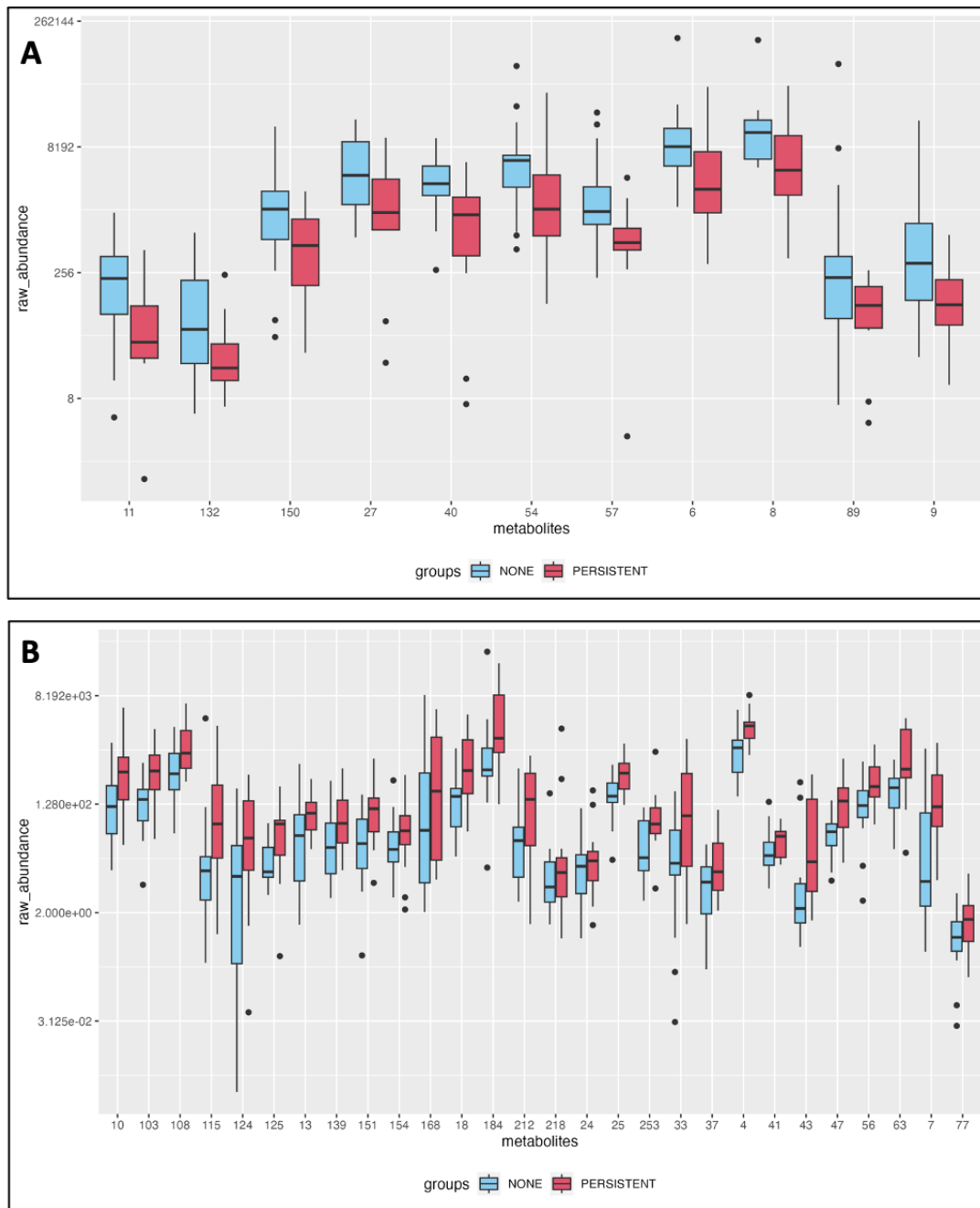


Figure 4.3 Box plot comparisons of discriminating metabolite abundances between infants in Persistent eczema group and infants in None eczema group. All metabolites shown have significantly different mean value of $p < 0.05$ (Wilcoxon test, Bonferroni correction for multiple comparisons) between the Persistent and None group. The y-axis shows log₂-transformed raw abundance values, while x-axis displays each metabolite identified by its unique identifier number used within this study. Dark red color indicates the Persistent group, while the light blue color indicates the None group. **(A)** 11 selected unique metabolites with p -value < 0.05 , and median ratio of Persistent/None < 0.5 . **(B)** 28 selected metabolites with p -value < 0.05 and median ratio of Persistent/None > 2.0 .

Analyses of fecal-transplanted, humanized mouse metabolome

Mice samples taken from in a previous experiment included 4 different gut microbiota: InfantA, InfantB, AdultC, and Mouse[206]. InfantA, InfantB, and AdultC samples all came from mice that were germ-free, then received fecal-transplant from different human samples. Mouse group contained a conventional mouse microbiota as they never received any fecal-transplant[206]. Each microbiota group was separated into halves, where one half received the sham-treatment of phosphate buffered-saline (PBS), while the other half was treated with house dust mites (HDM).

Metabolome clustered clearly by base microbiome

To visualize the overall spread of metabolome data, PCA was performed on the 736 metabolites present in the 8 experimental groups. With all 80 samples included, there was one extreme outlier in the PCA scores plot belonging in the PBS-treated conventional Mouse microbiota group (Figure 4.4A). Once the outlier was removed and PCA repeated, general clustering by microbiota could be seen (Figure 4.4B). Samples in InfantA-grouping, both PBS- and HDM-treated groups were closer together within the upper left quadrant (Figure 4.4B). Samples in InfantB groups had a slightly wider spread, mostly residing in the bottom left quadrant and spreading into the upper left quadrant (Figure 4.4B). Samples in AdultC grouping fell exclusively on the right quadrants, and equally in upper and lower quadrants on that side (Figure 4.4B). Mouse conventional group seemed to be most widely spread, spanning from the very bottom of the Hotelling's ellipse and close to the top border of the ellipse, but still enclosed on the right hand side of the quadrants (Figure 4.4B). PLS-DA was performed on the full set of samples with the outlier from the first PCA included. In the PLS-DA, the groups were clearly clustered by their microbiome types, and PBS- and HDM-treated groups within were intermingled (Figure 4.4C). InfantA groups clustered closely in the bottom right quadrant, InfantB groups clustered in the upper right quadrant, AdultC groups clustered in the upper left quadrant, and the conventional Mouse group clustered in the bottom left quadrant (Figure 4.4C).

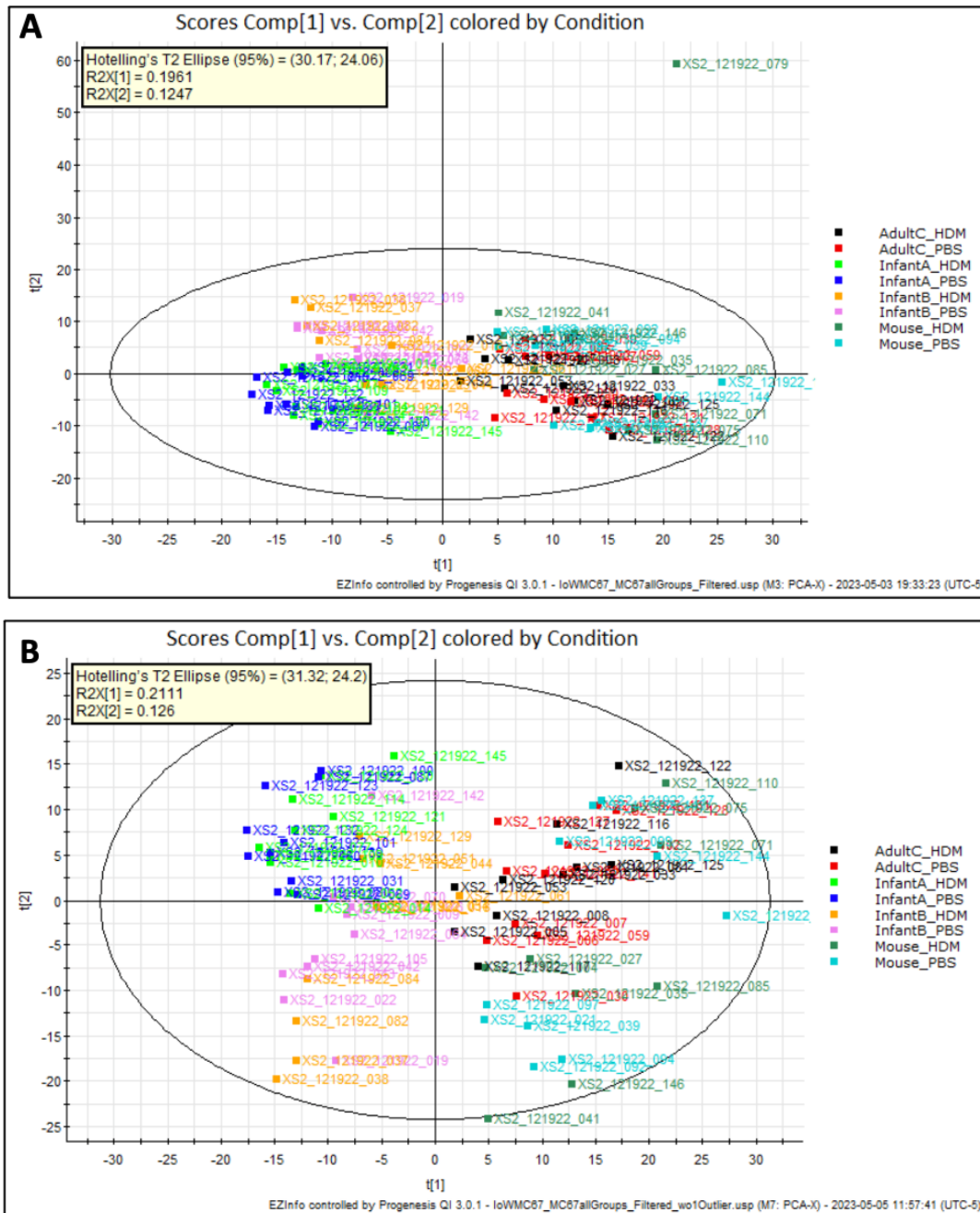
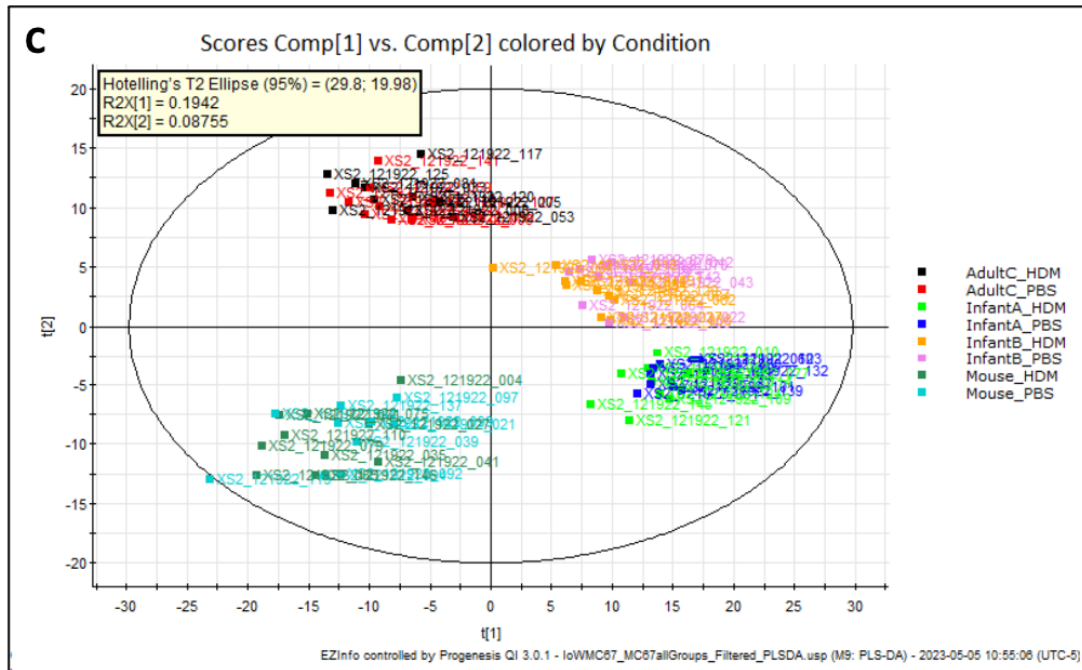


Figure 4.4 Ordination analyses of murine gut metabolome. (A-B) Each color represents each experimental group. First part of the label in the legend refers to the gut microbiome group of the mice. The second part of the label indicates the treatment group, PBS is sham-treated group and HDM was the allergen treated group. 736 metabolites were used. **(A)** PCA with metabolite abundances scaled with Unit Variance and individually transformed. One samples in dark green is an extreme outlier as it lies well beyond the Hotelling's ellipse. **(B)** PCA repeated with the single outlier removed, using Unit Variance scaling and individual transformation. **(C)** PLS-DA of all samples with abundances scaled with Unit Variance and transformed individually.

Figure 4.4 (cont'd)



Metabolome profile differs for each mouse group with different gut microbiome

Ordination analyses were repeated for all four microbiome groups that were sham-treated with PBS to investigate the differences in the metabolome influenced by their gut microbiome. In the PCA, the two mouse groups with gut microbiota stemming from human infants with or without allergy, InfantA and InfantB, fell on the left side of the plot, with some overlapping (Figure 4.5A). The group with human adult-based microbiome, AdultC, fell on the right hand side of the plot, both above and below the middle line (Figure 4.5A). Those with the conventional Mouse microbiota also fell on the right hand side, with wider vertical spread within the group (Figure 4.5A). In PLS-DA, the clustering was tighter within the groups, with each group contained within a single quadrant (Figure 4.5B). Infant A group and InfantB group were clustered most closely to each other; InfantA clustering in the bottom right quadrant and InfantB in the upper right quadrant (Figure 4.5B). AdultC group clustered in the upper left quadrant and conventional Mouse group clustered in the lower left quadrant (Figure 4.5B).

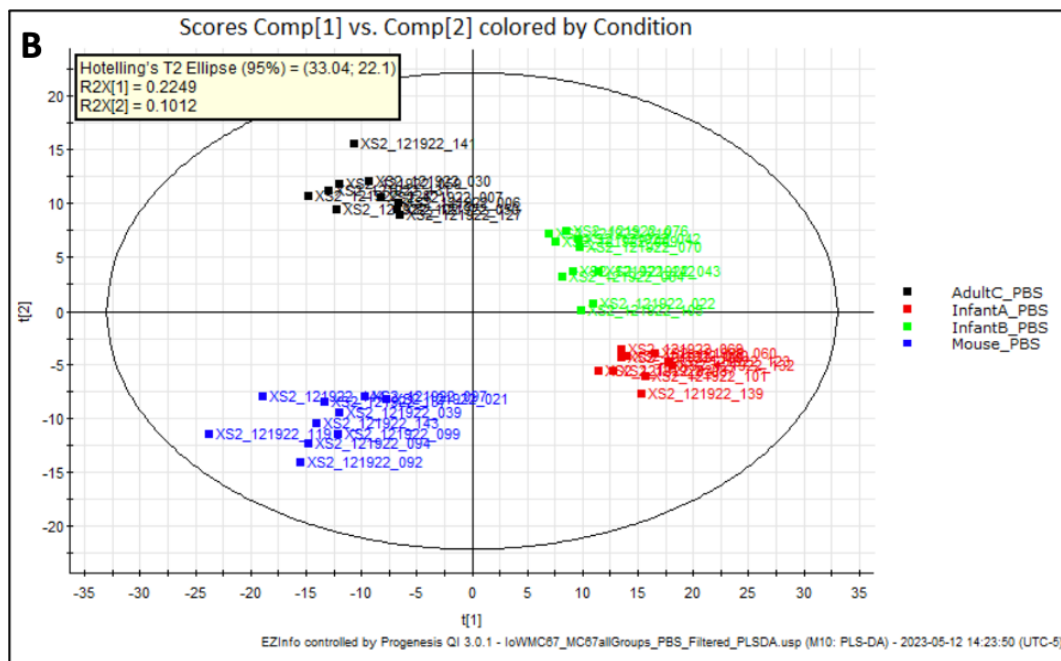
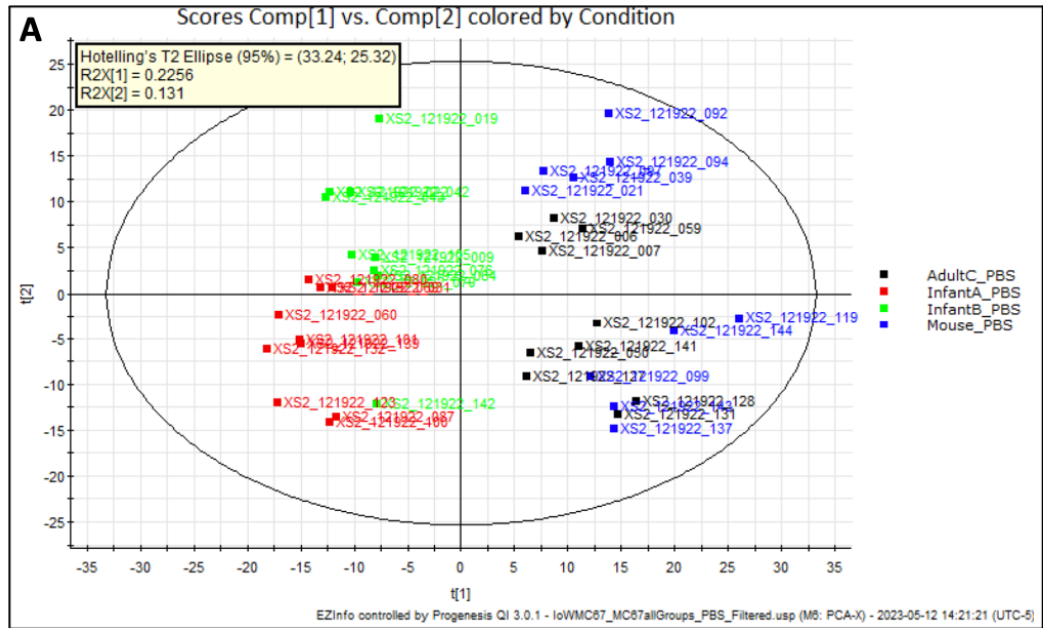


Figure 4.5 Ordination analyses of sham-treated mouse metabolome grouped by microbiome. 735 metabolites were included in the analyses. All samples and groups received the sham-treatment (PBS) in the previous experiment. Each group is indicated by the color as shown in the figure legend. **(A)** PCA scores plot of the four microbiota groups, scaled with Unit Variance and log transformed. All samples fell within the Hotelling's ellipse. **(B)** PLS-DA of the four microbiota groups scaled with Unit Variance, log transformed, and predicting 92% of the variance.

More than half of humanized and conventional mouse gut metabolome significantly differed

Fecal gut metabolite abundances of each humanized mouse group (InfantA, InfantB, and AdultC) were compared to that of conventional mouse group using PBS-treated groups for each microbiota groups to assess the differences in the basal level of metabolites.

For the comparison of the conventional mouse group to InfantA mouse groups, together they had 1454 unique metabolites after filtering, of which 903 metabolites (62.1% of total) had significant mean difference with p -value < 0.05 , and 541 metabolites (59.9% of total) had significant mean difference with p -value < 0.01 , both after correction for multiple comparisons (data not shown). Out of the 541 metabolites with significantly different abundance, 25 total metabolites were further selected based on the median ratio of the abundance between the groups being above 100,000 in either direction. Seven metabolites were identified for having at least 100,000-fold lower median in the InfantA mouse metabolome compared to the conventional mouse metabolome (Figure 4.6A). 18 other metabolites were identified for having at least 100,000-fold higher median in the InfantA mouse metabolome compared to the conventional mouse metabolome (Figure 4.6B). These 25 unique metabolites represent the most striking differentiating features of the metabolome of the InfantA mouse group and conventional mouse group.

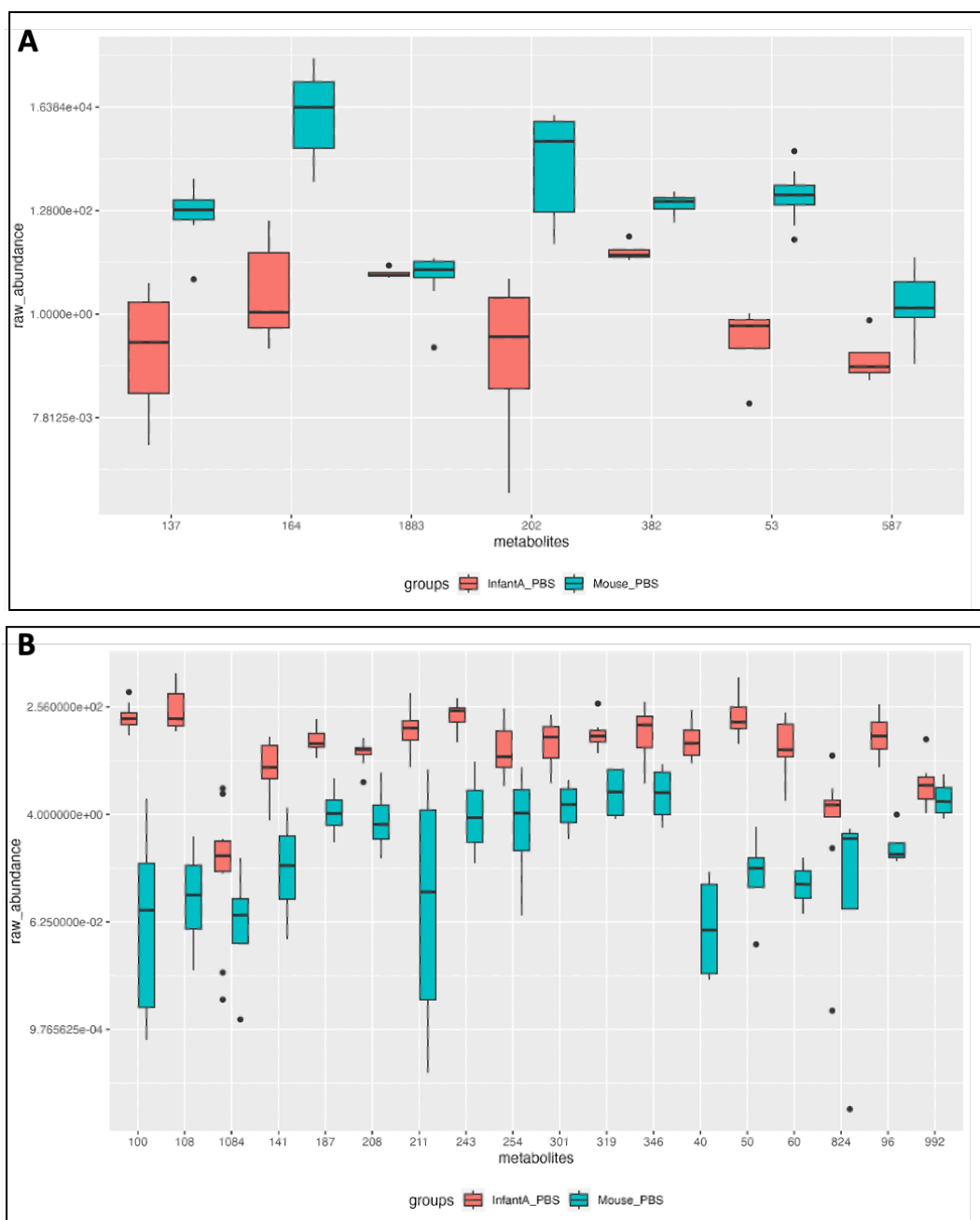


Figure 4.6 Comparisons of metabolite abundances between humanized InfantA mouse group and conventional mouse group. All metabolites shown have mean difference significance p -value < 0.01 (Wilcoxon test, corrected for multiple comparison with Bonferroni correction) between the humanized InfantA mouse group and conventional mouse group, both PBS-treated. The y-axis is log-2 transformed for better visualization, post p -value calculation. Each unique metabolite is indicated as an integer on the X-axis, functioning as their unique identifier within this study. **(A)** Selected seven unique metabolites with at least 100,000 fold difference in their median values with higher median in the conventional mouse group. **(B)** Selected 18 unique metabolites with higher median value in humanized InfantA mouse group by at least 100,000 fold.

When comparing InfantB mouse group's metabolome to that of conventional mouse metabolome, they had 1284 unique measured metabolites post-filtering together, 885 unique metabolites (68.9% of total) that were significant at $p < 0.05$, and 592 unique metabolites (41.2%) that were significant at $p < 0.01$ (data not shown). Out of the 592 unique metabolites with significant abundance difference of $p < 0.01$, 27 were further identified for having at least 100,000 fold differences in the medians between InfantB and conventional mouse. 5 metabolites were identified for being lower in InfantB than in conventional mice by at least 100,000 fold (figure 4.7A), while 22 were identified for being higher in the InfantB than in conventional mice (figure 4.7B).

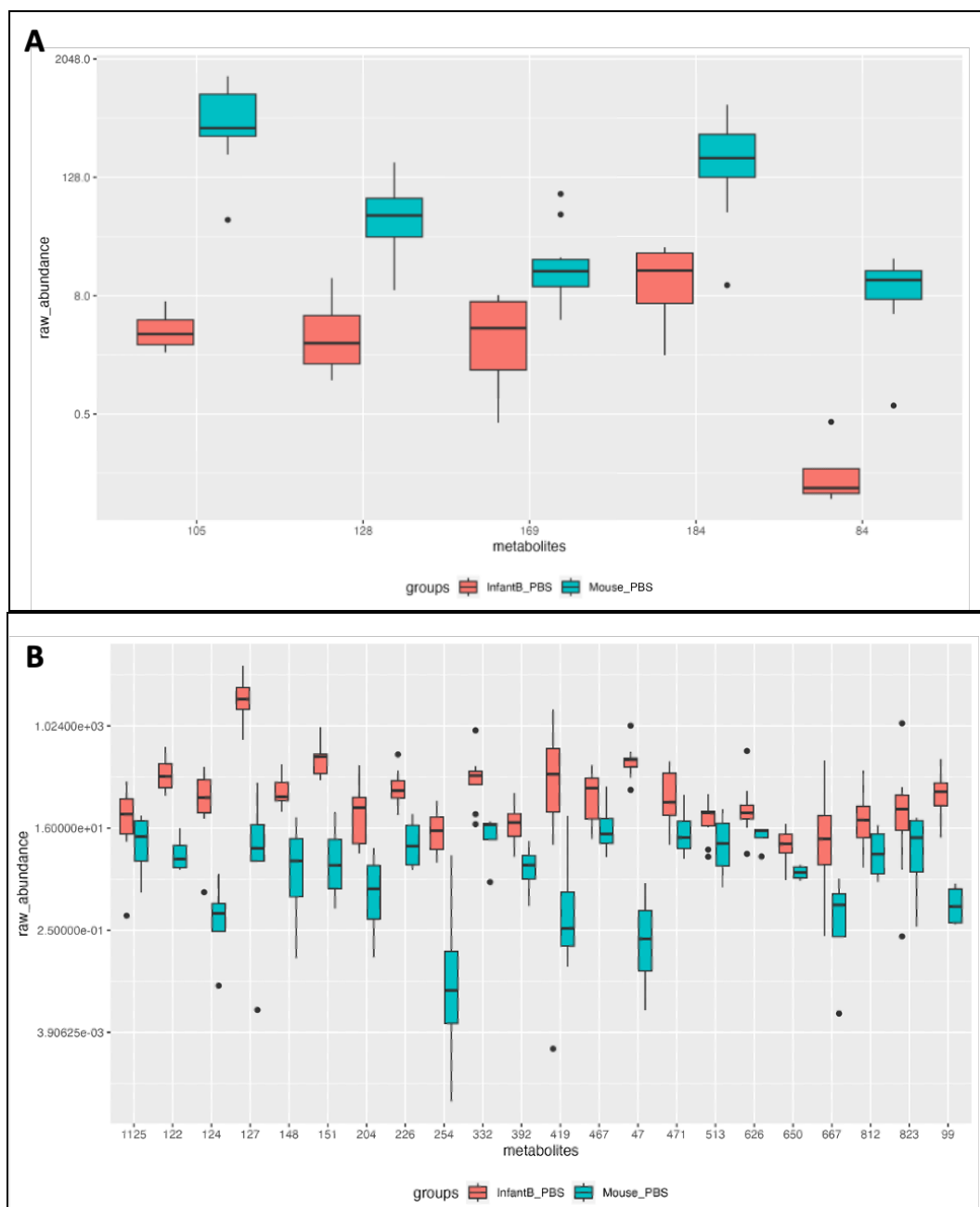


Figure 4.7 Comparisons of metabolite abundances between humanized InfantB mouse group and conventional mouse group. All metabolites shown have mean difference significance p -value < 0.01 (Wilcoxon test, corrected for multiple comparison with Bonferroni correction) between the humanized InfantB mouse group and conventional mouse group, both PBS-treated. The y-axis is log-2 transformed for better visualization, post p -value calculation. Each unique metabolite is indicated as an integer on the X-axis, functioning as their unique identifier within this study. **(A)** Selected five unique metabolites with at least 100,000 fold difference in their median values with higher median in the conventional mouse group. **(B)** Selected 22 unique metabolites with higher median value in humanized InfantB mouse group by at least 100,000 fold.

For the comparison of AdultC mouse group and conventional mouse group, of the total 691 unique metabolites retained after filtering, 425 unique metabolites (61.5%) were significantly different at $p < 0.05$, and 258 unique metabolites (37.3%) were significant at $p < 0.01$. Out of the 258 unique metabolites, 9 total metabolites had at least 100,000 fold differences in their medians between the groups. Only one metabolite was identified as having 100,000 higher median in conventional mouse group (metabolite 25), and 8 metabolites had higher medians in AdultC groups than conventional mouse group (Figure 4.8).

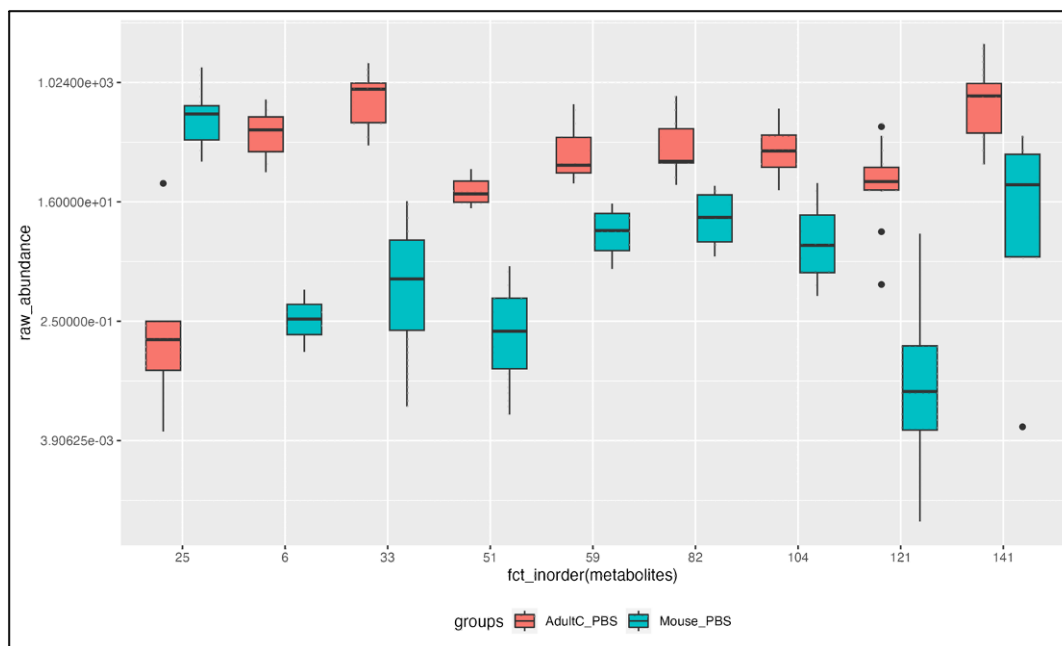


Figure 4.8 Comparisons of metabolite abundances between humanized InfantB mouse group and conventional mouse group. All metabolites shown have mean difference significance p -value < 0.01 (Wilcoxon test, corrected for multiple comparison with Bonferroni correction) between the humanized InfantB mouse group and conventional mouse group, both PBS-treated. The y-axis is \log_2 transformed for better visualization, post p -value calculation. Each unique metabolite is indicated as an integer on the X-axis, functioning as their unique identifier within this study. Selected nine unique metabolites with at least 100,000 fold difference in their median values are shown. The metabolite on the very left (25) is the only metabolite with median 100,000 fold higher in the conventional mouse group than AdultC group. The remaining 8 metabolites had medians 100,000 fold higher in the AdultC group than in conventional mouse group.

HDM treatment altered gut metabolome in mice

Despite not being the main driver of the clustering and spreading of the metabolome data

amongst the 8 mouse groups, the groups receiving HDM expressed an altered gut metabolome profile compared to their sham- groups. The separation is not as clear in the PCA scores plot of all groups separated based on HDM- or PBS-treatment (Figure 4.9A), however it becomes more clear in the PLS-DA where the HDM-treated groups cluster to the right and PBS-treated groups to the left (Figure 9B). Although with four different microbiota still present in the dataset, their effect on the spread is still prominent.

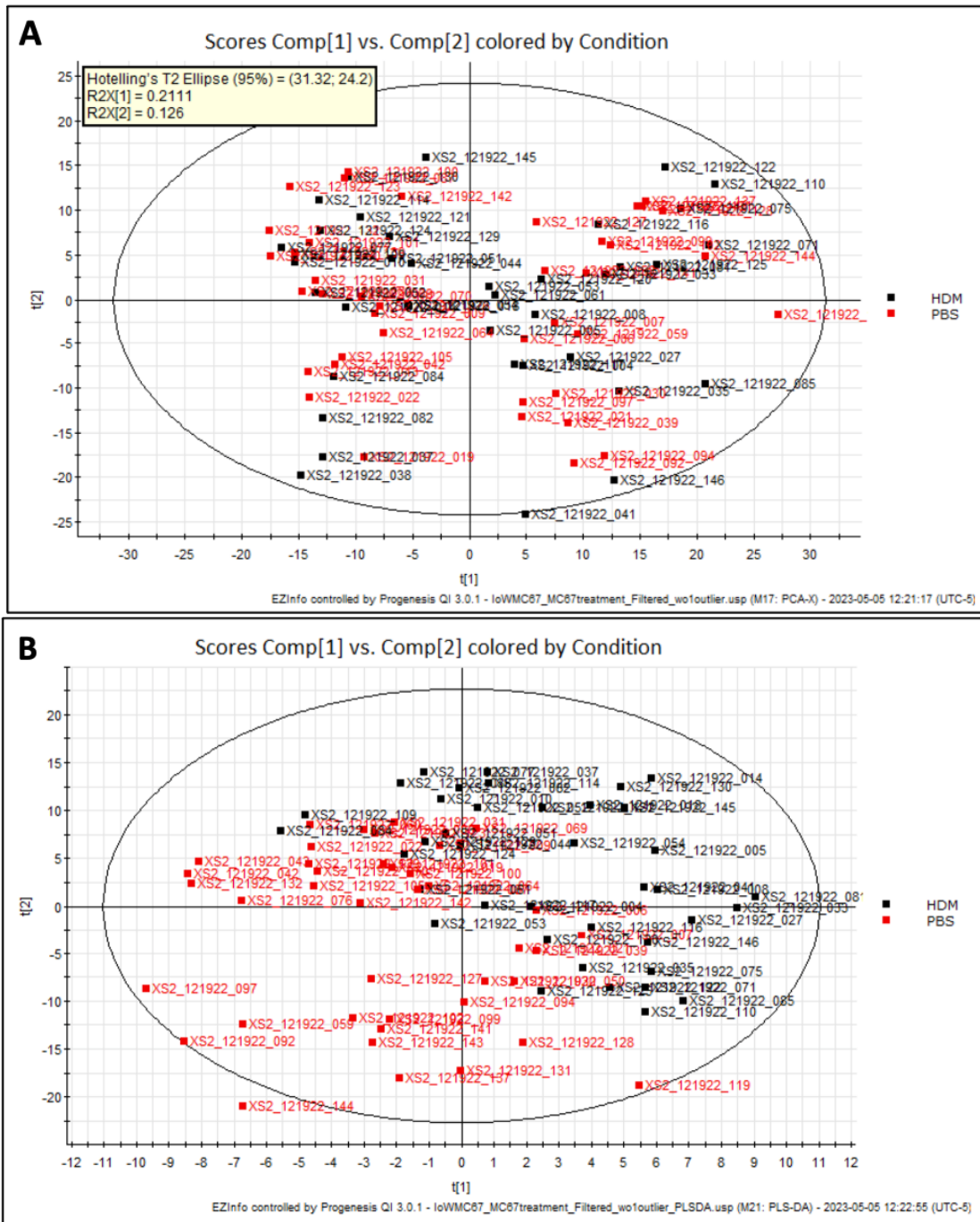


Figure 4.9 Ordination analyses of 736 metabolites, grouped by PBS- or HDM- treatment. **(A)** PCA scores plot generated with abundance scaled using Unit Variance and individually transformed. **(B)** PLS-DA scores plot scaled with Unit variance and transformed individually.

When separated by each microbiota groups to eliminate the effect of the microbiota differences driving the spread of the data, better spread between the PBS- and HDM-treated groups can be observed (Figure 4.10). For InfantA, PCA shows a tendency for the PBS-treated

samples to cluster in the top half and HDM-treated samples in the bottom half with some exceptions (Figure 4.10A). The separation between the treatment group is emphasized in the PLS-DA scores plot where the HDM-treated samples move to the right-hand side of the plot away from the PBS-treated samples (Figure 4.10B). In the PCA of InfantB group, there was less clustering and more spread of the PBS-treated group, while the HDM-treated group had narrower spread (Figure 4.10C). In PLS-DA, InfantB group had one HDM-treated sample that laid outside of the Hotelling's ellipse, indicating it as a potential outlier in this analysis (Figure 4.10D). The treatment groups within the ellipse separated with samples from each perspective treatment groups clustering together on each side (Figure 4.10D). AdultC PCA displayed the least clear clustering by the treatment groups, where samples from both treatment group was more spread out across all 4 quadrants without any clear clustering (Figure 4.10E). The PLS-DA of AdultC group did show horizontal separation between the treatment groups, however, it also had the widest vertical spread of the samples within each of the groups (Figure 4.10F). In the conventional Mouse group PCA, there was a small cluster near the horizontal midline consisting of samples from both treatment groups, but no clear clustering by the groups (Figure 4.10G). However in PLS-DA, the two treatment groups were more tightly clustered with all the samples from HDM-treated groups clustering in the upper right quadrant and most of the PBS-treated samples clustering in the bottom left quadrant on the opposite side (Figure 4.10H).

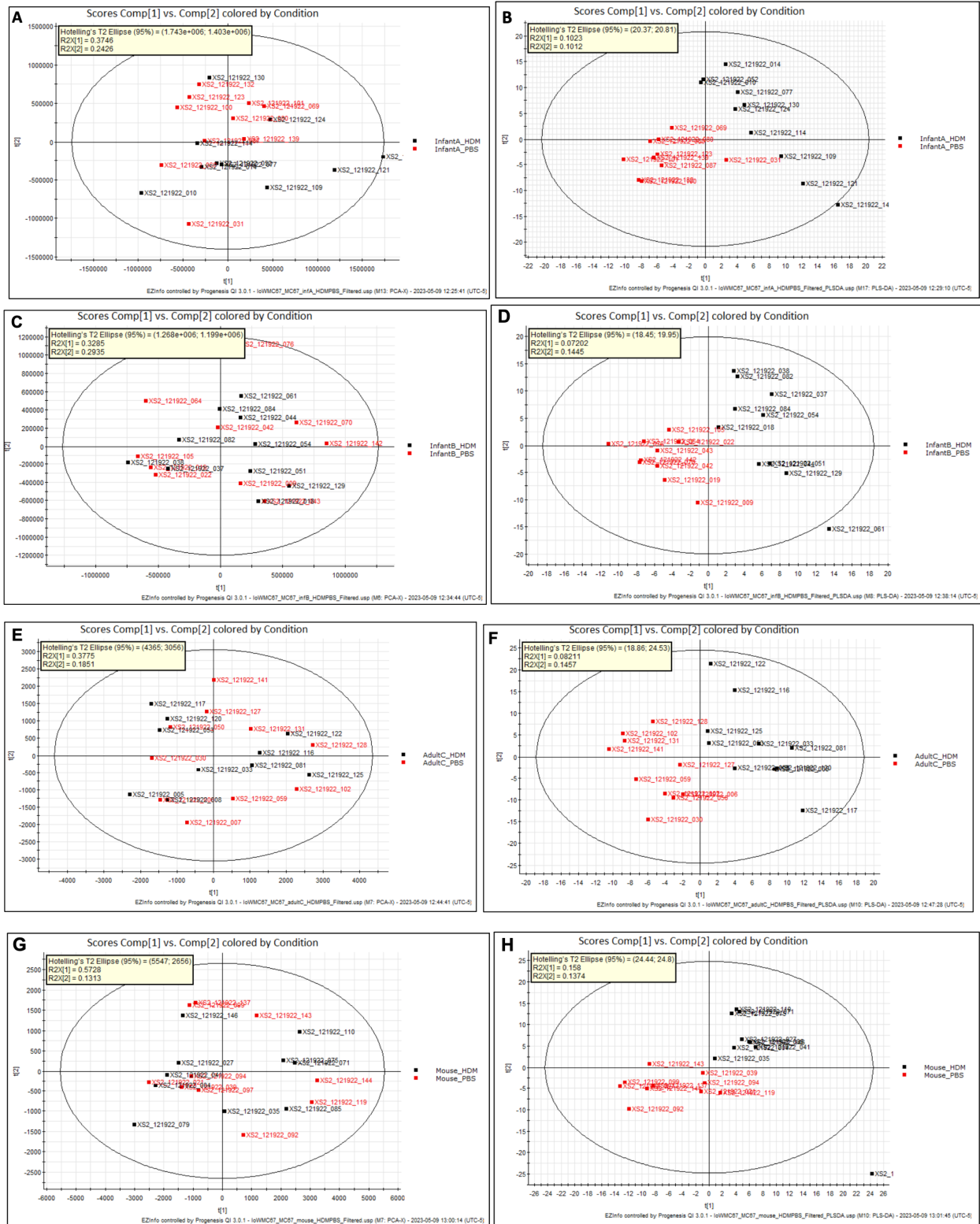


Figure 4.10 Ordination analyses of metabolites for each microbiota group, grouped by PBS- or HDM-treatment. Black color indicates HDM-treated samples and red color indicates the PBS-treated samples. The black ellipse represent the 95% Hotelling's ellipse. **(A)** PCA

Figure 4.10 (cont'd)

scores plot of 731 metabolites in InfantA group with center scaling and individual transformation. **(B)** PLS-DA scores plot of 731 metabolites in InfantA group with unit variance scaling and log transformation. **(C)** PCA of 732 metabolites in InfantB group with center scaling and log transformation. **(D)** PLS-DA of 732 metabolites in InfantB group with Unit Variance scaling and log transformation. **(E)** PCA of 731 metabolites in AdultC group with center scaling and log transformation. **(F)** PLS-DA of 731 metabolites in AdultC group with Unit Variance scaling and log transformation. **(G)** PCA of 730 metabolites in conventional Mouse group with center scaling and log transformation. **(H)** PLS-DA of 730 metabolites in conventional mouse group with Unit Variance scaling and log transformation.

HDM treatment significantly changed the abundances of several metabolites

Fecal gut metabolite abundances of each treatment group were compared to each other within each microbiota group to assess the differences of metabolite expression induced by the allergen treatment. Metabolites were selected by applying the more stringent filtering described in the methods on the metabolite raw abundance data for each comparison.

Within the InfantA group, there were 78 metabolites that remained after the stringent filtering, indicating the metabolites most responsible for distinguishing between the HDM- and PBS-treated groups within the InfantA microbiota group. Of those 78, 25 metabolites were shown to be significantly different in their means by having re-calculated p-values < 0.05 (data not shown). These 25 significant metabolites and their abundances are shown per metabolite and the treatment group in Figure 11. 14 of the 25 metabolites had higher medians in the PBS-treated groups compared to the HDM-treated groups, as shown by the bold black line within the boxes (Figure 4.11). Eleven other metabolites had median values higher in the HDM-treated group compared to the PBS-treated group (Figure 4.11).

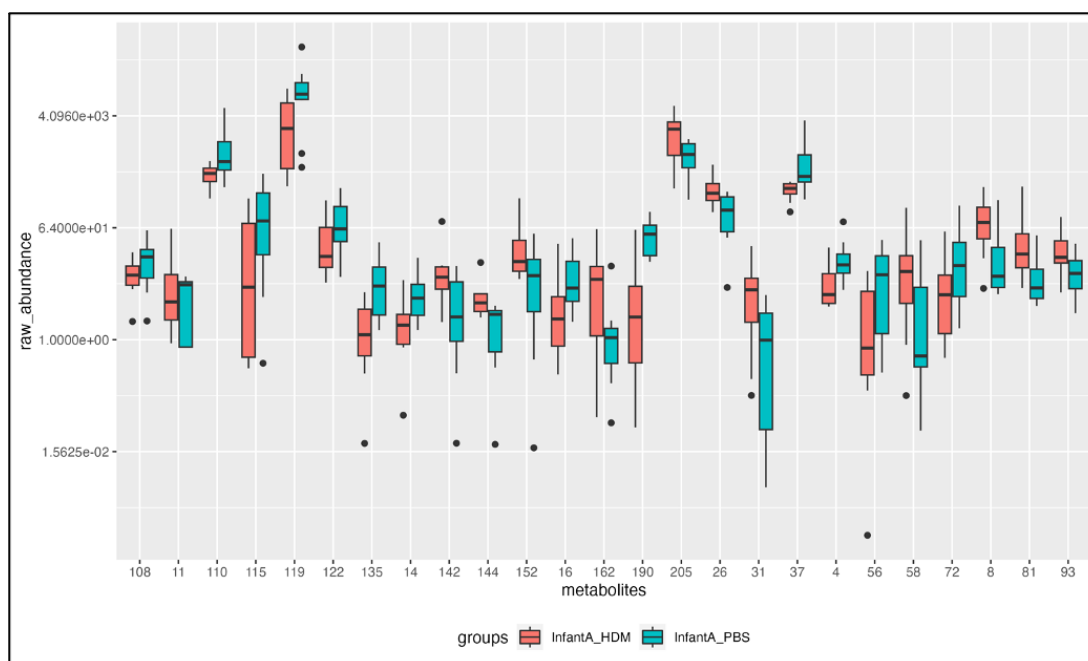


Figure 4.11 Comparison of significantly different metabolite abundances between PBS- and HDM-treated InfantA mice. All 25 metabolites shown have statistically significant mean difference of p-value < 0.05 (Wilcoxon test, corrected for multiple comparison with Bonferroni correction) between the HDM-treated and PBS-treated groups. The y-axis is log-2 transformed for better visualization, post p-value calculation. Each unique metabolite is indicated as an integer on the X-axis, functioning as their unique identifier within this study.

The InfantB groups retained 119 metabolites upon the same stringent filtering process and had 56 unique metabolites that were statistically significant (p-value < 0.05) upon re-calculation. Out of the 56 metabolites, 32 metabolites were further selected using the median ratio of HDM-treated group/PBS-treated group. 12 metabolites were selected for having the median ratio < 0.2, indicating a notably higher abundance in the PBS-treated group (Figure 4.12A). 20 metabolites were selected for having the median ratio > 2.0, indicating at least a doubling of the median values in the HDM-treated group compared to the PBS-treated group (Figure 4.12B).

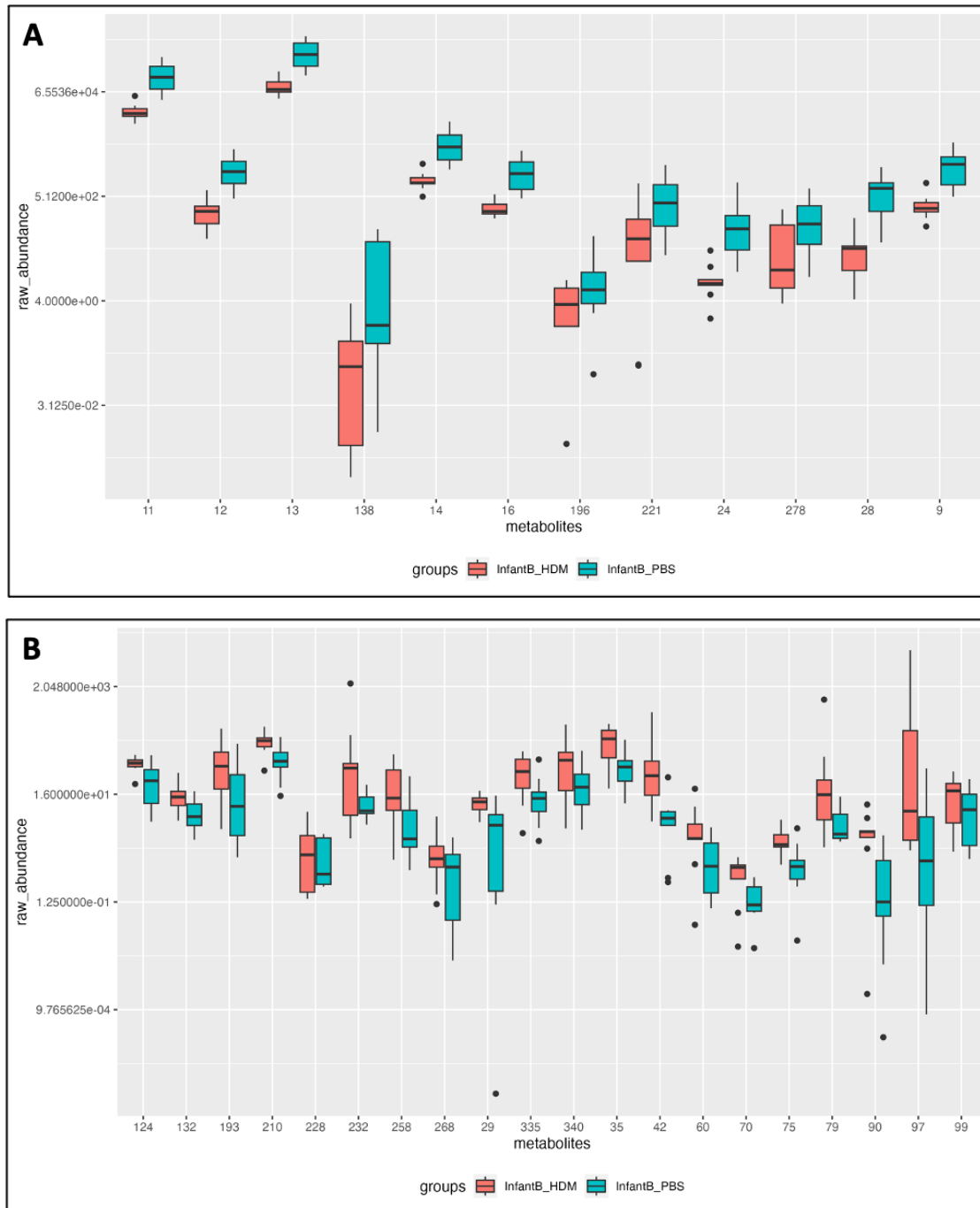


Figure 4.12 Comparison of significantly different metabolite abundances between PBS- and HDM-treated InfantB mice. All metabolites shown have statistically significant mean difference of p -value < 0.05 (Wilcoxon test, corrected for multiple comparison with Bonferroni correction) between the HDM-treated and PBS-treated groups. The y-axis is log-2 transformed for better visualization, post p -value calculation. Each unique metabolite is indicated as an integer on the X-axis, functioning as their unique identifier within this study. **(A)** 12 metabolites with median ratio of HDM-treated/PBS-treated < 0.2 . **(B)** 20 metabolites with HDM-treated/PBS-treated ratio > 2.0 .

Adult C group retained a total of 131 metabolites upon stringent filtering, and 38 of those metabolites were identified as statistically significant in their mean differences (p-value < 0.05). Out of the 38 significant metabolites, 7 were selected for having HDM-treated/PBS-treated group median ratio of < 0.3, indicating they are more abundance in the PBS-treated groups compared to the HDM-treated groups (Figure 4.13A). 17 other were selected for having HDM-treated/PBS-treated group median ratio of > 3.0, indicating at least 3-fold higher abundance in mice treated with HDM compared to mice treated with PBS (Figure 4.13B).

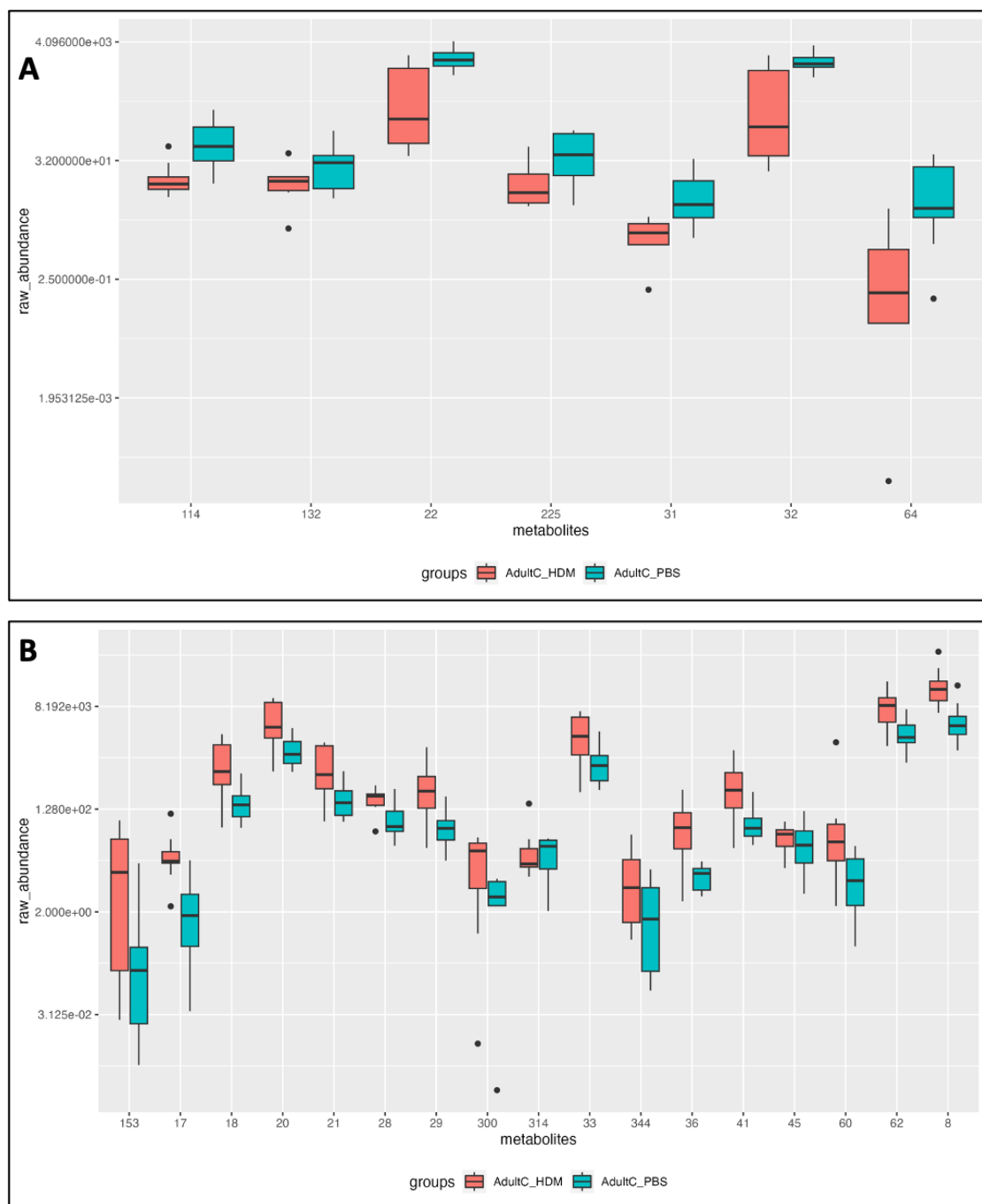


Figure 4.13 Comparison of significantly different metabolite abundances between PBS- and HDM-treated AdultC mice. All metabolites shown have statistically significant mean difference of p -value < 0.05 (Wilcoxon test, corrected for multiple comparison with Bonferroni correction) between the HDM-treated and PBS-treated groups. The y-axis is log-2 transformed for better visualization, post p -value calculation. Each unique metabolite is indicated as an integer on the X-axis, functioning as their unique identifier within this study. **(A)** 7 metabolites with HDM/PBS median ratio < 0.3 . **(B)** 17 metabolites with HDM/PBS median ratio > 3.0 .

In the conventional Mouse group, total of 125 metabolites remained following the stringent filtering process, of which 42 metabolites were shown to be statistically significant in their abundance means (p -value < 0.05). Of the 42 further selected metabolites, three metabolites were selected for also having the HDM-treated/PBS-treated group median ratio < 1.0 , and 19 metabolites were selected for having the HDM-treated/PBS-treated group median ratio > 2.0 (Figure 4.14). These metabolites represent those that are significant in the differences of their abundance across the compared groups, thus distinguishing the metabolomic profiles of the compared groups.

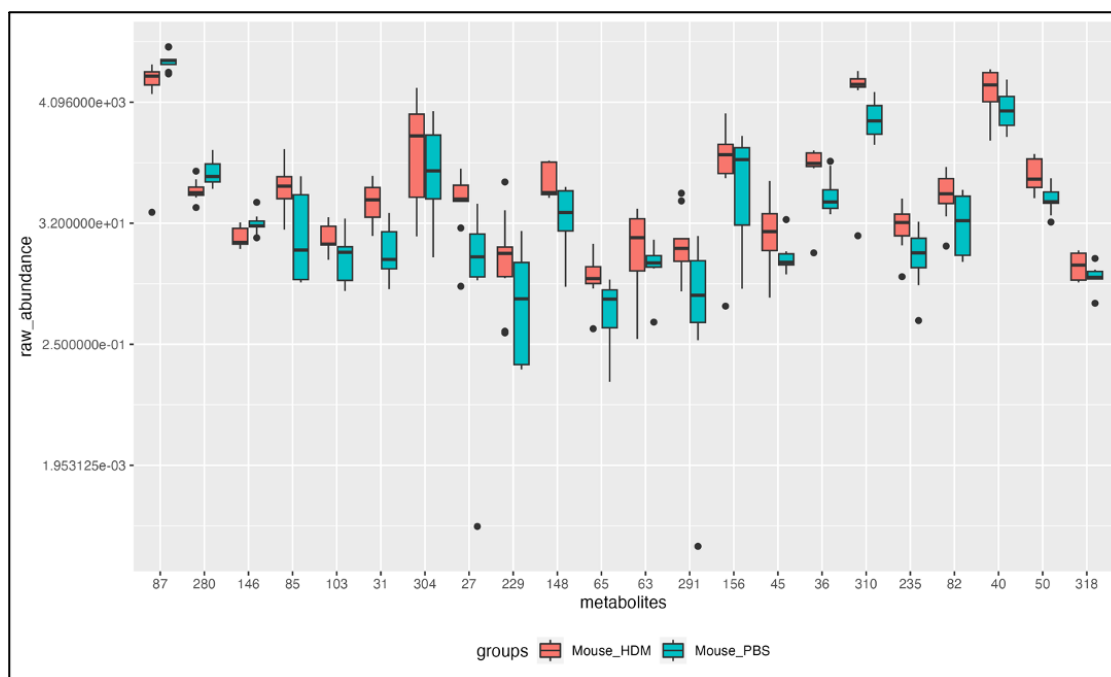


Figure 4.14 Comparison of significantly different metabolite abundances between PBS- and HDM-treated conventional Mouse group. All 22 metabolites shown have statistically significant mean difference of p -value < 0.05 (Wilcoxon test, corrected for multiple comparison with Bonferroni correction) between the HDM-treated and PBS-treated groups. The y-axis is log-2 transformed for better visualization, post p -value calculation. Each unique metabolite is indicated as an integer on the X-axis, functioning as their unique identifier within this study. 3 metabolites on the left most side had HDM/PBS median ratio < 1.0 , while the remaining 19 metabolites had HDM/PBS median ratio > 2.0 .

Discussion

Using 31 fecal samples from human infants and 80 cecal samples from mice, total of 8675 unique metabolites were measured to be used for analyses. 744 of those metabolites were selected based on abundance, fold change differences, and pre-calculated p-values to be used for ordination analyses to visualize the similarities of metabolite profiles. Human infant metabolite profiles were most different when comparing the Persistent group, the infants diagnosed with eczema persistently during the first 3 years of life, and None group, the infants that never developed eczema during the first 3 years. 50 unique metabolites were identified for being significantly different ($p < 0.05$) between the Persistent and None group. Hippuric acid and dihydrocortisol were amongst the metabolites most significantly in higher abundance in the None group, those who lacked eczema. Asn-Ser-Thr and an unknown compound with a formula $C_{16}H_{26}N_6O_5$ were amongst the metabolites most significantly in higher abundance in the Persistent group, those with chronic childhood eczema. Mouse metabolome were heavily clustered by the base gut microbiome group. The humanized microbiota mouse groups, which all showed increased airway-hyperresponsiveness previously[206], expressed more than half of metabolite profiles that were significantly different from the conventional mouse microbiota group that did not show an increased airway-hyperresponsiveness. HDM-treatment also altered the measured fecal metabolome in each of the mouse groups, although not as significantly as the basal gut microbiota differences.

In the initial analyses of human infant's metabolite profiles using the three eczema diagnosis groups, Persistent, Intermediate, and None, PCA showed very little spread based on the group identity. Although PLS-DA was able to separate the data by the groups more than PCA, overlap of the groups still occurred. To minimize the overlaps and noise, using the two most clinically relevant groups, Persistent and None were used for further analyses. PCA analysis of Persistent and None group still did not show spread of data based on the clinical grouping. PLS-DA did show a better separation of samples by the groups, however the clustering by the group was still rather wide. Given the influence of the gut microbiome in gut metabolome, it was expected that the ordination analyses of infant fecal metabolome will yield similar overlapping seen in its equivalent 16S microbiota ordination analyses[204]. The lack of clear clustering can also be explained by the fact that these samples came from real human infants, all having reported to have been on varying diets, a factor known to affect the gut microbiome and

especially gut metabolome greatly [98].

Despite the ordination overlaps, there were several metabolites identified as being significantly different in abundance between the samples from infants with “Persistent” eczema and infants having “None” eczema diagnosis. Using a stringent filtering process to identify the metabolites most distinguishing between the two groups, 113 metabolites were identified. Of the 113, 50 metabolites had a significantly ($p < 0.05$) different mean difference between the Persistent and None groups. 39 metabolites were then further identified using the abundance median ratios. Of the 11 metabolites that had significant mean difference, and twice as high abundance median in the None group compared to the Persistent group, 2 metabolites were manually identified as hippuric acid and dihydrocortisol. Hippuric acid is a uremic toxin that is endogenously produced by metabolism in mammals [209, 210]. A metabolomics study comparing the metabolite profiles of germ-free mice to conventional mice observed hippuric acid to be 17-fold higher in conventional mice than in germ-free mice, suggesting the importance of the gut microbiome in hippuric acid accumulation[211]. As it was higher in the infants without early childhood eczema, the infants with early childhood eczema may be missing certain microbial flora that contribute to the hippuric acid accumulation. Dihydrocortisol is a steroid derivative molecule that is endogenously produced in animals including humans and can also be exogenously sourced through consumption of animal meat[212-216]. Dihydrocortisol has been studied across different settings. One study suggested that it as a potential mineralcorticoid in humans[217], while another showed a potential of measuring dihydrocortisol to assess the levels of beef cattle welfare[218]. As dihydrocortisol was also higher in infants without eczema, it may be a potential marker for not developing childhood eczema. The two compounds manually identified that had twice as high median ratios in the Persistent group compared to None were the tripeptide Asn-Ser-Thr and metabolite-24 as an unknown compound with a formula of $C_{16}H_{26}N_6O_5$. Currently there are no known specific biological functionalities tied directly to Asn-Ser-Thr nor $C_{16}H_{26}N_6O_5$, a metabolite most likely another tripeptide. However, given amino acids are the building blocks of proteins, they may be part of specific protein degradation that are increased in the infants with persistent early childhood eczema.

Mouse groups showed cleaner clustering by experimental groups than the human infant samples, which were expected as all the mice used were of the same genotype sharing the same diet and caging environment, reducing environmentally induced variability. This was also seen in

their equivalent 16S microbiota analyses previously[206]. In analyses including all 8 groups, 4 microbiota groups with 2 treatment groups each, the treatment groups clusters overlapped within the same microbiota group in PCA and PLS-DA, suggesting that the gut microbiota has a larger effect on the metabolic profiles than the allergen-exposure treatment (HDM). The role of the underlying gut microbiome shaping the gut metabolome was further highlighted in the following analyses using just the 4 microbiota groups, all sham(PBS)-treated. Visualized without the effect of the allergen(HDM)-treatment, the metabolic profiles were mostly clustered by the underlying microbiota in PCA, and seen clearly clustered in PLS-DA. Although in PCA, AdultC microbiota group and the conventional Mouse microbiota groups were seen to be split into 2 separate clusters within each group, where each of those clusters were in close proximity to the other group. This phenomenon was not observed in the PLS-DA analysis.

In the previous experiment, all 3 of the humanized microbiota mouse groups were measured to have significantly decreased baseline lung mechanics capabilities as well as having significantly increased airway hyper-responsiveness, a pathology commonly associated with asthma[206]. This results were in support of the other published studies suggesting the importance the role of the gut microbiota in the development of allergy and asthma[4, 80-83]. To explore the mechanism in which the 3 different humanized gut microbiota of mice altered the lung functionalities, metabolite profiles of the 3 humanized microbiota mouse groups were each compared to that of the conventional mouse microbiota group. InfantA group, which received the fecal-transplant from infants with persistent eczema, had 541 metabolites with abundances statistically significant ($p < 0.01$) compared to the conventional Mouse group. 25 of those metabolites had abundance median difference of at least 100,000-fold. Seven of these metabolites were in significantly higher abundance in the conventional mouse group, while 18 remaining metabolites were in significantly higher abundance in the InfantA group. Similarly, InfantB group had 592 metabolites with abundances statistically significant ($p < 0.01$) compared to the conventional Mouse group, 27 of which had median difference of at least 100,000 fold, with five higher in conventional Mouse group and 22 higher in InfantB group. AdultC group had fewer significantly different metabolites at 258 ($p < 0.01$), and one metabolite that was 100,000 fold higher median in the conventional Mouse group and eight metabolites 100,000 fold higher in the AdultC group. Although their metabolite identities are currently unassigned, these metabolites represent a subset of metabolites that distinguishes the humanized microbiota mice

with decreased lung functions from the conventional mouse groups without the decreased lung functions.

House dust mites (HDM) serves as a common allergen associated with development and triggering of allergic asthma in humans[78, 79]. HDM was used to induce allergic phenotypes in all four groups of mice in the previous experiment[206]. Although the HDM-treatment did not differentiate the metabolic profiles as much as the underlying gut microbiota, it still induced changes and shift in the measurable metabolome. The differentiation induced by HDM-treatment was slightly variable between the microbiota types as seen by the spread and clustering of the samples in ordination analyses, suggesting the effect of the gut microbiota in the host- and/or gut microbial-metabolism in response to an allergen exposure. The shift in the metabolome due to the HDM-treatment was characterized by a group of metabolites. The median fold changes as well as the total number of metabolites that were statistically significant were much less in number than the metabolites differentiating between the microbiota types, however, a collection of metabolites were still identified to be significantly differentiating between the HDM-treated groups and sham(PBS)-treated groups. Within the InfantA group, HDM-treatment made total of 25 metabolites to be significantly different ($p < 0.05$) compared to the PBS-treated group. InfantB group had 32 metabolites that were significant ($p < 0.05$) and having at least two-fold difference in the abundance median between the HDM- and PBS-treated groups. AdultC group had 38 significant ($p < 0.05$) metabolites with at least three-fold difference, and conventional Mouse group had 22 significant ($p < 0.05$) metabolites with at least 1 to 2-fold abundance median differences. The presence of metabolites significantly differing in their abundance in HDM- and PBS-treated group displayed that an allergen (HDM) exposure significantly alters the gut metabolic profiles. The shift in the gut metabolome may be driven by the alteration of the gut microbiota either in their composition or their metabolic activities from the exposure to HDM. Several studies have shown that exposure and sensitization to inhaled allergens can alter the composition of the gut microbiome[219-221]. Other studies have also observed that the host-response to the allergen exposures are influenced by the gut microbiota[4, 80, 81, 222], suggesting that this shift in metabolome seen with HDM-treatment is most likely due to the complex interplay and dual feedback of allergen altering the gut microbiota composition, and gut microbiota altering the host-response to the allergen.

This study established the differences of the metabolite profiles between disease states

(early childhood eczema) and identified a group of gut metabolites that distinguished those groups in humans, such as hippuric acid. In addition, the differences in the gut metabolome of fecal-transplanted with humanized gut microbiota mice were established, along with a group of metabolites that were significantly distinguished between the groups. The altering effect of HDM-treatment on gut metabolome was also established in mouse models, both with humanized microbiota and with a conventional mouse microbiota. To further the understanding of different metabolic signatures of each groups studied, measuring sample metabolites using a different mass spectrometry method may assist this current dataset by providing more extensive metabolic profiles. More work is needed to further identify the metabolites to allow a more clinically-translatable insight into metabolic production that could be directly tied to either a specific gut microbial members or an environmental/dietary exposures in relation to allergy development. Most of the detected metabolites have yet to be identified, highlighting the need for a more extensive metabolite databases in the current state of the field of metabolomic profiling studies. More investigations of gut chemistry and biochemistry, as well as roles of individual taxa and microbial members of the gut are needed to better understand the interactions of metabolites between the host and the microbiota, as well as within the microbiota, which will help shed the light on their role in disease manifestation, as well as development of better treatments and preventions.

REFERENCES

1. Tanno, L.K., et al., Categorization of allergic disorders in the new World Health Organization International Classification of Diseases. *Clin Transl Allergy*, 2014. **4**: p. 42.
2. Arrieta, M.C., et al., Early infancy microbial and metabolic alterations affect risk of childhood asthma. *Sci Transl Med*, 2015. **7**(307): p. 307ra152.
3. Jones, S.M., et al., Efficacy and safety of oral immunotherapy in children aged 1-3 years with peanut allergy (the Immune Tolerance Network IMPACT trial): a randomised placebo-controlled study. *Lancet*, 2022. **399**(10322): p. 359-371.
4. Zimmermann, P., et al., Association between the intestinal microbiota and allergic sensitization, eczema, and asthma: A systematic review. *J Allergy Clin Immunol*, 2019. **143**(2): p. 467-485.
5. CDC, N.C.f.H.S., More Than a Quarter of U.S. Adults and Children Have at Least One Allergy. 2023.
6. Bieber, T., Atopic dermatitis. *N Engl J Med*, 2008. **358**(14): p. 1483-94.
7. Chan Ho Na, J.C., Eric L. Simpson, Quality of Life and Disease Impact of Atopic Dermatitis and Psoriasis on Children and Their Families. *Children*, 2019. **6**(12)(133).
8. Camfferman, D., et al., Eczema and sleep and its relationship to daytime functioning in children. *Sleep Med Rev*, 2010. **14**(6): p. 359-69.
9. Chamlin, S.L., et al., The price of pruritus: sleep disturbance and cosleeping in atopic dermatitis. *Arch Pediatr Adolesc Med*, 2005. **159**(8): p. 745-50.
10. Stores, G., A. Burrows, and C. Crawford, Physiological sleep disturbance in children with atopic dermatitis: a case control study. *Pediatr Dermatol*, 1998. **15**(4): p. 264-8.
11. Holm, E.A., et al., Life quality assessment among patients with atopic eczema. *Br J Dermatol*, 2006. **154**(4): p. 719-25.
12. Absolon, C.M., et al., Psychological disturbance in atopic eczema: the extent of the problem in school-aged children. *Br J Dermatol*, 1997. **137**(2): p. 241-5.
13. Mitchell, A.E., et al., Parenting and childhood atopic dermatitis: A cross-sectional study of relationships between parenting behaviour, skin care management, and disease severity in young children. *Int J Nurs Stud*, 2016. **64**: p. 72-85.
14. Daud, L.R., M.E. Garralda, and T.J. David, Psychosocial adjustment in preschool children with atopic eczema. *Arch Dis Child*, 1993. **69**(6): p. 670-6.
15. Patel, K.R., et al., Association between atopic dermatitis, depression, and suicidal ideation: A systematic review and meta-analysis. *J Am Acad Dermatol*, 2019. **80**(2): p. 402-410.
16. Wadonda-Kabondo, N., et al., Association of parental eczema, hayfever, and asthma with atopic dermatitis in infancy: birth cohort study. *Arch Dis Child*, 2004. **89**(10): p. 917-21.
17. Matsuoka, S., et al., Prevalence of specific allergic diseases in school children as related to parental atopy. *Pediatr Int*, 1999. **41**(1): p. 46-51.
18. Schultz Larsen, F., Atopic dermatitis: a genetic-epidemiologic study in a population-based twin sample. *J Am Acad Dermatol*, 1993. **28**(5 Pt 1): p. 719-23.

19. Larsen, F.S., N.V. Holm, and K. Henningsen, Atopic dermatitis. A genetic-epidemiologic study in a population-based twin sample. *J Am Acad Dermatol*, 1986. **15**(3): p. 487-94.
20. Biagini Myers, J.M. and G.K. Khurana Hershey, Eczema in early life: genetics, the skin barrier, and lessons learned from birth cohort studies. *J Pediatr*, 2010. **157**(5): p. 704-14.
21. Williams, H. and C. Flohr, How epidemiology has challenged 3 prevailing concepts about atopic dermatitis. *J Allergy Clin Immunol*, 2006. **118**(1): p. 209-13.
22. Wahn, U., Wahn, U. "The immunology of fetuses and infants: What drives the allergic march. *Allergy*, 2000. **55**(7): p. 591-599.
23. Wang, I.J., et al., Effect of gestational smoke exposure on atopic dermatitis in the offspring. *Pediatr Allergy Immunol*, 2008. **19**(7): p. 580-6.
24. Schafer, T., et al., Maternal smoking during pregnancy and lactation increases the risk for atopic eczema in the offspring. *J Am Acad Dermatol*, 1997. **36**(4): p. 550-6.
25. Kramer, U., et al., The effect of environmental tobacco smoke on eczema and allergic sensitization in children. *Br J Dermatol*, 2004. **150**(1): p. 111-8.
26. LL. Muizzuddin N, M.K., Vallon P, Maes D. , Effect of cigarette smoke on skin. *J Soc Cosmet Chem*, 1997. **48**(5): p. 235-242.
27. Flohr, C., D. Pascoe, and H.C. Williams, Atopic dermatitis and the 'hygiene hypothesis': too clean to be true? *Br J Dermatol*, 2005. **152**(2): p. 202-16.
28. McNally, N.J., et al., Is there a geographical variation in eczema prevalence in the UK? Evidence from the 1958 British Birth Cohort Study. *Br J Dermatol*, 2000. **142**(4): p. 712-20.
29. McKeever, T.M., et al., Siblings, multiple births, and the incidence of allergic disease: a birth cohort study using the West Midlands general practice research database. *Thorax*, 2001. **56**(10): p. 758-62.
30. Karmaus, W. and C. Botezan, Does a higher number of siblings protect against the development of allergy and asthma? A review. *J Epidemiol Community Health*, 2002. **56**(3): p. 209-17.
31. Williams, H.C., D.P. Strachan, and R.J. Hay, Childhood eczema: disease of the advantaged? *BMJ*, 1994. **308**(6937): p. 1132-5.
32. Pickett, K.E. and R.G. Wilkinson, Income inequality and health: a causal review. *Soc Sci Med*, 2015. **128**: p. 316-26.
33. McKenzie, C., et al., The nutrition-gut microbiome-physiology axis and allergic diseases. *Immunol Rev*, 2017. **278**(1): p. 277-295.
34. Irvine, A.D. and P. Mina-Osorio, Disease trajectories in childhood atopic dermatitis: an update and practitioner's guide. *Br J Dermatol*, 2019. **181**(5): p. 895-906.
35. Prevention, C.f.D.C.a., Asthma, Most Recent National Asthma Data 2021. 2023.
36. Yang, C.L., J.M. Gaffin, and D. Radhakrishnan, Question 3: Can we diagnose asthma in children under the age of 5 years? *Paediatr Respir Rev*, 2019. **29**: p. 25-30.
37. Cave, A.J. and L.L. Atkinson, Asthma in preschool children: a review of the diagnostic challenges. *J Am Board Fam Med*, 2014. **27**(4): p. 538-48.

38. Silverberg, J.I. and J.M. Hanifin, Adult eczema prevalence and associations with asthma and other health and demographic factors: a US population-based study. *J Allergy Clin Immunol*, 2013. **132**(5): p. 1132-8.
39. Pate CA, Z.H., Qin X, Johnson C, Hummelman E, Malilay J, Asthma Surveillance — United States, 2006–2018, in *MMWR Surveill Summ* 2021. 2021. p. 1-32.
40. Brannan, J.D. and M.D. Lougheed, Airway hyperresponsiveness in asthma: mechanisms, clinical significance, and treatment. *Front Physiol*, 2012. **3**: p. 460.
41. Postma, D.S. and H.A. Kerstjens, Characteristics of airway hyperresponsiveness in asthma and chronic obstructive pulmonary disease. *Am J Respir Crit Care Med*, 1998. **158**(5 Pt 3): p. S187-92.
42. Ruan, Z., et al., Asthma susceptible genes in children: A meta-analysis. *Medicine (Baltimore)*, 2020. **99**(45): p. e23051.
43. Schauberger, E.M., et al., Identification of ATPAF1 as a novel candidate gene for asthma in children. *J Allergy Clin Immunol*, 2011. **128**(4): p. 753-760 e11.
44. Ziyab, A.H., et al., Allergic sensitization and filaggrin variants predispose to the comorbidity of eczema, asthma, and rhinitis: results from the Isle of Wight birth cohort. *Clin Exp Allergy*, 2014. **44**(9): p. 1170-8.
45. Chen, S., et al., Consistency and Variability of DNA Methylation in Women During Puberty, Young Adulthood, and Pregnancy. *Genet Epigenet*, 2017. **9**: p. 1179237X17721540.
46. Zhang, H., et al., The interplay of DNA methylation over time with Th2 pathway genetic variants on asthma risk and temporal asthma transition. *Clin Epigenetics*, 2014. **6**(1): p. 8.
47. Soto-Ramirez, N., et al., The interaction of genetic variants and DNA methylation of the interleukin-4 receptor gene increase the risk of asthma at age 18 years. *Clin Epigenetics*, 2013. **5**(1): p. 1.
48. Yousefi, M., et al., The methylation of the LEPR/LEPROT genotype at the promoter and body regions influence concentrations of leptin in girls and BMI at age 18 years if their mother smoked during pregnancy. *Int J Mol Epidemiol Genet*, 2013. **4**(2): p. 86-100.
49. Mukherjee, A.B. and Z. Zhang, Allergic asthma: influence of genetic and environmental factors. *J Biol Chem*, 2011. **286**(38): p. 32883-9.
50. von Mutius, E., Environmental factors influencing the development and progression of pediatric asthma. *J Allergy Clin Immunol*, 2002. **109**(6 Suppl): p. S525-32.
51. O'Dwyer, D.N., R.P. Dickson, and B.B. Moore, The Lung Microbiome, Immunity, and the Pathogenesis of Chronic Lung Disease. *J Immunol*, 2016. **196**(12): p. 4839-47.
52. Kozik, A.J. and Y.J. Huang, The microbiome in asthma: Role in pathogenesis, phenotype, and response to treatment. *Ann Allergy Asthma Immunol*, 2019. **122**(3): p. 270-275.
53. Martinez, F.D. and S. Guerra, Early Origins of Asthma. Role of Microbial Dysbiosis and Metabolic Dysfunction. *Am J Respir Crit Care Med*, 2018. **197**(5): p. 573-579.
54. Stokholm, J., et al., Maturation of the gut microbiome and risk of asthma in childhood. *Nat Commun*, 2018. **9**(1): p. 141.

55. Simon, A.K., G.A. Hollander, and A. McMichael, Evolution of the immune system in humans from infancy to old age. *Proc Biol Sci*, 2015. **282**(1821): p. 20143085.
56. Halkias, J., et al., CD161 contributes to prenatal immune suppression of IFN γ -producing PLZF⁺ T cells. *J Clin Invest*, 2019. **129**(9): p. 3562-3577.
57. Mishra, A., et al., Microbial exposure during early human development primes fetal immune cells. *Cell*, 2021. **184**(13): p. 3394-3409 e20.
58. Rackaityte, E., et al., Viable bacterial colonization is highly limited in the human intestine in utero. *Nat Med*, 2020. **26**(4): p. 599-607.
59. Mold, J.E., et al., Fetal and adult hematopoietic stem cells give rise to distinct T cell lineages in humans. *Science*, 2010. **330**(6011): p. 1695-9.
60. Romagnani, S., Immunologic influences on allergy and the TH1/TH2 balance. *J Allergy Clin Immunol*, 2004. **113**(3): p. 395-400.
61. Sender, R., S. Fuchs, and R. Milo, Revised Estimates for the Number of Human and Bacteria Cells in the Body. *PLoS Biol*, 2016. **14**(8): p. e1002533.
62. Clemente, J.C., et al., The impact of the gut microbiota on human health: an integrative view. *Cell*, 2012. **148**(6): p. 1258-70.
63. Statistics, N.C.f.H., Allergies and Hay Fever, United States, 2023. 2023: Hyattsville, Maryland.
64. Feehley, T., et al., Healthy infants harbor intestinal bacteria that protect against food allergy. *Nat Med*, 2019. **25**(3): p. 448-453.
65. Jota Baptista, C.V., A.I. Faustino-Rocha, and P.A. Oliveira, Animal Models in Pharmacology: A Brief History Awarding the Nobel Prizes for Physiology or Medicine. *Pharmacology*, 2021. **106**(7-8): p. 356-368.
66. Ericsson, A.C., M.J. Crim, and C.L. Franklin, A brief history of animal modeling. *Mo Med*, 2013. **110**(3): p. 201-5.
67. Laboratory, T.J. Our History. [cited 2023; Available from: <https://www.jax.org/about-us/history#nobel-prizes-et-al>].
68. Makowska, I.J. and D.M. Weary, A Good Life for Laboratory Rodents? *ILAR J*, 2021. **60**(3): p. 373-388.
69. Robinson, N.B., et al., The current state of animal models in research: A review. *Int J Surg*, 2019. **72**: p. 9-13.
70. Dominguez-Oliva, A., et al., The Importance of Animal Models in Biomedical Research: Current Insights and Applications. *Animals (Basel)*, 2023. **13**(7).
71. Swearingen, J.R., Choosing the right animal model for infectious disease research. *Animal Model Exp Med*, 2018. **1**(2): p. 100-108.
72. Nials, A.T. and S. Uddin, Mouse models of allergic asthma: acute and chronic allergen challenge. *Dis Model Mech*, 2008. **1**(4-5): p. 213-20.
73. Taube, C., A. Dakhama, and E.W. Gelfand, Insights into the pathogenesis of asthma utilizing murine models. *Int Arch Allergy Immunol*, 2004. **135**(2): p. 173-86.

74. Seyyede Masoume Athari, E.M.N., Seyyed Shamsadin Athari, Animal model of allergy and asthma; protocol for researches. Protocol Exchange, 2019.
75. Wenzel, S. and S.T. Holgate, The mouse trap: It still yields few answers in asthma. *Am J Respir Crit Care Med*, 2006. **174**(11): p. 1173-6; discussion 1176-8.
76. Kumar, R.K., C. Herbert, and P.S. Foster, The "classical" ovalbumin challenge model of asthma in mice. *Curr Drug Targets*, 2008. **9**(6): p. 485-94.
77. Huss, K., et al., House dust mite and cockroach exposure are strong risk factors for positive allergy skin test responses in the Childhood Asthma Management Program. *J Allergy Clin Immunol*, 2001. **107**(1): p. 48-54.
78. Panzner, P., et al., Cross-sectional study on sensitization to mite and cockroach allergen components in allergy patients in the Central European region. *Clin Transl Allergy*, 2018. **8**: p. 19.
79. Stefka, A.T., et al., Commensal bacteria protect against food allergen sensitization. *Proc Natl Acad Sci U S A*, 2014. **111**(36): p. 13145-50.
80. Cahenzli, J., et al., Intestinal microbial diversity during early-life colonization shapes long-term IgE levels. *Cell Host Microbe*, 2013. **14**(5): p. 559-70.
81. Herbst, T., et al., Dysregulation of allergic airway inflammation in the absence of microbial colonization. *Am J Respir Crit Care Med*, 2011. **184**(2): p. 198-205.
82. Wang, Y., et al., A study on the method and effect of the construction of a humanized mouse model of fecal microbiota transplantation. *Front Microbiol*, 2022. **13**: p. 1031758.
83. Shimbori, C., et al., Gut bacteria interact directly with colonic mast cells in a humanized mouse model of IBS. *Gut Microbes*, 2022. **14**(1): p. 2105095.
84. Park, J.C. and S.H. Im, Of men in mice: the development and application of a humanized gnotobiotic mouse model for microbiome therapeutics. *Exp Mol Med*, 2020. **52**(9): p. 1383-1396.
85. Wrzosek, L., et al., Transplantation of human microbiota into conventional mice durably reshapes the gut microbiota. *Sci Rep*, 2018. **8**(1): p. 6854.
86. Eiseman, B., et al., Fecal enema as an adjunct in the treatment of pseudomembranous enterocolitis. *Surgery*, 1958. **44**(5): p. 854-9.
87. Kumar, V. and M. Fischer, Expert opinion on fecal microbiota transplantation for the treatment of *Clostridioides difficile* infection and beyond. *Expert Opin Biol Ther*, 2020. **20**(1): p. 73-81.
88. Aroniadis, O.C. and L.J. Brandt, Fecal microbiota transplantation: past, present and future. *Curr Opin Gastroenterol*, 2013. **29**(1): p. 79-84.
89. Weingarden, A.R. and B.P. Vaughn, Intestinal microbiota, fecal microbiota transplantation, and inflammatory bowel disease. *Gut Microbes*, 2017. **8**(3): p. 238-252.
90. Leonardi, I., et al., Fungal Trans-kingdom Dynamics Linked to Responsiveness to Fecal Microbiota Transplantation (FMT) Therapy in Ulcerative Colitis. *Cell Host Microbe*, 2020. **27**(5): p. 823-829 e3.

91. Dhamoon, J.J.P.A.S., Physiology, Digestion. 2023, Treasure Island, FL: StatPearls Publishing.
92. Oliphant, K. and E. Allen-Vercoe, Macronutrient metabolism by the human gut microbiome: major fermentation by-products and their impact on host health. *Microbiome*, 2019. **7**(1): p. 91.
93. Culp, E.J. and A.L. Goodman, Cross-feeding in the gut microbiome: Ecology and mechanisms. *Cell Host Microbe*, 2023. **31**(4): p. 485-499.
94. Germerodt, S., et al., Pervasive Selection for Cooperative Cross-Feeding in Bacterial Communities. *PLoS Comput Biol*, 2016. **12**(6): p. e1004986.
95. Hill, M.J., Intestinal flora and endogenous vitamin synthesis. *Eur J Cancer Prev*, 1997. **6 Suppl 1**: p. S43-5.
96. Rowland, I., et al., Gut microbiota functions: metabolism of nutrients and other food components. *Eur J Nutr*, 2018. **57**(1): p. 1-24.
97. Kim, C.H., Immune regulation by microbiome metabolites. *Immunology*, 2018. **154**(2): p. 220-229.
98. Macfarlane, S. and G.T. Macfarlane, Regulation of short-chain fatty acid production. *Proc Nutr Soc*, 2003. **62**(1): p. 67-72.
99. Tan, J., et al., Dietary Fiber and Bacterial SCFA Enhance Oral Tolerance and Protect against Food Allergy through Diverse Cellular Pathways. *Cell Rep*, 2016. **15**(12): p. 2809-24.
100. Depner, M., et al., Maturation of the gut microbiome during the first year of life contributes to the protective farm effect on childhood asthma. *Nat Med*, 2020. **26**(11): p. 1766-1775.
101. Thorburn, A.N., et al., Evidence that asthma is a developmental origin disease influenced by maternal diet and bacterial metabolites. *Nat Commun*, 2015. **6**: p. 7320.
102. Roduit, C., et al., High levels of butyrate and propionate in early life are associated with protection against atopy. *Allergy*, 2019. **74**(4): p. 799-809.
103. Crestani, E., et al., Untargeted metabolomic profiling identifies disease-specific signatures in food allergy and asthma. *J Allergy Clin Immunol*, 2020. **145**(3): p. 897-906.
104. Nakada, E.M., et al., Conjugated bile acids attenuate allergen-induced airway inflammation and hyperresponsiveness by inhibiting UPR transducers. *JCI Insight*, 2019. **4**(9).
105. Willart, M.A., et al., Ursodeoxycholic acid suppresses eosinophilic airway inflammation by inhibiting the function of dendritic cells through the nuclear farnesoid X receptor. *Allergy*, 2012. **67**(12): p. 1501-10.
106. Yamazaki, K., et al., Ursodeoxycholic acid inhibits eosinophil degranulation in patients with primary biliary cirrhosis. *Hepatology*, 1999. **30**(1): p. 71-8.
107. Turi, K.N., et al., Unconjugated bilirubin is associated with protection from early-life wheeze and childhood asthma. *J Allergy Clin Immunol*, 2021. **148**(1): p. 128-138.

108. van der Sluijs, K.F., et al., Systemic tryptophan and kynurenine catabolite levels relate to severity of rhinovirus-induced asthma exacerbation: a prospective study with a parallel-group design. *Thorax*, 2013. **68**(12): p. 1122-30.
109. Hu, Y., et al., Decreased expression of indolamine 2,3-dioxygenase in childhood allergic asthma and its inverse correlation with fractional concentration of exhaled nitric oxide. *Ann Allergy Asthma Immunol*, 2017. **119**(5): p. 429-434.
110. Unuvar, S., et al., Neopterin Levels and Indoleamine 2,3-Dioxygenase Activity as Biomarkers of Immune System Activation and Childhood Allergic Diseases. *Ann Lab Med*, 2019. **39**(3): p. 284-290.
111. Finkelstein, R.A., H.T. Norris, and N.K. Dutta, Pathogenesis Experimental Cholera in Infant Rabbits. I. Observations on the Intraintestinal Infection and Experimental Cholera Produced with Cell-Free Products. *J Infect Dis*, 1964. **114**: p. 203-16.
112. Scheutz, F., et al., Multicenter evaluation of a sequence-based protocol for subtyping Shiga toxins and standardizing Stx nomenclature. *J Clin Microbiol*, 2012. **50**(9): p. 2951-63.
113. Schiavo, G., et al., Botulinum neurotoxins are zinc proteins. *J Biol Chem*, 1992. **267**(33): p. 23479-83.
114. Fujimura, K.E., et al., Neonatal gut microbiota associates with childhood multisensitized atopy and T cell differentiation. *Nat Med*, 2016. **22**(10): p. 1187-1191.
115. Levan, S.R., et al., Elevated faecal 12,13-diHOME concentration in neonates at high risk for asthma is produced by gut bacteria and impedes immune tolerance. *Nat Microbiol*, 2019. **4**(11): p. 1851-1861.
116. Gould, H.J. and Y.B. Wu, IgE repertoire and immunological memory: compartmental regulation and antibody function. *Int Immunol*, 2018. **30**(9): p. 403-412.
117. Sanchez-Jimenez, F., et al., Pharmacological potential of biogenic amine-polyamine interactions beyond neurotransmission. *Br J Pharmacol*, 2013. **170**(1): p. 4-16.
118. Stiemsma, L.T. and S.E. Turvey, Asthma and the microbiome: defining the critical window in early life. *Allergy Asthma Clin Immunol*, 2017. **13**: p. 3.
119. Riedler, J., et al., Exposure to farming in early life and development of asthma and allergy: a cross-sectional survey. *Lancet*, 2001. **358**(9288): p. 1129-33.
120. Ege, M.J., et al., Exposure to environmental microorganisms and childhood asthma. *N Engl J Med*, 2011. **364**(8): p. 701-9.
121. Olszak, T., et al., Microbial exposure during early life has persistent effects on natural killer T cell function. *Science*, 2012. **336**(6080): p. 489-93.
122. Zuccotti, G., et al., Probiotics for prevention of atopic diseases in infants: systematic review and meta-analysis. *Allergy*, 2015. **70**(11): p. 1356-71.
123. Ichinohe, T., et al., Microbiota regulates immune defense against respiratory tract influenza A virus infection. *Proc Natl Acad Sci U S A*, 2011. **108**(13): p. 5354-9.
124. Spergel, J.M. and A.S. Paller, Atopic dermatitis and the atopic march. *J Allergy Clin Immunol*, 2003. **112**(6 Suppl): p. S118-27.

125. von Kobyletzki LB, B.C., Hasselgren M, Larsson M, Lindström CB, Svensson Å, Eczema in early childhood is strongly associated with the development of asthma and rhinitis in a prospective cohort. *BMC Dermatol*, 2012. **12**(11).
126. Abrahamsson, T.R., et al., Low diversity of the gut microbiota in infants with atopic eczema. *J Allergy Clin Immunol*, 2012. **129**(2): p. 434-40, 440 e1-2.
127. Abrahamsson, T.R., et al., Low gut microbiota diversity in early infancy precedes asthma at school age. *Clin Exp Allergy*, 2014. **44**(6): p. 842-50.
128. Tariq, S.M., et al., The prevalence of and risk factors for atopy in early childhood: a whole population birth cohort study. *J Allergy Clin Immunol*, 1998. **101**(5): p. 587-93.
129. Arshad, S.H., et al., Cohort Profile: The Isle Of Wight Whole Population Birth Cohort (IOWBC). *Int J Epidemiol*, 2018. **47**(4): p. 1043-1044i.
130. Arshad, S.H., et al., Cohort Profile Update: The Isle of Wight Whole Population Birth Cohort (IOWBC). *Int J Epidemiol*, 2020. **49**(4): p. 1083-1084.
131. Becker AB, A.E., Asthma guidelines: the Global Initiative for Asthma in relation to national guideline. *Curr Opin Allergy Clin Immunol*, 2017. **17**(2): p. 99-103.
132. Sadeghnejad A, K.W., Davis S, Kurukulaaratchy RJ, Matthews S, Arshad SH, Raised cord serum immunoglobulin E increases the risk of allergic sensitisation at ages 4 and 10 and asthma at age 10. *Thorax*, 2004. **59**(11): p. 936-942.
133. Severity scoring of atopic dermatitis: the SCORAD index. Consensus Report of the European Task Force on Atopic Dermatitis. *Dermatology*, 1993. **186**(1): p. 23-31.
134. Asher, M.I., et al., International Study of Asthma and Allergies in Childhood (ISAAC): rationale and methods. *Eur Respir J*, 1995. **8**(3): p. 483-91.
135. Patil, V.K., et al., Interaction of prenatal maternal smoking, interleukin 13 genetic variants and DNA methylation influencing airflow and airway reactivity. *Clin Epigenetics*, 2013. **5**(1): p. 22.
136. Soto-Ramirez, N., et al., Modes of infant feeding and the occurrence of coughing/wheezing in the first year of life. *J Hum Lact*, 2013. **29**(1): p. 71-80.
137. Karmaus, W., et al., Long-term effects of breastfeeding, maternal smoking during pregnancy, and recurrent lower respiratory tract infections on asthma in children. *J Asthma*, 2008. **45**(8): p. 688-95.
138. Brooks, P.T., et al., Transplanted human fecal microbiota enhanced Guillain Barre syndrome autoantibody responses after *Campylobacter jejuni* infection in C57BL/6 mice. *Microbiome*, 2017. **5**(1): p. 92.
139. Hall, M. and R.G. Beiko, 16S rRNA Gene Analysis with QIIME2. *Methods Mol Biol*, 2018. **1849**: p. 113-129.
140. Amir, A., et al., Deblur Rapidly Resolves Single-Nucleotide Community Sequence Patterns. *mSystems*, 2017. **2**(2).
141. Rognes, T., et al., VSEARCH: a versatile open source tool for metagenomics. *PeerJ*, 2016. **4**: p. e2584.

142. Santos, T., et al., Use of MALDI-TOF mass spectrometry fingerprinting to characterize *Enterococcus* spp. and *Escherichia coli* isolates. *J Proteomics*, 2015. **127**(Pt B): p. 321-31.
143. Team, R.C., R: A Language and Environment for Statistical Computing. 2020, R Foundation for Statistical Computing: Vienna, Austria.
144. SAS Institute Inc. SAS and all other SAS Institute Inc. product or service names are registered trademarks or trademarks of SAS Institute Inc., C., NC, USA.
145. Sbihi, H., et al., Thinking bigger: How early-life environmental exposures shape the gut microbiome and influence the development of asthma and allergic disease. *Allergy*, 2019. **74**(11): p. 2103-2115.
146. Bisgaard, H., et al., Childhood asthma after bacterial colonization of the airway in neonates. *N Engl J Med*, 2007. **357**(15): p. 1487-95.
147. Hilty, M., et al., Disordered microbial communities in asthmatic airways. *PLoS One*, 2010. **5**(1): p. e8578.
148. Lal, C.V., et al., The Airway Microbiome at Birth. *Sci Rep*, 2016. **6**: p. 31023.
149. Lynch, S.V., et al., Effects of early-life exposure to allergens and bacteria on recurrent wheeze and atopy in urban children. *J Allergy Clin Immunol*, 2014. **134**(3): p. 593-601 e12.
150. Penders, J., et al., Establishment of the intestinal microbiota and its role for atopic dermatitis in early childhood. *J Allergy Clin Immunol*, 2013. **132**(3): p. 601-607 e8.
151. Louisa Owens, I.A.L., Guicheng Zhang, Stephen Turner & Peter N Le Souëf, Prevalence of allergic sensitization, hay fever, eczema, and asthma in a longitudinal birth cohort. *Journal of Asthma and Allergy*, 2018. **11**: p. 173-180.
152. Ta, L.D.H., et al., A compromised developmental trajectory of the infant gut microbiome and metabolome in atopic eczema. *Gut Microbes*, 2020. **12**(1): p. 1-22.
153. Sher, A.A., et al., Conjugative RP4 Plasmid-Mediated Transfer of Antibiotic Resistance Genes to Commensal and Multidrug-Resistant Enteric Bacteria In Vitro. *Microorganisms*, 2023. **11**(1).
154. Jolley, K.A., J.E. Bray, and M.C.J. Maiden, Open-access bacterial population genomics: BIGSdb software, the PubMLST.org website and their applications. *Wellcome Open Res*, 2018. **3**: p. 124.
155. Zhou, Z., et al., The Enterobase user's guide, with case studies on *Salmonella* transmissions, *Yersinia pestis* phylogeny, and *Escherichia* core genomic diversity. *Genome Res*, 2020. **30**(1): p. 138-152.
156. Könönen, E., 250 - Anaerobic Cocci and Anaerobic Gram-Positive Nonsporulating Bacilli. 8 ed. Mandell, Douglas, and Bennett's Principles and Practice of Infectious Diseases, ed. R.D. John E. Bennett, Martin J. Blaser. Vol. 2. 2015.
157. Berenger, B.M., et al., Anaerobic urinary tract infection caused by *Veillonella parvula* identified using cystine-lactose-electrolyte deficient media and matrix-assisted laser desorption ionization-time of flight mass spectrometry. *IDCases*, 2015. **2**(2): p. 44-6.
158. Ito, Y., et al., The first case of *Veillonella atypica* bacteremia in a patient with renal pelvic tumor. *Anaerobe*, 2022. **73**: p. 102491.

159. Andréanne Morin, C.G.M., Casper-Emil T. Pedersen, Jakob Stokholm, Bo L. Chawes, Ann-Marie Malby Schoos, Katherine A. Naughton, Jonathan Thorsen, Martin S. Mortensen, Donata Vercelli, Urvis Trivedi, Søren J. Sørensen, Hans Bisgaard, Dan L. Nicolae, Klaus Bønnelykke, Carole Ober, Epigenetic landscape links upper airway microbiota in infancy with allergic rhinitis at 6 years of age. *Journal of Allergy and Clinical Immunology*, 2020. **146**(6): p. 1358-1366.
160. Salameh, M., et al., The role of gut microbiota in atopic asthma and allergy, implications in the understanding of disease pathogenesis. *Scand J Immunol*, 2020. **91**(3): p. e12855.
161. Zheng, H., et al., Altered Gut Microbiota Composition Associated with Eczema in Infants. *PLoS One*, 2016. **11**(11): p. e0166026.
162. Centers for Disease, C.a.P., Most recent National Asthma Data. 2019(Last updated May, 2019).
163. Ziyab, A.H., et al., DNA methylation of the filaggrin gene adds to the risk of eczema associated with loss-of-function variants. *J Eur Acad Dermatol Venereol*, 2013. **27**(3): p. e420-3.
164. Ziyab, A.H., et al., Association of filaggrin variants with asthma and rhinitis: is eczema or allergic sensitization status an effect modifier? *Int Arch Allergy Immunol*, 2014. **164**(4): p. 308-18.
165. Arshad, S.H., et al., Cohort Profile Update: The Isle of Wight Whole Population Birth Cohort (IOWBC). *Int J Epidemiol*, 2020.
166. Adami, A.J. and S.J. Bracken, Breathing Better Through Bugs: Asthma and the Microbiome. *Yale J Biol Med*, 2016. **89**(3): p. 309-324.
167. Wu, Z.X., et al., Prenatal and early, but not late, postnatal exposure of mice to sidestream tobacco smoke increases airway hyperresponsiveness later in life. *Environ Health Perspect*, 2009. **117**(9): p. 1434-40.
168. Chapman, D.G. and C.G. Irvin, Mechanisms of airway hyper-responsiveness in asthma: the past, present and yet to come. *Clin Exp Allergy*, 2015. **45**(4): p. 706-19.
169. Ito, J.T., et al., Extracellular Matrix Component Remodeling in Respiratory Diseases: What Has Been Found in Clinical and Experimental Studies? *Cells*, 2019. **8**(4).
170. Biesbroek, G., et al., Early respiratory microbiota composition determines bacterial succession patterns and respiratory health in children. *Am J Respir Crit Care Med*, 2014. **190**(11): p. 1283-92.
171. Teo, S.M., et al., The infant nasopharyngeal microbiome impacts severity of lower respiratory infection and risk of asthma development. *Cell Host Microbe*, 2015. **17**(5): p. 704-15.
172. Bisgaard, H., et al., Reduced diversity of the intestinal microbiota during infancy is associated with increased risk of allergic disease at school age. *J Allergy Clin Immunol*, 2011. **128**(3): p. 646-52 e1-5.
173. Fujimura, K.E., et al., House dust exposure mediates gut microbiome *Lactobacillus* enrichment and airway immune defense against allergens and virus infection. *Proc Natl Acad Sci U S A*, 2014. **111**(2): p. 805-10.

174. Huang, Y.J. and H.A. Boushey, The microbiome in asthma. *J Allergy Clin Immunol*, 2015. **135**(1): p. 25-30.
175. Kong, H.H., et al., Temporal shifts in the skin microbiome associated with disease flares and treatment in children with atopic dermatitis. *Genome Res*, 2012. **22**(5): p. 850-9.
176. Collins, J., et al., Humanized microbiota mice as a model of recurrent *Clostridium difficile* disease. *Microbiome*, 2015. **3**: p. 35.
177. Directors, A.B.o., Guidelines for Methacholine and Exercise Challenge Testing—1999. American Thoracic Society 1999.
178. Woo, L.N., et al., A 4-Week Model of House Dust Mite (HDM) Induced Allergic Airways Inflammation with Airway Remodeling. *Sci Rep*, 2018. **8**(1): p. 6925.
179. Gandhi, V.D., et al., House dust mite interactions with airway epithelium: role in allergic airway inflammation. *Curr Allergy Asthma Rep*, 2013. **13**(3): p. 262-70.
180. Brown, T.A., et al., Early life microbiome perturbation alters pulmonary responses to ozone in male mice. *Physiol Rep*, 2020. **8**(2): p. e14290.
181. Lommatzsch, M., Airway hyperresponsiveness: new insights into the pathogenesis. *Semin Respir Crit Care Med*, 2012. **33**(6): p. 579-87.
182. Ver Heul, A., J. Planer, and A.L. Kau, The Human Microbiota and Asthma. *Clin Rev Allergy Immunol*, 2019. **57**(3): p. 350-363.
183. Bonaz, B., T. Bazin, and S. Pellissier, The Vagus Nerve at the Interface of the Microbiota-Gut-Brain Axis. *Front Neurosci*, 2018. **12**: p. 49.
184. Trompette, A., et al., Gut microbiota metabolism of dietary fiber influences allergic airway disease and hematopoiesis. *Nat Med*, 2014. **20**(2): p. 159-66.
185. Vanoirbeek, J.A., et al., Noninvasive and invasive pulmonary function in mouse models of obstructive and restrictive respiratory diseases. *Am J Respir Cell Mol Biol*, 2010. **42**(1): p. 96-104.
186. Patel, K.R., et al., Mast cell-derived neurotrophin 4 mediates allergen-induced airway hyperinnervation in early life. *Mucosal Immunol*, 2016. **9**(6): p. 1466-1476.
187. Patel, K.R., et al., Targeting acetylcholine receptor M3 prevents the progression of airway hyperreactivity in a mouse model of childhood asthma. *FASEB J*, 2017. **31**(10): p. 4335-4346.
188. Bonvini, S.J., et al., Novel airway smooth muscle-mast cell interactions and a role for the TRPV4-ATP axis in non-atopic asthma. *Eur Respir J*, 2020. **56**(1).
189. Mendez-Enriquez, E. and J. Hallgren, Mast Cells and Their Progenitors in Allergic Asthma. *Front Immunol*, 2019. **10**: p. 821.
190. Traina, G., Mast Cells in Gut and Brain and Their Potential Role as an Emerging Therapeutic Target for Neural Diseases. *Front Cell Neurosci*, 2019. **13**: p. 345.
191. Team, R.C., A language and environment for statistical computing. 2020.

192. Mansfield, L.S., et al., C57BL/6 and congenic interleukin-10-deficient mice can serve as models of *Campylobacter jejuni* colonization and enteritis. *Infect Immun*, 2007. **75**(3): p. 1099-115.
193. Nault, R., et al., Development of a computational high-throughput tool for the quantitative examination of dose-dependent histological features. *Toxicol Pathol*, 2015. **43**(3): p. 366-75.
194. Kujur, W., et al., Caerulomycin A inhibits Th2 cell activity: a possible role in the management of asthma. *Sci Rep*, 2015. **5**: p. 15396.
195. Adami, A.J., et al., Early-life antibiotics attenuate regulatory T cell generation and increase the severity of murine house dust mite-induced asthma. *Pediatr Res*, 2018. **84**(3): p. 426-434.
196. Lee, K.S., et al., Inhibition of phosphoinositide 3-kinase delta attenuates allergic airway inflammation and hyperresponsiveness in murine asthma model. *FASEB J*, 2006. **20**(3): p. 455-65.
197. Kwak, Y.G., et al., Involvement of PTEN in airway hyperresponsiveness and inflammation in bronchial asthma. *J Clin Invest*, 2003. **111**(7): p. 1083-92.
198. Zaiss, M.M., et al., The Intestinal Microbiota Contributes to the Ability of Helminths to Modulate Allergic Inflammation. *Immunity*, 2015. **43**(5): p. 998-1010.
199. McCullagh, P. and J.A. Nelder, *Generalized Linear Models*. Second Edition. 1989, London: Chapman and Hall.
200. Penders, J., et al., The role of the intestinal microbiota in the development of atopic disorders. *Allergy*, 2007. **62**(11): p. 1223-36.
201. Zheng, P., et al., Gut Microbiome and Metabolomics Profiles of Allergic and Non-Allergic Childhood Asthma. *J Asthma Allergy*, 2022. **15**: p. 419-435.
202. Hinako Terauchi, J.A.B., Yu Jiang, Hongmei Zhang, Phillip T. Brooks, Samantha Waite, John W. Holloway, Wilfried Karmaus, Susan L. Ewart, S. Hasan Arshad, Linda S. Mansfield, Predominance of *Veillonella* and other allergy agonists in 3-month-old infant gut microbiota was associated with development of eczema in early childhood in the Isle of Wight Birth Cohort. 2023: In Review at PLOS ONE.
203. Lee-Sarwar, K., et al., Association of the gut microbiome and metabolome with wheeze frequency in childhood asthma. *J Allergy Clin Immunol*, 2022. **150**(2): p. 325-336.
204. Ivon Moya Uribe, H.T., Julia A. Bell, Alexander Zanetti, Sanket Jantre, Marianne Huebner, S. Hasan Arshad, Susan L. Ewart, Linda S. Mansfield, Fecal microbiota transplants of three distinct human communities to germ-free mice exacerbated inflammation and decreased lung function in their offspring. 2023: In Review for mBio.
205. Stagliano, M.C., et al., Bioassay-directed fractionation for discovery of bioactive neutral lipids guided by relative mass defect filtering and multiplexed collision-induced dissociation. *Rapid Commun Mass Spectrom*, 2010. **24**(24): p. 3578-84.

206. Ekanayaka, E.A., M.D. Celiz, and A.D. Jones, Relative mass defect filtering of mass spectra: a path to discovery of plant specialized metabolites. *Plant Physiol*, 2015. **167**(4): p. 1221-32.
207. Wishart, D., et al., T3DB: the toxic exposome database. *Nucleic Acids Res*, 2015. **43**(Database issue): p. D928-34.
208. Lim, E., et al., T3DB: a comprehensively annotated database of common toxins and their targets. *Nucleic Acids Res*, 2010. **38**(Database issue): p. D781-6.
209. Wikoff, W.R., et al., Metabolomics analysis reveals large effects of gut microflora on mammalian blood metabolites. *Proc Natl Acad Sci U S A*, 2009. **106**(10): p. 3698-703.
210. Wishart, D.S., et al., HMDB 5.0: the Human Metabolome Database for 2022. *Nucleic Acids Res*, 2022. **50**(D1): p. D622-D631.
211. Wishart, D.S., et al., HMDB 4.0: the human metabolome database for 2018. *Nucleic Acids Res*, 2018. **46**(D1): p. D608-D617.
212. Wishart, D.S., et al., HMDB 3.0--The Human Metabolome Database in 2013. *Nucleic Acids Res*, 2013. **41**(Database issue): p. D801-7.
213. Wishart, D.S., et al., HMDB: a knowledgebase for the human metabolome. *Nucleic Acids Res*, 2009. **37**(Database issue): p. D603-10.
214. Wishart, D.S., et al., HMDB: the Human Metabolome Database. *Nucleic Acids Res*, 2007. **35**(Database issue): p. D521-6.
215. Marver, D. and I.S. Edelman, Dihydrocortisol: a potential mineralocorticoid. *J Steroid Biochem*, 1978. **9**(1): p. 1-7.
216. Tarantola, M., et al., Beef cattle welfare assessment: use of resource and animal-based indicators, blood parameters and hair 20 β -dihydrocortisol. *Italian Journal of Animal Science*, 2020. **19**(1): p. 341-350.
217. Nomura, A., et al., Relationship between gut microbiota composition and sensitization to inhaled allergens. *Allergol Int*, 2020. **69**(3): p. 437-442.
218. Mutlu, E.A., et al., Inhalational exposure to particulate matter air pollution alters the composition of the gut microbiome. *Environ Pollut*, 2018. **240**: p. 817-830.
219. Yamaguchi, T., et al., Effect of gut microbial composition and diversity on major inhaled allergen sensitization and onset of allergic rhinitis. *Allergol Int*, 2023. **72**(1): p. 135-142.
220. Borbet, T.C., et al., Influence of the early-life gut microbiota on the immune responses to an inhaled allergen. *Mucosal Immunol*, 2022. **15**(5): p. 1000-1011.
221. Scalbert, A., et al., Mass-spectrometry-based metabolomics: limitations and recommendations for future progress with particular focus on nutrition research. *Metabolomics*, 2009. **5**(4): p. 435-458.
222. Chen, J., et al., Spatiotemporal modeling of microbial metabolism. *BMC Syst Biol*, 2016. **10**: p. 21.
223. Saa, P., et al., Modeling approaches for probing cross-feeding interactions in the human gut microbiome. *Comput Struct Biotechnol J*, 2022. **20**: p. 79-89.

CHAPTER 5: Conclusions and future directions

Allergy affects nearly third of the adult population and over quarter of child population in the United States[5]. Eczema, or atopic dermatitis, is a chronic skin allergic condition affecting over 10% of the total population of children in the US[5], where the majority of cases (60%) develop within the first year of life[6]. Despite not being life-threatening on its own, eczema is known to have significant impact on the quality of life throughout childhood and adolescence if the disease persists [7, 8, 10-12, 14, 15]. Most children diagnosed with eczema in early childhood is believed to “outgrow” the condition with age by current clinical consensus, however it has been observed that those who do not “outgrow” the condition are more likely to develop additional allergic comorbidities such as severe eczema and allergic asthma with age in a phenomenon named “atopic march”[34]. Asthma is a chronic airway disease affecting 6.5% of children in the US[36], and is characterized by wheezing, shortness of breath, coughing, chest tightness, and difficulty breathing[1]. Allergic asthma is a subtype of asthma where symptoms are aggravated by exposure to allergens[1], and is commonly associated with Type 2 immune response[61].

Given the phenomenon of atopic march combined with observations of early life environment affecting the risk of allergy development[27-29, 55], education of the early system has been suggested to play an important role in the susceptibility to developing allergy. Early immune system is educated through exposures to environmental antigens, many of which are microbial species that gets ingested by the infant that becomes commensal residents of their gut microbiota[56]. Gut microbiota has been associated with a wide array of pathologies and diseases, both allergic and non-allergic, in humans[63]. Although the exact etiology remains unknown, in case of allergic disease development, gut microbiome composition during the first year of life is thought to have a significant impact[54, 55]. Many studies have identified an association with either a specific bacterial taxon, or a collection of bacterial taxa especially within the first year of life, with development of allergic diseases[3, 4, 65]. Other studies have sought to explore the possible molecular mechanism of how the gut microbiota can affect allergy development by focusing on the gut metabolome[2, 33, 99, 102]. Given these previous studies, we sought to further close the gap of knowledge on how a gut composition of both bacteria and their metabolites are influencing allergy development. We hypothesized that specific compositions of the gut microbiota and the gut metabolome affect the development of allergy. Both a human infant allergy cohort and a mouse model of asthma were utilized to address this

question.

First using the Isle of Wight infant allergy cohort, we tested the hypothesis that a particular composition of the early life gut microbiota is associated with the development of eczema and atopy in infants. Out of the 56 infants used in this study, 18 were graded to have “persistent” eczema, 21 to have “Intermediate” eczema, and 17 to have “None” based on the number of eczema diagnosis in the first 36 months of their life. Upon analyzing their gut microbiota obtained with 16SV4 rRNA amplicon sequencing, several previously allergy-associated taxa (*Bifidobacterium*, *Escherichia-Shigella*, *Prevotella*, and *Veillonella*) were identified as major contributors to the differences in the gut microbiota between the clinical groups. *Bifidobacterium* and *Escherichia-Shigella* were further identified as having the most importance in differentiating between a group with higher prevalence of both eczema and atopy diagnosis from another group with less allergy prevalence. Atopy was also found to strengthen the correlation between eczema diagnosis and microbiota composition. Finally, *Veillonella* was identified as having statistically significant association with eczema status at 3 months of age. This study confirmed the relevance of certain bacterial taxa in their relation to allergy in infancy and early childhood. Bacterial taxa previously associated with allergy in other cohorts were also observed to differentiate those with allergy and those without. These results suggests the need to further explore these bacterial species for their involvement in allergy development. The relatively small sample size along with a higher variability characteristic of human studies did provide some challenges and limitation in computations of statistical significance. There still lies a strength in the use of this cohort, given its longitudinal and multi-generational aspect, allowing for additional follow up analyses of the same infants studied here. At the time of this study, the infants had yet to reach an age where they can be accurately diagnosed with asthma[37, 38]. Revisitation of the same cohort past their early infancy will provide value to further explore the shift in their gut microbiome with age, and additional clinical diagnoses will allow for the exploration of the microbial effects on atopic march. Variability introduced by uncontrolled environmental factors is a nature of human subject studies, which can be accommodated by using an animal model.

A mouse model of asthma was developed to further study the effect of specific gut microbiota composition on allergic phenotypes. The infant fecal samples used and analyzed from the Isle of Wight allergy cohort discussed in the previous section were transplanted into germ-

free C57BL/6 mice to create A) mice with allergy-prone gut microbiome, and B) mice with allergy-averse gut microbiome. Upon successful fecal-transplantation and breeding of the transplanted mice, the two new infant-based mouse groups were used to test our hypothesis that *Enterobacteriaceae*-dominant gut microbiota from eczemic infants will cause increased T helper 2 (Type 2) inflammation and decreased lung function after house dust mite antigen (HDM) exposure in the transplanted mice, while *Bacteroidaceae*-dominant gut microbiota from non-eczemic infants will be protective. The mice transplanted with fecal samples of select infants with “Persistent” eczema diagnosis and *Enterobacteriaceae*-dominance in the gut microbiota was named “InfantA,” while the mice transplanted with fecal samples of select infants with no eczema diagnosis and *Bacteroidaceae*-dominance in the gut microbiota was named “InfantB.” These two groups were compared to a positive control group named “AdultC,” a previously established Th-2 prone fecal-transplanted mice [140], and a negative control group with untouched, conventional mouse microbiota named “Mouse.” Despite receiving a fecal transplant from infants lacking allergy, “InfantB” mouse group showed a decrease in lung functions and an increase in airway hyper-responsiveness (AHR) alongside “InfantA” and “AdultC” groups, in comparison to the conventional “Mouse” group. The impairment of lung functions was seen in all three humanized gut microbiota mouse groups without any treatment with an allergen, suggesting that carrying of a humanized gut microbiota lead to the lowered lung functions. In addition, treatment with an allergen (HDM) increased AHR in all three humanized gut microbiota mouse groups compared to the conventional mouse group. Immuno- and histopathological analyses performed did not identify any inflammatory characteristics to be statistically significant, although elevated in the three humanized gut microbiota mice.

Albeit the expressions of similar phenotypes, gut microbiota compositions of these mice were shown to be distinct between all four groups based on 16S amplicon sequencing data. All three humanized gut microbiota mouse groups carried varying set of bacterial taxa previously associated with allergy and inflammation. “InfantA” carried *Bacteroides*, *Lachnospiraceae*, *Turicibacter*, *Clostridium*, *Escherichia coli/Shigella*, *Coprobacter*, *Lachnoclostridium*, *Klebsiella*, *Haemophilus*. “InfantB” carried *Bacteroides*, *Lachnospiraceae*, *Alistipes*, *Turicibacter*, *Clostridium*, *Parabacteroides*, *Sutterella*, *Parasutterella*, *Haemophilus*, and *Veillonella*. “AdultC” carried *Bacteroides*, *Lachnospiraceae*, *Turicibacter*, *Parabacteroides*, *Alistipes*, *Ruminiclostridium*, *Sutterella*, *Parasutterella* and *Haemophilus*. On the other hand,

“Mouse” group carried a set of unique bacterial taxa previously associated with protection from allergy: *Clostridia (Clostridiales)*, *Faecalibacterium*, and *Ruminococcus-Coprococcus*. The lack of statistically significant measured inflammatory responses is most likely due to the use of acute sensitization protocol, with its relatively short sensitization period did not allow for the full development of adaptive immune response[180]. The allergen exposed mice in this experiment still displayed significant changes in the baseline lung functions as well as allergen induced AHR, thus making them a viable mouse model of asthma with humanized gut microbiota. Testing of repeatability of this result with longer sensitization would extend the comparative relevance of this model to the chronic nature of asthma, although the limitation arising from chronic sensitization models should also be noted[73]. The similarities of phenotype among the three humanized gut microbiota mouse groups suggests that disease phenotypes are not induced by a singular bacterial taxon, but rather, a combination of multiple bacterial taxa which may differ by individual. Further characterization of the commonalities and differences of these microbiota compositions between varying disease phenotypes is needed to understand the possible mechanisms in which a select group of bacterial taxa could affect the host disease phenotypes. Methods such as whole genome sequencing followed by culturing will aid in species-level identification of bacteria, which will allow more insight into the mechanistic interactions of the microbiome and the host. The differences in the bacterial composition of the three humanized gut microbiota mice also suggests the possibility that it is not the presence of specific bacterial taxa that affect the host disease phenotype, but rather what is produced within the gut. This question can be addressed by measuring the gut metabolite contents using proteomics tools such as mass-spectrometry.

Based on the microbiome analyses of both the infants from Isle of Wight allergy cohort and the humanized mouse models of asthma, we decided to pursue the search for the underlying mechanisms of association between an allergic/asthmatic phenotype and the gut microbiome using metabolomics and liquid chromatography-mass spectrometry. We hypothesized that there are distinct differences in the metabolite profiles between groups expressing a disease phenotype compared to the groups that did not. In analyzing the samples from Isle of Wight allergy cohort, the metabolite profiles were most distinct between the infants with “Persistent” eczema and infants having “None” of eczema diagnoses; a difference characterized by 113 unique metabolites. Within the 113 metabolites, hippuric acid and dihydrocortisol were identified to be

higher in the “None” group, with statistically significance ($p < 0.05$) in both mean and median abundance value. Two more metabolites, Asn-Ser-Thr and $C_{16}H_{26}N_6O_5$, were also identified to be statistically significant ($p < 0.05$), but this time higher in the “Persistent” group. Analyses of the ceca samples from the mouse model of asthma study also revealed that the gut metabolite profiles were significantly distinct by the microbiota groups. Each of the three humanized gut microbiota mouse groups were significantly distinct to the conventional mouse group in their metabolite profiles, with over 600 to 1000 unique metabolites characterizing these differences. The HDM-treatment also significantly altered the gut metabolite profiles compared to the sham (PBS)-treatment. Each microbiota grouping had a set of unique metabolites in distinct abundances between the HDM- and PBS-treated groups that were statistically significant, but the number of metabolites characterizing the distinct differences were fewer in number than the microbiome comparisons, ranging from 78 to 131 metabolites. The metabolites in the mouse groups were unidentified. Despite majority of the metabolites being unidentified, this study clearly displayed the difference in the metabolic profiles between the clinical and experimental groups for both humans and mice. These results further confirmed the underlying role of the gut microbiota and the gut contents regarding allergy development. Pursuing the identities of the differentiating metabolites will further contribute to fill the gap of knowledge on the exact molecular mechanism of gut-mediated allergy development.

Current major limitation of metabolomic studies is the difficulty in metabolite annotations[223]. Much of this difficulty stems from the lack of established standardized protocols due to the very recent technical advancements[223] combined with the sheer complexity of metabolic cross-feeding that occurs within the gut[94, 95]. Main source of metabolites in the gut stems from consumed food[94], yet there is a great uncertainty on exactly how the consumed dietary nutrients interact with the host and the members of the gut microbiota[223]. Many researchers have opted to using a mathematical model to understand this complex metabolite network within the gut[224, 225]. However, it is still limited by the lack of knowledge on the individual members that make up the gut microbiota[225]. To fill this gap will require a large-scale interdisciplinary effort; microbiologists to identify and characterize more of the unidentified bacterial species within the gut microbiome as well as their metabolic genotype/phenotypes, chemists and biochemists to identify the unidentified measurable metabolites along with their molecular characteristics and role in the gut environment, mathematicians and

statisticians to better model and analyze the complex network of metabolic exchange, clinicians to facilitate clinical studies and provide clinical insight, engineers to improve the mechanic measurement tools, and many others with appropriate specialties.

Study of the role of gut microbiome and metabolome on disease phenotypes is an ever-growing field with an ever-growing knowledge, and knowledge gaps that follow. This study aimed to contribute to the field by identifying specific bacterial taxa associated with eczema in infants, as well as lowered lung functionality and increased AHR in mouse models of asthma. A collection of metabolic profiles that distinguishes between disease phenotypes in infants and mice were also identified. These findings can now be used as a basis for future studies that aims to explore the roles and the mechanisms of human gut microbiome and metabolome on allergy and asthma.

REFERENCES

1. Tanno, L.K., et al., Categorization of allergic disorders in the new World Health Organization International Classification of Diseases. *Clin Transl Allergy*, 2014. **4**: p. 42.
2. Arrieta, M.C., et al., Early infancy microbial and metabolic alterations affect risk of childhood asthma. *Sci Transl Med*, 2015. **7**(307): p. 307ra152.
3. Jones, S.M., et al., Efficacy and safety of oral immunotherapy in children aged 1-3 years with peanut allergy (the Immune Tolerance Network IMPACT trial): a randomised placebo-controlled study. *Lancet*, 2022. **399**(10322): p. 359-371.
4. Zimmermann, P., et al., Association between the intestinal microbiota and allergic sensitization, eczema, and asthma: A systematic review. *J Allergy Clin Immunol*, 2019. **143**(2): p. 467-485.
5. CDC, N.C.f.H.S., More Than a Quarter of U.S. Adults and Children Have at Least One Allergy. 2023.
6. Bieber, T., Atopic dermatitis. *N Engl J Med*, 2008. **358**(14): p. 1483-94.
7. Chan Ho Na, J.C., Eric L. Simpson, Quality of Life and Disease Impact of Atopic Dermatitis and Psoriasis on Children and Their Families. *Children*, 2019. **6**(12)(133).
8. Camfferman, D., et al., Eczema and sleep and its relationship to daytime functioning in children. *Sleep Med Rev*, 2010. **14**(6): p. 359-69.
9. Chamlin, S.L., et al., The price of pruritus: sleep disturbance and cosleeping in atopic dermatitis. *Arch Pediatr Adolesc Med*, 2005. **159**(8): p. 745-50.
10. Stores, G., A. Burrows, and C. Crawford, Physiological sleep disturbance in children with atopic dermatitis: a case control study. *Pediatr Dermatol*, 1998. **15**(4): p. 264-8.
11. Holm, E.A., et al., Life quality assessment among patients with atopic eczema. *Br J Dermatol*, 2006. **154**(4): p. 719-25.
12. Absolon, C.M., et al., Psychological disturbance in atopic eczema: the extent of the problem in school-aged children. *Br J Dermatol*, 1997. **137**(2): p. 241-5.
13. Mitchell, A.E., et al., Parenting and childhood atopic dermatitis: A cross-sectional study of relationships between parenting behaviour, skin care management, and disease severity in young children. *Int J Nurs Stud*, 2016. **64**: p. 72-85.
14. Daud, L.R., M.E. Garralda, and T.J. David, Psychosocial adjustment in preschool children with atopic eczema. *Arch Dis Child*, 1993. **69**(6): p. 670-6.
15. Patel, K.R., et al., Association between atopic dermatitis, depression, and suicidal ideation: A systematic review and meta-analysis. *J Am Acad Dermatol*, 2019. **80**(2): p. 402-410.
16. Wadonda-Kabondo, N., et al., Association of parental eczema, hayfever, and asthma with atopic dermatitis in infancy: birth cohort study. *Arch Dis Child*, 2004. **89**(10): p. 917-21.
17. Matsuoka, S., et al., Prevalence of specific allergic diseases in school children as related to parental atopy. *Pediatr Int*, 1999. **41**(1): p. 46-51.
18. Schultz Larsen, F., Atopic dermatitis: a genetic-epidemiologic study in a population-based twin sample. *J Am Acad Dermatol*, 1993. **28**(5 Pt 1): p. 719-23.

19. Larsen, F.S., N.V. Holm, and K. Henningsen, Atopic dermatitis. A genetic-epidemiologic study in a population-based twin sample. *J Am Acad Dermatol*, 1986. **15**(3): p. 487-94.
20. Biagini Myers, J.M. and G.K. Khurana Hershey, Eczema in early life: genetics, the skin barrier, and lessons learned from birth cohort studies. *J Pediatr*, 2010. **157**(5): p. 704-14.
21. Williams, H. and C. Flohr, How epidemiology has challenged 3 prevailing concepts about atopic dermatitis. *J Allergy Clin Immunol*, 2006. **118**(1): p. 209-13.
22. Wahn, U., Wahn, U. "The immunology of fetuses and infants: What drives the allergic march. *Allergy*, 2000. **55**(7): p. 591-599.
23. Wang, I.J., et al., Effect of gestational smoke exposure on atopic dermatitis in the offspring. *Pediatr Allergy Immunol*, 2008. **19**(7): p. 580-6.
24. Schafer, T., et al., Maternal smoking during pregnancy and lactation increases the risk for atopic eczema in the offspring. *J Am Acad Dermatol*, 1997. **36**(4): p. 550-6.
25. Kramer, U., et al., The effect of environmental tobacco smoke on eczema and allergic sensitization in children. *Br J Dermatol*, 2004. **150**(1): p. 111-8.
26. LL. Muizzuddin N, M.K., Vallon P, Maes D. , Effect of cigarette smoke on skin. *J Soc Cosmet Chem*, 1997. **48**(5): p. 235-242.
27. Flohr, C., D. Pascoe, and H.C. Williams, Atopic dermatitis and the 'hygiene hypothesis': too clean to be true? *Br J Dermatol*, 2005. **152**(2): p. 202-16.
28. McNally, N.J., et al., Is there a geographical variation in eczema prevalence in the UK? Evidence from the 1958 British Birth Cohort Study. *Br J Dermatol*, 2000. **142**(4): p. 712-20.
29. McKeever, T.M., et al., Siblings, multiple births, and the incidence of allergic disease: a birth cohort study using the West Midlands general practice research database. *Thorax*, 2001. **56**(10): p. 758-62.
30. Karmaus, W. and C. Botezan, Does a higher number of siblings protect against the development of allergy and asthma? A review. *J Epidemiol Community Health*, 2002. **56**(3): p. 209-17.
31. Williams, H.C., D.P. Strachan, and R.J. Hay, Childhood eczema: disease of the advantaged? *BMJ*, 1994. **308**(6937): p. 1132-5.
32. Pickett, K.E. and R.G. Wilkinson, Income inequality and health: a causal review. *Soc Sci Med*, 2015. **128**: p. 316-26.
33. McKenzie, C., et al., The nutrition-gut microbiome-physiology axis and allergic diseases. *Immunol Rev*, 2017. **278**(1): p. 277-295.
34. Irvine, A.D. and P. Mina-Osorio, Disease trajectories in childhood atopic dermatitis: an update and practitioner's guide. *Br J Dermatol*, 2019. **181**(5): p. 895-906.
35. Hill, D.A. and J.M. Spergel, The atopic march: Critical evidence and clinical relevance. *Ann Allergy Asthma Immunol*, 2018. **120**(2): p. 131-137.
36. Prevention, C.f.D.C.a., Asthma, Most Recent National Asthma Data 2021. 2023.
37. Yang, C.L., J.M. Gaffin, and D. Radhakrishnan, Question 3: Can we diagnose asthma in children under the age of 5 years? *Paediatr Respir Rev*, 2019. **29**: p. 25-30.

38. Cave, A.J. and L.L. Atkinson, Asthma in preschool children: a review of the diagnostic challenges. *J Am Board Fam Med*, 2014. **27**(4): p. 538-48.
39. Silverberg, J.I. and J.M. Hanifin, Adult eczema prevalence and associations with asthma and other health and demographic factors: a US population-based study. *J Allergy Clin Immunol*, 2013. **132**(5): p. 1132-8.
40. Pate CA, Z.H., Qin X, Johnson C, Hummelman E, Malilay J, Asthma Surveillance — United States, 2006–2018, in *MMWR Surveill Summ* 2021. 2021. p. 1-32.
41. Brannan, J.D. and M.D. Lougheed, Airway hyperresponsiveness in asthma: mechanisms, clinical significance, and treatment. *Front Physiol*, 2012. **3**: p. 460.
42. Postma, D.S. and H.A. Kerstjens, Characteristics of airway hyperresponsiveness in asthma and chronic obstructive pulmonary disease. *Am J Respir Crit Care Med*, 1998. **158**(5 Pt 3): p. S187-92.
43. Ruan, Z., et al., Asthma susceptible genes in children: A meta-analysis. *Medicine (Baltimore)*, 2020. **99**(45): p. e23051.
44. Schaubberger, E.M., et al., Identification of ATPAF1 as a novel candidate gene for asthma in children. *J Allergy Clin Immunol*, 2011. **128**(4): p. 753-760 e11.
45. Ziyab, A.H., et al., Allergic sensitization and filaggrin variants predispose to the comorbidity of eczema, asthma, and rhinitis: results from the Isle of Wight birth cohort. *Clin Exp Allergy*, 2014. **44**(9): p. 1170-8.
46. Chen, S., et al., Consistency and Variability of DNA Methylation in Women During Puberty, Young Adulthood, and Pregnancy. *Genet Epigenet*, 2017. **9**: p. 1179237X17721540.
47. Zhang, H., et al., The interplay of DNA methylation over time with Th2 pathway genetic variants on asthma risk and temporal asthma transition. *Clin Epigenetics*, 2014. **6**(1): p. 8.
48. Soto-Ramirez, N., et al., The interaction of genetic variants and DNA methylation of the interleukin-4 receptor gene increase the risk of asthma at age 18 years. *Clin Epigenetics*, 2013. **5**(1): p. 1.
49. Yousefi, M., et al., The methylation of the LEPR/LEPROT genotype at the promoter and body regions influence concentrations of leptin in girls and BMI at age 18 years if their mother smoked during pregnancy. *Int J Mol Epidemiol Genet*, 2013. **4**(2): p. 86-100.
50. Mukherjee, A.B. and Z. Zhang, Allergic asthma: influence of genetic and environmental factors. *J Biol Chem*, 2011. **286**(38): p. 32883-9.
51. von Mutius, E., Environmental factors influencing the development and progression of pediatric asthma. *J Allergy Clin Immunol*, 2002. **109**(6 Suppl): p. S525-32.
52. O'Dwyer, D.N., R.P. Dickson, and B.B. Moore, The Lung Microbiome, Immunity, and the Pathogenesis of Chronic Lung Disease. *J Immunol*, 2016. **196**(12): p. 4839-47.
53. Kozik, A.J. and Y.J. Huang, The microbiome in asthma: Role in pathogenesis, phenotype, and response to treatment. *Ann Allergy Asthma Immunol*, 2019. **122**(3): p. 270-275.
54. Martinez, F.D. and S. Guerra, Early Origins of Asthma. Role of Microbial Dysbiosis and Metabolic Dysfunction. *Am J Respir Crit Care Med*, 2018. **197**(5): p. 573-579.

55. Stokholm, J., et al., Maturation of the gut microbiome and risk of asthma in childhood. *Nat Commun*, 2018. **9**(1): p. 141.
56. Simon, A.K., G.A. Hollander, and A. McMichael, Evolution of the immune system in humans from infancy to old age. *Proc Biol Sci*, 2015. **282**(1821): p. 20143085.
57. Halkias, J., et al., CD161 contributes to prenatal immune suppression of IFN γ -producing PLZF⁺ T cells. *J Clin Invest*, 2019. **129**(9): p. 3562-3577.
58. Mishra, A., et al., Microbial exposure during early human development primes fetal immune cells. *Cell*, 2021. **184**(13): p. 3394-3409 e20.
59. Rackaityte, E., et al., Viable bacterial colonization is highly limited in the human intestine in utero. *Nat Med*, 2020. **26**(4): p. 599-607.
60. Mold, J.E., et al., Fetal and adult hematopoietic stem cells give rise to distinct T cell lineages in humans. *Science*, 2010. **330**(6011): p. 1695-9.
61. Romagnani, S., Immunologic influences on allergy and the TH1/TH2 balance. *J Allergy Clin Immunol*, 2004. **113**(3): p. 395-400.
62. Sender, R., S. Fuchs, and R. Milo, Revised Estimates for the Number of Human and Bacteria Cells in the Body. *PLoS Biol*, 2016. **14**(8): p. e1002533.
63. Clemente, J.C., et al., The impact of the gut microbiota on human health: an integrative view. *Cell*, 2012. **148**(6): p. 1258-70.
64. Statistics, N.C.f.H., Allergies and Hay Fever, United States, 2023. 2023: Hyattsville, Maryland.
65. Feehley, T., et al., Healthy infants harbor intestinal bacteria that protect against food allergy. *Nat Med*, 2019. **25**(3): p. 448-453.
66. Jota Baptista, C.V., A.I. Faustino-Rocha, and P.A. Oliveira, Animal Models in Pharmacology: A Brief History Awarding the Nobel Prizes for Physiology or Medicine. *Pharmacology*, 2021. **106**(7-8): p. 356-368.
67. Ericsson, A.C., M.J. Crim, and C.L. Franklin, A brief history of animal modeling. *Mo Med*, 2013. **110**(3): p. 201-5.
68. Laboratory, T.J. Our History. [cited 2023; Available from: <https://www.jax.org/about-us/history#nobel-prizes-et-al>].
69. Makowska, I.J. and D.M. Weary, A Good Life for Laboratory Rodents? *ILAR J*, 2021. **60**(3): p. 373-388.
70. Robinson, N.B., et al., The current state of animal models in research: A review. *Int J Surg*, 2019. **72**: p. 9-13.
71. Dominguez-Oliva, A., et al., The Importance of Animal Models in Biomedical Research: Current Insights and Applications. *Animals (Basel)*, 2023. **13**(7).
72. Swearingen, J.R., Choosing the right animal model for infectious disease research. *Animal Model Exp Med*, 2018. **1**(2): p. 100-108.
73. Nials, A.T. and S. Uddin, Mouse models of allergic asthma: acute and chronic allergen challenge. *Dis Model Mech*, 2008. **1**(4-5): p. 213-20.

74. Taube, C., A. Dakhama, and E.W. Gelfand, Insights into the pathogenesis of asthma utilizing murine models. *Int Arch Allergy Immunol*, 2004. **135**(2): p. 173-86.
75. Seyyede Masoume Athari, E.M.N., Seyyed Shamsadin Athari, Animal model of allergy and asthma; protocol for researches. *Protocol Exchange*, 2019.
76. Wenzel, S. and S.T. Holgate, The mouse trap: It still yields few answers in asthma. *Am J Respir Crit Care Med*, 2006. **174**(11): p. 1173-6; discussion 1176-8.
77. Kumar, R.K., C. Herbert, and P.S. Foster, The "classical" ovalbumin challenge model of asthma in mice. *Curr Drug Targets*, 2008. **9**(6): p. 485-94.
78. Huss, K., et al., House dust mite and cockroach exposure are strong risk factors for positive allergy skin test responses in the Childhood Asthma Management Program. *J Allergy Clin Immunol*, 2001. **107**(1): p. 48-54.
79. Panzner, P., et al., Cross-sectional study on sensitization to mite and cockroach allergen components in allergy patients in the Central European region. *Clin Transl Allergy*, 2018. **8**: p. 19.
80. Stefka, A.T., et al., Commensal bacteria protect against food allergen sensitization. *Proc Natl Acad Sci U S A*, 2014. **111**(36): p. 13145-50.
81. Cahenzli, J., et al., Intestinal microbial diversity during early-life colonization shapes long-term IgE levels. *Cell Host Microbe*, 2013. **14**(5): p. 559-70.
82. Herbst, T., et al., Dysregulation of allergic airway inflammation in the absence of microbial colonization. *Am J Respir Crit Care Med*, 2011. **184**(2): p. 198-205.
83. Wang, Y., et al., A study on the method and effect of the construction of a humanized mouse model of fecal microbiota transplantation. *Front Microbiol*, 2022. **13**: p. 1031758.
84. Shimbori, C., et al., Gut bacteria interact directly with colonic mast cells in a humanized mouse model of IBS. *Gut Microbes*, 2022. **14**(1): p. 2105095.
85. Park, J.C. and S.H. Im, Of men in mice: the development and application of a humanized gnotobiotic mouse model for microbiome therapeutics. *Exp Mol Med*, 2020. **52**(9): p. 1383-1396.
86. Wrzosek, L., et al., Transplantation of human microbiota into conventional mice durably reshapes the gut microbiota. *Sci Rep*, 2018. **8**(1): p. 6854.
87. Eiseman, B., et al., Fecal enema as an adjunct in the treatment of pseudomembranous enterocolitis. *Surgery*, 1958. **44**(5): p. 854-9.
88. Kumar, V. and M. Fischer, Expert opinion on fecal microbiota transplantation for the treatment of *Clostridioides difficile* infection and beyond. *Expert Opin Biol Ther*, 2020. **20**(1): p. 73-81.
89. Aroniadis, O.C. and L.J. Brandt, Fecal microbiota transplantation: past, present and future. *Curr Opin Gastroenterol*, 2013. **29**(1): p. 79-84.
90. Weingarden, A.R. and B.P. Vaughn, Intestinal microbiota, fecal microbiota transplantation, and inflammatory bowel disease. *Gut Microbes*, 2017. **8**(3): p. 238-252.

91. Leonardi, I., et al., Fungal Trans-kingdom Dynamics Linked to Responsiveness to Fecal Microbiota Transplantation (FMT) Therapy in Ulcerative Colitis. *Cell Host Microbe*, 2020. **27**(5): p. 823-829 e3.
92. Grigoryan, Z., et al., Fecal microbiota transplantation: Uses, questions, and ethics. *Med Microecol*, 2020. **6**.
93. Dhamoon, J.J.P.A.S., *Physiology, Digestion*. 2023, Treasure Island, FL: StatPearls Publishing.
94. Oliphant, K. and E. Allen-Vercoe, Macronutrient metabolism by the human gut microbiome: major fermentation by-products and their impact on host health. *Microbiome*, 2019. **7**(1): p. 91.
95. Culp, E.J. and A.L. Goodman, Cross-feeding in the gut microbiome: Ecology and mechanisms. *Cell Host Microbe*, 2023. **31**(4): p. 485-499.
96. Germerodt, S., et al., Pervasive Selection for Cooperative Cross-Feeding in Bacterial Communities. *PLoS Comput Biol*, 2016. **12**(6): p. e1004986.
97. Hill, M.J., Intestinal flora and endogenous vitamin synthesis. *Eur J Cancer Prev*, 1997. **6 Suppl 1**: p. S43-5.
98. Rowland, I., et al., Gut microbiota functions: metabolism of nutrients and other food components. *Eur J Nutr*, 2018. **57**(1): p. 1-24.
99. Kim, C.H., Immune regulation by microbiome metabolites. *Immunology*, 2018. **154**(2): p. 220-229.
100. Macfarlane, S. and G.T. Macfarlane, Regulation of short-chain fatty acid production. *Proc Nutr Soc*, 2003. **62**(1): p. 67-72.
101. Tan, J., et al., Dietary Fiber and Bacterial SCFA Enhance Oral Tolerance and Protect against Food Allergy through Diverse Cellular Pathways. *Cell Rep*, 2016. **15**(12): p. 2809-24.
102. Depner, M., et al., Maturation of the gut microbiome during the first year of life contributes to the protective farm effect on childhood asthma. *Nat Med*, 2020. **26**(11): p. 1766-1775.
103. Thorburn, A.N., et al., Evidence that asthma is a developmental origin disease influenced by maternal diet and bacterial metabolites. *Nat Commun*, 2015. **6**: p. 7320.
104. Roduit, C., et al., High levels of butyrate and propionate in early life are associated with protection against atopy. *Allergy*, 2019. **74**(4): p. 799-809.
105. Crestani, E., et al., Untargeted metabolomic profiling identifies disease-specific signatures in food allergy and asthma. *J Allergy Clin Immunol*, 2020. **145**(3): p. 897-906.
106. Nakada, E.M., et al., Conjugated bile acids attenuate allergen-induced airway inflammation and hyperresponsiveness by inhibiting UPR transducers. *JCI Insight*, 2019. **4**(9).
107. Willart, M.A., et al., Ursodeoxycholic acid suppresses eosinophilic airway inflammation by inhibiting the function of dendritic cells through the nuclear farnesoid X receptor. *Allergy*, 2012. **67**(12): p. 1501-10.

108. Yamazaki, K., et al., Ursodeoxycholic acid inhibits eosinophil degranulation in patients with primary biliary cirrhosis. *Hepatology*, 1999. **30**(1): p. 71-8.
109. Turi, K.N., et al., Unconjugated bilirubin is associated with protection from early-life wheeze and childhood asthma. *J Allergy Clin Immunol*, 2021. **148**(1): p. 128-138.
110. van der Sluijs, K.F., et al., Systemic tryptophan and kynurenine catabolite levels relate to severity of rhinovirus-induced asthma exacerbation: a prospective study with a parallel-group design. *Thorax*, 2013. **68**(12): p. 1122-30.
111. Hu, Y., et al., Decreased expression of indoleamine 2,3-dioxygenase in childhood allergic asthma and its inverse correlation with fractional concentration of exhaled nitric oxide. *Ann Allergy Asthma Immunol*, 2017. **119**(5): p. 429-434.
112. Unuvar, S., et al., Neopterin Levels and Indoleamine 2,3-Dioxygenase Activity as Biomarkers of Immune System Activation and Childhood Allergic Diseases. *Ann Lab Med*, 2019. **39**(3): p. 284-290.
113. Heath-Pagliuso, S., et al., Activation of the Ah receptor by tryptophan and tryptophan metabolites. *Biochemistry*, 1998. **37**(33): p. 11508-15.
114. Peltola, J., et al., Toxic-metabolite-producing bacteria and fungus in an indoor environment. *Appl Environ Microbiol*, 2001. **67**(7): p. 3269-74.
115. Fujimura, K.E., et al., Neonatal gut microbiota associates with childhood multisensitized atopy and T cell differentiation. *Nat Med*, 2016. **22**(10): p. 1187-1191.
116. Levan, S.R., et al., Elevated faecal 12,13-diHOME concentration in neonates at high risk for asthma is produced by gut bacteria and impedes immune tolerance. *Nat Microbiol*, 2019. **4**(11): p. 1851-1861.
117. Gould, H.J. and Y.B. Wu, IgE repertoire and immunological memory: compartmental regulation and antibody function. *Int Immunol*, 2018. **30**(9): p. 403-412.
118. Sanchez-Jimenez, F., et al., Pharmacological potential of biogenic amine-polyamine interactions beyond neurotransmission. *Br J Pharmacol*, 2013. **170**(1): p. 4-16.
119. Caminero, A., et al., Mechanisms by which gut microorganisms influence food sensitivities. *Nat Rev Gastroenterol Hepatol*, 2019. **16**(1): p. 7-18.
120. Stiemsma, L.T. and S.E. Turvey, Asthma and the microbiome: defining the critical window in early life. *Allergy Asthma Clin Immunol*, 2017. **13**: p. 3.
121. Riedler, J., et al., Exposure to farming in early life and development of asthma and allergy: a cross-sectional survey. *Lancet*, 2001. **358**(9288): p. 1129-33.
122. Ege, M.J., et al., Exposure to environmental microorganisms and childhood asthma. *N Engl J Med*, 2011. **364**(8): p. 701-9.
123. Olszak, T., et al., Microbial exposure during early life has persistent effects on natural killer T cell function. *Science*, 2012. **336**(6080): p. 489-93.
124. Zuccotti, G., et al., Probiotics for prevention of atopic diseases in infants: systematic review and meta-analysis. *Allergy*, 2015. **70**(11): p. 1356-71.

125. Ichinohe, T., et al., Microbiota regulates immune defense against respiratory tract influenza A virus infection. *Proc Natl Acad Sci U S A*, 2011. **108**(13): p. 5354-9.
126. Spergel, J.M. and A.S. Paller, Atopic dermatitis and the atopic march. *J Allergy Clin Immunol*, 2003. **112**(6 Suppl): p. S118-27.
127. von Kobyletzki LB, B.C., Hasselgren M, Larsson M, Lindström CB, Svensson Å, Eczema in early childhood is strongly associated with the development of asthma and rhinitis in a prospective cohort. *BMC Dermatol*, 2012. **12**(11).
128. Abrahamsson, T.R., et al., Low diversity of the gut microbiota in infants with atopic eczema. *J Allergy Clin Immunol*, 2012. **129**(2): p. 434-40, 440 e1-2.
129. Abrahamsson, T.R., et al., Low gut microbiota diversity in early infancy precedes asthma at school age. *Clin Exp Allergy*, 2014. **44**(6): p. 842-50.
130. Tariq, S.M., et al., The prevalence of and risk factors for atopy in early childhood: a whole population birth cohort study. *J Allergy Clin Immunol*, 1998. **101**(5): p. 587-93.
131. Arshad, S.H., et al., Cohort Profile: The Isle Of Wight Whole Population Birth Cohort (IOWBC). *Int J Epidemiol*, 2018. **47**(4): p. 1043-1044i.
132. Arshad, S.H., et al., Cohort Profile Update: The Isle of Wight Whole Population Birth Cohort (IOWBC). *Int J Epidemiol*, 2020. **49**(4): p. 1083-1084.
133. Becker AB, A.E., Asthma guidelines: the Global Initiative for Asthma in relation to national guideline. *Curr Opin Allergy Clin Immunol*, 2017. **17**(2): p. 99-103.
134. Sadeghnejad A, K.W., Davis S, Kurukulaaratchy RJ, Matthews S, Arshad SH, Raised cord serum immunoglobulin E increases the risk of allergic sensitisation at ages 4 and 10 and asthma at age 10. *Thorax*, 2004. **59**(11): p. 936-942.
135. Severity scoring of atopic dermatitis: the SCORAD index. Consensus Report of the European Task Force on Atopic Dermatitis. *Dermatology*, 1993. **186**(1): p. 23-31.
136. Asher, M.I., et al., International Study of Asthma and Allergies in Childhood (ISAAC): rationale and methods. *Eur Respir J*, 1995. **8**(3): p. 483-91.
137. Patil, V.K., et al., Interaction of prenatal maternal smoking, interleukin 13 genetic variants and DNA methylation influencing airflow and airway reactivity. *Clin Epigenetics*, 2013. **5**(1): p. 22.
138. Soto-Ramirez, N., et al., Modes of infant feeding and the occurrence of coughing/wheezing in the first year of life. *J Hum Lact*, 2013. **29**(1): p. 71-80.
139. Karmaus, W., et al., Long-term effects of breastfeeding, maternal smoking during pregnancy, and recurrent lower respiratory tract infections on asthma in children. *J Asthma*, 2008. **45**(8): p. 688-95.
140. Brooks, P.T., et al., Transplanted human fecal microbiota enhanced Guillain Barre syndrome autoantibody responses after *Campylobacter jejuni* infection in C57BL/6 mice. *Microbiome*, 2017. **5**(1): p. 92.
141. Hall, M. and R.G. Beiko, 16S rRNA Gene Analysis with QIIME2. *Methods Mol Biol*, 2018. **1849**: p. 113-129.

142. Amir, A., et al., Deblur Rapidly Resolves Single-Nucleotide Community Sequence Patterns. *mSystems*, 2017. **2**(2).
143. Rognes, T., et al., VSEARCH: a versatile open source tool for metagenomics. *PeerJ*, 2016. **4**: p. e2584.
144. Santos, T., et al., Use of MALDI-TOF mass spectrometry fingerprinting to characterize *Enterococcus* spp. and *Escherichia coli* isolates. *J Proteomics*, 2015. **127**(Pt B): p. 321-31.
145. Team, R.C., *R: A Language and Environment for Statistical Computing*. 2020, R Foundation for Statistical Computing: Vienna, Austria.
146. SAS Institute Inc. SAS and all other SAS Institute Inc. product or service names are registered trademarks or trademarks of SAS Institute Inc., C., NC, USA.
147. Sbihi, H., et al., Thinking bigger: How early-life environmental exposures shape the gut microbiome and influence the development of asthma and allergic disease. *Allergy*, 2019. **74**(11): p. 2103-2115.
148. Bisgaard, H., et al., Childhood asthma after bacterial colonization of the airway in neonates. *N Engl J Med*, 2007. **357**(15): p. 1487-95.
149. Hilty, M., et al., Disordered microbial communities in asthmatic airways. *PLoS One*, 2010. **5**(1): p. e8578.
150. Lal, C.V., et al., The Airway Microbiome at Birth. *Sci Rep*, 2016. **6**: p. 31023.
151. Lynch, S.V., et al., Effects of early-life exposure to allergens and bacteria on recurrent wheeze and atopy in urban children. *J Allergy Clin Immunol*, 2014. **134**(3): p. 593-601 e12.
152. Penders, J., et al., Establishment of the intestinal microbiota and its role for atopic dermatitis in early childhood. *J Allergy Clin Immunol*, 2013. **132**(3): p. 601-607 e8.
153. Louisa Owens, I.A.L., Guicheng Zhang, Stephen Turner & Peter N Le Souëf, Prevalence of allergic sensitization, hay fever, eczema, and asthma in a longitudinal birth cohort. *Journal of Asthma and Allergy*, 2018. **11**: p. 173-180.
154. Ta, L.D.H., et al., A compromised developmental trajectory of the infant gut microbiome and metabolome in atopic eczema. *Gut Microbes*, 2020. **12**(1): p. 1-22.
155. Sher, A.A., et al., Conjugative RP4 Plasmid-Mediated Transfer of Antibiotic Resistance Genes to Commensal and Multidrug-Resistant Enteric Bacteria In Vitro. *Microorganisms*, 2023. **11**(1).
156. Jolley, K.A., J.E. Bray, and M.C.J. Maiden, Open-access bacterial population genomics: BIGSdb software, the PubMLST.org website and their applications. *Wellcome Open Res*, 2018. **3**: p. 124.
157. Zhou, Z., et al., The Enterobase user's guide, with case studies on *Salmonella* transmissions, *Yersinia pestis* phylogeny, and *Escherichia* core genomic diversity. *Genome Res*, 2020. **30**(1): p. 138-152.
158. Könönen, E., 250 - Anaerobic Cocci and Anaerobic Gram-Positive Nonsporulating Bacilli. 8 ed. Mandell, Douglas, and Bennett's Principles and Practice of Infectious Diseases, ed. R.D. John E. Bennett, Martin J. Blaser. Vol. 2. 2015.

159. Berenger, B.M., et al., Anaerobic urinary tract infection caused by *Veillonella parvula* identified using cystine-lactose-electrolyte deficient media and matrix-assisted laser desorption ionization-time of flight mass spectrometry. *IDCases*, 2015. **2**(2): p. 44-6.
160. Ito, Y., et al., The first case of *Veillonella atypica* bacteremia in a patient with renal pelvic tumor. *Anaerobe*, 2022. **73**: p. 102491.
161. Andréanne Morin, C.G.M., Casper-Emil T. Pedersen, Jakob Stokholm, Bo L. Chawes, Ann-Marie Malby Schoos, Katherine A. Naughton, Jonathan Thorsen, Martin S. Mortensen, Donata Vercelli, Urvish Trivedi, Søren J. Sørensen, Hans Bisgaard, Dan L. Nicolae, Klaus Bønnelykke, Carole Ober, Epigenetic landscape links upper airway microbiota in infancy with allergic rhinitis at 6 years of age. *Journal of Allergy and Clinical Immunology*, 2020. **146**(6): p. 1358-1366.
162. Salameh, M., et al., The role of gut microbiota in atopic asthma and allergy, implications in the understanding of disease pathogenesis. *Scand J Immunol*, 2020. **91**(3): p. e12855.
163. Zheng, H., et al., Altered Gut Microbiota Composition Associated with Eczema in Infants. *PLoS One*, 2016. **11**(11): p. e0166026.
164. Centers for Disease, C.a.P., Most recent National Asthma Data. 2019 (Last updated May, 2019).
165. Ziyab, A.H., et al., DNA methylation of the filaggrin gene adds to the risk of eczema associated with loss-of-function variants. *J Eur Acad Dermatol Venereol*, 2013. **27**(3): p. e420-3.
166. Ziyab, A.H., et al., Association of filaggrin variants with asthma and rhinitis: is eczema or allergic sensitization status an effect modifier? *Int Arch Allergy Immunol*, 2014. **164**(4): p. 308-18.
167. Arshad, S.H., et al., Cohort Profile Update: The Isle of Wight Whole Population Birth Cohort (IOWBC). *Int J Epidemiol*, 2020.
168. Adami, A.J. and S.J. Bracken, Breathing Better Through Bugs: Asthma and the Microbiome. *Yale J Biol Med*, 2016. **89**(3): p. 309-324.
169. Wu, Z.X., et al., Prenatal and early, but not late, postnatal exposure of mice to sidestream tobacco smoke increases airway hyperresponsiveness later in life. *Environ Health Perspect*, 2009. **117**(9): p. 1434-40.
170. Chapman, D.G. and C.G. Irvin, Mechanisms of airway hyper-responsiveness in asthma: the past, present and yet to come. *Clin Exp Allergy*, 2015. **45**(4): p. 706-19.
171. Ito, J.T., et al., Extracellular Matrix Component Remodeling in Respiratory Diseases: What Has Been Found in Clinical and Experimental Studies? *Cells*, 2019. **8**(4).
172. Biesbroek, G., et al., Early respiratory microbiota composition determines bacterial succession patterns and respiratory health in children. *Am J Respir Crit Care Med*, 2014. **190**(11): p. 1283-92.
173. Teo, S.M., et al., The infant nasopharyngeal microbiome impacts severity of lower respiratory infection and risk of asthma development. *Cell Host Microbe*, 2015. **17**(5): p. 704-15.

174. Bisgaard, H., et al., Reduced diversity of the intestinal microbiota during infancy is associated with increased risk of allergic disease at school age. *J Allergy Clin Immunol*, 2011. **128**(3): p. 646-52 e1-5.
175. Fujimura, K.E., et al., House dust exposure mediates gut microbiome Lactobacillus enrichment and airway immune defense against allergens and virus infection. *Proc Natl Acad Sci U S A*, 2014. **111**(2): p. 805-10.
176. Huang, Y.J. and H.A. Boushey, The microbiome in asthma. *J Allergy Clin Immunol*, 2015. **135**(1): p. 25-30.
177. Kong, H.H., et al., Temporal shifts in the skin microbiome associated with disease flares and treatment in children with atopic dermatitis. *Genome Res*, 2012. **22**(5): p. 850-9.
178. Collins, J., et al., Humanized microbiota mice as a model of recurrent *Clostridium difficile* disease. *Microbiome*, 2015. **3**: p. 35.
179. Directors, A.B.o., Guidelines for Methacholine and Exercise Challenge Testing—1999. American Thoracic Society 1999.
180. Woo, L.N., et al., A 4-Week Model of House Dust Mite (HDM) Induced Allergic Airways Inflammation with Airway Remodeling. *Sci Rep*, 2018. **8**(1): p. 6925.
181. Gandhi, V.D., et al., House dust mite interactions with airway epithelium: role in allergic airway inflammation. *Curr Allergy Asthma Rep*, 2013. **13**(3): p. 262-70.
182. Brown, T.A., et al., Early life microbiome perturbation alters pulmonary responses to ozone in male mice. *Physiol Rep*, 2020. **8**(2): p. e14290.
183. Lommatzsch, M., Airway hyperresponsiveness: new insights into the pathogenesis. *Semin Respir Crit Care Med*, 2012. **33**(6): p. 579-87.
184. Ver Heul, A., J. Planer, and A.L. Kau, The Human Microbiota and Asthma. *Clin Rev Allergy Immunol*, 2019. **57**(3): p. 350-363.
185. Bonaz, B., T. Bazin, and S. Pellissier, The Vagus Nerve at the Interface of the Microbiota-Gut-Brain Axis. *Front Neurosci*, 2018. **12**: p. 49.
186. Trompette, A., et al., Gut microbiota metabolism of dietary fiber influences allergic airway disease and hematopoiesis. *Nat Med*, 2014. **20**(2): p. 159-66.
187. Vanoirbeek, J.A., et al., Noninvasive and invasive pulmonary function in mouse models of obstructive and restrictive respiratory diseases. *Am J Respir Cell Mol Biol*, 2010. **42**(1): p. 96-104.
188. Patel, K.R., et al., Mast cell-derived neurotrophin 4 mediates allergen-induced airway hyperinnervation in early life. *Mucosal Immunol*, 2016. **9**(6): p. 1466-1476.
189. Patel, K.R., et al., Targeting acetylcholine receptor M3 prevents the progression of airway hyperreactivity in a mouse model of childhood asthma. *FASEB J*, 2017. **31**(10): p. 4335-4346.
190. Bonvini, S.J., et al., Novel airway smooth muscle-mast cell interactions and a role for the TRPV4-ATP axis in non-atopic asthma. *Eur Respir J*, 2020. **56**(1).

191. Mendez-Enriquez, E. and J. Hallgren, Mast Cells and Their Progenitors in Allergic Asthma. *Front Immunol*, 2019. **10**: p. 821.
192. Traina, G., Mast Cells in Gut and Brain and Their Potential Role as an Emerging Therapeutic Target for Neural Diseases. *Front Cell Neurosci*, 2019. **13**: p. 345.
193. Team, R.C., A language and environment for statistical computing. 2020.
194. Mansfield, L.S., et al., C57BL/6 and congenic interleukin-10-deficient mice can serve as models of *Campylobacter jejuni* colonization and enteritis. *Infect Immun*, 2007. **75**(3): p. 1099-115.
195. Nault, R., et al., Development of a computational high-throughput tool for the quantitative examination of dose-dependent histological features. *Toxicol Pathol*, 2015. **43**(3): p. 366-75.
196. Kujur, W., et al., Caerulomycin A inhibits Th2 cell activity: a possible role in the management of asthma. *Sci Rep*, 2015. **5**: p. 15396.
197. Adami, A.J., et al., Early-life antibiotics attenuate regulatory T cell generation and increase the severity of murine house dust mite-induced asthma. *Pediatr Res*, 2018. **84**(3): p. 426-434.
198. Lee, K.S., et al., Inhibition of phosphoinositide 3-kinase delta attenuates allergic airway inflammation and hyperresponsiveness in murine asthma model. *FASEB J*, 2006. **20**(3): p. 455-65.
199. Kwak, Y.G., et al., Involvement of PTEN in airway hyperresponsiveness and inflammation in bronchial asthma. *J Clin Invest*, 2003. **111**(7): p. 1083-92.
200. Zaiss, M.M., et al., The Intestinal Microbiota Contributes to the Ability of Helminths to Modulate Allergic Inflammation. *Immunity*, 2015. **43**(5): p. 998-1010.
201. McCullagh, P. and J.A. Nelder, *Generalized Linear Models*. Second Edition. 1989, London: Chapman and Hall.
202. Penders, J., et al., The role of the intestinal microbiota in the development of atopic disorders. *Allergy*, 2007. **62**(11): p. 1223-36.
203. Zheng, P., et al., Gut Microbiome and Metabolomics Profiles of Allergic and Non-Allergic Childhood Asthma. *J Asthma Allergy*, 2022. **15**: p. 419-435.
204. Hinako Terauchi, J.A.B., Yu Jiang, Hongmei Zhang, Phillip T. Brooks, Samantha Waite, John W. Holloway, Wilfried Karmaus, Susan L. Ewart, S. Hasan Arshad, Linda S. Mansfield, Predominance of *Veillonella* and other allergy agonists in 3-month-old infant gut microbiota was associated with development of eczema in early childhood in the Isle of Wight Birth Cohort. 2023: In Review at PLOS ONE.
205. Lee-Sarwar, K., et al., Association of the gut microbiome and metabolome with wheeze frequency in childhood asthma. *J Allergy Clin Immunol*, 2022. **150**(2): p. 325-336.
206. Ivon Moya Uribe, H.T., Julia A. Bell, Alexander Zanetti, Sanket Jantre, Marianne Huebner, S. Hasan Arshad, Susan L. Ewart, Linda S. Mansfield, Fecal microbiota transplants of three distinct human communities to germ-free mice exacerbated inflammation and decreased lung function in their offspring. 2023: In Review for mBio.

207. Stagliano, M.C., et al., Bioassay-directed fractionation for discovery of bioactive neutral lipids guided by relative mass defect filtering and multiplexed collision-induced dissociation. *Rapid Commun Mass Spectrom*, 2010. **24**(24): p. 3578-84.
208. Ekanayaka, E.A., M.D. Celiz, and A.D. Jones, Relative mass defect filtering of mass spectra: a path to discovery of plant specialized metabolites. *Plant Physiol*, 2015. **167**(4): p. 1221-32.
209. Wishart, D., et al., T3DB: the toxic exposome database. *Nucleic Acids Res*, 2015. **43**(Database issue): p. D928-34.
210. Lim, E., et al., T3DB: a comprehensively annotated database of common toxins and their targets. *Nucleic Acids Res*, 2010. **38**(Database issue): p. D781-6.
211. Wikoff, W.R., et al., Metabolomics analysis reveals large effects of gut microflora on mammalian blood metabolites. *Proc Natl Acad Sci U S A*, 2009. **106**(10): p. 3698-703.
212. Wishart, D.S., et al., HMDB 5.0: the Human Metabolome Database for 2022. *Nucleic Acids Res*, 2022. **50**(D1): p. D622-D631.
213. Wishart, D.S., et al., HMDB 4.0: the human metabolome database for 2018. *Nucleic Acids Res*, 2018. **46**(D1): p. D608-D617.
214. Wishart, D.S., et al., HMDB 3.0--The Human Metabolome Database in 2013. *Nucleic Acids Res*, 2013. **41**(Database issue): p. D801-7.
215. Wishart, D.S., et al., HMDB: a knowledgebase for the human metabolome. *Nucleic Acids Res*, 2009. **37**(Database issue): p. D603-10.
216. Wishart, D.S., et al., HMDB: the Human Metabolome Database. *Nucleic Acids Res*, 2007. **35**(Database issue): p. D521-6.
217. Marver, D. and I.S. Edelman, Dihydrocortisol: a potential mineralocorticoid. *J Steroid Biochem*, 1978. **9**(1): p. 1-7.
218. Tarantola, M., et al., Beef cattle welfare assessment: use of resource and animal-based indicators, blood parameters and hair 20 β -dihydrocortisol. *Italian Journal of Animal Science*, 2020. **19**(1): p. 341-350.
219. Nomura, A., et al., Relationship between gut microbiota composition and sensitization to inhaled allergens. *Allergol Int*, 2020. **69**(3): p. 437-442.
220. Mutlu, E.A., et al., Inhalational exposure to particulate matter air pollution alters the composition of the gut microbiome. *Environ Pollut*, 2018. **240**: p. 817-830.
221. Yamaguchi, T., et al., Effect of gut microbial composition and diversity on major inhaled allergen sensitization and onset of allergic rhinitis. *Allergol Int*, 2023. **72**(1): p. 135-142.
222. Borbet, T.C., et al., Influence of the early-life gut microbiota on the immune responses to an inhaled allergen. *Mucosal Immunol*, 2022. **15**(5): p. 1000-1011.
223. Scalbert, A., et al., Mass-spectrometry-based metabolomics: limitations and recommendations for future progress with particular focus on nutrition research. *Metabolomics*, 2009. **5**(4): p. 435-458.

224. Chen, J., et al., Spatiotemporal modeling of microbial metabolism. *BMC Syst Biol*, 2016. **10**: p. 21.
225. Saa, P., et al., Modeling approaches for probing cross-feeding interactions in the human gut microbiome. *Comput Struct Biotechnol J*, 2022. **20**: p. 79-89.